Using pXRF for the Analysis of Ancient Pottery

AN EXPERT WORKSHOP IN BERLIN 2014

Morten Hegewisch
Małgorzata Daszkiewicz
Gerwulf Schneider
(eds.)

edition | topoi

BERLIN STUDIES OF THE ANCIENT WORLD

THE AIM OF THE SECOND WORKSHOP on the use of portable energy-dispersive X-ray fluorescence (pXRF) organized by the Cluster of Excellence TOPOI was to exchange experiences and discuss the basic requirements for the use of pXRF as a tool for chemical analysis of archaeological ceramics. During two days, 49 participants from eight European countries discussed nineteen lectures, twelve of which are published here as papers presenting research on ceramics and glass of various periods from Bulgaria, Germany, Greece, Rumania, Ukraine, Sudan, Syria and the United Kingdom. The focus was on analysing bulk pottery and on the possibilities of non-destructive determination of chemical composition. The number of chemical elements significant for provenance studies and determinable with sufficient precision and accuracy plays a major role. This was compared with chemical analysis using WDXRF, ICP-MS, NAA. The different examples prove that the chances of positive outcomes depend very much on the individual cases.

75 BERLIN STUDIES OF
THE ANCIENT WORLD

BERLIN STUDIES OF THE ANCIENT WORLD · 75

EDITED BY TOPOI EXCELLENCE CLUSTER

Using pXRF for the Analysis of Ancient Pottery

AN EXPERT WORKSHOP IN BERLIN 2014

EDITED BY

Morten Hegewisch
Małgorzata Daszkiewicz
Gerwulf Schneider

Bibliographic information published by the Deutsche Nationalbibliothek
The Deutsche Nationalbibliothek lists this publication in the Deutsche Nationalbibliographie; detailed bibliographic data are available in the Internet at http://dnb.d-nb.de.

Cover image: Sherds of alamannian pottery from excavations on „Runder Berg“ in Urach (Baden-Württemberg). Photo: Gerwulf Schneider.

Design concept: Stephan Fiedler

Distributed by
Westarp Verlagsservicegesellschaft mbH

Printed by
Druckerei Kühne & Partner GmbH & Co. KG

ISBN 978-3-9819685-9-0
ISSN (Print) 2366-6641
ISSN (Online) 2366-665X
DOI 10.17171/3-75
URN urn:nbn:de:kobv:188-refubium-29632-6

First published 2021

www.edition-topoi.org

CONTENTS

Morten Hegewisch, Michael Meyer

Introduction

Summary

Research Group A-6 *Economic Spaces* within the Excellence Cluster Topoi *The Formation and Transformation of Space and Knowledge in Ancient Civilizations* analyses economic structures in space. Its focus is on the organization of the manufacture and distribution of goods and on the spatially-related consumption thereof; ceramics are the principle object of research. The workshop on the use of portable energy-dispersive X-ray fluorescence (pXRF) for the analysis of ceramics was intended as an opportunity for the exchange of experiences and the discussion of basic prerequisites for working with the class of instruments it centered around. The aim of this volume is not a summary of the state of research, but rather the presentation of application examples.

Keywords: portable energy-dispersive X-ray fluorescence (pXRF); exchange of experiences; new methodological approaches; applicability for ceramics; international research

Die Forschungsgruppe A-6 Economic Spaces im Exzellenzcluster Topoi „Die Entstehung und Transformation von Raum und Wissen in alten Zivilisationen“ analysiert wirtschaftliche Strukturen im Raum. Ihr Schwerpunkt liegt auf der Organisation, der Herstellung und Verteilung von Waren und deren räumlich bedingter Verbrauch; Keramik ist das Hauptforschungsobjekt. Der Workshop über den Einsatz von tragbarer energiedispersiver Röntgenfluoreszenz (pXRF) zur Analyse von Keramik war als Gelegenheit für den Erfahrungsaustausch und die Diskussion der Grundvoraussetzungen für die Arbeit mit dieser Geräteklasse gedacht. Das Ziel des vorliegenden Bands ist keine Zusammenfassung des Forschungsstands, sondern vielmehr die Präsentation von Anwendungsbeispielen, aus denen andere Forschergruppen lernen können.

Keywords: tragbare energiedispersive Röntgenfluoreszenz (pXRF); Erfahrungsaustausch; neue methodische Ansätze; Anwendbarkeit für Keramik; internationale Forschung

Morten Hegewisch, Małgorzata Daszkiewicz und Gerwulf Schneider (eds.) | Using pXRF for the Analysis of Ancient Pottery – an Expert Workshop in Berlin 2014 | Berlin Studies of the Ancient World 75 (ISBN TODO; DOI: 10.17171/3-75) | www.edition-topoi.org

Research Group A-6 *Economic Spaces* within the Excellence Cluster TOPOI *The Formation and Transformation of Space and Knowledge in Ancient Civilizations* analyses economic structures in space. Its focus is on the organization of the manufacture and distribution of goods and on the spatially-related consumption thereof; ceramics are the principle object of research. The researchers attempt to identify and interpret production sites and distribution and consumption areas of specific groups of ceramics, primarily through natural science-based analyses, though also through stylistic analyses. The research group deliberately pursues a comparative perspective in two respects: firstly, by comparing conditions in diverse cultural spaces and epochs of the Ancient World and secondly, by conducting illustrative investigations on the production and distribution of other goods enabling comparison.

Research Group A-6 held a workshop entitled "Der Einsatz transportabler RFA-Geräte für Keramikanalysen/Application of portable X-ray fluorescence to the analysis of archaeological ceramics" on 20 and 21 June 2014. Organized and led by Michael Meyer, Małgorzata Daszkiewicz, Gerwulf Schneider, and Morten Hegewisch, the workshop took place at the Topoi Building Dahlem at Freie Universität Berlin.

The workshop on the use of portable energy-dispersive X-ray fluorescence (pXRF)[1] for the analysis of ceramics was intended as an opportunity for the exchange of experiences and the discussion of basic prerequisites for working with the class of instruments it centered around.

The aim of this volume is not a summary of the state of research, but rather the presentation of examples of applications.

In addition to the group's members, researchers from Finland, Germany, Greece, Israel, Poland, Qatar, Sweden and the United Kingdom were invited to contribute. The use of pXRF was the prerequisite for contributing to the workshop as a speaker. The workshop provided an opportunity to compare experiences with two instruments from different manufacturers: Thermo Fischer Scientific Niton's XL3t 900S GOLDD analyzer and Bruker's TRACER-III SD. Only occasional mention was made of instruments manufactured by other companies.

Portable XRF instruments have been in use, in the archaeological sciences and elsewhere, since the 2000s. Use of transportable XRF equipment for ceramic analyses and other purposes began back in the 1970s. The first papers and rigorous methodological approaches appeared in that same decade.[2]

The technology did not come into widespread national and international use until the 2000s. There are several reasons for this delay. One is that WD-XRF and INAA were

1 The abbreviation pXRF is used to refer to these instruments throughout the text. Other abbreviations can be found elsewhere in the literature such as p XFA, p-ED-XRF, HH-XRF (for handheld XRF).

2 Cesareo et al. 1972.

already well-established techniques with standardized procedures permitting high measurement accuracy that were already being used successfully – the use of WD-XRF in the archaeology of the Roman provinces can serve as an example in the European context. Another reason for the lag in development of the portable technology was that the new class of instruments addressed here is not primarily suited to the study of archaeological ceramics (where the aim is mainly to detect light elements), the instruments being far better suited to the rapid and reliable identification of metals – for the purposes of recycling metal scrap for instance – an area in which the technology was swiftly adopted.

It also took the expenditure of considerable time and effort to overcome the new technique's "teething troubles," which were manifest particularly in conjunction with adapting hardware and software to suit the new objects of analysis. In addition, although this new technology is less expensive and, importantly, does not require the extraction of samples from objects for analysis, it was not initially clear whether the results it generates genuinely reflect past conditions or whether they might only be the product of an incorrect application of the technique. Accordingly, there was a very real need for a thorough evaluation of this technology, i.e. one not limited to only certain aspects, and to compare it to long-established and mature methods and techniques, and the framework of Topoi made it possible to address.

This comparison has drawn its share of criticism however. Marcus Helfert[3], for instance, has noted:

> Thus P-ED XRF is compared directly with INAA, with emphasis on the inferior precision and accuracy of the results of the former and the more limited spectrum of elements it can measure […]. Yet it has been clear from the outset that the two methods cannot be subjected to a point-for-point comparison, as the instrumental components and sample preparation are so dissimilar. There is therefore little point in comparative studies in comparing the highest class of equipment with what is quasi the lowest and then emphasizing the inferior performance potential of the latter.[4]

One has to agree with that, yet when the extensive deployment of this technology is at issue, then this very potential does have to be assessed in comparison with the established, and expensive older methods – partly to determine whether or not the qualicty of the data is adequate for specific questions in economic archaeology. However, Behrendt, Mielke and Mecking found three studies in which 10–45% of the sherds analyzed with pXRF were classified incorrectly in comparison to classic laboratory analysis.[5]

3 Helfert 2013, 17.
4 Helfert 2013, 7.
5 Behrendt, Mielke, and Mecking 2012.

Within the framework of the Excellence Cluster Topoi, Research Group A-6 *Economic Spaces* was able to carry out the broadly-based evaluation of this technique, the results of which will be presented in detail in future publications. During the evaluation, a sophisticated sample strategy for diachronically dated objects located in multiple regions was developed within an archaeological/archaeometry working group whose members focus on a wide range of fields and methodologies. The strategy involves combining pXRF with the re-firing technique (MRG analysis[6]) as well as the modification of the sample selection and methodology prior to the actual analysis of samples in the laboratory. It is this combination that makes it possible to identify points where "tweaks" can directly affect data quality and impact the interpretation of the results.

It would have been pointless to use the funds available for the Topoi project to gather extensive sets of data, thus generating results with no way of estimating their accuracy or their useful life. The consequences for broad sub-fields of archaeological scholarship in various countries would have been substantial, particularly in connection with inaccurate data, particularly given the fact that in archaeological disciplines the same research results sometimes continue to be used over the course of decades. Instead, the in-depth evaluation of the technique as such made it possible to develop new methodological approaches over a longer period and lines of inquiry that had not previously been thought of.

Regarding international research, the problems broached here have been widely recognized and discussed in the context of a great many national and international publications.[7] The universities have also taken developments in this area into account, having integrated archaeometry into the archaeological curricula or even gone so far as to establish it as a minor field of study, as the Goethe-Universität Frankfurt has done.[8]

This volume marks a step along this path, describing the difficulties confronting those using this technique while also illustrating the possibilities that have opened up for archaeology.

A great many researchers were invited to the workshop. The archaeological ceramics they have studied came from Bulgaria, Germany, Greece, Jordan, Romania, Ukraine, Sudan, Syria and the United Kingdom. The examples they presented encompassed analyses of Neolithic and Bronze Age pottery, Greek amphoras, Roman terra sigillata, Germanic wheel-thrown pottery and other goods.

6 Daszkiewicz and Schneider 2001; Daszkiewicz and Maritan 2017.

7 Behrendt and Mielke 2013; Donais et al. 2010; Frahm, Doonan, and Kilikoglou 2014; Hanauska and Sonnemann 2013; Helfert and Böhme 2010; Helfert 2013; Mazar et al. 2010; Mecking, Mielke, and Behrendt 2013; Morgenstein and Redmont 2005; Pettersson 2013; Potts and West 2008; Potts, William-Thorbe, and Webb 1997; Shugar 2013; Tykot et al. 2013; Papmehl-Dufay et al. 2013.

8 Helfert 2013, 42, n. 1.

Most of the papers presented at the workshop were submitted for publication in an extended form. In addition, this volume contains a paper by Toni Walter and Marc Fellinger, who were able to provide answers to important questions in the concluding discussion. Two shorter portions of the paper given by Małgorzata Daszkiewicz and Ewa Bobryk have previously been published[9] and their text has been supplemented here by the addition of the surface area measurements of salt containers.

In their presentations, the natural scientists at the workshop emphasized the aspects of general applicability for ceramics (and other applications) and the reliability of the measurement data. Controversial topics of discussion were measurement times per sample (how many minutes per measurement, how many measurements per sample, how many samples associated with a reasonable investment of time and resources), calibration (exchange of reference samples, fixed reference samples or pressed powder tablets, comparability of databases), non-destructive analysis (fresh fracture, cleaned or abraded surface) and radiation protection.

In relation to promoting standardization and comparability, the following points emerged from the discussion:

– When presenting results, researchers should note that the analyses were done using p-ED-XRF without sample extraction rather than with the considerably more reliable analysis of powdered samples (or of powders) with WD-XRF – merely stating that the XRF was the method used is not sufficient. Numbers of measurements per sample and the relevant measurement times should also be reported.

– It would be helpful to publish tests on reproducibility and trueness of pXRF analyses at the same time.

– Sample preparation (unchanged or abraded surface, fresh fracture) must be noted.

– For purposes of data comparability, every effort must be made to enable the exchange of suitable reference samples, which are identified when the data is published.

The workshop contributions provide an impressive view of the possibilities, but also the limitations of the analysis of archaeological ceramics (and glasses) with pXRF and without the extraction of powdered samples from the objects. One saw that the success of use of the technique is highly project-dependent, or rather, dependent on the ceramics being analyzed. In many cases, pXRF can provide good answers to archaeological

9 Daszkiewicz and Bobryk 2013; Daszkiewicz, Schneider, et al. 2013.

questions about the origin of ceramic objects and the distribution of certain groups of materials, while in other cases non-destructive analyses are not sufficiently conclusive. The projects presented here may be helpful when planning projects. At a minimum, it would always be wise to start by carrying out a pilot project with analyses, using WD-XRF, for example, in order to ascertain which elements must be detected with a given degree of precision in order to fulfil the research aims.

Bibliography

Behrendt and Mielke 2013
Sonja Behrendt and Dirk Paul Mielke. "Probleme und Perspektiven archäometrischer Untersuchungen großer Keramikmengen. Ein Projektbericht." *Universitätsforschungen zur Prähistorischen Archäologie* 218 (2013), 93–121.

Behrendt, Mielke, and Mecking 2012
Sonja Behrendt, Dirk Paul Mielke, and Oliver Mecking. "Die portable Röntgenfluoreszenzanalyse (P-RFA) in der Keramikforschung: Grundlagen und Potenzial." *Restaurierung und Archäologie* 5 (2012). Mainz, 93–110.

Cesareo et al. 1972
Roberto Cesareo, Franco V. Frazzoli, Carlo Mancini, Sebastiano Sciutti, Maurizio Marabelli, Peter Mora, Pasquale Rotondi, and Giuliani Urbani. "Non-Destructive Analysis of Chemical Elements in Paintings and Enamels." *Archaeometry* 14 (1972), 65–78.

Daszkiewicz and Bobryk 2013
Małgorzata Daszkiewicz and Ewa Bobryk. "Gypsum on Pottery Surfaces Detected by pXRF – Alteration, Forming or Geometry?" In *Archäometrie und Denkmalpflege*. Ed. by A. Hauptmann, O. Mecking, and M. Prange. Metalla Sonderheft 6. Bochum: Bauhaus-Universität Weimar, 2013, 154–158.

Daszkiewicz and Maritan 2017
Małgorzata Daszkiewicz and Lara Maritan. "Experimental Firing and Re-firing, Chapt. 27." In *The Oxford Handbook of Archaeological Ceramic Analysis*. Ed. by A. Hunt. Oxford: Oxford University Press, 2017, 487–508.

Daszkiewicz and Schneider 2001
Małgorzata Daszkiewicz and Gerwulf Schneider. "Klassifizierung von Keramik durch Nachbrennen von Scherben." *Zeitschrift für Schweizerische Archäologie und Kunstgeschichte* 58 (2001), 25–32.

Daszkiewicz, Schneider, et al. 2013
Małgorzata Daszkiewicz, Gerwulf Schneider, Stefan G. Schmid, and Ewa Bobryk. "Grouping of Nabataean Pottery from Petra (Jordan) Using pXRF and Other Techniques." In *Archäometrie und Denkmalpflege*. Ed. by A. Hauptmann, O. Mecking, and M. Prange. Metalla Sonderheft 6. Bochum: Bauhaus-Universität Weimar, 2013, 138–142.

Donais et al. 2010
Mary Kate Donais, Bradley Duncan, David B. George, and Claudio Bizzarri. "Comparisons of Ancient Mortars and Hydraulic Cements through in situ Analyses by Portable X-Ray Fluorescence Spectrometry." *X-Ray Spectrometry* 39 (2010), 146–153.

Frahm, Doonan, and Kilikoglou 2014
Ellery Frahm, Roger C.P. Doonan, and Vassilis Kilikoglou. "Handheld Portable X-Ray Fluorescence of Aegean Obsidians." *Archaeometry* 56 (2014), 228–263.

Hanauska and Sonnemann 2013
Petra Hanauska and Thorsten Sonnemann. "Die mittelalterliche Keramik der Rheingauer Töpferorte Dillenhausen und Aulhausen: Wie gleich ist gleich?" *Universitätsforschungen zur Prähistorischen Archäologie* 218 (2013), 82–92.

Helfert 2013
Markus Helfert. "Die portable energiedispersive Röntgenfluoreszenzanalyse (P-ED-RFA) – Studie zu methodischen und analytischen Grundlagen ihrer Anwendung in der archäologischen Keramikforschung." *Universitätsforschungen zur Prähistorischen Archäologie* 218 (2013), 13–47.

Helfert and Böhme 2010
Markus Helfert and Dieter Böhme. "Herkunftsbestimmung von römischer Keramik mittels portabler energiedispersiver Röntgenfluoreszenzanalyse (P-ED-RFA) – Erste Ergebnisse einer anwendungsbezogenen Teststudie." In *Naturwissenschaftliche Analysen vor- und frühgeschichtlicher Keramik I: Methoden, Anwendungsbereiche, Auswertemöglichkeiten*. Ed. by B. Ramminger and O. Stilborg. Bonn: Dr. Rudolf Habelt GmbH, 2010, 11–30.

Mazar et al. 2010
Eilat Mazar, Wayne Horowitz, Takayoshi Oshima, and Yuval Goren. "A Cuneiform Tablet from the Ophel in Jerusalem." *Israel Exploration Journal* 60 (2010), 4–21.

Mecking, Mielke, and Behrendt 2013
Oliver Mecking, Dirk Paul Mielke, and Sonja Behrendt. "Methodenvergleich, Anwendungsbeispiele und Grundlagen der portablen Röntgenfluoreszenzanalyse (P-RFA) in der Keramikforschung." *Universitätsforschungen zur Prähistorischen Archäologie* 218 (2013), 49–67.

Morgenstein and Redmont 2005
Maury Morgenstein and Carol A. Redmont. "Using Portable Energy Dispersive X-Ray Fluorescence (EDXRF) Analysis for On-Site Study of Ceramic Sherds at El Hibeh, Egypt." *Journal of Archaeological Science* 32 (2005), 1513–1623.

Papmehl-Dufay et al. 2013
Ludvig Papmehl-Dufay, Ole Stilborg, Anders Lindahl, and Sven Isaksson. "For Everyday Use and Special Occasions – A Multi-Analytical Study of Pottery from two Early Neolithic Funnel Beaker (TRB) Sites on the Island of Öland, SE-Sweden." *Universitätsforschungen zur Prähistorischen Archäologie* 218 (2013), 123–152.

Pettersson 2013
Paul Eklöv Pettersson. "Analyses of Crucibles from Southern and Western Sweden Using Handheld XRF." *Universitätsforschungen zur Prähistorischen Archäologie* 218 (2013), 69–79.

Potts, William-Thorbe, and Webb 1997
Philip J. Potts, Olwen William-Thorbe, and Peter C. Webb. "The Bulk Analysis of Silicate Rocks by Portable X-Ray Fluorescence: Effect of Sample Mineralogy in Relation to the Size of the Excited Volume." *Geostandard Newsletter* (1997), 21–41.

Potts and West 2008
Philipp J. Potts and Margaret West, eds. *Portable X-Ray Fluorescence Spectrometry – Capabilities for in situ Analysis*. Cambridge: Royal Society of Chemistry, 2008.

Shugar 2013
Aaron N. Shugar. "Portable X-Ray Fluorescence and Archaeology: Limitations of the Instrument and Suggested Methods to Achieve Desired Results." *Archaeological Chemistry* VIII (2013), 173–193.

Tykot et al. 2013
Robert H. Tykot, Nancy M. White, J. P. Du Vernay, J. S. Freeman, Christopher Hays, M. Koppe, C. N. Hunt, Richard A. Weinstein, and D. S. Woodward. "Advantages and Disadvantages of pXRF for Archaeological Ceramic Analysis: Prehistoric Pottery Distribution and Trade in NW Florida." In *Archaeological Chemistry VIII*. Ed. by R. A. Armitage and J. H. Burton. Florida: American Chemical Society, 2013, 233–244.

MORTEN HEGEWISCH

Morten Hegewisch is archaeologist with a scientific focus on Roman Imperial age in Germanic regions and is specialized on Germanic pottery. He worked at the Roman-Germanic Commission of the German Archaeological Institute, at the Rheinisches Landesmuseum Bonn, at the Museum of Westlausitz, for the Excellence Cluster Topoi, the Rheinische Friedrich-Wilhelms-Universität Bonn, at now permanent at the Institute of Prehistoric Archeology of the Free University Berlin as editor of the Praehistorische Zeitschrift.

Dr. Morten Hegewisch
Institut für Prähistorische Archäologie
Freie Universität Berlin
Fabeckstraße 23–25
14195 Berlin, Germany
E-mail: hegewisc@zedat.fu-berlin.de

MICHAEL MEYER

Michael Meyer (Dr. phil. Marburg 1990, habilitation at Humboldt-Universität zu Berlin 2005), is a professor of Prehistoric Archaeology at Freie Universität Berlin and has been the spokesperson of the Excellence Cluster Topoi from 2011 to 2019. His research focus lies on the archaeology of the centuries before and after the birth of Christ, on settlement, conflict and economic archaeology.

Prof. Dr. Michael Meyer
Institut für Prähistorische Archäologie
Freie Universität Berlin
Fabeckstraße 23–25
14195 Berlin, Germany
E-mail: michael.meyer@fu-berlin.de

Oliver Mecking

The Influence of Temper on pXRF Measurements and Comparison of pXRF Results with Those of Classic Laboratory Analyses

Summary

As pXRF measures only small volumes at the surface of a ceramic object, grain sizes of the temper and the non-homogeneous distribution of elements in the clay have a significant effect on measurement results. These effects were reproduced using a variety of sherds manufactured by the researcher. In addition, pXRF results were checked against those of classic laboratory analyses in two cases, involving ceramics from Haarhausen and Eythra. In this context, pXRF was unable to reproduce the results of classic laboratory analysis on geochemically similar sherds. In the case of geochemically differing sherds, it was possible to reproduce the results of the laboratory analysis at a rate of 70–100%.

Keywords: pXRF; temper; grain sizes; Haarhausen; Eythra

Da die p-RFA nur kleine Volumina an der Oberfläche misst, haben die Korngrößen der Magerung und die nicht homogene Verteilung der Elemente im Ton einen wichtigen Einfluss auf die Messung. Diese Einflüsse wurden an unterschiedlichen selbst hergestellten Scherben nachvollzogen. Weiter wurde an zwei Beispielen – Haarhausen und Eythra – die Ergebnisse der p-RFA mit klassischer Laboranalytik überprüft. Dabei hat sich gezeigt, dass bei geochemisch ähnlichen Scherben die Ergebnisse der klassischen Laboranalytik nicht reproduziert werden konnten. Bei geochemischen Unterschieden können die Ergebnisse der Laboranalytik zu 70 bis 100% wiedergefunden werden.

Keywords: pRFA; Magerung; Korngrößen; Haarhausen; Eythra

Morten Hegewisch, Małgorzata Daszkiewicz und Gerwulf Schneider (eds.) | Using pXRF for the Analysis of Ancient Pottery – an Expert Workshop in Berlin 2014 | Berlin Studies of the Ancient World 75 (ISBN TODO; DOI: 10.17171/3-75) | www.edition-topoi.org

1 Introduction

Geochemical analyses of ceramics are an important element of archaeological work on ceramics. These analyses investigate either the mineralogical phase composition of the pottery (thin sections) or the element pattern of the pottery. They make it possible to distinguish among different clay recipes or detect technological differences. When misfired pottery samples from a pottery production site are available, attribution to the kiln is possible by comparing sherds from other finding sites with the sherds from pottery production waste.

Large quantities of ceramics are found at excavations. With scientific analyses, researchers seek answers to questions of economic archaeology. Obtaining these answers requires the analysis of a sufficiently large number of sherds. The investigation of multiple finding sites has great potential benefit for archaeological interpretations, however is only rarely feasible due to the time requirements and high costs associated with laboratory analysis. pXRF holds out fascinating possibilities for research questions of this kind, because it allows investigators to analyze, quickly and inexpensively, a larger series of samples in the field.[1] However, the objects being analyzed are ceramics, which do not present a homogeneous sample body, and pXRF instruments analyze only a small volume at the surface of an object due to the low escape depth of the fluorescence radiation. This can result in substantial errors if pXRF is employed incorrectly. For this reason, an accurate understanding of the measurement process is important to ensure the reliable interpretation of results. This article therefore first describes the basic methodology, before turning to examples for the use of pXRF. In connection with examples, the pXRF results are compared to those of classic laboratory methods to permit an assessment of the possible applications pXRF.

2 Methodological basis

Portable XRF involves the measurement of a volume at the surface of a sample. The measurement site thus plays a decisive role. The work of many researchers has made it very clear that analyses on the outer surfaces of pottery can be problematic – either due to coatings applied to the surface or to the effects of time spent in the ground – in connections with Fe, Ca, K and other elements.[2] For this reason, pXRF measurements are now taken at fresh fractures.[3] Other problems have been described as well. The shape

1 See Morgenstein and Redmount 2006; Helfert, Mecking, et al. 2011 and others.

2 See Ikeoka et al. 2012; Behrendt, Mielke, and Mecking 2012; Behrendt, Mielke, and Tagle 2012 and others.

3 See Aimers, Farthing, and Shugar 2012; Behrendt, Mielke, and Mecking 2012; Daszkiewicz and Schneider 2011 and others.

of the sample has a significant influence on the analysis, for instance.[4] Furthermore, the duration of the measurement has a significant effect on data quality.[5]

2.1 Influence of temper

The largest source of error in pXRF analyses other than those mentioned is associated with the composition of ceramics. Ceramics consist of a clay matrix and aplastic inclusions. Thus, ceramics do not constitute a homogeneous matrix. Whether one or multiple measurements are taken, one must always ask whether the measurements are representative of the entire sherd (for rocks.[6] Classic laboratory analysis avoids these problems by grinding up various amounts of the sherd. Approximately 100 mg suffices with fine pottery, while up to 4 grams may be necessary for coarse pottery.[7] With pXRF, this kind of sample preparation is not performed. It is therefore essential to obtain an understanding of the physics of X-ray fluorescence radiation. The energy of a given element determines the escape depth of its X-ray fluorescence radiation.[8] The lower the energy is, the lower the escape depth. One can estimate the volume measured by estimating the escape depth of the element[9] and multiplying that by the spot size area (here, 8 mm diameter). By multiplying this volume by the estimated density[10] of pottery of approx. 2 g /cm^3, one can determine the weight associated with the volume measured for each individual element. These weights vary by as much as two orders of magnitude, falling between 0.5 and 50 mg (Tab. 1). This may mean that because of the non-homogeneous distribution the measurement of iron or potassium content, for instance, is not representative for the ceramic, while it may be representative in the case of Sr, Rb, Y and Zr. The weights of ceramic material measured (Tab. 1) indicate that the results are more likely to be representative in the case of the elements Sr, Rb, Y, Nb and Zr, for which large volumes are measured, than are those obtained for the lighter elements. In pXRF systems that have a smaller or larger spot size, the volumes measured, and with them the weights measured, differ accordingly.

The masses calculated for the different elements make it clear that temper can have an influence on the analysis. If the grain diameter of the temper is within the range of the size of the measurement window, it is unlikely that an analysis will accurately reflect the relative proportions of clay and temper. Thus, the measurement data can be erroneous. In an initial assessment, the effect can be described as varying with the grain size of the

4 Forster et al. 2011.
5 Behrendt, Mielke, and Mecking 2012.
6 See Potts, Williams-Thorpe, and Webb 1997.
7 See Schneider et al. 1989.
8 See e.g. Stern 1995; Liritzis and Zacharias 2011; Potts, Williams-Thorpe, and Webb 1997.
9 See Mecking 2010b and Helfert and Böhme 2010 on this.
10 See Curet 1997 and Wieckhorst 1995 on density.

	Weight in mg		Weight in mg
Mg	0.47	Mn	2.51
Al	0.82	Fe	3.52
Si	1.17	Cu	6.23
P	0.14	Zn	8.04
K	0.54	Rb	29.66
Ca	0.65	Sr	31.06
Ti	1.21	Zr	44.84
V	1.66	Nb	53.38
Cr	2.01	Y	37.40

Tab. 1 Estimated weight of material analyzed using pXRF with a spot size of 8 mm.

additives. Lack of homogeneity in the clay matrix can be the source of a second significant effect. How can these two effects be assessed? Temper, whether deliberately added or naturally present in the clay, differs in composition from the clay that contains it. Tempers can have quite different chemical compositions. For instance, a temper might consist solely of quartz, which would only cause a "dilution" of the results, since it would merely boost the proportion of silicon, reducing the proportions of the other elements accordingly. Other tempers, such as feldspar types, zircons or granites, change the trace element pattern of the ceramic. Thus, not only the grain size but also the composition of the temper particles has an impact on results. A variety of ceramics were produced in the laboratory in order to assess these effects.[11] A commonly available homogenized clay was used for this purpose. Granite, quartz, quartz-monazite, gabbro and marble were mixed with the clay as temper components. These were crushed and then sorted by grain sizes using sieves into fractions from 0.1 to 4 mm. These different grain-size fractions were then mixed with the clay in differing proportions (from 5 to 30 percent by mass) by hand, to reproduce the work of an ancient potter. The resulting mixtures were then shaped into oblong objects and fired at 800°C. After the firing, the objects were cut and analyzed at four different sites on their surfaces. A Niton XL3tGOLDD+ Hybrid with an Ag tube was used for the analyses, without helium flushing. The spot (measurement surface) has a diameter of 8 mm. The results described below can therefore be directly transferred only to analyses in which the spot size is also 8mm in diameter. Nonetheless, they can also provide some guidance for analyses performed using instruments with other spot sizes.

11 Behrendt, Mielke, and Mecking 2012.

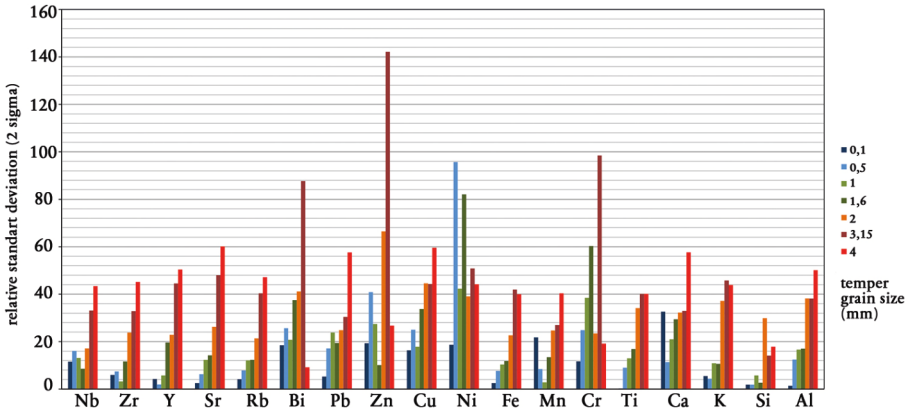

Fig. 1 Relative standard deviation for results from analysis of samples tempered with 20% of quartz.

As described above, one can distinguish between two types of temper effects. The first type is associated with tempers consisting chiefly of a single element that is also present in the pottery, and the second type is associated with tempers that bring a significant increase in the concentration of one or more elements into the clay. In order to describe the influence of the temper on the measurement results, the sherds were measured at four different sites. Relative standard deviations (2 sigma) were calculated from the results of these four measurements. The larger the relative standard deviation, the greater is the risk that measured values might differ from the true values. Looking at the results for the ceramics with 20% quartz temper (Fig. 1), for example, one sees that the relative standard deviations remain low up to a grain-size of 1–1.6 mm, at which point the values begin to increase rapidly, rising above 40% for almost all of elements.[12]

The elements with the greatest escape depths (Zr, Nb, Y, Sr, Rb) are associated with smaller dispersion ranges than the other elements do. Due to the inferior counting statistics, the elements Zn, Cu, Cr and to some extent Pb are associated with considerable scattering, even in the cases with samples with smaller grain sizes. The relative standard deviations then begin to increase markedly from a grain size of 1.6 mm. This means that fewer measurements are needed to obtain representative results for ceramics with quartz tempers with grain sizes of less than 1.6 mm. With grain sizes above 1.6 mm, the number of measurements should be increased to ensure that the results are representative. To depict the effect of temper on the mean value, two different groups were formed. One group consisted of ceramics with temper grain diameters less than or equal to 1 mm. In this group, the effect exerted by the temper was minor. This group

12 Behrendt, Mielke, and Mecking 2012.

		Zr	Y	Sr	Rb	Nb	Fe	Ti	K	Ca
Single measurement	≤ 1 mm	9	11	16	16	25	13	15	34	2
	≥1.6 mm	58	66	74	60	51	59	54	63	66
Mean value over 2 measurements	≤ 1 mm	7	7	6	6	15	5	4	9	5
	≥1.6 mm	22	25	26	20	23	18	25	40	23
Mean value over 4 measurements	≤ 1 mm	2	5	5	4	8	4	3	3	5
	≥1.6 mm	7.4	10	10	8	11	4	5.3	4.2	15

Tab. 2 Relative ranges for different mean values obtained for the samples with 20% quartz temper.

therefore constitutes the comparison group. To establish the comparison basis, all of the individual mean values associated with the individual temper grain sizes were divided by the mean value of the measurement results from the samples with temper grain sizes of 0.1–1 mm, and the quotient multiplied by 100. These values were used to generate the ranges for the measurements of up to 1 mm and from 1.6 mm on up. Thus, by comparing these two values, one can depict the influence of the temper associated with the four measurements at different sites. Instrumental background was determined by running a glass standard (BCR 126A) on every measurement day over the course of 1,5 years. The contents measured for the individual elements varied between 2 and 4.5% in this context. The relative ranges for all elements increase. For instance, in the case of measurement results for Zr, Sr, Fe and K associated with grain-sizes under 1 mm, the relative ranges are below 5% and thus within the instrumental background (Tab. 2). With the larger grain sizes these values rise to 10%. One can detect effects here, but multiple measurements can partially compensate for them. These effects are significantly greater in the case of elements at concentrations closer to the detection limit. In the extreme case of the Cr values, for instance, it increased from 12 to 76%.

How great is the effect when only one measurement is carried out on the sample and this result used for the interpretation? Here again, relative ranges were generated using the individual measurements for the ceramics with temper grain sizes less than or equal to 1 mm or greater than 1.6 mm. For the less than 1 mm grain size group, the ranges for the elements Zr, Y, Sr, Rb and Nb are between 9 and 25% For the ceramics with temper diameters greater than 1.6 mm, the values were considerably higher, reaching as high as 74% (Tab. 2). This was also seen in connection with the lighter elements, like Fe, Ti, K and Ca. The ranges for smaller temper diameters are between 12 and 34%. The ranges increase with larger grain-size diameters, coming in between 54 and 66%. This indicates

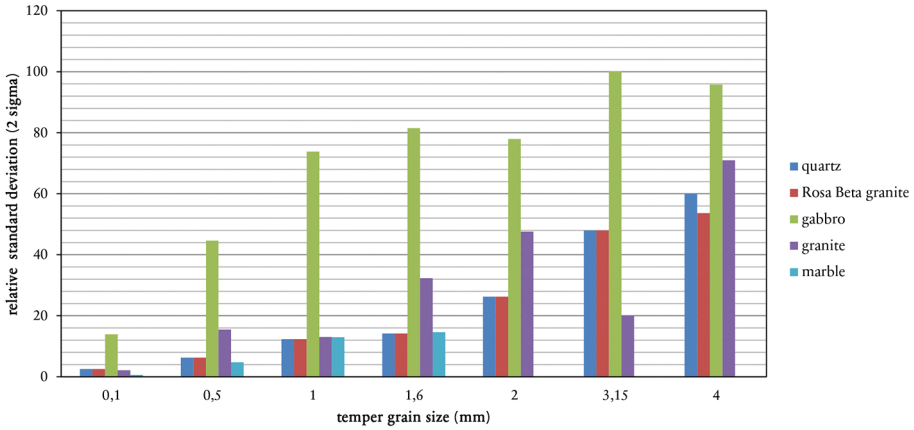

Fig. 2 Change of the coefficient of variation for Sr with different tempers, 20% temper content.

very clearly that that multiple measurements are necessary with coarser ceramics.

If we now assume that the analyses of ceramics should always consist of 2 measurements, we can calculate the mean for each pair of measurements and compare these values with one another. The ranges of the mean values determined decrease considerably compared to those for the individual measurements. For instance, the relative ranges for Zr, Y, Sr, Rb and Nb fall to values of 7–15% for ceramics with temper diameters of up to 1 mm. In the case of the larger grain diameters, the ranges decrease considerably, coming in between 20 and 26% for these elements (Tab. 2). Similar effects are also seen for the lower-energy elements. There, the values for Fe, Ti, Ca and K are low for grain sizes of up to 1 mm. The values associated with larger grain sizes, of 1.6 mm or greater, are considerably higher, but still below those obtained using the single measurements (Tab. 2). This shows that one can get by with two measurements when analyzing ceramics with quartz temper of smaller grain sizes. If the grain size is 1.6 mm or greater, at least two, and preferably more, measurements should be taken. This means that it is possible to analyze ceramics with quartz temper in grain sizes above 1.6 mm. When four measurements are taken, measurement error for ceramics with grain sizes above 1.6 mm is between two and four times greater than that associated smaller grain sizes. Nonetheless, for most elements the error is still under 10%.

The type of temper is also important: the results of measurements on ceramics made with a 20% non-quartz temper mix can differ considerably from those for ceramics with the same percentage of quartz temper. This can best be discussed by looking at the example of Sr. The addition of temper changes the strontium content of the sample. For 20% quartz and quartz-monazite, the strontium content in the ceramics came in

at 54 ppm (value calculated from the mean value for samples with temper grain sizes of 0.1, 0.5 and 1 mm). When granite was added this mean value rose to 88 ppm of strontium. When gabbro was added instead of granite, the values rose to 159 ppm Sr. This has a considerable effect on the relative coefficients of variation of the measurement results (Fig. 2). The influence of gabbro is already evident at a grain size of 0.1 mm and the value of the relative coefficient of variation (2 sigma) is 14%. It is under 3% for all other tempers. With 1 mm temper, the coefficient of variation for the gabbro was 74%, far higher than that associated with any other kind of temper. Similar differences were recorded for ceramics with larger temper particles. These differences can also be detected for granite, though they are not as striking and do not emerge as clearly with all grain sizes. When measurements were performed at four different sites in order to counteract this effect, the mean values associated with quartz monazite temper grain sizes between 0.1 and 1 mm vary from 53 to 56 ppm. With quartz temper they are in the same range. Granite is associated with a somewhat greater dispersion, between 84 and 92 ppm. With gabbro the dispersion is over a somewhat broader range of 150 to 175 ppm. In the case of quartz temper, when dealing with the larger temper diameters, it was possible to cope with the inhomogeneities by taking four separate measurements, as was shown above. The situation with granite is different. The dispersion ranges, between 75 and 140, increase considerably. With gabbro, the values are between 150 and 190 ppm Sr. With this sample (20% gabbro), one finds even greater effects when looking at the individual measurements. For the ceramics with temper diameters of up to 1 mm, the relative range of the strontium values is 75%. The relative range associated with the samples with grain sizes of 1.6 or larger is 150%. Generating a mean value from two measurements, the relative range of those was 22% for the ceramics with temper sizes of 1 mm or below and 93% for the larger grain sizes. These results show that a temper which introduces an element in higher concentrations can lead to substantially greater measurement error in connection with temper of larger grain sizes. Unlike the case with quartz, performing four measurements can only compensate for this to a limited extent. Thus in this case, the strontium values could only be used for the evaluation in exceptional cases.

When marble was added to the clay, an unexpected observation was made. It was not possible to manufacture clay with all of the grain sizes. At grain sizes of 2 to 3 mm or larger, the samples were no longer stable. Thus, most of the samples fall into the range that can be described on the basis of the previous analyses as not being subject to any great influence. This absence of an influence is also seen for many elements. For instance, the relative standard deviation (2 sigma) for the Zr values was under 12% for all four temper concentrations. A different picture is presented in the case of elements that are introduced to the sample in larger quantities with the temper. The relative standard deviation (2 sigma) associated with the Ca values was 36% for grain sizes of up

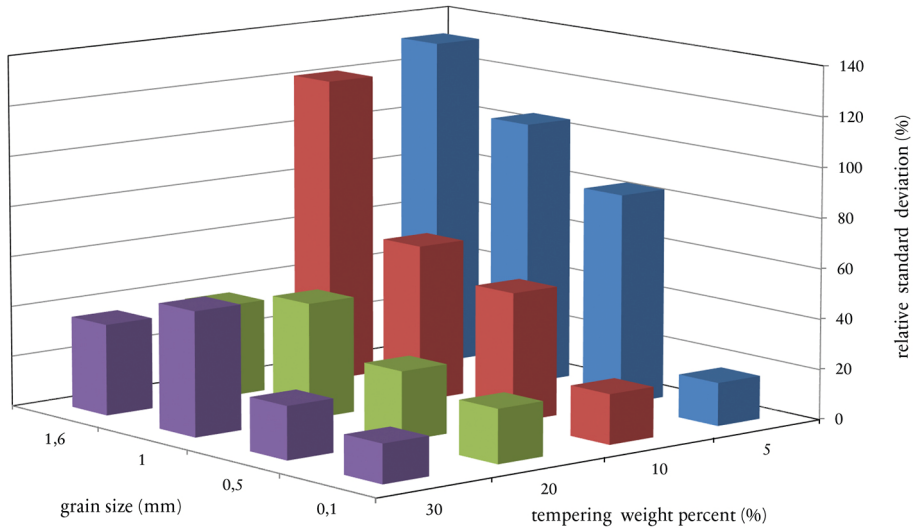

Fig. 3 Coefficient of variation for Ca, measured on ceramics with different proportions of marble temper.

to 1.6 mm and 30% temper ceramics. Here, again, the smaller grain sizes showed smaller effects. However, when the proportion of temper was reduced, the values increased. For instance, the 2-sigma relative standard deviation at 20% temper content increases to 45%, increasing again to 130% in the 5% temper mixture (Fig. 3). It is interesting to see how great the effect on the mean value of the measurements is in this case too. Here again, the relative ranges, which were generated from the mean values of the four measurements, can serve as the unit of measurement. The highest values, at 60%, are associated with the 5% temper content. They then decrease with the addition of more temper, coming in at only 15% for the 30% temper mixture.

Here again, it was only possible to consider grain sizes of up to 1.6 mm. These large deviations are not associated with the other elements. When only two measurements are taken, the probability of error is greater. This can be applied to other temper mixtures. When the ceramic contains a low percentage of temper and the temper consists of only a few elements, one should expect a more noticeable error. The error grows larger as the proportion of temper decreases. This was probably caused by an uneven distribution of the temper. In addition, since the volumes measured for Ca are very small, the values are highly sensitive to small-scale changes. If we assume that the temper distribution in sherds varies within a small range, e.g. between 5% and 4.5%, we can calculate these effects. Assuming that the clay has a CaO content of 2% and was mixed with a temper consisting of 100% Ca) and assuming a random variation of 0.5% in absolute terms in the temper distribution, these two values would differ by 6.7%. Given a difference of 4

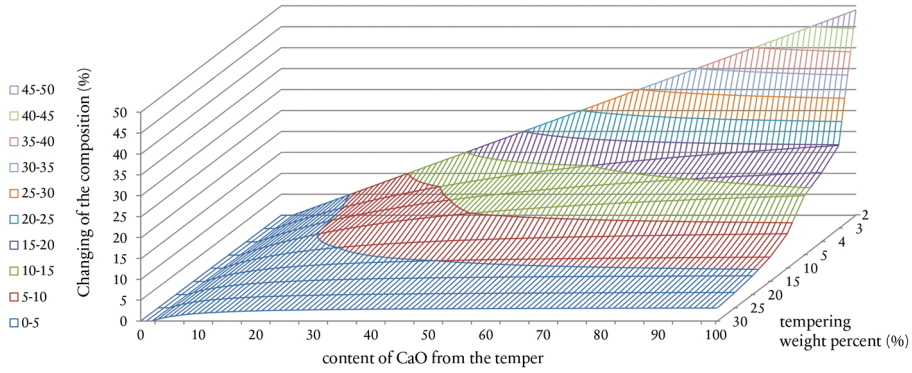

Fig. 4 Theoretic calculation for the effect of a 1% change of temper with different temper amounts and different Ca concentrations.

and 5% in the proportion of temper in the ceramic, the variation runs to approx. 14%. If the proportion of temper is 20%, the effect is considerably smaller. Calculating this for different percentages of temper and different CaO contents in the temper (Fig. 4), one sees that the differences increase with smaller quantities of temper and with high percentages of CaO in the temper. If one adds a temper containing up to 12% CaO (to a clay containing 2%), values lie at 5% at a maximum and thus within the range of measurement error. Assuming an error of 10%, the temper could contain up to 22% CaO. With higher CaO concentrations in the temper, the effects increase considerably in some cases. The quantity of temper exerts the greatest influence though. For instance, the maximal calculated error for a 2% temper mixture is 50%. At a temper proportion of 5%, the maximum calculated error is 14%, and it continues to decrease from there. At a temper proportion of 10%, for instance, it is 10%; and it then falls rapidly below the 5% mark.

This explains why the effect was observed primarily in the group with of ceramics with small proportions of temper. This can also be applied to other types of temper where the temper brings a significantly higher proportion of trace elements into the ceramics. One can think of a variety of tempers which might have such effects. For instance, Flügel et al. describe marble tempers in Roman ceramics from Southern Germany.[13] With this temper, Ca and Sr values would need to be interpreted with great care, since there might be greater scattering. The same applies, naturally, to any other tempers containing calcium, see for example Daszkiewicz regarding limestone,[14] Kalm

13 C. Flügel, Joachimski, and E. Flügel 1997.

14 Daszkiewicz, Schneider, and Bobryk 2008.

Instrument	K	Ca	Ti	Fe	Rb	Sr
Tracer	0.39	0.97	0.37	0.54	0.60	0.93
Analyticon	0.81	0.86	0.39	0.54	0.54	0.94
Oxford	0.58	0.79	0.23	0.49	0.24	0.83

Tab. 3 Comparison of values for selected elements measured in the laboratory with three different pXRF instruments and in the laboratory using the R^2 values.

regarding shells,[15] Daszkiewicz regarding bones.[16] Adding slag[17] could affect the values for copper, lead or iron, depending on the type of slag in question. Zircon temper can present a particular problem, resulting in a greater scattering in the zircon values.[18] However, these effects can be caused by any element that is added to the ceramic mixture with small amounts of temper if the concentration of the element in the temper is high relative to its concentration in the clay.

2.2 Comparison of different pXRF instruments

The use of pXRF is resulting in the compilation of more and more sets of data. In the future, these data sets will contribute to interpretations. In order to make this data useful, it is essential that it be possible to compare data from different instruments and/or laboratories. To provide some initial insight onto this issue, a set of 19 sherds were analyzed with three different instruments. One was the Bruker Nano Tracer Turbo,[19] another was the NITON XL3t GOLDD+Hybrid from Thermo. These two instruments were calibrated with standards.[20] The third instrument was the Oxford X-MET7500. The fundamental parameters were used without standards for the quantification. All of the sherds were also analyzed using laboratory methods.

Looking at the element Rb, for instance, the pXRF values correlate to varying degrees with those from the laboratory analysis. The R^2 value for the Tracer results was 0.6, for the Analyticon it was 0.54 and for the Oxford instrument it was 0.24 (see Tab. 3). The first point that one notices with these values is that, as one would expect, one sees poorer correlation with the lab values with the instruments that do not have adapted standards. Instruments should therefore always be calibrated using standards. However, differences arise even among instruments that have been calibrated using standards. Some of these are only very minor, such as in the iron and strontium counts, while for other elements they are considerably larger. The fact that one instrument might be superior in one respect while the other is better in another suggests that there is considerable opportunity for improvement in pXRF associated with instrument calibration.[21]

15 Kalm 1996.
16 Daszkiewicz, Schneider, and Bobryk 2008.
17 See, e.g. Töchterle et al. 2013.

		Zr	Sr	Rb	Pb	Zn	Cu	Fe	Ti	Ca	K
Tracer	Mean value	186	247	79	20	102	56	3.47	0.43	7.35	2.32
	SD	14	68	13	5	35	12	0.64	0.04	2.83	0.47
Analyticon	Mean value	203	261	85	20	69	36	4.29	0.49	6.95	1.89
	SD	14	69	13	3	24	10	0.70	0.06	2.62	0.33

Tab. 4 Comparison of values for selected elements measured in the laboratory with three different pXRF instruments and in the laboratory using the R^2 values.

However, the R^2 values provide only limited insight into the comparison of the two calibrated instruments. The values could correlate well with one another well and yet still exhibit systematic deviations or higher scattering. When the mean values for the 19 fragments are calculated and compared with one another, one finds elements for which the differences are less than 10%, like Pb, Sr, Rb, Zr and Ca (Tab. 4). Other elements, like Zn, Cu, Fe, Ti and K, exhibit differences as high as 50%. This can lead to errors when data from the literature is incorporated into interpretations. This problem could be avoided by having the same set of sherds or standards analyzed with both instruments and reconciling the values on the basis of a comparison of the two sets of data. This is assuming, naturally, that a systematic error is at issue.

The mean values and the R^2 values, which can be compared with one another, are one aspect. Individual values can show greater differences. One element for which one sees very good correlations is strontium. When one sets the individual measured values alongside the laboratory values (Fig. 5), the first thing one sees is that the values from the Oxford instruments are considerably poorer than those from the other instruments. This is because this instrument was used without standards. The values from the other instruments are more consistent. Looking at the individual values, many sherds correlate very well. Some individual sherds show differences of up to 20% between the two measurements though. These errors must be taken into consideration when evaluating results.

18 See, e.g. Knappett et al. 2011.

19 For the measurement data with the tracer, see Behrendt, Mielke, and Tagle 2012. We would like to take this opportunity to thank Mrs Behrendt very much for making the sherds available for the comparative measurements.

20 See Behrendt, Mielke, and Tagle 2012 on the Tracer and Helfert, Mecking, et al. 2011 on the Niton.

21 See also, e.g., Pessanha, Guilherme, and Carvalho 2009 and Aimers, Farthing, and Shugar 2012 on this.

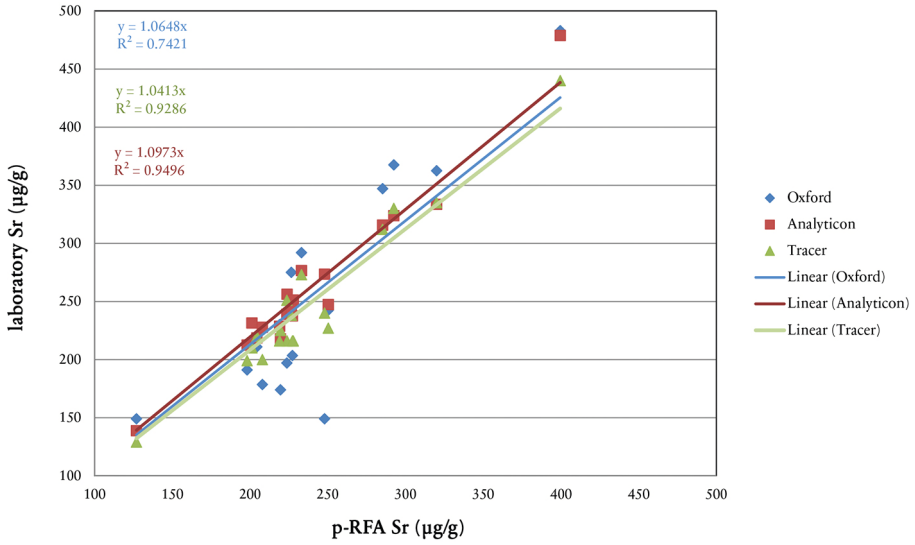

Fig. 5 Comparison of Sr values obtained with the three different pXRF instruments and comparison of these with results from the laboratory analyses.

In order to estimate the errors for interpretation purposes, the measurements from the Tracer and Analyticon instruments were combined within one data set and subjected to a cluster analysis. This allowed the samples to be classified into three large groups. Where the differences between the measurements were minor, both measurement results for the sherds should end up in the same cluster. When the values for all elements were included in the cluster analysis, two of the 19 sherds were classed into two different clusters (10% are classified incorrectly). This means that they were interpreted incorrectly. Reducing the number of elements (here, Zn and Cu are taken out of consideration, because the counting rate is low) the result for the clustering is that four sherds end up in different clusters (20% of the sherds are incorrectly classified). These results make it clear that great care must be taken when carrying out comparisons with data from the literature.

3 Examples for the use of pXRF – possibilities and limitations of pXRF

Apart from these general considerations, it is important to make the comparison with the laboratory data to gain an understanding of the possibilities and limitations of

pXRF.[22] Due to the smaller volumes of samples analyzed, the quality of the pXRF results is inferior to that of the results of the laboratory analysis, the samples for which are homogenized prior to analysis, and thus a larger sample volume is analyzed. In addition, fewer elements are measured with pXRF, and the results for individual elements like copper, for instance, are associated with a higher standard deviation.[23] For the use of pXRF in archaeology, it is important to assess the significance of these errors for the interpretation. Two different projects were selected with the aim of establishing a sound foundation for this assessment with respect to data. For them, sherds were first measured with classic sample preparation.[24] The same samples were then analyzed with the pXRF. Comparing the two series of measurements enables us to assess the possibilities and limitations of pXRF.

3.1 Grey wheel-thrown pottery from Thuringia (Roman imperial period)

To date, three kilns have been excavated in Haarhausen. These three kilns were built using Roman construction methods.[25] Grey wheel-thrown ware was manufactured at the kilns during the Roman imperial period. These pottery forms have been documented at approximately 200 finding sites in Thuringia.[26] Given that only three or four kilns have been found[27] so far, one naturally asks whether these supplied all of Thuringia with pottery or whether other kilns might have contributed to the supply of the area. This additional supply might have come from additional production sites in the Thuringian basin, or pottery may have been imported from neighboring regions. Researchers are using geo-chemical techniques in an effort to answer this question, which represents a classic question for scientific ceramics analysis.[28] Because this and other questions of economic archaeology require the investigation of large numbers of find sites and thus of sherds, pXRF, due to its high sample throughput rate, seems predestined for this task. Frienstedt and Haarhausen, were selected as the finding sites to test the possibilities of pXRF.

For each site, 30 sherds were analyzed using pXRF (double measurements) and using the classic laboratory method. The data from the classic laboratory analysis were evaluated first. In the second step, the pXRF data were subjected to the same type of evaluation. For 67% of the sherds, both methods assigned the sherds to the same

22 See also Speakman et al. 2011 and Aimers, Farthing, and Shugar 2012 on this.
23 See Behrendt, Mielke, and Mecking 2012.
24 For measurement with XRF and ICP-MS, for details on the sample preparation and evaluation, see Mecking 2010a.
25 See Dušek 1992 on this, for more recent literature see Hegewisch 2011.
26 Dušek 1992.
27 Hegewisch 2011.
28 See e.g. Mommsen 2003; Mommsen, Beier, and Kesslering-Poth 1991; Picon, Vichy, and Meille 1971; Rother 1992.

groups.[29] Approximately one third of the sherds were classified incorrectly. Two thirds were classified correctly. However, other, previously investigated sites[30] suggest that approximately one third of the sherds do not come from Haarhausen. Thus, the analysis with pXRF is only useful to a limited extent in the case of the grey wheel-thrown ware. But why is it that not all of the sherds were classified correctly?

The first scientific analyses of ceramics from Haarhausen were undertaken by Schneider and Busch.[31] The pottery production-site finds from Mainfranken, which were manufactured in a similar manner, were also analyzed.[32] The potassium and iron values for the ceramics from Haarhausen are high relative to ceramics from other sites. Using bivariate plots of the elements, potassium and iron, one can easily distinguish between the pottery from Haarhausen and that from Mainfranken (Fig. 6). The average potassium content for the sherds from Eßleben (in Mainfranken) is 3.2%, while the average value for Haarhausen is higher (mean: 4.95% K_2O). There are also differences in the iron content. Haarhausen sherds have an average iron content of 6.8% Fe_2O_3 while the values for the Eßleben sherds are lower, at 5.65% Fe_2O_3. The plot of the Frienstedt values also demonstrates how well these two values lend themselves to distinguishing some sherds from the sherds from Haarhausen (Fig. 7).

While the sherds from Frienstedt fall in the same area as Eßleben, this does not necessarily mean that they originated there. To determine whether that is the case, additional elements must be taken into consideration. However, because Haarhausen sherds have high potassium and iron values, these are important parameters. Assuming that the errors associated with fine ceramics are minor (see section on temper), it should be possible to distinguish between the two groups using pXRF as well. It is interesting to note that this clear separation between the two groups disappears in the plot of the pXRF values for these elements (Fig. 8). What causes this? One can see from the plots that the scattering of the potassium values is greater. The laboratory potassium values were therefore plotted (Fig. 9) against the values measured with pXRF (in this case the mean values obtained from the two measurements). The relative deviations for the pXRF values for potassium in comparison to the classic laboratory analysis are as high as 30%. Since the potassium content differs by about 1.75% (absolute value) between the two groups, it is quite difficult to separate the groups.

To ascertain the reason for this, a portion of the sherds were mapped with a micro XRF analyzer. One can see in the image (Fig. 10) that the distribution of potassium within the sherd is highly inhomogeneous. Similar observations were made with respect to the elements Sr and Rb.[33] In some places potassium is substantially enriched. One can see this in the results from pXRF analyses as well. For this purpose, up to 8

29 See Mecking, Mielke, and Behrendt 2013.
30 See Mecking 2003.
31 Schneider 1992; Busch 1992.
32 Biegert 2002.
33 Mecking, Mielke, and Behrendt 2013.

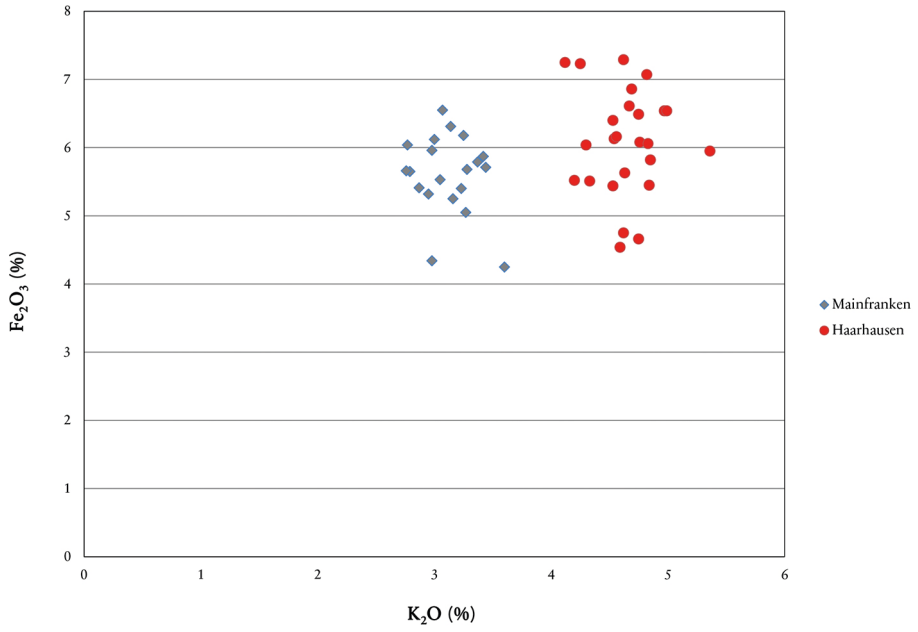

Fig. 6 Potassium vs. iron contents for sherds from Haarhausen Schneider 1992 and Mainfranken Biegert 2002. The measurement values were generated by classic laboratory analyses (WD-XRF).

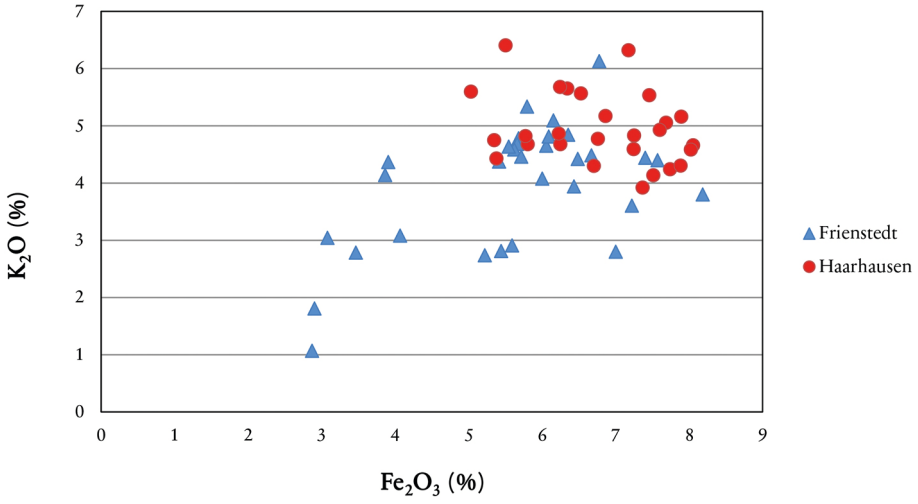

Fig. 7 Potassium vs. iron contents for the sherds from Frienstedt and Haarhausen analyzed with classic laboratory techniques.

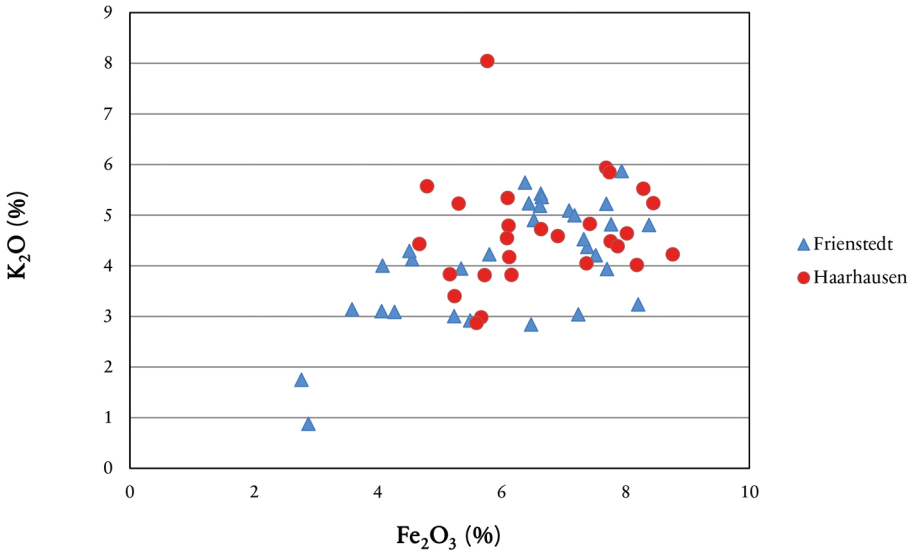

Fig. 8 Potassium vs. iron contents for the sherds from Frienstedt and Haarhausen analyzed with pXRF.

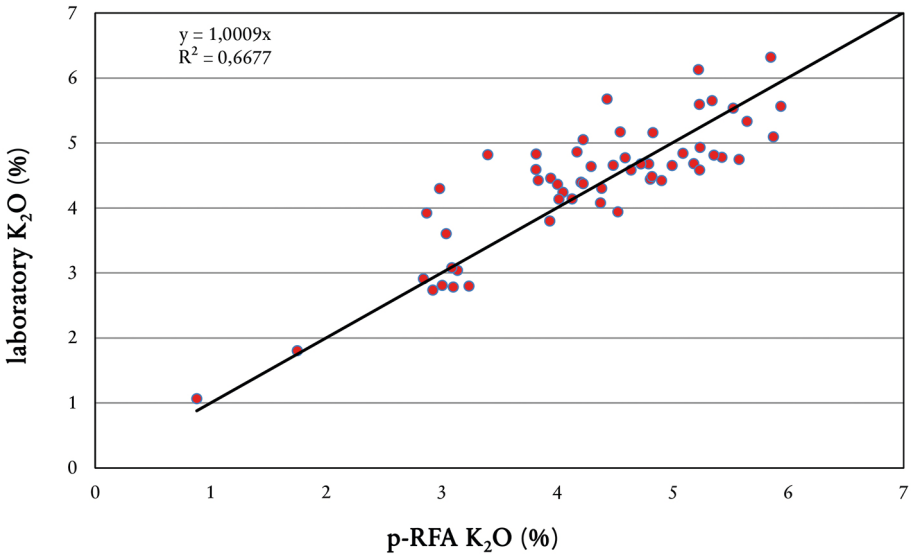

Fig. 9 pXRF potassium values (two measurements per sherd) vs. laboratory potassium data for the analyzed sherds from Frienstedt and Haarhausen.

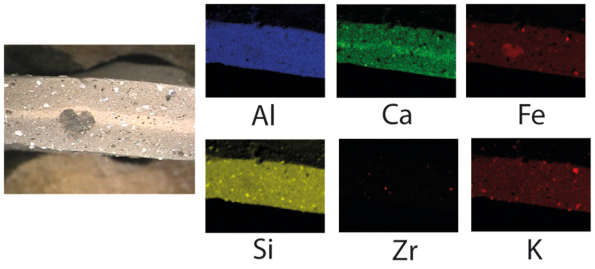

Fig. 10 Element distribution for a sherd from Haarhausen (Ker 634).

different measuring spots on a single sherd were analyzed with the pXRF instrument. In the case of sherd Ker 634, for instance, the first five pXRF results yielded K_2O values between 4.1 and 4.4%. The final three measurements yielded values of 3.7, 3.2 and 2.5% K_2O however. This explains why the values differ so greatly. Which spot on a sherd is measured is a matter of chance, and thus so too is the mean value that results. This is why the potassium values for the grey wheel-thrown pottery are so difficult to interpret. This can occur in connection with other elements at other finding sites.[34]

If the poor recovery rates are due to inhomogeneities in the ceramics, then performing analyses at more sites should improve the results. To test this hypothesis, a set of sherds were analyzed once again. This time pXRF measurements were taken at up to six different sites on each sherd. Mean values were calculated from the results. This changes the values for potassium and iron significantly. One sees this when one generates the R^2 values for the regression lines for the laboratory values and the pXRF measurements. In the case of the 6-measurement analyses, the R^2 values are 0.90 for iron and 0.84 for potassium. With fewer measurements, these values are lower. The bivariate plot of the elements potassium and iron shows that increasing the number of measurement points considerably improved the result. In the case of the double measurements, the information provided by the plot is of only limited significance. In the case of the results from measuring at different measuring spots, pXRF was able to reproduce the picture provided by the laboratory analysis relatively well (Fig. 11).

The results revealed that the influence on the potassium content was greatest in connection with high concentrations. With lower percentages, the double measurements fit better with the laboratory measurements than they did in the case of higher percentages. The cause for the poor reproducibility of the results of classic laboratory analyses using pXRF was therefore the uneven distribution of the elements within the sherds. One can compensate for this problem by increasing the number of pXRF analyses but doing so leads to a decrease in the number of sherds measured in a given period.

34 Speakman et al. 2011 have already pointed out the problems associated with inhomogeneities.

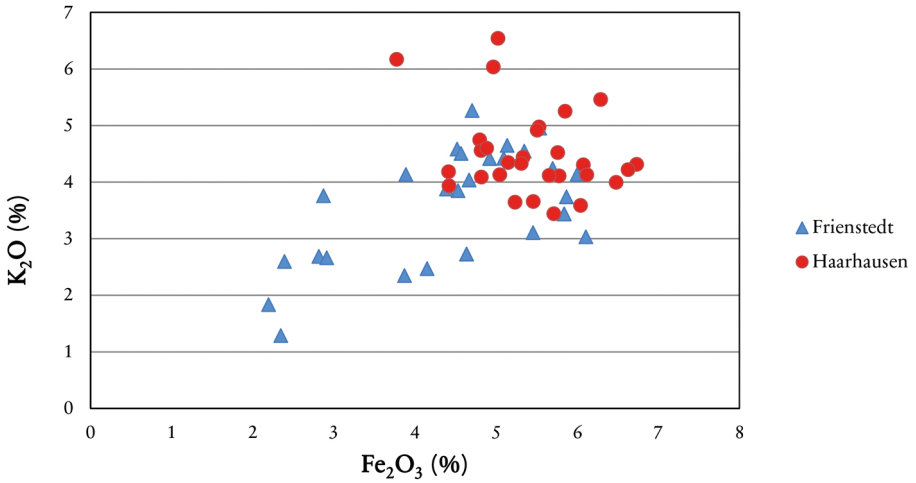

Fig. 11 Potassium vs. iron content from the pXRF measurements (up to six measurement spots per sherd) for the sherds from Haarhausen and Frienstedt.

3.2 Eythra

In a further series, samples from the Neolithic site Eythra[35] were analyzed. These were first investigated using classic laboratory methods. A total of 42 elements were measured using XRF (Na, Mg, Al, Si, P, S, K, Ca, Ti, Mn, Fe, Sr, Rb and Zr) and ICP-MS (Ba, Ce, Co, Cr, Cs, Cu, Dy, Er, Eu, Ga, Gd, Ho, La, Li, Lu, Nd, Ni, Pb, Sc, Sm, Tb, Th, Tm, U, V, Y, Yb, and Zn).[36] The first series of samples incorporated samples from the earliest and earlier linear ware (LBK). In further analyses, younger sherds were analyzed, with the youngest in the series representing stroke-ornamented ware (STK). The aim of the analyses was to capture changes in technique and/or clay recipes at one site over a longer period. The findings would then be correlated with the archaeological findings to understand whether technological change was associated with cultural, or whether the two kinds of change occurred independently of one another. For instance, the analyses were able to show that in the earliest and earlier LBK the proportion of iron-containing temper particles decreased over this period.[37] In addition, the trace element pattern revealed different clay recipes: it was possible to identify 10 clusters with the help of cluster analyses performed on the results from the classic laboratory analyses. The clusters were verified by a discriminant analysis of the clusters, taking

35 The sherds are analyzed in a collaboration within the framework of the DFG project "Eythra" between the University of Leipzig and the Saxony State Office for Archaeology. For details on the site see Cladders et al. 2012.

36 See Mecking, Behrendt, et al. 2012.

37 Mecking, Mielke, and Behrendt 2013.

measurement error into account. Two of the clusters, which encompassed a total of 11 sherds, contained only finds of the earliest LBK. Most of the other clusters contained samples of both the earliest and earlier LBK. Based on these analyses, one can conclude that the clay recipes changed to some extent over time, despite continuity of settlement. An attempt was made to reproduce these results using pXRF. The fact that some of the pottery was coarsely tempered posed an additional complication for the pXRF analysis. Measurements were taken at 2 or more sites per sherd for the pXRF analysis. A cluster analysis was performed with the mean values from these measurements. It was not possible to distinguish the clusters identified in the laboratory data. The cluster analysis of the laboratory data identified two clusters that contained only sherds of the earliest LBK, on the basis of the pXRF data, these sherds were distributed among various clusters which also contained sherds of the earlier LBK. Thus, the evaluation of the pXRF data generated a result completely different from that obtained in the classic laboratory analyses.

3.3 Summary of the comparison of p-RXF analysis with laboratory analysis

Why does pXRF work very well in some cases and more poorly in others? pXRF is more limited with respect to the selection of elements in comparison to laboratory analysis. In addition, the scattering of measured values is greater in pXRF than is the case with lab analysis. Moreover, scattering of the values increases with increasing size of the temper particles; and the pXRF results are more sensitive to the non-homogeneous distribution of elements within the sherd, which naturally has an influence on the results and their interpretation. Kuleff and Djingova noted the following with regard to a sufficient number of elements for the statistical analysis:

> These principles encourage the specialists working in the field of provenance study of pottery to increase continuously the number of determined elements. The justification of this approach was determined by Hartbottle (1991) who proved that at less than 10 elements the probability for misclassification increases significantly. Usually nowadays it is accepted that for a representative classification of archaeological ceramics about 20–25 elements should be determined. (Some authors suggest at least 15 elements see Schneider, 1993).[38]

Since pXRF can measure up to 14 elements but can yield large errors in the case of some elements present in small amounts, it is evident that the use of these instruments is not sufficient to clarify all of these issues. pXRF is best used in contexts where the

38 Kuleff and Djingova 1996, 61; Hartbottle 1991; Schneider 1993.

geochemical differences are easily identified. An example for this might be the Roman imperial period grey wheel-thrown ware in Thuringia. Other authors have reached this same conclusion. Speakman et al., for instance, describe the analysis of Mimbres and Jornada pottery from the American Southwest with INAA and pXRF in this way.[39] It was possible to separate out several groups with the pXRF. Certain subgroups could be better distinguished in bivariate plots of elements with INAA thanks to the greater precision and additional elements.[40] Another example from the literature is the analysis of the Phoenician pottery from Spain.[41] In this case, four regional groups were identified using NAA. The same sherds were then measured with pXRF. The regional groups found with NAA could be distinguished in the pXRF data at a rate of 78 and 100%. The greater the geochemical similarity between clay recipes, the greater the error associated with the results, as in the case with Eythra, for instance. The difficulty with the Eythra sherds is exacerbated by the fact that some of the sherds contain tempers of very large diameter, increasing the measurement error. This shows one limitation associated with pXRF: it cannot reliably distinguish between geochemically similar clays.

Researchers should certainly ascertain how many measurements on the sherds are required in order to obtain reproducible results before performing the measurements (see example of grey wheel-thrown ware). This can best be done by taking several measurements of a certain number of sherds. In the case of coarse pottery, the temper can cause values to vary to a greater degree. This can cause problems when it is necessary distinguish among groups of greater geochemical similarity. In connection with any measurements though, researchers should bear in mind that 0 to 30% of individual sherds may be classified incorrectly. Ideally therefore, a selection of the sherds should first be analyzed to ascertain whether and how pXRF might be useful. Using the data from the smaller series, one could assess the quality of the data that a larger series would be expected to produce. It is clear from the discussion above that pXRF analyses demand both analytical and in-depth geo-chemical knowledge.

39 Speakman et al. 2011.

40 Speakman et al. 2011, fig. 6.

41 Behrendt, Mielke, and Mecking 2012; Behrendt, Mielke, and Tagle 2012; Mecking, Mielke, and Behrendt 2013.

Bibliography

Aimers, Farthing, and Shugar 2012
Jim J. Aimers, Doris J. Farthing, and Aaron N. Shugar. "Handheld XRF Analysis of Maja Ceramics. A Pilot Study Presenting Issues Related to Quantifiacation and Calibration." In *Handheld XRF for Art and Archaeology*. Ed. by A. N. Shugar and J. L. Mass. Studies in Archaeological Scienes 3. Leuven: Leuven University Press, 2012, 423–448.

Behrendt, Mielke, and Mecking 2012
Sonja Behrendt, Dirk Paul Mielke, and Oliver Mecking. "Die portable Röntgenfluoreszenzanalyse (p-RFA) in der Keramikforschung. Grundlagen und Potenzial." *Restaurierung und Archäologie* 5 (2012), 93–110.

Behrendt, Mielke, and Tagle 2012
Sonja Behrendt, Dirk Paul Mielke, and Roald Tagle. "Provenienzanalysen im Vergleich. Neue Wege zur archäometrischen Untersuchung phönizischer Keramik." *Madrider Mitteilungen* 53 (2012), 187–219.

Biegert 2002
Susanne Biegert. "Analysen lokaler grauer Drehscheibenkeramik aus Unterfranken und Thüringen." *Bayrische Vorgeschichtsblätter* 67 (2002), 113–115.

Busch 1992
Helmut Busch. "Chemische Analysen und Brenntemperaturbestimmungen grauer Drehscheibenkeramik aus Thüringer Fundorten." In *Römische Handwerker im germanischen Thüringen*. Ed. by S. Dušek. Weimarer Monographien zur Ur- und Frühgeschichte 27. Stuttgart: Theiss, 1992, 166–170.

Cladders et al. 2012
Maria Cladders, Harald Stäuble, Thomas Tischendorf, and Sabine Wolfram. "Zur linen- und stichbandkeramischen Besiedlung von Eythra, Lkr. Leipzig." In *Siedlungstrukturen und Kulturwandel in der Bandkeramik*. Ed. by R. Smolnik. Arbeits- und Forschungsberichte zur sächsischen Bodendenkmalpflege, Beiheft 25. Dresden: Landesamt für Archäologie, 2012, 146–159.

Curet 1997
L. Antonio Curet. "Technological Changes in Prehistoric Ceramics from Eastern Puerto Rico. An Exploratory Study." *Journal of Archaeological Science* 24 (1997), 497–504.

Daszkiewicz and Schneider 2011
Małgorzata Daszkiewicz and Gerwulf Schneider. "Archäokeramische Klassifizierung am Beispiel kaiserzeitlicher Drehscheibenkeramik aus Brandenburg." *Bonner Beiträge zur vor- und frühgeschichtlichen Archäologie* 13 (2011), 17–33.

Daszkiewicz, Schneider, and Bobryk 2008
Małgorzata Daszkiewicz, Gerwulf Schneider, and Ewa Bobryk. "Archäokeramologische Untersuchungen an endneolithischer Keramik aus Wattendorf und Voitmannsdorf." In *Endneolithische Siedlungsstrukturen in Oberfranken II-Wattendorf-Motzenstein. Eine schnurkeramische Siedlung auf der Nördlichen Frankenalb*. Ed. by J. Müller and T. Seregély. Universitätsforschungen zur prähistorischen Archäologie 155. Bonn: Habelt, 2008, 69–84.

Dušek 1992
Sigrid Dušek. *Römische Handwerker im germanischen Thüringen*. Stuttgart: Konrad Theiss, 1992.

C. Flügel, Joachimski, and E. Flügel 1997
Christof Flügel, Michael Joachimski, and Erik Flügel. "Römische Keramik mit Mamormagerung. Herkunftsbestimmung mit Hilfe von stabilen Isotopen (Auerbergtöpfe aus Süddeutschland)." *Archäologisches Korrespondenzblatt* 27 (1997), 265–284.

Forster et al. 2011
Nicola Forster, Peter Grave, Nancy Vickery, and Lisa Kealhofer. "Nondestructive Analysis Using PXRF. Methodology and Application to Archaeological Ceramics." *X-Ray Spectrometry* 40 (2011), 389–398.

Hartbottle 1991
German Hartbottle. "The Efficiencies and Error-Rates of Euclidean and Mahalanobis Searches in Hypergeometries Ceramic Composition." In *Proceedings of the 27th Symposium on Archaeometry*. Ed. by E. Pernicka and G. Wagner. Basel: Birkhaeuser Verlag, 1991, 413–424.

Hegewisch 2011
Morten Hegewisch. "Zur Drehscheibenkeramik im Westen der Germania Magna. Anfänge, Weiterentwicklung und Verbreitung." *Bonner Beiträge zur vor- und frühgeschichtlichen Archäologie* 13 (2011), 119–174.

Helfert and Böhme 2010
Markus Helfert and Dieter Böhme. "Herkunftsbestimmung von römischer Keramik mittels portabler energiedispersiver Röntgenfluoreszenzanalyse (p-ED-RFA). Erste Ergebnisse einer anwendungsbezogenen Teststudie." In *Naturwissenschaftliche Analysen vor- und frühgeschichtlicher Keramik I. Methoden, Anwendungsbereiche, Auswertungsmöglichkeiten*. Ed. by B. Ramminger, O. Stilborg, and M. Helfert. Universitätsforschungen zur prähistorischen Archäologie 176. Bonn: Habelt, 2010, 11–30.

Helfert, Mecking, et al. 2011
Markus Helfert, Oliver Mecking, Franziska Lang, and Hans-Markus von Kaenel. "Neue Perspektiven für die Keramikanalytik. Zur Evaluation der portablen energiedispersiven Röntgenfluoreszenzanalyse (P-ED-RFA) als neues Verfahren für die geochemische Analyse von Keramik in der Archäologie." *Frankfurter elektronische Rundschau zur Altertumskunde* 14 (2011), 1–30.

Ikeoka et al. 2012
Renato A. Ikeoka, Carlos R. Appoloni, Paulo S. Parreira, Fábio Lopes, and Arkley M. Bandeira. "PXRF and Multivariate Statistics Analysis of Pre-Colonial Pottery from Northeast of Brazil." *X-Ray Spectrometry* 41 (2012), 12–15.

Kalm 1996
Volli Kalm. "X-Ray Diffraction Analysis of Neolithic Ceramics. An Example from the Narva Area, South-Eastern Coast of the Gulf of Finland." *PACT* 51 (1996), 385–396.

Knappett et al. 2011
Carl Knappett, Duncan Pirrie, Matthew R. Power, Irene Nikolakopoulou, Jill Hildtich, and Gavyn K. Rollinson. "Mineralogical Analysis and Provenancing of Ancient Ceramics Using Automated SEM-EDS Analysis." *Journal of Archaeological Science* 38 (2011), 219–232.

Kuleff and Djingova 1996
Ivelin Kuleff and Rumiana Djingova. "Provenance Study of Pottery. Choice of Elements to be Determined." *Revue d'Árcheometrie* 20 (1996), 57–67.

Liritzis and Zacharias 2011
Ioannis Liritzis and Nikolaos Zacharias. "Portable XRF of Archaeological Artifacts. Current Research, Potentials and Limitations." In *X-Ray Fluorescence Spectrometry (XRF) in Geoarchaeology*. Ed. by M. S. Shackley. New York: Springer, 2011, 109–142.

Mecking 2003
Oliver Mecking. "Herkunftsbestimmung an grauer Drehscheibenkeramik des 3. Jahrhunderts aus Thüringen." In *Archäometrie und Denkmalpflege. Kurzberichte 2003*. Ed. by O. Hahn, C. Goedicke, R. Fuchs, and I. Horn. Berlin: Deutsche Mineralogische Gesellschaft, 2003, 43–45.

Mecking 2010a
Oliver Mecking. "Die Rekonstruktion der Goldschmiedetechniken aufgrund der chemischen Analytik." In *Der Schatzfund. Analysen – Herstellungstechniken – Rekonstruktion*. Ed. by S. Ostritz. Die mittelalterliche jüdische Kultur in Erfurt 2. Langenweißbach: Beier & Beran, 2010, 10–225.

Mecking 2010b
Oliver Mecking. "Naturwissenschaftliche Untersuchungen eines Töpferofens der Bernburger Kultur aus Erfurt-Gispersleben." In *Naturwissenschaftliche Analysen vor- und frühgeschichtlicher Keramik I. Methoden, Anwendungsbereiche, Auswertungsmöglichkeiten*. Ed. by B. Ramminger, O. Stilborg, and M. Helfert. Universitätsforschungen zur prähistorischen Archäologie 176. Bonn: Habelt, 2010, 117–126.

Mecking, Behrendt, et al. 2012
Oliver Mecking, Sonja Behrendt, Isabel Hohle, and Sabine Wolfram. "Geochemische und technologische Keramikanalysen zum Übergang von ältester zu älterer Linienbandkeramik in Eythra und Zwenkau-Nord, Lkr. Leipzig." In *Siedlungsstrukturen und Kulturwandel in der Bandkeramik*. Ed. by R. Smolnik. Arbeits- und Forschungsberichte zur sächsischen Bodendenkmalpflege, Beiheft 25. Dresden: Landesamt für Archäologie, 2012, 261–273.

Mecking, Mielke, and Behrendt 2013
Oliver Mecking, Dirk Paul Mielke, and Sonja Behrendt. "Anwendungsbeispiele und Grundlagen der portablen Röntgenfloureszenzanalyse (P-RFA) in der Keramikforschung." In *Naturwissenschaftliche Analysen vor- und frühgeschichtlicher Keramik III. Methoden, Anwendungsbereiche, Auswertungsmöglichkeiten*. Ed. by B. Ramminger, O. Stilborg, and M. Helfert. Universitätsforschungen zur prähistorischen Archäologie 238. Bonn: Habelt, 2013, 49–67.

Mommsen 2003
Hans Mommsen. "Attic Pottery Production, Imports and Export during the Mycenaean Period by Neutron Activation Analysis." *Mediterranean Archaeology and Archaeometry* 3 (2003), 13–30.

Mommsen, Beier, and Kesslering-Poth 1991
Hans Mommsen, Thomas Beier, and Lydia Kesslering-Poth. "Neutronenaktivierungsanalyse von Scherben aus einem Töpferofen aus der Geburtsstunde Bonns." *Archaeo-Physika* 12.2 (1991), 367–382.

Morgenstein and Redmount 2006
Maury Morgenstein and Carol A. Redmount. "Redmount, Using Portable Energy Dispersive X-Ray Fluorescence (EDXRF) Analysis for On-Site Study of Ceramic Sherds at El Hibeh, Egypt." *Journal of Archaeological Science* 32 (2006), 1613–1623.

Pessanha, Guilherme, and Carvalho 2009
Sofia Pessanha, Ana Guilherme, and Maria L. Carvalho. "Comparison of Matrix Effects on Portable and Stationary XRF Spectrometers for Cultural Heritage Samples." *Applied Physics A Material Science and Processing* 97 (2009), 497–505.

Picon, Vichy, and Meille 1971
Maurice Picon, Michèle Vichy, and Eliane Meille. "Composition of the Lezoux, Lyon and Arezzo Samaian Ware." *Archaeometry* 13.2 (1971), 191–208.

Potts, Williams-Thorpe, and Webb 1997
Philip J. Potts, Olwen Williams-Thorpe, and Peter C. Webb. "The Bulk Analysis of Silicate Rocks by Portable X-Ray Fluorescence. Effect of Sample Mineralogy in Relation to the Size of the Excited Volume." *Geostandard Newsletter* 22 (1997), 29–41.

Rother 1992
Anette Rother. "Ergebnisse der chemischen Analyse von Steinzeug aus dem Rheinland." *Berliner Beiträge zur Archäometrie* 11 (1992), 123–136.

Schneider 1992
Gerwulf Schneider. "Chemische Zusammensetzung von Keramik aus Haarhausen." In *Römische Handwerker im germanischen Thüringen*. Ed. by S. Dušek. Weimarer Monographien zur Ur- und Frühgeschichte 27. Stuttgart: Konrad Theiss, 1992, 171–174.

Schneider 1993
Gerwulf Schneider. "X-Ray Fluorescence Analysis and the Production and Distribution of Terra Sigillata and Firmalampen." In *X-Ray Fluorescence Analysis and the Production and Distribution of Terra Sigillata and Firmalampen*. Ed. by W.V. Harris. Journal of Roman Archaeology, Suppl. Ser. 6. 1993, 129–137.

Schneider et al. 1989
Gerwulf Schneider, Andreas Burmeister, Christian Goedicke, Hans W. Heinnicke, Barbara Kleimann, Heinz Knoll, Marino Maggetti, and Rolf Rottländer. "Naturwissenschaftliche Kriterien und Verfahren zur Beschreibung von Keramik." *Acta praehistorica et archaeologica* 21 (1989), 7–39.

Speakman et al. 2011
Robert J. Speakman, Nicole C. Little, Darrell Creel, Myles R. Miller, and Javier G. Inanez. "Sourcing Ceramics with Portable XRF Spectrometers? A Comparison with INAA Using Mimbres Pottery from the American Southwest." *Journal of Archaeological Science* 38 (2011), 3483–3496.

Stern 1995
Willem Stern. "On Non-Destructive Analysis of Gold Objects." In *Prehistoric Gold in Europe. Mines, Metallurgy, and Manufacture*. Ed. by G. Morteani and J. Northover. NATO ASI Series. Series E, Applied Sciences 280. Dordrecht and Boston: Kluwer Academic, 1995, 317–328.

Töchterle et al. 2013
Ulrike Töchterle, Gert Goldenberg, Philipp Schneider, and Peter Tropper. "Spätbronzezeitliche Verhüttungsdüsen aus dem Bergbaurevier Mauken im Unterinntal, Nordtirol. Typologie, mineralogische-petragraphische Zusammensetzung und experimentelle Rekonstruktionsversuche." *Der Anschnitt* 65 (2013), 2–19.

Wieckhorst 1995
Thomas Wieckhorst. "Analytische Untersuchungen an glasierten Keramiken der frühen Neuzeit." *Berliner Beiträge zur Archäometrie* 13 (1995), 125–206.

Illustration and table credits

ILLUSTRATIONS: 1–11 O. Mecking.

TABLES: 1–4 O. Mecking.

OLIVER MECKING

Oliver Mecking studied chemistry and pre- and early history in Kiel (1990–1996). In 2000, he completed his dissertation in the field of chemistry on the topic of archaeological ceramics under the supervision of Prof. Dr. Dr. h.c. Lagaly. Since then, he has headed the archaeometry laboratory of the Thüringisches Landesamt für Denkmalpflege und Archäologie in Weimar and carried out archaeometry projects on ceramics, glasses, non-ferrous and precious metals, technical ceramics, soil samples and cements.

Dr. Oliver Mecking
Thüringisches Landesamt für Denkmalpflege und Archäologie
Archäometrielabor
Humboldtstraße 11
99423 Weimar, Germany
E-mail: oliver.mecking@tlda.thueringen.de

Anno Hein

Revisiting the Groups – Exploring the Feasibility of Portable EDXRF in Provenance Studies of Transport Amphorae in the Eastern Aegean

Summary

This research investigates the applicability of portable energy dispersive X-ray fluorescence (pXRF) analysis for provenance studies of ceramics. The approach is tested on Hellenistic transport amphorae from the Eastern Aegean which were already analyzed by neutron activation analysis (NAA). The results from the two methods are compared for accuracy, reproducibility, and their ability to provide a basis for chemical classification. The study shows that pXRF should be used as complementary tool, rather than as a replacement for laboratory techniques. Suitable for a large number of non-invasive measurements, it can be applied for initial surveys of assemblages to select samples for further investigation and to classify further material based on reference material classified by NAA.

Keywords: NAA; pXRF; accuracy; reproducibility; transport amphorae; Eastern Aegean

In der vorliegenden Studie wird die Anwendbarkeit von pRFA in Provenienzstudien archäologischer Keramik untersucht. Die Vorgehensweise wird an Fragmenten hellenistischer Transportamphoren aus der Ost-Ägäis getestet, die bereits mit Neutronenaktivierungsanalyse (NAA) untersucht wurden. Die Ergebnisse beider Methoden werden verglichen bezüglich Genauigkeit, Reproduzierbarkeit und als mögliche Grundlage zur chemischen Klassifizierung. Laut der Studie sollte pRFA als komplementäre Methode benutzt werden, nicht als Ersatz für genauere Laboranalysen. Geeignet für eine große Zahl nicht-invasiver Messungen, kann die Methode angewendet werden, um nach der ersten Begutachtung einer Probensammlung geeignete Stücke für weitergehende Laboranalysen auszuwählen und bereits mit NAA klassifizierte Referenzproben weiter zu bestimmen.

Keywords: NAA; pRFA; Genauigkeit; Reproduzierbarkeit; Transportamphoren; Ost-Ägäis

Morten Hegewisch, Małgorzata Daszkiewicz und Gerwulf Schneider (eds.) | Using pXRF for the Analysis of Ancient Pottery – an Expert Workshop in Berlin 2014 | Berlin Studies of the Ancient World 75 (ISBN TODO; DOI: 10.17171/3-75) | www.edition-topoi.org

1 Introduction

Since the first case studies more than 50 years ago[1] it has been demonstrated that the chemical examination of archaeological ceramics can contribute substantially to the understanding of production, dissemination and trade of specific ceramic wares. Basis of the chemical approach in ceramic provenance studies is the assumption that ceramics from particular production places present characteristic chemical patterns which can be distinguished from other production places. The diverse raw materials used in the fabrication of ceramics are certainly the main reason of the feasibility of this approach. In general it can be assumed that chemical differences between different natural sources exceed differences observed within a given source, which is expressed in the 'Provenience postulate'.[2] Therefore, in the case that different clays or clay pastes were used for their fabrication ceramics should be distinguishable on the basis of their chemical composition. However, the natural variation of the used raw materials is interfered by the variation of the clay paste preparation if for example different components were mixed or if raw materials were refined.

Apart from clay selection and preparation also the analytical method, or more specifically its analytical uncertainty, contributes to the chemical variation within an examined assemblage of ceramics, which eventually can obscure actual differences between different ceramic wares. For this reason commonly methods with high analytical precision are preferred, such as neutron activation analysis (NAA), inductively coupled plasma mass spectroscopy (ICPMS) or wavelength dispersive X-ray fluorescence (WD-XRF). Additionally, in view of comparability of different studies the accuracy of the applied method, i.e. the closeness to the real values, should be considered. Provided sufficient long-term precision, standard reference materials can be used to monitor accuracy and to calibrate different methods in order to compare results.[3] In this way reference databases can be established comprising characteristic chemical patterns for production sites and ceramic ware groups which new results can be compared to.[4] Another aspect for the selection of a suitable method for ceramic analysis is the element suite which is covered by the analysis. Basically, as many element concentrations as possible should be measured in order to find significant differences between chemical patterns. Due to geochemical constraints and chemical alterations during ceramic production and after deposition, however, certain elements appear to be more meaningful than others. Particularly minor and trace elements proved to be generally more significant for studying provenance while major elements provide rather information about technological choice of the potter.

1 Sayre and Dodson 1957; Catling, Blin-Stoyle, and Richards 1961.
2 Weigand, Harbottle, and Sayre 1977.
3 Hein, Tsolakidou, et al. 2002.
4 Hein and Kilikoglou 2012.

Hence, under purely analytical considerations the above mentioned laboratory based methods appear to be definitely eligible for ceramic analyses. They require, however, sampling of the material. On the other hand when dealing with archaeological objects usually non-invasive approaches are preferred, which can be applied optionally also on-site. Therefore, during the recent years portable and non-destructive methods, such as handheld or bench top energy dispersive XRF (EDXRF), gained in importance in archaeological science in general[5] and also in studies of archaeological ceramics in particular.[6] Apart from the sample integrity the portable EDXRF offers also faster measurements which in connection with the omission of sample preparation allow for considerably larger numbers of objects to be examined. This might compensate up to some extent for analytical restraints of the method.

The present study was initiated in order to test the feasibilities and limits of the application of portable EDXRF (pEDXRF) in provenance studies of archaeological ceramics. Therefore, fragments of a sufficiently well-known ceramic ware, East Aegean Hellenistic transport amphorae, a part of which already had been analysed with NAA, were examined with pEDXRF and the results were statistically evaluated. Scope of this feasibility study was to explore up to which extent pEDXRF can be integrated in ceramic provenance studies and whether it can provide additional information.

1.1 Transport amphorae

The material selected for the present feasibility study was an assemblage of transport amphorae from the islands of Kos and Rhodes. During the Hellenistic and Roman period both islands were major producers of wine, which was traded and consumed in the whole Mediterranean Region and beyond.[7] The wine was transported in amphorae which were supposedly fabricated close to the places where it was cultivated. These amphorae were mass products with a high level of standardization as they had to fulfill specific functions and at the same time they had to represent their content. Characteristic design features of the transport amphorae indicated the provenance of the wine. Therefore, Koan and Rhodian amphorae are basically quite easily to distinguish. Nevertheless the study of the chemical variation of these specific amphora types reveals information about the organization of their production and its development over time.

Apart from the archaeological question there were also other reasons to select wine amphorae for this feasibility study. As transport containers for liquids they present commonly a comparably fine and homogeneous fabric. On the other hand their bodies are sufficiently thick so that pEDXRF can be applied on sections or on breaks of body sherds

5 Shugar and Mass 2012.

6 Goren, Mommsen, and Klinger 2011; Speakman et al. 2011; Hunt and Speakman 2015.

7 Empereur and Hesnard 1987.

without the use of an additional collimator reducing the size of the measurement spot. Finally, usually no elaborate surface treatment is observed so that even surface measurements can provide information about the ceramic body.

2 Analytical methods

2.1 pEDXRF

The pEDXRF measurements were carried out using a NITON XL3t GOLDD+ handheld system. For the present study the preset methods 'mining' and 'soil' were tested, both suitable for ceramic analyses. However, the results which will be presented here were obtained in 'soil' mode because this method provides a larger suite of trace elements. The life time of the measurement, which was carried out in air, was 120 seconds for each sample measuring in three energy ranges. For the measurement the system was fixed in a stand so that the sample could be placed from above. The measurement area had an estimated diameter of c. 6 millimeters and a photograph of each area was recorded with the integrated camera.

2.2 NAA and WDXRF

The statistical evaluation of the results was compared with NAA results concerning the same material (Tab. 1). The NAA was carried out at N.C.S.R. "Demokritos" and the Missouri University Research Reactor, respectively. In both cases samples of c. 100 to 130 milligram were powdered and irradiated together with standard reference materials. In a period of one until three weeks after irradiation γ-spectra of the samples were recorded in order to estimate concentrations of 25 to 30 elements.[8] Apart from NAA also WDXRF was included in the study mainly for a comparison of measurements and an assessment of the analytical performance of the pEDXRF. Therefore, the Bruker S8 Tiger system at the Fitch Laboratory at the British School at Athens was used.[9]

3 Results and discussion

3.1 Accuracy

In order to estimate the accuracy of the pEDXRF a powdered and homogenized sample of calcareous clay from Attica was measured which had been analysed by NAA and by

8 Kilikoglou et al. 2007.

9 Georgakopoulou et al. 2017.

	$NAA_{Demokritos}$		$WD\text{-}XRF_{Fitch}$		$pEDXRF_{Demokritos}$	
	mean	σ in %	mean	σ in %	value	error in %
As	30.5	1.3			32.4	12
Ba	214	10	226	5.5	174	23
$Ca_{\%}$	10.7	1.7	10.6	0.4	11.4	0.6
Ce	73.7	2.1	66	5.1		
Co	24.6	3.6	23	4.5	—— *<LOD* ——	
Cr	137	1.8	158	6.7	151	16
Cs	6.36	2.6			—— *<LOD* ——	
Cu			50	2.8	46	22
Eu	1.54	2.0				
$Fe_{\%}$	4.90	1.6	4.88	0.5	4.30	0.5
Hf	4.70	4.6				
$K_{\%}$	1.55	11	1.59	0.4	1.86	2.1
La	39.2	1.3	38	7.7		
Lu	0.44	2.6				
Mn			785	0.6	625	7.6
$Na_{\%}$	0.60	1.9	0.58	2.6		
Nd	39.2	19	34	15		
Ni	127	17	133	18	111	15
Pb			37	8.0	31	13
Rb	98	3.3	88	1.3	90	3.3
Sb	1.81	4.0			—— *<LOD* ——	
Sc	17.6	1.5			220	34
Sm	7.06	1.7				
Sr			109	1.1	103	2.5
Ta	1.22	4.6				
Tb	0.85	6.1				
Th	10.9	1.8	9	12	7.7	30
$Ti_{\%}$	0.22	2.4	0.46	0.9	0.42	2.8
U	2.73	5.2			—— *<LOD* ——	
V			120	4.7	104	26
Yb	3.75	5.2				
Zn	124	4.6	110	1.1	108	7.0
Zr	192	14	162	2.4	166	2.0

Tab. 1 Element concentrations in a homogenized calcareous clay from Attica measured with NAA, WDXRF and pEDXRF: The concentrations are given in ppm except for those of Ca, Fe, K, Na and Ti, which are given in wt%. Not listed are further major elements, which were measured by WDXRF and which are also measured by pEDXRF if the 'mining' is used. The standard deviation for NAA and WDXRF is based on replicate measurements while the experimental error for pEDXRF was provided by the system.

WDXRF before. In Tab. 1 the results of the pEDXRF measurement are compared with results of replicate measurements with NAA and WDXRF. The pEDXRF expectedly does not reach the level of precision of the two other methods. Nevertheless, the estimated values are sufficiently close to the other measurements even for element concentrations down to the tens of ppm level. Only the scandium concentration presents an obvious discrepancy with the assumed real value. However, due to the quite large analytical error a calibration towards other methods, in view of potentially making use of reference databases, appears to be inapplicable at the present stage.

3.2 Reproducibility

Before examining the chemical variability of the studied amphorae on the basis of pEDXRF analyses the reproducibility of the method was assessed by replicate measurements. In order to exclude any effect of the sample geometry first eleven ceramic disks were used which had been cut out of large body sherds and had been polished afterwards in order to obtain completely flat surfaces. The disks, which had a diameter of 30 millimeter and a thickness of c. 5 to 6 millimeters, had been actually prepared for material tests of the ceramics. Each disk was measured in three different arbitrarily selected areas. For the statistical evaluation 16 elements are used: Ba, Ca, Cr, Cs, Cu, Fe, K, Mn, Ni, Pb, Rb, Sr, Ti, V, Zn and Zr. Most other element concentrations potentially determined by the method are below the limit of detection for the majority of the samples, apart from As, Sc, Th and U. Sc is excluded though because of the observed discrepancy from the real value and As because of its known high variation in fired ceramics. The Th and U concentration eventually are apparently quite close to the limit of detection and in several cases below the limit of detection. Therefore a large experimental error can be expected.[10]

For the statistical evaluation the total variation of the data has been determined.[11] The total variation 1.80 though is expectedly quite high as material from different production places is considered. The largest variation is contributed by Cr, Ni and Ca. For hierarchical cluster analysis (Fig. 1), the data have been log ratio transformed using the Zn concentration as common divisor as it presents the lowest variation. In the case of the Rhodian samples indeed with one exception each sample triple forms a cluster which can be clearly distinguished from triples of the other samples. Only in the case of Sample RHO A674 one measurement appears to present a different composition compared to the other two. A closer inspection of the results reveals that this discrepancy is caused mainly by a high potassium concentration measured in the respective area, possibly due

10 Behrendt, Mielke, and Mecking 2012.

11 Aitchinson 1986; Buxeda i Garrigos and Kilikoglou 2001.

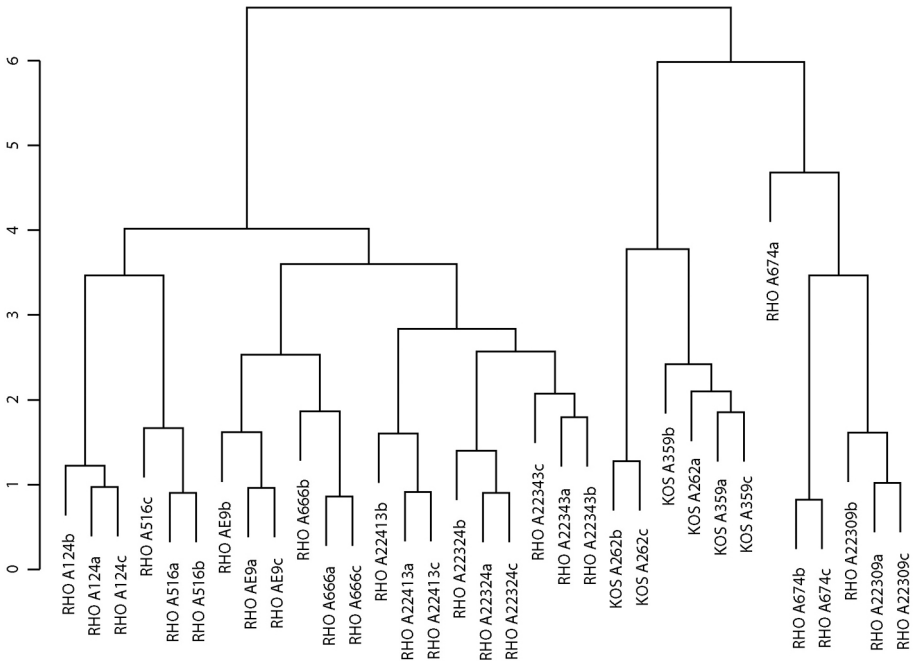

Fig. 1 Hierarchical clustering of the pEDXRF measurements of polished ceramic disks: Concentrations of 16 elements are used, which were log-ratio transformed with the Zn concentration as common divisor. The presented clustering is based on average linkage.

to an inclusion. On the other hand the clustering indicates the general feasibility of the method to distinguish the Koan ceramics from the Rhodian ceramics as the two samples from Koan amphorae are clearly separated from the Rhodian samples. However, the two triples of the Koan samples cannot be clearly separated. One measurement of KOS A262 appears in a cluster with the KOS A359 triple. This is apparently related to an increased copper concentration in the particular measurement.

In the next step the amphora fragments from which the disks were cut off have been included in the study with additional measurements of broken sections and of external and internal surfaces. Again the results are statistically treated on the basis of the same 16 element concentrations. The total variation has increased up to 2.10. Apart from Cr, Ni and Ca in this dataset also Pb and K contribute to the comparably high variation. Fig. 2 presents a hierarchical clustering of the log ratio transformed data using in this case the Fe concentration as a common divisor. While the measurements of the broken sections appear to be in general connected with the clusters of the measurements of the cut and polished disks the surface measurements are in most cases separated. Even though the actual surface layer might be rather thin it has to be considered that XRF

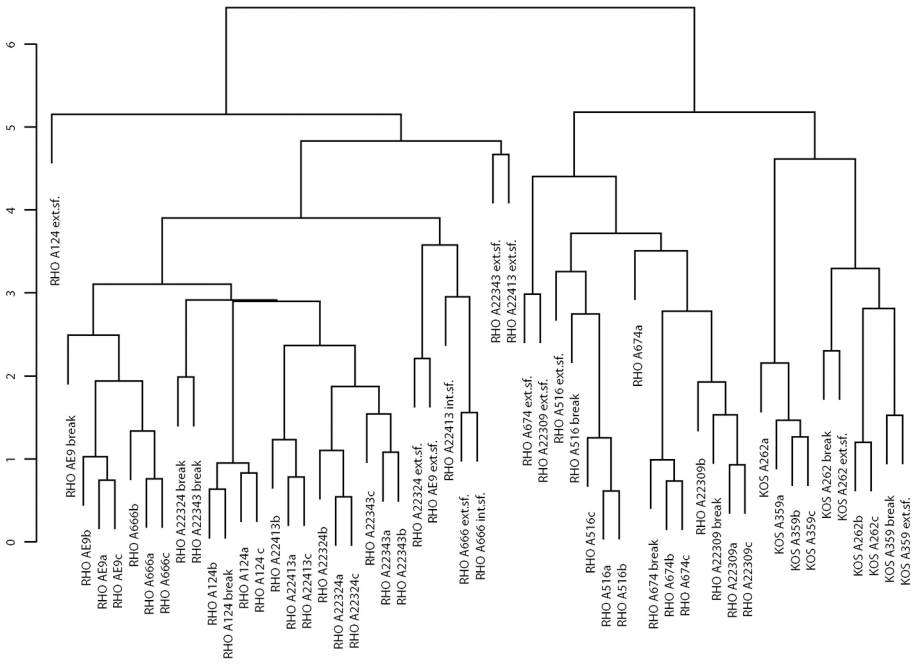

Fig. 2 Hierarchical clustering of the pEDXRF measurements of polished ceramic disks and measurements of fresh breaks and surfaces of the same fragments: Concentrations of 16 elements are used, which were log-ratio transformed with the Fe concentration as common divisor. The presented clustering is based on average linkage. The dashed line indicates the methodological variation, as in most cases the three measurements from the discs clustered below the respective distance.

is a surface sensitive method with different effective thickness of the analysed layer for different elements.[12] If the different surface compositions are related to a specific surface treatment during fabrication or to post-depositional alteration still has to be examined. Nevertheless, the results clearly indicate that measurements of fresh breaks should be preferred to surface measurements.

3.3 Koan amphorae

Following the above presented preparatory measurements the method was tested on 41 amphora fragments from Kardamaina, an amphora production centre in south-central Kos. These fragments were part of an assemblage which had been already examined with NAA.[13] The amphorae were fabricated and used during the Hellenistic Period from the

12 Behrendt, Mielke, and Mecking 2012.

13 Hein, Georgopoulou, et al. 2008.

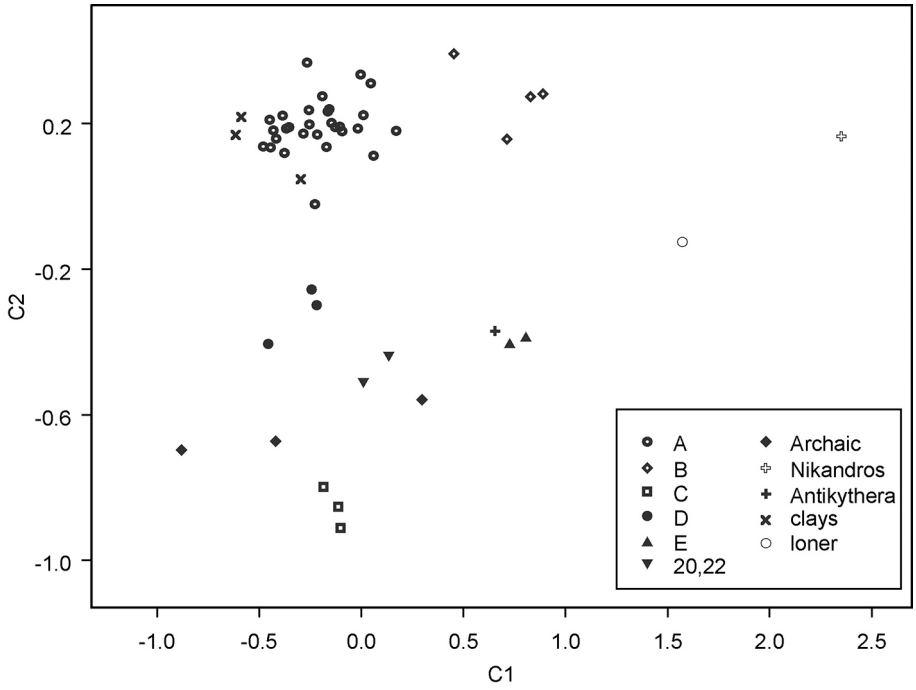

Fig. 3 Principal component analysis of NAA result of Hellenistic transport amphorae from Kardamaina, Kos, and related material: Presented are the first two principal components indicating a large and supposedly local group A which comprises amphorae from the whole Hellenistic period.

4th to 1st century BC. The conclusion of the NAA study was that during the whole period the used raw materials and the firing technology did not change while the vessel shape underwent a considerable modification. Fig. 3 presents a principle component analysis of the NAA results. The majority of the samples independent of vessel type presented a characteristic pattern which besides resembled the composition of a specific local clay. Furthermore, several smaller chemical groups were found, possibly presenting other production centres on the island or maybe on the nearby coast of Asia Minor.

Apart from 41 amphora fragments already measured by NAA, the measurements of KOS A262 and KOS A359, both assumedly belonging to the main ware group, and of a fired briquette fabricated from the local clay were measured. For the statistical evaluation again the above listed 16 element concentrations are used with the Fe concentration as common divisor for the log-ratio transformation. The total variation is 0.98 with the Pb and Cs concentrations contributing the highest variation. In the hierarchical cluster analysis (Fig. 4) the main cluster comprises exclusively samples which belong to Group A defined by NAA. Furthermore, two small clusters of five and two samples, respectively, are clearly separated corresponding to the NAA groups B and E. The samples of

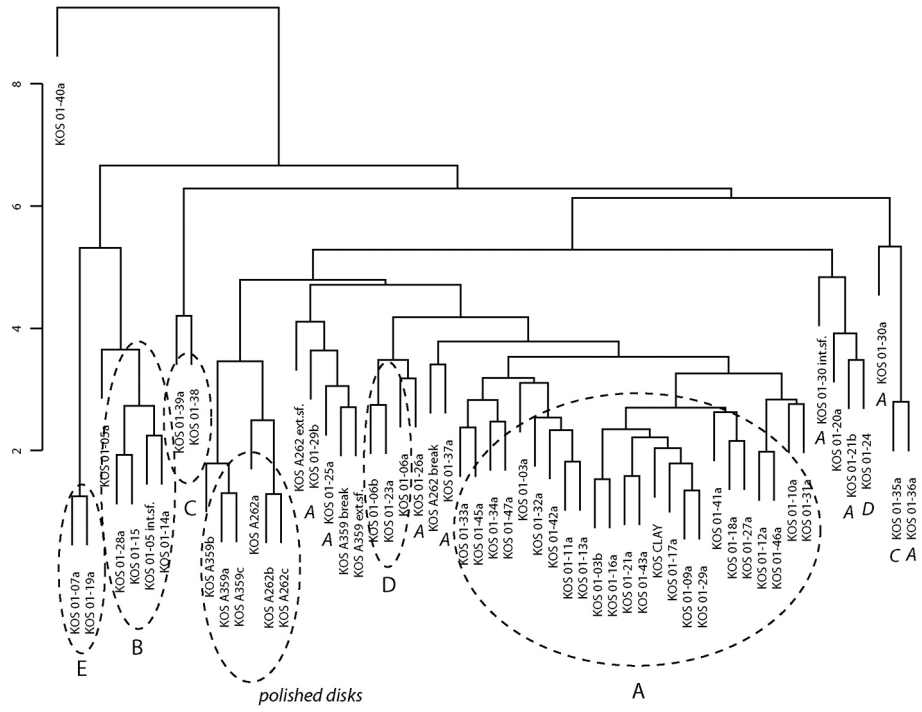

Fig. 4 Hierarchical clustering of pEDXRF measurements of Koan amphorae: Concentrations of 16 elements are used, which were log-ratio transformed with the Fe concentration as common divisor. The presented clustering is based on average linkage.

two other small NAA groups, C and D, are separated from the main cluster as well. However, the respective samples are scattered in various clusters, which partly comprise also samples of the main NAA group A. On the other hand the measurements of the polished disks of Kos A262 and KOS A359 are separated from the main cluster while the measurements of fresh breaks and surfaces of the same samples appear to be closer related to NAA group A. This was again mainly related to higher Cu concentrations measured on the polished surfaces. Therefore, Cu was removed from the evaluation and furthermore also Pb and Cs in order to exclude any effect of contamination. In this way the total variation was reduced to 0.55 with Ca, Mn and Sr contributing the highest variation. The hierarchical cluster analysis (Fig. 5) indicates again a clear separation of NAA groups B and E from the main cluster and also a clearer separation of NAA group C. Sample KOS A262 eventually appears to present a different composition compared to the main cluster, in which on the other hand all measurements of KOS A359 are now included.

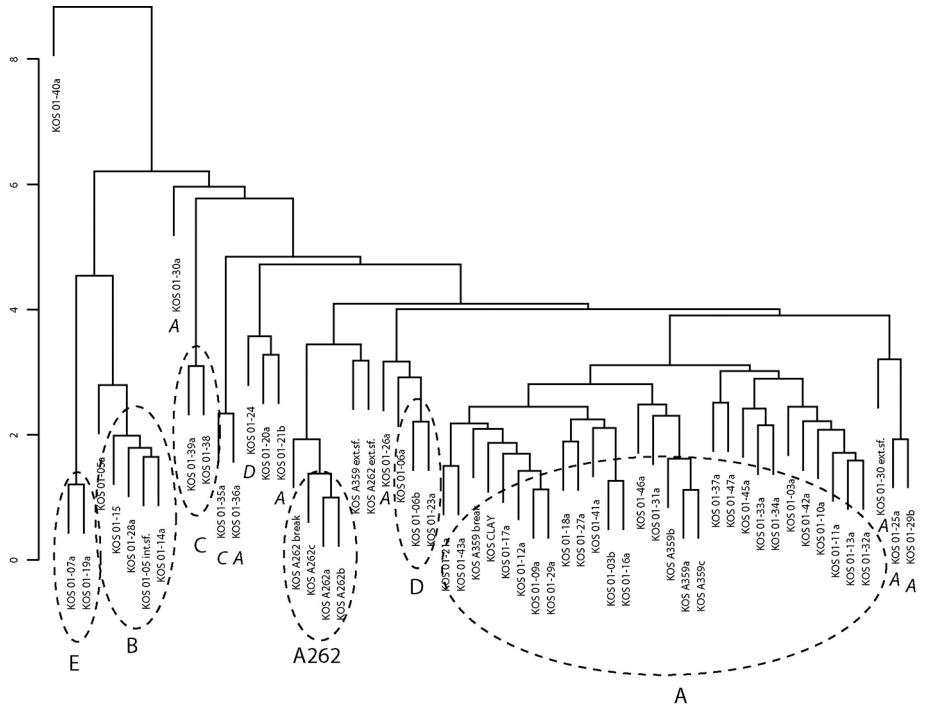

Fig. 5 Hierarchical clustering of pEDXRF measurements of Koan amphorae: Compared to the clustering in Fig. 4 Cs, Cu and Pb are excluded. The data were log-ratio transformed with the Fe concentration as common divisor. The presented clustering is based on average linkage.

In order to test the method on unknown samples 15 further amphora fragments from Kardamaina, part of them from the Roman period, and one amphora handle found in Kos town were measured. The same 13 elements as above were used for the statistical evaluation resulting in a total variation of 0.73. Three of the new samples, KOS 14-01, KOS 14-02 and KOS 14-04, were beforehand identified as imports from Rhodes or Knidos, and they can be also separated in the hierarchical clustering (Fig. 6). Most of the other samples are included in the main cluster, among them two over-fired wasters, KOS 14-07 and KOS 14-08. The amphora handle from Kos town is separated from the main cluster and appears to be related to NAA group C.

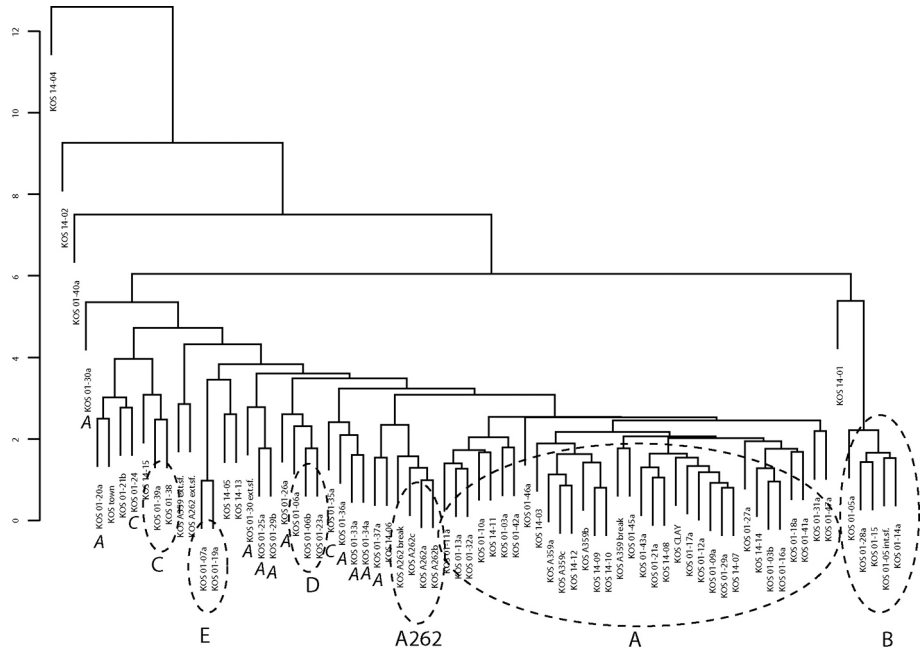

Fig. 6 Hierarchical clustering of the pEDXRF measurements of Koan amphorae including new material: Concentrations of 13 elements concordant with Fig. 5 were used and log-ratio transformed with the Fe concentration as common divisor. The presented clustering is based on average linkage.

3.4 Rhodian amphorae

The second case study for testing the pEDXRF method concerns Hellenistic amphorae from Rhodes.[14] The examined assemblage is considerably larger than the assemblage of the Koan amphorae. Furthermore, the amphorae, even though presenting in general the Rhodian amphora production, were supposedly produced at different places. The NAA analysis of 118 fragments indicated a quite large chemical variation of the material. Fig. 7 presents a hierarchical cluster analysis of the NAA results. The assemblage can be roughly divided in five clusters, the largest of which comprises approximately half of the material. Further statistical evaluation of the NAA results, however, allowed for subdividing these clusters, indicating variation of raw materials even at specific production places.

In a first test pEDXRF was applied on 85 of the already analysed samples, because these were taken as fragments and not as powders. Considering 16 elements the total

14 Palamida et al. 2016.

Fig. 7 Hierarchical clustering of 118 NAA measurements of Hellenistic Rhodian amphorae: Concentrations of 17 elements were used, which were log-ratio transformed with the Sm concentration as common divisor. The presented clustering is based on average linkage.

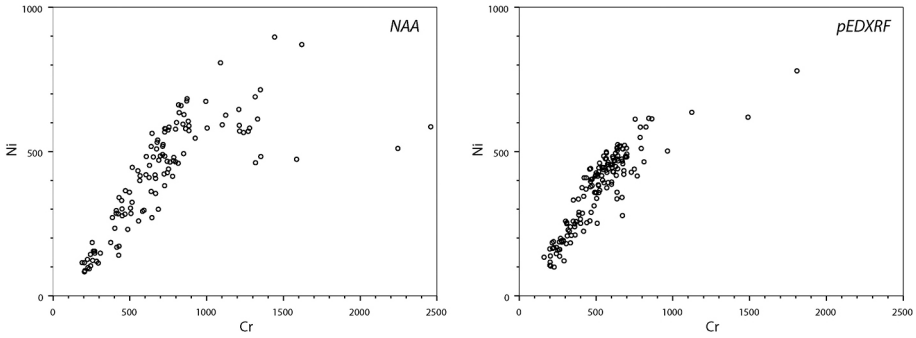

Fig. 8 Nickel and chromium concentrations of Rhodian amphorae measured by NAA (left) and by pEDXRF (right): The concentrations are given in ppm.

variation of 1.91 is considerably higher than in the case of the Koan amphorae. The highest variation is again contributed by Pb and Cs, which are not considered in the following statistical evaluation, reducing the total variation eventually to 1.46. In the specific case of Rhodes also Cr and Ni present a comparably high variation. The reason is that part of the clay deposits, which were exploited for the amphora production, were probably related to ophiolithic outcrops in the North of the island. In Fig. 8 the Ni and Cr concentrations measured by NAA and pEDXRF present in general a similar trend. However, the concentrations measured by pEDXRF appear to be better defined. The apparently smaller variation emerged probably because the effectively measured sample amount was larger than the NAA sample with a more homogeneous distribution of chromium and nickel rich inclusions.

Fig. 9 presents a hierarchical cluster analysis of the 85 samples on the basis of 14 element concentrations which have been log-ratio transformed with Fe as common divisor. Similarly to NAA a main cluster becomes apparent comprising approximately half of the samples. NAA groups B and C, however, appear in one cluster with no separation at least on the basis of the 14 element concentrations used. On the other hand the three samples of NAA group E appear in a clearly separated cluster. The NAA group D, finally, cannot be confirmed by pEDXRF, probably also because only a few fragments are still available to be measured.

Continuing the pEDXRF test 110 additional fragments were measured with pEDXRF which had not been analysed by NAA before. The same 14 elements are used for the statistical evaluation and the total variation is with 1.36 actually slightly smaller. Fig. 10 presents the hierarchical cluster analysis of the log-ratio transformed data using again Fe as common divisor. Increasing the measured assemblage to 205 samples results in a quite similar picture with a main cluster apparently corresponding to NAA group A and two separate clusters comprising samples belonging to NAA groups B and C and

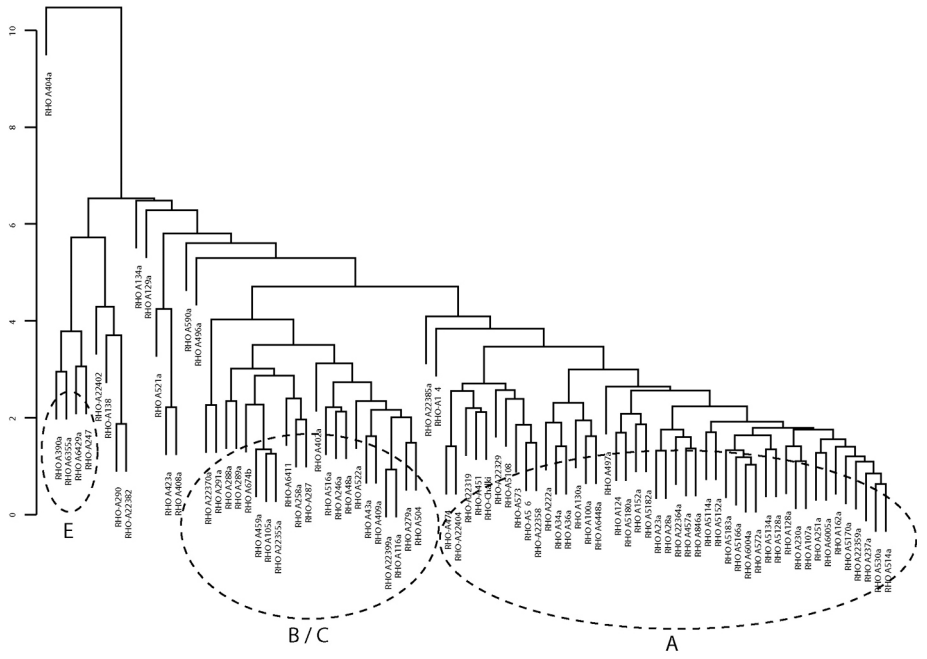

Fig. 9 Hierarchical clustering of the pEDXRF measurements of 85 Rhodian amphorae already measured with NAA: Concentrations of 14 elements were used, excluding Cs and Pb, and log-ratio transformed with the Fe concentration as common divisor. The presented clustering is based on average linkage.

NAA group E.

4 Conclusions

The results achieved so far indicate the general feasibility of pEDXRF for examining the chemical variation within an assemblage of archaeological ceramics. Furthermore, it can be used for a tentative distinction of different ceramic ware groups on the basis of their chemical variation. Particularly in archaeological science, the pEDXRF certainly offers some advantages compared to commonly applied laboratory measurements. It can be used on-site without moving the object or a sample of the objects, respectively. It is in principle non-invasive even though a sufficiently clean sample area is required. Finally, the method is comparably fast and cost-effective so that sufficiently larger numbers of objects can be analysed than with laboratory measurements. Nevertheless, there are certain analytical restraints to be considered. Due to the surface sensitivity of the method a comparably large and sufficiently clean measurement area has to be selected.

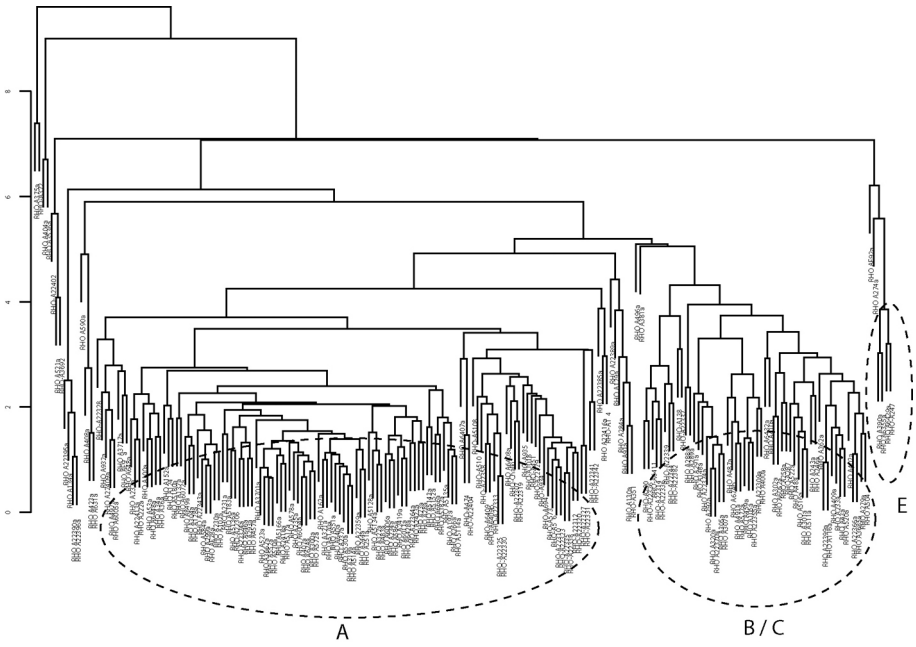

Fig. 10 Hierarchical clustering of the pEDXRF measurements of Rhodian amphorae including new material: Concentrations of 14 elements were used, excluding Cs and Pb, and log-ratio transformed with the Fe concentration as common divisor. The presented clustering is based on average linkage.

In the present case study fresh breaks of amphora fragments were found to be suitable for the analysis. Even though the surface treatment of the amphorae was obviously only marginal, comparative measurements of the surfaces on the other hand presented in most cases a clearly different chemical composition. Another issue is the insufficient precision for the trace elements which introduces additional variation into the data and complicates the assessment of accuracy in view of calibrating the data. This in combination with a comparably small suite of elements, which can be measured, preclude at the present stage the use of reference databases comprising results obtained with other methods, such as NAA or WDXRF.

In view of these analytical restrictions the application of pEDXRF in ceramic provenance studies as standalone technique appears to be questionable. Nevertheless, it can be certainly used as a complementary method to a more effective laboratory method. One reasonable approach would be the initial survey of a large ceramic assemblage with pEDXRF in order to plan the sampling strategy and potentially to reduce the number of samples to be analysed with more expensive methods.[15] On the other hand, ceramic

15 Anno Hein, Agata Dobosz and Vassilis Kilikoglou.

samples, which have been already chemically classified with a more effective method, can be included in an expanded pEDXRF study of a larger assemblage of the same ceramic wares. The present study demonstrated that statistical evaluation of the analytical data employing eventually a kind of supervised learning allows for adequate classification of the unknown samples.

"Portable ED-XRF as Tool for Optimizing Sampling Strategy – Case Study of a Hellenistic Amphora Assemblage from Paphos (Cyprus)", forthcoming.

Bibliography

Aitchinson 1986
John Aitchinson. *The Statistical Analysis of Compositional Data*. London: Chapman and Hall, 1986.

Behrendt, Mielke, and Mecking 2012
Sonja Behrendt, Dirk Paul Mielke, and Oliver Mecking. "Die portable Röntgenfluoreszenzanalyse (p-RFA) in der Keramikforschung. Grundlagen und Potenzial." *Restaurierung und Archäologie* 5 (2012), 93–110.

Buxeda i Garrigos and Kilikoglou 2001
Jaume Buxeda i Garrigos and Vassilis Kilikoglou. "Total Variation as a Measure of Variability in Chemical Data-Sets. A Festschrift in Honor of Edward V. Sayre." In *Patterns and Process*. Ed. by L. Van Zelst. Washington D. C.: Smithsonian Center for Materials Research and Education, 2001, 185–198.

Catling, Blin-Stoyle, and Richards 1961
Hector W. Catling, Audrey E. Blin-Stoyle, and E. E. Richards. "Spectrographic Analysis of Mycenaean and Minoan Pottery." *Archaeometry* 4 (1961), 31–38.

Empereur and Hesnard 1987
Jean Yves Empereur and Antoinette Hesnard. "Les amphores hellénistiques." In *Céramiques hellénistiques et romaines*. Ed. by J. P. Morel. Vol. 2. Paris: Les Belles Lettres, 1987, 7–71.

Georgakopoulou et al. 2017
Myrto Georgakopoulou, Anno Hein, Noémi S. Müller, and Evangelia Kiriatzi. "Development and Calibration of a WDXRF Routine Applied to Provenance Studies on Archaeological Ceramics." *X-Ray Spectrometry* 46.3 (2017), 186–199.

Goren, Mommsen, and Klinger 2011
Yuval Goren, Hans Mommsen, and Jörg Klinger. "Non-Destructive Provenance Study of Cuneiform Tablets Using Portable X-Ray Fluorescence (pXRF)." *Journal of Archaeological Science* 38 (2011), 684–696.

Hein, Georgopoulou, et al. 2008
Anno Hein, Victoria Georgopoulou, Eleni Nodarou, and Vassilis Kilikoglou. "Koan Amphorae from Halasarna. Investigations in a Hellenistic Amphorae Production Centre." *Journal of Archaeological Science* 35 (2008), 1049–1061.

Hein and Kilikoglou 2012
Anno Hein and Vassilis Kilikoglou. "CeraDAT. Prototype of a Web Based Relational Database for Archaeological Ceramics." *Archaeometry* 54 (2012), 230–243.

Hein, Tsolakidou, et al. 2002
Anno Hein, Alexandra Tsolakidou, Ioannis Iliopoulos, Hans Mommsen, Jaume Buxeda i Garrigos, Giuseppe Montana, and Vassilis Kilikoglou. "Standardisation of Elemental Analytical Techniques Applied to Provenance Studies of Archaeological Ceramics. An Inter Laboratory Calibration Study." *The Analyst* 127 (2002), 542–553.

Hunt and Speakman 2015
Alice M. W. Hunt and Robert J. Speakman. "Portable XRF Analysis of Archaeological Sediments and Ceramics." *Journal of Archaeological Science* 53 (2015), 626–638.

Kilikoglou et al. 2007
Vassilis Kilikoglou, Apostolos P. Grimanis, Alexandra Tsolakidou, Anno Hein, Dimitra Malamidou, and Zoi Tsirtsoni. "Neutron Activation Patterning of Archaeological Materials at the National Centre for Scientific Research "Demokritos". The Case of Black-On-Red Neolithic Pottery from Macedonia, Greece." *Archaeometry* 49 (2007), 301–319.

Palamida et al. 2016
Chara Palamida, Fani K. Seroglou, Mark L. Lawall, and Angeliki Yiannikouri. "The Emergence of 'Hellenistic' Transport Amphoras: The Example of Rhodes." In *Traditions and Innovations: Tracking the Development of Pottery from the Late Classical to the Early Imperial Periods*. Ed. by S. Japp and P. Kögler. Wien: Phoibos, 2016, 135–150.

Sayre and Dodson 1957
Edward V. Sayre and Robert W. Dodson. "Neutron Activation Study of Mediterranean Potsherds." *American Journal of Archaeology* 61 (1957), 35–41.

Shugar and Mass 2012
Aaron N. Shugar and Jennifer L. Mass. "Introduction." In *Handheld XRF for Art and Archaeology*. Ed. by A. N. Shugar and J. L. Mass. Studies in Archaeological Sciences 3. Leuven: Leuven University Press, 2012, 17–36.

Speakman et al. 2011
Robert J. Speakman, Nicole C. Little, Darrell Creel, Myles R. Miller, and Javier G. Iñañez. "Sourcing Ceramics with portable XRF Spectrometers? A Comparison with INAA Using Mimbres Pottery from the American Southwest." *Journal of Archaeological Science* 38 (2011), 2483–3496.

Weigand, Harbottle, and Sayre 1977
Phil C. Weigand, Garman Harbottle, and Edward V. Sayre. "Turquoise Sources and Source Analysis. Mesoamerica and the Southwestern USA." In *Exchange Systems in Prehistory. Studies in Archaeology*. Ed. by T. K. Earle and J. E. Ericson. New York: Academic Press, 1977, 15–34.

Illustration and table credits

ILLUSTRATIONS: **1–10** A. Hein.

TABLES: **1** A. Hein.

ANNO HEIN

Anno Hein studied physics at the University of Bonn (diploma in 1993, PhD in 1996). He worked at the N.C.S.R. "Demokritos" as a post-doctoral fellow and associate researcher. After collaborating in various projects on archaeological science in Greece, he took on a permanent position as a researcher at the N.C.S.R. "Demokritos" in 2010. His main research interest is the study of ceramics and composite materials, with a particular focus on archaeological materials.

Dr. Anno Hein
Institute of Nanoscience and Nanotechnology
N.C.S.R. "Demokritos"
15310 Aghia Paraskevi, Greece
E-mail: a.hein@inn.demokritos.gr

Richard Jones, Louisa Campbell

Testing Composition by pXRF Analysis against Ceramic Shape, Style and Stamp: A Case Study from Samian Found on Hadrian's Wall

Summary

Attributing a source to Roman samian (or Terra Sigillata) pottery has generally been accomplished on the basis of style, decoration, and potters' stamps. However, chemical composition can also play an important role. Our investigation concerns the application of pXRF analysis to situations where sampling for destructive analysis is not possible. This paper reports the results for typologically well-characterized samian, including many stamped sherds, from South Shields fort on Hadrian's Wall. The encouraging results showed that examples of samian ascribed to a particular production center had a uniform, recognizable composition and that comparison with published WD-XRF data gave a provenance assignment that was in agreement with expectations.

Keywords: pXRF; Roman pottery; samian; Gaul; slip

Die Zuordnung römischer Terra Sigillata zu ihren Produktionsorten geschah allgemein auf der Grundlage von Stil, Dekor und Töpferstempeln. Aber auch die chemische Zusammensetzung kann eine wichtige Rolle spielen. Unsere Untersuchung betrifft die Anwendung der pRFA bei Situationen wo eine Probennahme für nicht zerstörungsfreie Analyse unmöglich ist. Dieser Beitrag liefert Ergebnisse für typologisch sicher bestimmte Terra Sigillata, einschließlich vieler gestempelter Scherben, vom South Shields Fort am Hadrian-Wall. Die ermutigenden Ergebnisse zeigten, dass bestimmten Produktionszentren zugeschriebene Beispiele von Terra Sigillata eine einheitliche, erkennbare Zusammensetzung hatten und der Vergleich mit publizierten WD-RFA-Daten eine Herkunftsbestimmung ermöglichte, die in guter Übereinstimmung mit der Erwartung war.

Keywords: pRFA; römische Keramik; Terra Sigillata; Gallien; Glanztonüberzug

We are grateful to the Association for Roman Archaeology for financial support for this project; Paul Bidwell at Tyne & Wear Museums for assistance; and Nick Hodgson, Secretary for the Newcastle Society of Antiquaries, for the kind permission to reproduce illustrations.

Morten Hegewisch, Małgorzata Daszkiewicz und Gerwulf Schneider (eds.) | Using pXRF for the Analysis of Ancient Pottery – an Expert Workshop in Berlin 2014 | Berlin Studies of the Ancient World 75 (ISBN TODO; DOI: 10.17171/3-75) | www.edition-topoi.org

R. J. thanks Ken Grainger and John Hurley at Niton UK for discussions about calibration algorithms, and Gerwulf Schneider and Philippe Sciau for discussions of the results.

1 Introduction

In addition to the contributions to this volume, there have been several reports in the recent archaeological science literature about the application of portable XRF (pXRF) to pottery from archaeological contexts to resolve issues of the pottery's identity, technology and especially origin. For the last of these issues, the reports on prehistoric ceramics – clay tablets found at Hattuša (Boğazköy) and Tell el Amarna,[1] Early-Middle Bronze Age pottery on Cyprus[2] and Chalcolithic pottery in Turkey[3] – have presented encouraging results, while at the same time these studies have identified and characterised some of the limitations that are inherent in the analysis of ceramic surfaces. Statements can indeed be made about origin, generally in the form of associating samples of common composition to a common origin; there can be no claim that the output of pXRF is able to provide more precise and sophisticated information about origin. Rather than replacing the systematic high-quality, multi-element analysis of bulk samples that the destructive techniques, such as WD-XRF, NAA and ICP-ES and ICP-MS, can give, the role of pXRF at present should be seen in providing rapid, and if necessary *in situ*, analysis on a quantitatively larger scale than is usually possible when employing destructive techniques. pXRF thereby presents a broad, objective dimension of information which may set the questions that can be tackled by destructive techniques with access to their associated large databases. Further, the non-invasive and portable character of the technique has great potential for realising the latent research potential of collections under curatorial care.

This paper concerns samian ware (Terra Sigillata) which remains one of the most important and widely studied class of fine ware pottery in the Roman world. As outlined more fully below, there is a wealth of information about its shape and style and much is known about where and how it was made,[4] whilst more research work focusses on the broader social and economic aspects of this ware.[5] The significance of the frequent presence of potters' stamps on samian ware is well explored and understood.[6] Nevertheless, there are instances in which the identity of samian, that is, its assignment to a

1 Goren, Mommsen, and Klinger 2011.
2 Frankel and Webb 2012.
3 Forster et al. 2011.
4 Stanfield and Simpson 1958.
5 Fulford 2013.
6 Hartley and Dickinson 2008–2012.

particular workshop, is uncertain or ambiguous because of the absence of decoration or stamp; it may also be in poor condition. The clear role that chemical analysis can play in this situation led us to investigate samian recovered from various excavations along the Antonine Wall and its vicinity in Scotland.[7] We selected pXRF as the most appropriate analytical technique because all of the assemblages are now acquisitioned in museums that were able only to grant permission for non-destructive work, and, crucially, there were two methodological factors favouring this approach: first the fine textured fabric, and second the characteristic way that samian fractures so often gives a flat, clean break which is suitable for a surface analysis.

In the first phase of our programme of pXRF we analysed samian[8] from four forts along the Antonine Wall – Old Kilpatrick, West Dunbartonshire[9]; Balmuildy, Glasgow[10]; Cadder, East Dunbartonshire; and Bar Hill, East Dunbartonshire[11]. With that data we were able to resolve specific questions regarding the samian from two forts to the south of the Wall of mainly Flavian date[12] namely Castledykes, South Lanarkshire[13] and Loudon Hill, East Ayrshire. At these two forts where much of the samian was undiagnostic and unstamped, two chemical groups were defined: the examples of Flavian date consistently belonged to one group, likely of South Gaulish origin, and a smaller number which joined all the examples from the Antonine Wall whose sources were Lezoux and one other centre of production in Central Gaul.

In this paper we report the results of an internally more controlled exercise, based on well-studied samian from South Shields fort on Hadrian's Wall in northern England.[14] This pottery was selected to include samian that was confidently assigned on the basis of decorative style and in many cases the stamp to different production regions within Gaul. Knowing, as will be explained below, that these regions can be discriminated chemically, our purpose was to establish whether our methodology could yield results that were in accordance with the expectations based on published stylistic/stamp evidence[15] and then as a further check to compare on a qualitative basis our data with that obtained by WD-XRF for the same candidate production centres. A further aim was to add value by analysing the red slip as well as the fabric to determine whether the former's composition was characteristic of the production site in the same way that the body's composition should be. The main effort so far has been in characterising this slip from La Graufesenque and other centres in South Gaul[16] and in particular demon-

7 Jones and Campbell 2016.
8 Now stored in the Hunterian Museum, University of Glasgow.
9 Miller 1928.
10 Miller 1922.
11 Macdonald and Park 1906; Robertson, Scott, and Keppie 1975.
12 1st century AD.
13 Robertson 1964.
14 Dore, Greene, and Johns 1979.
15 Dore, Greene, and Johns 1979; Hartley and Dickinson 1979.
16 Sciau, Languille, et al. 2005; Sciau, Relaix, et al. 2006; Sciau, Sanchez, and Gliozzo 2020.

Fig. 1 Photographs of selected stamps.

strating that the clays of the slip and body were very likely not the same;[17] similar views are emerging about the black gloss on Attic vases.[18]

To put samian ware briefly into context, this class, based on vessel forms and potters' stamps (Fig. 1), plays a fundamental role in dating the Roman presence especially in Rome's frontier regions.[19] But over the last few decades there has been increasing interest in the production aspects of samian. Fülle[20] has explored the internal organisation of the industry at Arezzo, and excavations at numerous production sites,[21] for example at La Graufesenque,[22] have revealed the procedures in making and firing samian; these sites have offered plentiful material for chemical characterisation studies. The standardised technology adopted across Rome's northern provinces in the production of samian – the use of a usually fine-textured, pale coloured, low to medium calcareous clay which was then well fired – provides optimal conditions for such characterisation studies. Because many of the production centres can be reliably differentiated chemically, the role of chemical analysis in samian studies has been important in acting as an objective means of determining origin especially in those cases, which may not be infrequent, where the visual characteristics of the fabrics as set out in *The National Roman Fabric Reference Collection*[23] may be ambiguous or indecisive. Three European laboratories in particular have built up large databases of samian chemical compositions, all using conventional wavelength-dispersive X-ray fluorescence (XRF) spectrometry: Berlin[24], Lyon[25] and Fribourg[26]. One significant application of these databases is Picon's study of samian from

17 Picon 1997.
18 Aloupi-Siotis 2020.
19 E.g. Hartley 1972.
20 Fülle 1997.
21 Tyers 1996.
22 Genin and Vernhet 2002.
23 Tomber and Dore 1998.
24 Schneider 1978.
25 Picon, Vichy, and Meille 1971.
26 Maggetti 1981.

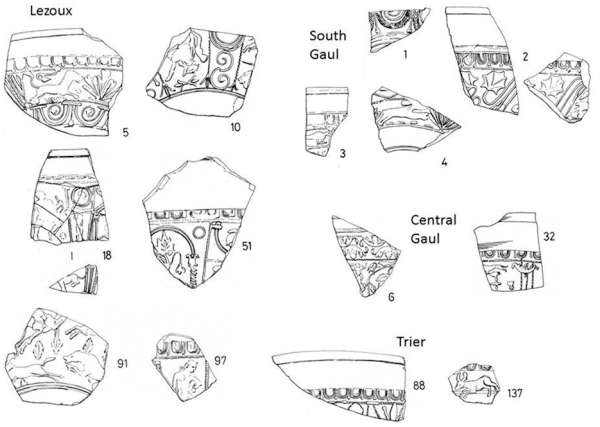

Fig. 2 Illustrations of selected sherds analysed (from Dore, Greene, and Johns 1979, scale 1:2).

the Roman fort at Haltern, showing that Lyon and Pisa, rather than Arezzo were the main suppliers to this fort.[27] Analysis by neutron activation of examples of samian bearing the stamp of Ateius found at Lyons showed decisively that they were products of the Lyon area rather than of this master potter's base at Arezzo;[28] it was inferred that Ateius had established a workshop in this part of Gaul.

2 Material

At the eastern end of Hadrian's Wall lies South Shields fort overlooking the River Tyne. Founded around AD 120, it later became the maritime supply fort for Hadrian's Wall, and was occupied until the Romans left Britain in the 5th century. Of the large assemblage of samian which has been published by Dore et al.[29] and the stamps by Hartley and Dickinson[30], 50 samian sherds[31] were selected for analysis. They are listed in Tab. 1 and some are illustrated in Fig. 2 and Fig. 3.

In order to test the reliability of the pXRF results we deliberately selected samples for analysis which could be relatively confidently ascribed to particular production centres and timeframes through alternative techniques. Rheinzabern and Lezoux feature prominently but other centres are represented as well (Fig. 4). The sherds were in good condition; there was an absence of concretion or surface coating resulting from burial or conservation treatment.

27 Schnurbein, Lasfargues, and Picon 1982; see also Greene 1992, 37.
28 Widemann et al. 1975.
29 Dore, Greene, and Johns 1979.
30 Hartley and Dickinson 1979.
31 Now in the South Shields Museum.

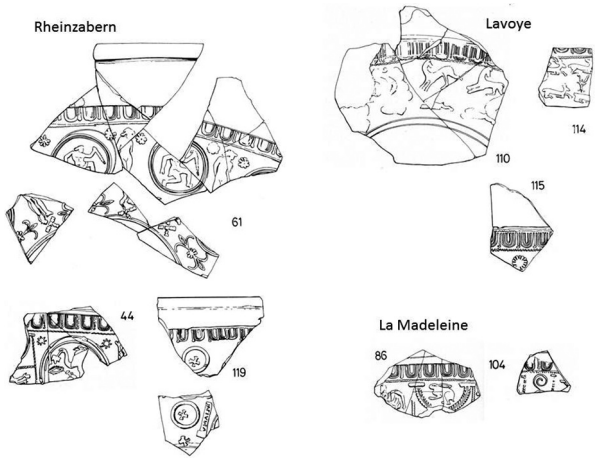

Fig. 3 Illustrations of selected sherds analysed (from Dore, Greene, and Johns 1979, scale 1:2).

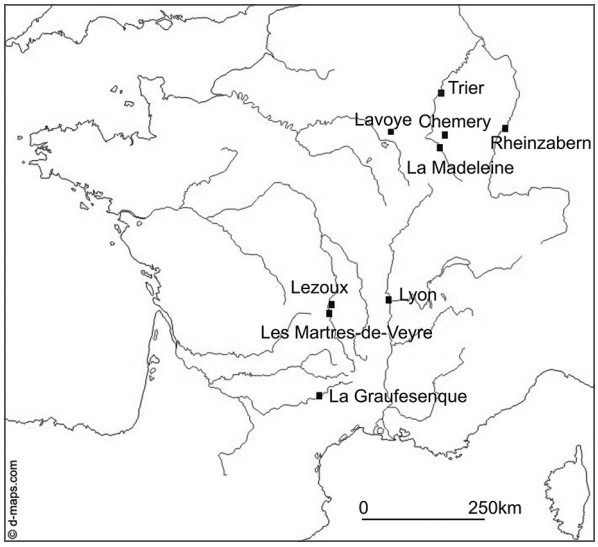

Fig. 4 Map of Gaul showing the samian production centres represented at South Shields Roman fort.

2.1 Method

The analyses were carried out with a portable Thermo Scientific Niton XL3t energy-dispersive XRF instrument with a 50 kV silver X-ray tube and a Geometrically Optimized Large Drift Detector. Each sherd was placed in the lead-lined sample compartment of a Niton-manufactured test stand allowing constant distance and geometry between the X-ray beam and the selected location on the sherd. Three locations were selected, having a fresh break and as flat a surface as possible; the analysis area was estimated at *c.* 10 mm². In a few cases the ring base was analysed as well as the fresh break; compar-

ison of the compositions of the ring base in the as-received state and following light sanding of the surface to remove possible surface weathering indicated increases in Fe, Mn and Ca contents in the former of the order of 5%. The count time in each analysis was 60 seconds.[32] Of the instrument's calibration algorithms provided by Niton – Soil, Testall Geo and Mining – Testall Geo gave the preferred results for the range of elements required, but it is nevertheless imperfect when judged against the values of accuracy obtained from analysis of NIST Till 4 and USGS standards (DNC1, AGV2, BCR2 and DTS2).[33] Tab. 2 shows that most elements were underestimated, a major exception being Cr which cannot be reliably determined at concentrations less than 100 ppm; the discrepancy between determined and certified values for this element extends to USGS DNC standard (Cr2 column in Tab. 2). For the four USGS standards simple regression analysis of the certified and determined values gave satisfactory coefficients of determination R^2 values apart from those for V and Cr. Correction factors were determined using the results obtained from the USGS standards whose compositions encompass those of the samian. At least three determinations of each element were examined and found for the most part to lie within 10% of each other, but where one of the determinations deviated by more than 20% it was discounted; analysis of Sr occasionally gave spurious values well in excess of 20%. At least one analysis was made of the slip layer on most sherds.

3 Results

The compositions are given in Tab. 3. Visual examination of the data suggests significant variation in Rb, Zr and Ti contents and this is borne out in the bivariate plots in Fig. 5. 97 with an anomalous high Rb content (244 ppm) is omitted from these plots. When the sample number is replaced by the proposed source based either on vessel form, decoration and where relevant stamp, good correlation is observed (Fig. 6).

- Group 1 encompasses all the examples of samian attributed to Rheinzabern in East Gaul.

- Group 2 contains samian primarily attributed to Lezoux together with one example from Les Martres de Veyre and seven that are loosely defined as Central Gaul.

32 20 seconds each on the main and low energy ranges and light element range; experimentation with longer times gave little improvement in the quality of the data.

33 Wolf and Wilson 2007.

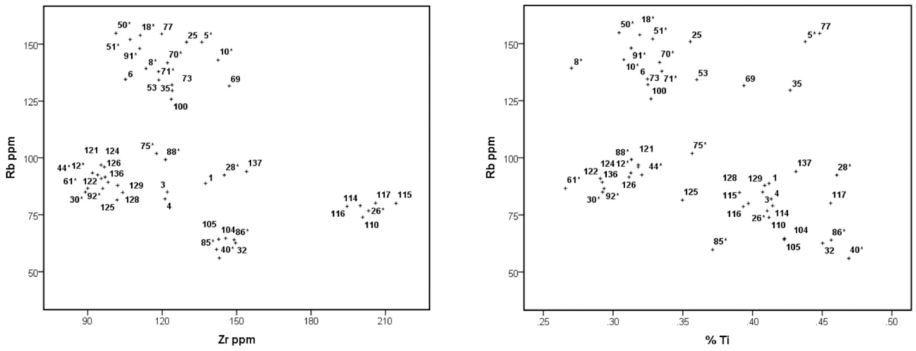

Fig. 5 Plots of Rb-Zr (left) and Rb-Ti (right) contents in samian from South Shields.

– Group 3 is also East Gaul as it comprises four examples from La Madeleine and two assigned stylistically to East Gaul. Dore et al.[34] assign **32** to Central Gaul while noting that its fabric and finish are very similar to that of samian from La Madeleine; its composition however places it firmly in our supposed East Gaul group.

– Group 4 comprises samian from Lavoye and one example, **26**, from Argonne or Trier, again exclusively East Gaul.

Two examples of supposed South Gaul samian, **3** and **4**, lie outside Group 1, as do two examples, **75** and **88**, both stamped that may be from Trier. Two further examples that are assigned to Trier, **28** and **137**, lie well outside Groups 1 and 3.

Multivariate treatment using average link cluster analysis on z score data yields a dendrogram (Fig. 7). There are four significant clusters and several outliers:

– Cluster 1 encompasses members of Groups 1, 3 and 4 and includes Trier **75**.

– Cluster 2 is equivalent to Group 2, i.e. Central Gaul. Anomalous sample **97** belongs weakly to this cluster.

– Cluster 3 consists of Group 1 members – **122**, **124**, **30**, **61**, **92**, **136** – and South Gaul **4** and (weakly) Trier **88**. This cluster separates from Cluster 1 owing primarily to higher Ca in the former.

34 Dore, Greene, and Johns 1979.

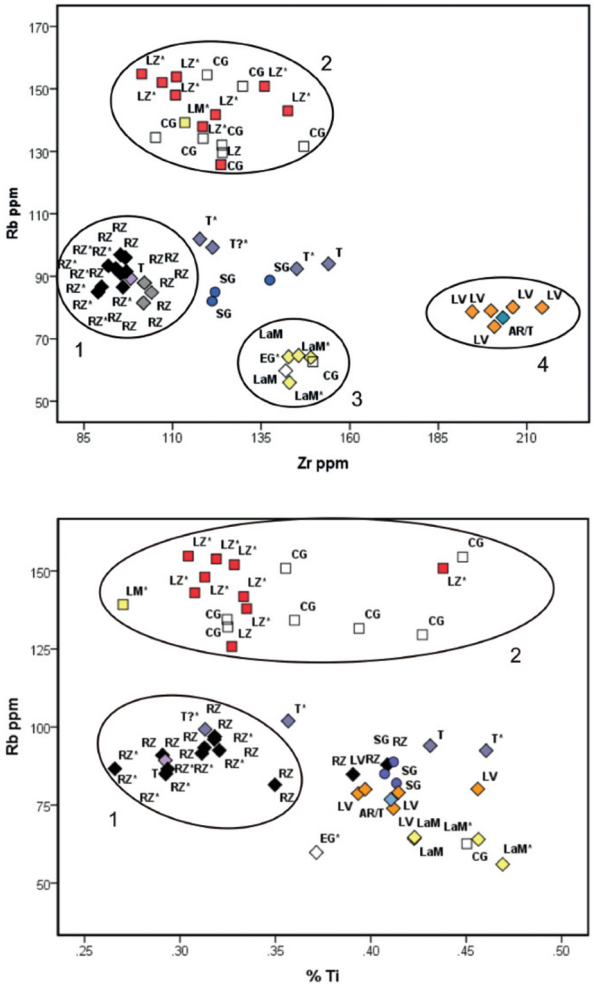

Fig. 6 As for Fig. 5 but the samples are annotated according to projected source based on style and/or stamp. * indicates stamped. *East Gaul diamond*: RZ black, Trier and AR/T blue, Lavoye (LV) orange, La Madeleine (LAM) yellow, E Gaul unclassified no colour. *Central Gaul square*: Lezoux red, Les Martres de Veyre (LM) yellow, C Gaul unclassified no colour. *South Gaul circle*, blue.

The outliers are **28** and **137** (high K), **126** (high Zn), **6** and **10** (high Sr), **3** (high Sr, Ca and Cu) and **110** (low Ca, Mn, Zn and V).

Thus, the cluster analysis has combined most members of the proposed East Gaul Groups 1, 2 and 3 into broad cluster 1 but has separated out a more calcareous East Gaul group. Principal components analysis of the same data set failed to provide a helpful classification since the first two PCs accounted for only 44% of the total variation in composition (PC1 24% dominated by Cr, Ti, –Ca; PC2 20% dominated by Al, Si).

The composition characteristics of the members of Groups 1, 3 and 4 and clusters 1 and 3, all tentatively assigned to East Gaul, are as follows: lower ranges of Ti, Zr, Rb and Sr; wide but on average lower Ca. Trier and La Madeleine have higher Zr and Ti

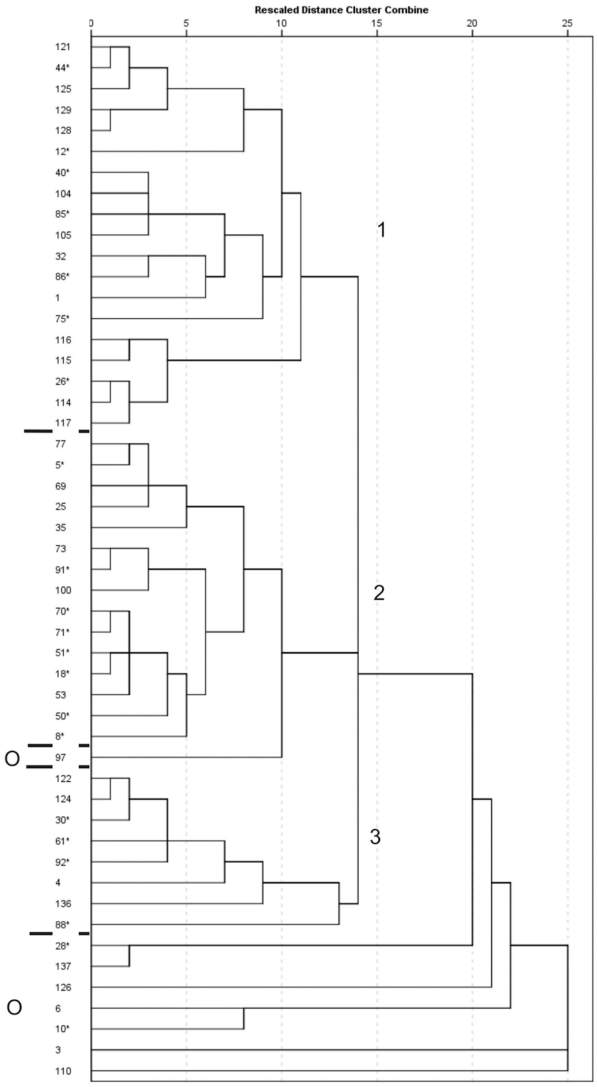

Fig. 7 Average link cluster analysis dendrogram. There are three clusters, 1–3, and Outliers (marked O) 97, 28, 137, 126, 6, 10, 3 and 110.

than Rheinzabern and Trier has notably wide Ca ranges (Fig. 8). Group 2 and Cluster 2, tentatively assigned to Central Gaul, have higher Rb, Sr and Ca contents and wide range of Ti contents.

At this point it can be stated that the samian assigned on the basis of style and/or stamp to particular workshops or regions in Gaul forms coherent chemical groups. There seem to be no discrepancies. With this encouraging picture in mind, the next step is to compare each group with the published data for samian from known work-

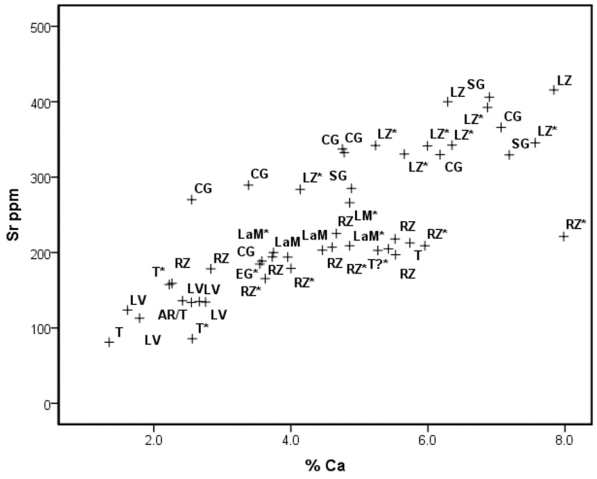

Fig. 8 Plot of Sr-Ca contents.

shops in Gaul, most of it obtained by WD-XRF[35] (Tab. 4). In view of the way the compositions from centres *within* East Gaul – Rheinzabern, Lavoye and La Madeleine – are discernibly different (Figs. 5 and 6), the compositions of several samian reference groups in East Gaul – Chemery, Blickweiler, Trier, Avocourt – have deliberately been included in Tab. 4.

Having corrected the pXRF data according to the figures given in Tab. 2, but treating the Cr comparison as semi-quantitative at best, the first comparison is Group 1 with Rheinzabern. Ca is higher in Group 1 than the Rheinzabern group mean but still within 1 standard deviation; the discrepancy in Mn is slightly larger, but there is excellent agreement in the discriminating elements, Rb, Zr and Ti. Group 2 agrees satisfactorily with the Lezoux group although the former's mean Rb, Sr, Zr and Mn are higher. Despite its very small size, Group 3 agrees adequately with the La Graufesenque group, and this is borne out well in Figs. 9a and 9b although there is total overlap with Lezoux in the Sr-Ca plot (Fig. 9c).

The samples assigned typologically to Trier do not have similar compositions. **75** and **88** share some similarities (e.g. in Rb-Zr) but probably do not have the same source. Neither matches the Trier ICP group (which lacks Rb and Zr determinations) convincingly. **28** and **137** form a pair but in Fig. 8 there is no consistency in the way they associate with a reference group. **136** lies closer to Rheinzabern than anywhere else, and **26** (classed as AR/T) consistently groups with the Lavoye examples in Figs. 5 and 6 and with Chemery and Avocourt in Fig. 9c.

35 Schneider 1978.

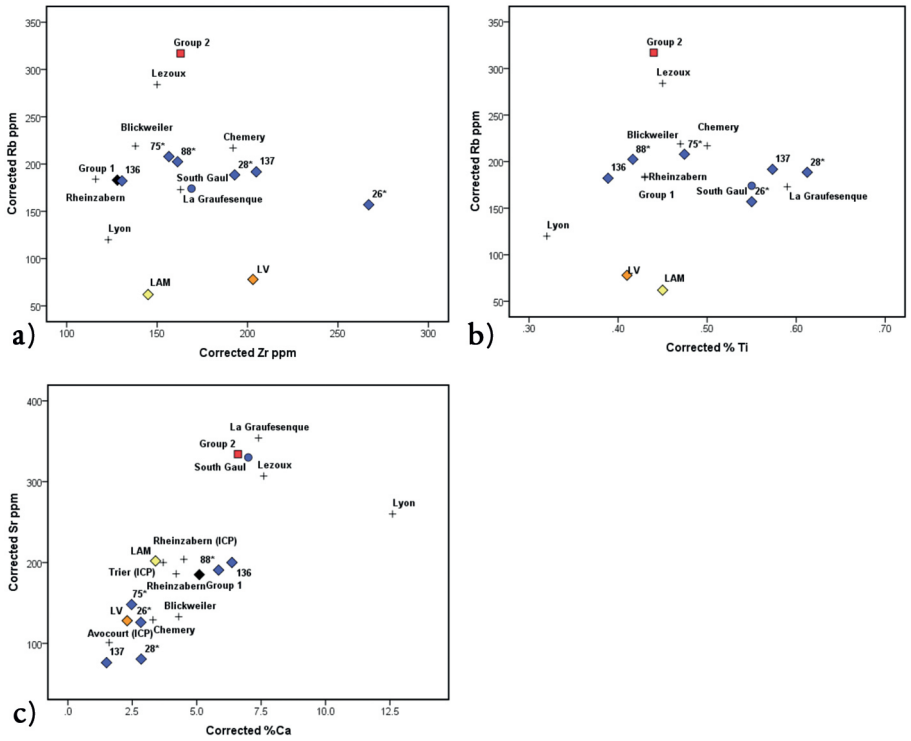

Fig. 9 Plots of *corrected mean* values of (a) Rb-Zr, (b) Rb-Ti and (c) Sr-Ca for Groups 1 and 2, South Gaul group, Lavoye, La Madeleine and individual Trier samples using the coloured symbols as in Fig. 2. The remaining points are the mean values for the Rheinzabern, Lezoux, La Graufesenque, Lyon, Chemery, Blickweiler, Trier and Avocourt reference groups (all indicated with +) as given in Tab. 4. The ranges for each of these groups can be determined from the % coefficient of variation values in Tab. 4.

The Lavoye and La Madeleine samian, which form two separate groups in Fig. 6 left and to a lesser extent in Fig. 6 right, retain their identity in Fig. 9 (which show *mean* values) owing to their lower Rb contents than any of the samian reference groups.

Semi-quantitative analysis of the *slip* layer revealed that it has, as expected, a different composition from that of the body. From the results in Tab. 5 it is apparent that the slip generally has a slightly higher iron content and significantly higher potassium and aluminium but lower calcium contents than the body. On the basis of microprobe analysis of examples of slip from La Graufesenque, Picon[36] used the finding of a K/Al ratio that was double that in the body to propose that the slip was prepared from a less calcareous clay than the body. Working with examples from the same site and from the smaller centre at Montans in the same region, Sciau et al.[37] concurred with this view,

36 Picon 1997, 90.

37 Sciau, Languille, et al. 2005.

demonstrating that the very thin slip,[38] fired at 1020–1080°C, comprised a homogeneous highly sintered layer with uniformly distributed iron and a wide range of quartz crystal sizes.[39]

The K/Al ratio as determined by pXRF is a function not only of the slip and body compositions but also the slip thickness as the X-ray beam penetrates through the slip to a depth of *c.* 100 microns. What pXRF detects therefore is a composite of the major signal arising from the slip coupled with a smaller component from the underlying body. Working on the assumption that the thickness does not vary significantly among the present samples, the results in Tab. 2 and 5 indicate that the three South Gaul specimens, **1**, **3** and **4**, have indeed higher values in the slip than in the body. In the plot of this ratio in the slip and body (Fig. 10) there is one broad cluster with outliers in the form of South Gaul (SG) **3** and Trier **136** and Trier **137**. The South Gaul samples are joined by other samples with ratios greater than 1 but they do not separate from the remaining samples, which themselves form a slight majority, having K/Al ratios less than 1. A potentially important implication is that the latter samples could represent the use of the *same* or similar clay for both slip and body. Turning to another ratio, K/Ca, a high value would point to enriched K in the slip coupled with a low calcareous clay in the slip. The difficulty is that a lower value of this ratio implies a more calcareous clay which could be in either the slip or the body, and to resolve this issue would require further investigation involving analysis by, for example, PIXE. In any case, all the slips, especially the South Gaul examples, have higher K/Ca values than the body except for three Lezoux specimens (**10**, **71** and **100**), one from Rheinzabern (**92**) and three from elsewhere in East Gaul (**26**, **85** and **86**) (Fig. 6).

Examining the distribution of the K/Al and K/Ca ratios among samian from the same production centre or region and bearing in mind the very limited numbers in the Trier and South Gaul groups, the following observations can be made: (1) the relative similarity of slip at Rheinzabern and Lezoux, (2) the relatively higher K/Ca but very uniform K/Al ratios at Trier and (3), as already noted, the higher K/Al values in South Gaul. These observations are compatible with the use of clays selected for the slip that differed from centre to centre, but they may also have a bearing on the level of quality control achieved at each centre.

4 Discussion

This exercise has produced encouraging results. It was designed to test the preliminary findings from our earlier investigation with pXRF analysis of 1st and 2nd C samian re-

38 Estimated at 15 microns thick by Tite, Bimson, and Freestone 1982.

39 Sciau, Relaix, et al. 2006.

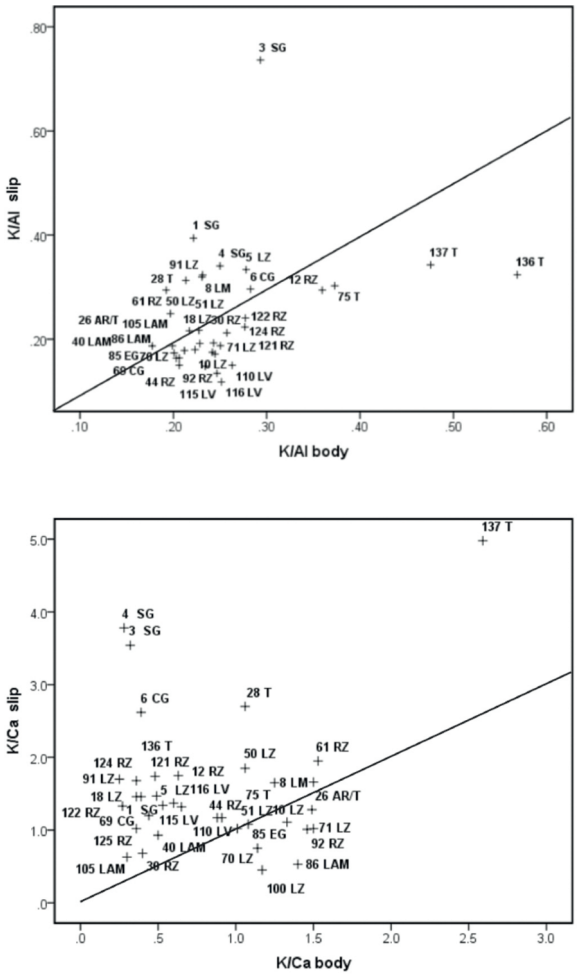

Fig. 10 Plot of (a) K/Al and (b) K/Ca ratios in selected examples of samian slip and body.

covered from forts on and close to the Antonine Wall. The sherds from South Shields on Hadrian's Wall forming the present study were deliberately selected to include examples that were attributable on the basis of decorative style or stamp to a wide range of sources in Gaul. At a first level, the emergent chemical groupings appear to align closely with the sherds' classification according to style and/or stamp, and as such provide a verifiable chemical fingerprint for centres of samian production. At a second level, progress has been made in assigning origin to some of these groupings by relating them to the published chemical (WD-XRF) database of samian production centres. The collective outcome helps validate the use of pXRF as a rapid, non-destructive analytical technique that is capable of interrogating large assemblages of samian sherds. Forthcoming phases

of our study are aiming to extend and exploit this capability. Already underway is study of material from excavations of an important Iron Age site at Traprain Law in East Lothian, close to the Roman port at Inveresk which lies to the east of the Antonine Wall. Much of the samian from Traprain Law is either poorly defined typologically or comprises few stamped pieces; in such cases pXRF can expect to take the lead in identifying source regions.

In tandem with the analysis of new material comes the process of addressing a number of methodological issues. One of these is the desirability of introducing a ceramic-specific calibration algorithm to the analysis protocol with Thermo-Niton instruments. Another is to improve the performance characteristics of the kind given in Tab. 2 that should come with the analysis of more ceramic standards; improved performance characteristics will facilitate assessment of the reliability of measurement of important but problematic elements such as Cr. Also assuming increasing importance is the matter of approaching the relationship between the respective compositions determined respectively by WD-XRF and pXRF more directly by analysing by the latter technique either the glass discs prepared for WD-XRF[40] or new samples of samian from the main centres such as Rheinzabern, Lezoux and La Graufesenque.

Finally, this study has contributed to the question of whether the relative technological uniformity of samian production in Gaul extended to the way the slip was prepared. To judge from pXRF analysis, whose limitation that it cannot account for variation in slip thickness has to be acknowledged, the answer would appear to be in the negative. The selection of a less calcareous clay for the slip than the body seems assured at centres in southern Gaul[41], but this was not a uniform procedure since there are examples of samian from elsewhere in Gaul for which the data is more compatible with the use of the same or similar clay for both slip and body. Such a situation is surely consistent with potters adapting their practices to raw materials that were locally available.[42] But more broadly, this line of enquiry raises interesting implications, not necessarily new, regarding quality control[43] and the extent to which, first, the sources of those raw materials changed over time at a given centre and, second, slip preparation was carried out at the individual workshop or centralised level.

40 As was done by Aimers, Farthing, and Shugar 2012 on Mayan ceramics.

41 See relevant results from South Gaul reported by Picon 2002 and Sciau, Vendier, and Dooryhee 2002 and references therein.

42 Despite the significant distance – 12 km – from a source of the red slip used on samian at La Graufesenque, as proposed by Picon 2002, Dannell 2002, 214, makes the important point that the slip may have been refined close to source, thereby reducing considerably its weight and volume during transport to the workshop.

43 See Dannell 2002, fig. 1.

Number in Hartley and Dickinson 1979 (*) or in Dore, Greene, and Johns 1979	Origin (typology/stamp)	Date AD	Stamp (see Hartley and Dickinson 1979)
1	S Gaul	By 90	
3	S Gaul	90–110	
4	S Gaul	90–100	
5*	Lezoux	120–145	Attius
6*	C Gaul	100–120	Austrus
8*	Les Martres de Veyre	120–150	Beliniccus
10*	Lezoux	155–185	Cambus
12*	Rheinzabern	Late 2nd early 3rd	Capitolinus
18*	Lezoux	170-200	Celsianius
25	C Gaul	?	
26*	Argonne/Trier	Mid 2nd	Comus
28*	Trier	Probably Antonine	Craca
30*	Rheinzabern	Late 2nd-early 3rd	Cunissa
32	C Gaul	125–150	
35	C Gaul	?	
40*	La Madeleine	130–160	Genitor
44*	Rheinzabern	180–220	Iulianus
50*	Lezoux	140–160?	Macrianus
51*	Lezoux	150–180	Macrinus
53	C Gaul	?	
61*	Rheinzabern	180–200	Martinus
69*	C Gaul	Antonine	Mercator
70*	Lezoux	150–180	Mossius
71*	Lezoux	160–190	Mox(s)ius
73	C Gaul	?	Mox(s)ius
75*	Trier	180–220	Parentinus

Tab. 1 Samian from South Shields fort analysed by pXRF, arranged according to the number given in Dore, Greene, and Johns 1979 and where stamped (*) by Hartley and Dickinson 1979.

Number in Hartley and Dickinson 1979 (*) or in Dore, Greene, and Johns 1979	Origin (typology/stamp)	Date AD	Stamp (see Hartley and Dickinson 1979)
77	C Gaul	After 150	
85*	E Gaul	c 130–160	Remicus
86*	La Madeleine	130–160	Sabellus
88*	Trier?	Probably late Antonine	Sadiodus
91*	Lezoux	155–190	Secundinus
92*	Rheinzabern	Late 2nd-early 3rd	Severianus
97	Lezoux	Probably early Antonine	Cinnamus?
100*	Lezoux	Mid-late Antonine	Unicus
104	La Madeleine	?	
105	La Madeleine	?	
110	Lavoye	?	
114	Lavoye	?	
115	Lavoye	?	
116	Lavoye	?	
117	Lavoye	?	
119	Rheinzabern	Late 2nd early 3rd	
121	Rheinzabern	Antonine	
122	Rheinzabern	?	
124	Rheinzabern	3rd	
125	Rheinzabern	3rd	
126	Rheinzabern	?	
128	Rheinzabern	3rd	
129	Rheinzabern	?	
136	Trier	Late 2nd early 3rd	
137	Trier	?	

Tab. 1 (Continued) Samian from South Shields fort analysed by pXRF, arranged according to the number given in Dore, Greene, and Johns 1979 and where stamped (*) by Hartley and Dickinson 1979.

	Si	Ti	Al	Fe	Mn	Ca	K	V	Cr	Cr2	Cu	Zn	Rb	Sr	Zr
Till 4 Mean (7)	26.8	3371	6.2	31692	562	6923	9853	231	170	99	219	77	85	120	288
SD	0.14	57	0.1	118	21	178	350	23	17		5.8	3.1	1.3	1.7	2.8
%CV	0.4	1.7	1.7	0.4	3.7	2.6	1.8	9.8	10		2.6	4.1	1.6	1.5	1
Certified		4840		39700	490	8900	27000	53	18	270	237	70	161	109	385
% Accuracy		70		80	87	78	74	23	11	36	92	91	53	91	75
% Accuracy for USGS stds (AGV2, BCR2, GSP2 and DNC1)	93, 83, 94, 77	84, 73, 88, 54	70, 80, 76, 74	97, 100, 86, 88	91, 95, 89, 98	89, 83, 89, 97	90, 79, 90, 74	24, 61, 10, 62	13, 12, 44, 37	36	nd	95, 82, 88, 83	54, 50, 53	88, 98, 91, 99	75, 73, 84, 66
R^2	0.98	0.968	0.986	0.975	0.998	0.988	0.998	0.268	–		nd	0.938	1	0.996	0.998
Correction factor	1.15	1.33	1.33	1.07	0.93	1.11	1.2	0.39		2.78	1.09	1.15	2.04	0.94	1.33

Tab. 2 Performance characteristics of the pXRF analysis: mean, standard deviation, %coefficient of variation and certified values for Till 4 standard. % Accuracy determinations based on data for Till 4 (all elements apart from Si and Al) and USGS standards (all elements except Cu). R^2 values obtained from USGS standards and correction factors determined from USGS accuracy values. All elements expressed as ppm except Si and Al (%). See text for Cr2.

Sherd number in Dore and Gillam 1979	Si	Ti	Al	Fe	Mn	Ca	K	V	Cr	Cu	Zn	Rb	Sr	Zr
1	20.0	0.41	8.6	4.4	730	4.9	1.9	340	42	31	120	89	285	137
3	18.1	0.41	7.5	3.57	1050	6.9	2.2	325	34	134	170	85	406	122
4	18.1	0.41	8.0	2.97	570	7.2	2.0	318	60	40	102	82	330	121
5*	22.7	0.44	7.9	3.68	662	4.1	2.2	316	36	31	123	151	284	136
6	19.4	0.32	6.7	4.02	428	4.9	1.9	276	21	62	108	134	797	105
8*	21.0	0.27	7.9	3.81	791	4.9	2.0	328	39	42	157	139	266	113
10*	22.3	0.31	8.9	4.29	609	3.7	1.6	273	25	53	155	143	1331	143
12*	21.7	0.31	6.4	2.71	802	3.6	2.3	342	74	84	172	93	165	92
18*	19.8	0.32	8.3	3.29	684	6.4	1.9	239	30	48	108	154	342	111
25	24.7	0.36	9.8	3.18	872	3.4	2.3	278	31	50	126	151	289	130
26*	23.4	0.41	8.1	3.12	474	2.6	1.8	343	62	50	96	77	134	203
28*	22.2	0.46	6.5	2.69	665	2.6	4.2	291	72	62	106	92	86	145
30*	16.9	0.29	4.5	2.75	630	4.9	1.8	268	52	48	113	85	209	89
32	23.8	0.45	9.8	3.77	745	3.6	1.7	326	57	37	139	63	185	150
35	23.3	0.43	9.2	4.39	502	2.6	1.8	256	29	35	158	130	270	124
40*	18.7	0.47	7.7	4.22	894	3.8	1.4	344	57	49	168	56	200	143
44*	23.8	0.32	7.8	2.81	581	4.0	1.8	294	64	50	120	93	179	94
50*	17.8	0.3	7.0	2.92	676	5.2	1.9	245	26	30	109	155	342	101
51*	21.4	0.33	10.1	3.28	704	5.7	2.1	267	36	53	117	152	331	107
53	22.6	0.36	10.4	3.49	928	6.2	1.9	257	32	37	133	134	330	119
61*	15.6	0.27	4.7	2.67	793	8.0	1.3	286	47	47	106	87	221	90
69	23.8	0.39	10.3	3.57	602	4.8	2.1	276	36	34	163	132	337	147
70*	21.5	0.33	8.3	3.18	792	6.0	1.9	273	28	38	144	142	341	122
71*	21.3	0.33	8.8	2.86	619	6.9	1.9	271	28	32	141	138	392	119
73	20.2	0.33	7.9	2.79	1103	7.1	1.8	261	31	48	166	132	366	124
75*	20.8	0.36	7.5	3.92	1107	2.2	2.8	322	28	58	172	102	158	118

Tab. 3 The chemical compositions of the samian from South Shields. Si, Ti, Al, Fe, Ca and K expressed as % element, the remainder as ppm element.

Sherd number in Dore and Gillam 1979	Si	Ti	Al	Fe	Mn	Ca	K	V	Cr	Cu	Zn	Rb	Sr	Zr
77	24.0	0.45	8.8	3.76	869	4.8	2.4	286	40	42	143	154	333	120
85*	17.0	0.37	7.6	3.91	1032	3.6	1.6	310	47	39	138	60	189	142
86*	23.0	0.46	9.4	3.8	703	5.4	1.6	283	65	65	152	64	205	149
88*	19.2	0.31	6.3	3.54	1573	5.3	2.8	253	32	49	80	99	203	121
91*	20.5	0.31	8.2	2.83	1123	7.6	1.9	260	29	34	130	148	346	111
92*	19.5	0.29	6.1	3	1200	6.0	1.5	326	49	49	114	87	209	96
97	24.6	0.34	10.3	3.93	612	6.3	2.2	263	27	34	123	244	400	149
100	20.9	0.33	8.5	2.76	1530	7.8	1.8	300	26	53	174	126	416	124
104	20.3	0.42	7.5	3.77	1099	3.7	1.7	289	47	60	169	65	194	146
105	17.9	0.42	6.6	3.9	1393	4.6	1.4	340	52	47	195	64	207	143
110	20.3	0.41	6.2	3.12	553	1.8	1.6	109	61	37	91	74	113	201
114	24.0	0.41	8.0	3.1	589	2.4	2.0	317	65	37	94	79	136	200
115	21.8	0.4	7.0	3.47	506	2.7	1.7	334	52	31	122	80	135	214
116	19.0	0.39	6.2	3.17	509	2.8	1.7	378	50	35	101	79	134	195
117	26.0	0.46	9.8	3.42	522	1.6	2.0	333	67	31	102	80	124	206
121	24.0	0.32	7.6	3.12	658	4.0	1.9	312	57	52	132	97	194	95
122	18.7	0.29	5.5	3.28	519	5.5	1.5	296	52	48	134	91	218	95
124	18.6	0.32	5.8	3.11	559	4.5	1.6	315	59	44	137	96	203	97
125	23.1	0.35	8.2	3.58	675	4.7	1.7	305	55	45	127	81	225	102
126	18.2	0.31	5.2	2.93	589	5.5	1.5	346	59	56	271	92	197	97
128	24.3	0.39	7.3	3.74	609	2.8	1.6	281	75	66	153	85	178	104
129	24.7	0.41	8.3	3.75	515	2.3	1.8	283	84	49	134	88	159	102
136	15.8	0.29	4.8	3.8	1081	5.7	2.7	347	72	47	128	89	213	98
137	23.3	0.43	7.4	2.8	668	1.4	3.5	288	55	69	124	94	81	154

Tab. 3 (Continued) The chemical compositions of the samian from South Shields.

Site	No. of samples	Al	Ti	Fe	Mn	Ca	K	Cr	Rb	Sr	Zn	Zr
Rheinzabern mean	51	9.9	0.43	4.0	0.043	4.2	2.71	125	184	186	123	116
Coefficient of variation (CV%)		1.8	0.17	2.4	13.2	1.8	3.58	4.7	5.5	15	11	9.1
Rheinzabern (ICP) mean	18	10	0.49	3.9	0.047	4.5	2.30	94		204	121	
Standard deviation (sd)		0.61	0.07	0.3	0.016	1.3	0.18	15		31	10	
Group 1 mean	12	8.6	0.43	3.3	0.063	5.1	2.04	168	183	185	164	128
sd		1.8	0.06	0.4	0.018	1.7	0.3	32	10	21	51	6
Trier (ICP) mean	4	8.9	0.485	4.6	0.085	3.7	3.85	107		200?	150	
Sd		0.13	0.02	0.6	0.016	0.7	0.32	21		20	7	
Avocourt (ICP) mean	15	9.6	0.64	4.3	0.031	1.6	2.50	87		101	108	
Sd		0.4	0.024	0.2	0.008	0.5	0.12	10		12	11	
Blickweiler mean	12	10.6	0.47	4.8	0.064	4.3	4.77	98	219	133	104	138
CV		1.6	3.17	3.9	3.26	17.1	3.17	6.1	4	9.6	4.1	4.4
Chemery mean	9	10.1	0.5	4.4	0.086	3.3	4.47	95	217	129	92	192
CV		0.8	3.25	1.7	5.9	1.6	1.42	2.5	1.9	3.2	8	5.6
Lezoux mean	15	11.3	0.45	3.7	0.057	7.6	2.83	82	284	307	144	150
CV		1.7	3.3	4.3	16.3	12.1	4.67	5.4	6	13	17	13
Group 2 mean	9	11.5	0.44	3.5	0.075	6.6	2.31	81	317	334	152	163
Sd		1.3	0.05	0.6	0.028	1.5	0.23	11	66	38	24	21
La Graufesenque mean	13	11.9	0.59	4.2	0.056	7.4	3.13	134	173	354	119	163
CV		0.6	1.4	0.7	14	6.1	3.33	2.8	6.2	21	8.9	7.6
Lyon mean	5	7.7	0.32	3.8	0.101	12.6	1.8	76	120	260	81	123
South Gaul this study (mean and range)	3	10.7 (10.0-11.5)	0.55 (0.54-0.55)	3.9 (3.2-4.7)	0.073 (0.053-0.098)	7.0 (5.4-8.0)	2.78 (2.6-3.0)	126 (95-168)	174 (167-181)	330 (268-382)	151 (117-196)	169 (161-135)

Tab. 4 Reference data from Schneider 1978 (WD-XRF) and Hart et al. 1987 (marked ICP); corrected pXRF data for Rheinzabern, Lezoux and South Gaul groups appear in grey highlight. Al to K are % element, the remainder are ppm element; sd standard deviation.

Number and source	Fe %	Ca %	K %	Al%	K/Ca slip	K/Ca body	K/Al slip	K/Al body
1 SG	4.3	2.4	3.48	8.8	1.46	0.39	0.39	0.22
3 SG	4.1	1.9	6.69	9.1	3.54	0.32	0.74	0.29
4 SG	4.1	1.2	4.53	13.3	3.78	0.28	0.34	0.25
5 LZ	4.0	2.4	3.22	9.6	1.34	0.53	0.33	0.28
6 CG	4.7	1.4	3.67	12.4	2.62	0.39	0.30	0.28
8 LM	4.4	1.9	3.12	9.8	1.66	1.50	0.32	0.25
10 LZ	4.5	2.3	2.53	14.5	1.11	1.33	0.17	0.25
12 RZ	3.0	1.9	3.36	11.4	1.75	0.63	0.29	0.36
18 LZ	4.9	1.9	2.79	14.6	1.46	0.36	0.19	0.23
26 AR/T	3.1	1.8	2.25	10.4	1.28	1.49	0.22	0.24
28 T	3.1	1.5	4.16	13.3	2.70	1.06	0.31	0.21
30 RZ	3.4	3.5	2.36	11.1	0.68	0.40	0.21	0.26
40 LAM	4.0	2.5	2.33	12.4	0.93	0.50	0.19	0.18
44 RZ	4.8	1.0	1.23	8.2	1.17	0.88	0.15	0.21
50 LZ	4.3	1.8	3.31	13.3	1.85	1.06	0.25	0.20
51 LZ	4.5	2.5	2.69	12.4	1.08	1.08	0.22	0.23
61 RZ	3.8	1.8	3.58	12.2	1.95	1.53	0.29	0.25
69 CG	5.0	2.0	2.36	14.4	1.20	0.44	0.16	0.20
70 LZ	3.0	2.5	2.51	10.0	1.02	1.01	0.19	0.25
71 LZ	4.1	3.0	3.04	15.8	1.02	1.50	0.19	0.26
75 T	4.6	2.2	3.58	11.8	1.65	1.25	0.30	0.37
85 EG	3.9	2.8	2.09	12.1	0.75	1.14	0.17	0.20
86 LAM	3.8	3.9	2.08	11.6	0.53	1.40	0.18	0.20
91 LZ	3.9	2.5	4.32	13.4	1.70	0.25	0.32	0.23
92 RZ	3.5	2.5	2.58	15.0	1.01	1.46	0.17	0.24
100 LZ	4.0	4.3	1.94	13.1	0.45	1.17	0.15	0.23
105 LAM	4.1	3.0	1.89	10.6	0.63	0.30	0.18	0.21

Tab. 5 Fe, Ca, K and Al contents and K/Ca in the red slip and K/Ca in the body. Instances of the body having a higher K/Ca ratio than the slip are grey highlighted.

Number and source	Fe %	Ca %	K %	Al%	K/Ca slip	K/Ca body	K/Al slip	K/Al body
110 LV	4.8	1.0	1.23	8.2	1.17	0.91	0.15	0.26
115 LV	4.1	1.2	1.52	11.3	1.32	0.65	0.13	0.25
116 LV	3.5	1.2	1.70	14.4	1.37	0.60	0.12	0.25
121 RZ	4.0	1.5	2.68	14.3	1.74	0.48	0.19	0.25
122 RZ	3.5	2.0	2.71	12.2	1.33	0.27	0.22	0.28
124 RZ	3.5	1.7	2.79	11.6	1.68	0.36	0.24	0.28
125 RZ	3.7	2.5	2.50	15.3	1.02	0.36	0.16	0.21
136 T	4.4	2.9	4.21	13.0	1.47	0.49	0.32	0.57
137 T	3.0	0.8	4.16	12.1	4.98	2.59	0.34	0.48

Tab. 5 (Continued) Fe, Ca, K and Al contents and K/Ca in the red slip and K/Ca in the body. Instances of the body having a higher K/Ca ratio than the slip are grey highlighted.

Bibliography

Aimers, Farthing, and Shugar 2012
Jim J. Aimers, Dori J. Farthing, and Aaron N. Shugar. "Handheld XRF Analysis of Maya Ceramics. A Pilot Study Representing Issues Related to Quantification and Calibration." In *Handheld XRF for Art and Archaeology*. Ed. by A. N. Shugar and J. L. Mass. Leuven: Leuven University Press, 2012, 423–448.

Aloupi-Siotis 2020
Eleni Aloupi-Siotis. "Ceramic Technology: How to Characterise Black Fe-Based Glass-Ceramic Coatings." *Archaeological and Anthropological Sciences* 12 (2020), 191–206.

Dannell 2002
Geoffrey B. Dannell. "Law and Practice. Further Thoughts on the Organization of the Potteries at La Graufesenque." In *Céramiques de la Graufesenque et autres productions d'époque romaine. Nouvelles recherches*. Ed. by M. Genin and A. Vernhet. Montagnac: Monique Mergoil, 2002, 211–242.

Dore and Gillam 1979
John Dore and J. P. Gillam, eds. *The Roman Fort at South Shields. Excavations 1875–1975*. Society of Antiquaries of Newcastle-upon-Tyne, Monograph Series. Newcastle: Society of Antiquaries, 1979.

Dore, Greene, and Johns 1979
John Dore, Kevin Greene, and Catherine Johns. "The Decorated Ware." In *The Roman Fort at South Shields. Excavations 1875–1975*. Ed. by J. Dore and J. P. Gillam. Society of Antiquaries of Newcastle-upon-Tyne, Monograph Series. Newcastle: Society of Antiquaries, 1979, 107–127.

Forster et al. 2011
Nicola Forster, Peter Grave, Nancy Vickery, and Lisa Kealhofer. "Non-Destructive Analysis Using PXRF. Methodology and Application to Archaeological Ceramics." *X-Ray Spectrometry* 40 (2011), 389–398.

Frankel and Webb 2012
David Frankel and Jennifer Webb. "Pottery Production and Distribution in Prehistoric Bronze Age Cyprus. An Application of PXRF Analysis." *Journal of Archaeological Science* 39 (2012), 1380–1387.

Fulford 2013
Michael Fulford. *Seeing Red. New Economic and Social Perspectives on Gallo-Roman Sigillata*. London: Institute of Classical Studies, 2013.

Fülle 1997
Gunnar Fülle. "The Internal Organisation of the Arretine Terra Sigillata Industry. Problems of Evidence and Interpretation." *Journal of Roman Studies* 87 (1997), 111–153.

Genin and Vernhet 2002
Martine Genin and Alain Vernhet. *Céramiques de la Graufesenque et autres productions d'époque romaine: nouvelles recherches hommages à Bettina Hoffmann*. Montagnac: Editions Monique Mergoil, 2002.

Goren, Mommsen, and Klinger 2011
Yuval Goren, Hans Mommsen, and Jörg Klinger. "Non-Destructive Provenance Study of Cuneiform Tablets Using Portable X-Ray Fluorescence (pXRF)." *Journal of Archaeological Science* 38 (2011), 684–696.

Greene 1992
Kevin Greene. *Roman Pottery*. London: British Museum Press, 1992.

Hart et al. 1987
F. Alan Hart, Jeremy M. V. Storey, Stuart J. Adams, Robin P. Symonds, and J. Nicholas Walsh. "An Analytical Study, Using Inductively Coupled Plasma (ICP) Spectrometry, of Samian and Colour-Coated Wares from the Roman Town at Colchester Together with Related Continental Samian Wares." *Journal of Archaeological Science* 14 (1987), 577–598.

Hartley 1972
Brian R. Hartley. "The Roman Occupations of Scotland. The Evidence of Samian Ware." *Britannia* 3 (1972), 1–55.

Hartley and Dickinson 1979
Brian R. Hartley and Brenda M. Dickinson. "The Potter's Stamps." In *The Roman Fort at South Shields. Excavations 1875–1975*. Ed. by J. Dore and J. P. Gillam. Society of Antiquaries of Newcastle-upon-Tyne, Monograph Series. Newcastle: Society of Antiquaries, 1979, 100–106.

Hartley and Dickinson 2008–2012
Brian R. Hartley and Brenda M. Dickinson. *Names on Terra Sigillata. An Index of Makers' Stamps & Signatures on Gallo-Roman Terra Sigillata (Samian Ware)*. London: Institute of Classical Studies, 2008–2012.

Jones and Campbell 2016
Richard E. Jones and Louisa Campbell. "Non-Destructive Analysis of Samian Ware from Scottish Military Sites." In *Insight from Innovation. New Light on Archaeological Ceramics. Papers in Honour of David Peacock*. Ed. by S. Coxon, E. Sibbesson, and B. Jervis. St Andrews: Highfield Press, 2016, 118–136.

Macdonald and Park 1906
George Macdonald and Alex Park. *The Roman Forts on the Bar Hill, Dumbartonshire*. Glasgow: James Maclehose & Sons, 1906.

Maggetti 1981
Marino Maggetti. "Composition of Roman Pottery from Lausanne (Switzerland)." In *Scientific Studies in Ancient Ceramics*. Ed. by M. J. Hughes. British Museum Occasional Paper 19. London: British Museum, 1981, 33–49.

Miller 1922
Stuart N. Miller. *The Roman Fort at Balmuildy (Summerston, Near Glasgow) on the Antonine Wall*. Glasgow: Maclehose, Jackson & Co., 1922.

Miller 1928
Stuart N. Miller. *The Roman Fort at Old Kilpatrick*. Glasgow: Jackson, Sylie & Co., 1928.

Picon 1997
Maurice Picon. "Les argiles des vernis rouges et jaunes des céramiques sigillées de La Graufesenque (Aveyron) et la céladonite utilisée comme pigment vert dans les peintures murals romaines." *Revue d'Archéométrie* 21 (1997), 86–96.

Picon 2002
Maurice Picon. "Les modes de cuisson, les pâtes et les vernis de la Graufesenque. Une mise au point." In *Céramiques de la Graufesenque et autres productions d'époque romaine. Nouvelles recherches*. Ed. by M. Genin and A. Vernhet. Montagnac: Monique Mergoil, 2002, 139–164.

Picon, Vichy, and Meille 1971
Maurice Picon, Michèle Vichy, and Eliane Meille. "Composition of the Lezoux, Lyon and Arezzo Samian Ware." *Archaeometry* 13 (1971), 191–208.

Robertson 1964
Anne S. Robertson. *The Roman Fort at Castledykes*. Edinburgh: Oliver & Boyd, 1964.

Robertson, Scott, and Keppie 1975
Anne S. Robertson, Margaret E. Scott, and Lawrende Keppie. *Bar Hill: A Roman Fort and Its Finds*. British Archaeological Reports 16. Oxford: BAR Publishing, 1975.

Schneider 1978
Gerwulf Schneider. "Anwendung quantitativer Materialanalysen auf Herkunftsbestimmungen antiker Keramik." *Berliner Beiträge zur Archäometrie* 3 (1978), 63–122.

Schnurbein, Lasfargues, and Picon 1982
Siegmar von Schnurbein, Jacques Lasfargues, and Maurice Picon. *Die unverzierte Terra Sigillata aus Haltern*. Münster: Aschendorff, 1982.

Sciau, Languille, et al. 2005
Philippe Sciau, Marie-Angélique Languille, Eric Dooryhee, Thomas Martin, and Alain Vernhet. "Studies of the Southern Gaul Sigillata Ceramics. The Workshops of la Graufesenque and Montans." In *Understanding People through Their Pottery. Proceedings of the 7th European Meeting on Ancient Ceramics (EMAC'03)*. Ed. by I. Prudêncio, I. Dias, and J. C. Waerenborgh. Lisbon: Instituto Português de Arqueologia, 2005, 243–249.

Sciau, Relaix, et al. 2006
Philippe Sciau, Sabrina Relaix, Christian Roucau, and Yolande Kihn. "Microstructural and Microchemical Characterization of Roman Period Terra Sigillate Slips from Archeological Sites in Southern France." *Journal of the American Ceramic Society* 89 (2006), 1053–1058.

Sciau, Sanchez, and Gliozzo 2020
Philippe Sciau, Corinne Sanchez, and Elisabetta Gliozzo. "Ceramic Technology: How to Characterize Terra Sigillata Ware." *Archaeological and Anthropological Sciences* 12 (2020), 211–233.

Sciau, Vendier, and Dooryhee 2002
Philippe Sciau, Laure Vendier, and Eric Dooryhee. "La diffraction des rayons X est-elle adaptée à l'étude des sigillées?" In *Céramiques de la Graufesenque et autres productions d'époque romaine. Nouvelles recherches*. Ed. by M. Genin and A. Vernhet. Montagnac: Monique Mergoil, 2002, 171–180.

Stanfield and Simpson 1958
Joseph A. Stanfield and Grace Simpson. *Central Gaulish Potters*. London: Oxford University Press, 1958.

Tite, Bimson, and Freestone 1982
Michael S. Tite, Mavis Bimson, and Ian C. Freestone. "An Examination of the High Gloss Surface Finishes on Greek Attic and Roman Samian Wares." *Archaeometry* 24 (1982), 117–126.

Tomber and Dore 1998
Roberta Tomber and John Dore. *The National Roman Fabric Reference Collection. A Handbook*. London: Museum of London Archaeology Service, 1998.

Tyers 1996
Paul A. Tyers. *Potsherd. Atlas of Roman Pottery*. London: B. T. Batsford, 1996.

Widemann et al. 1975
Francois Widemann, Maurice Picon, Frank Asaro, Helen V. Michel, and Isidor Perlman. "A Lyons Branch of the Pottery-Making Firm of Ateius of Arezzo." *Archaeometry* 17 (1975), 45–59.

Wolf and Wilson 2007
Ruth E. Wolf and Stephen A. Wilson. *USGS Fact Sheet 2007-3056*. Washington D. C.: US Geological Survey, 2007.

Illustration and table credits

ILLUSTRATIONS: **1** L. Campbell. **2–3** L. Campbell after Dore, Greene, and Johns 1979. **4–10** R. Jones. **TABLES:** **1–5** R. Jones and L. Campell.

RICHARD JONES

Richard Jones is Senior Lecturer in Archaeology at the University of Glasgow. His research interests are artefact (mainly ceramic) analysis, Aegean archaeology, and geophysical and geochemical survey.

Dr. Richard Jones
Archaeology, Gregory Building
University of Glasgow
Glasgow G12 8QQ, UK
E-mail: richard.jones@glasgow.ac.uk

LOUISA CAMPBELL

Louisa Campbell is a Lord Kelvin-Adam Smith Fellow in Archaeology at the University of Glasgow. She was coordinator of the EAA conference in Glasgow in 2015. Her research interests are artefact analysis (mainly Roman material culture), the archaeology of Roman Scotland, and the practical application of theoretical constructs in situations of culture contact.

Dr. Louisa Campbell
Archaeology, Gregory Building
University of Glasgow
Glasgow G12 8QQ, UK
E-mail: louisa.campbell@glasgow.ac.uk

Hans-Joachim Mucha, Hans-Georg Bartel

From Univariate to Multivariate Clustering with Application to Portable XRF Data

Summary

Nowadays, portable XRF makes it quite easy to obtain high-dimensional chemical fingerprints of archaeological objects, after which cluster analysis can be applied for finding subpopulations (clusters). We propose a bottom-up variable selection in cluster analysis, starting with univariate clustering. The hope is that the structure of interest may be contained in only a small subset of variables. Our proposal is based on bootstrapping. We look for clusters that can be reproduced to a high degree under resampling schemes. In applications related to archaeometry, our goal is to choose a model that is as simple as possible. In the case of Bronze Age pottery from Corneşti Iarcuri, we found that stable clustering results are based on up to three variables out of 18, namely Cl, Zr, and Y.

Keywords: clustering; bootstrapping; validation; variable selection; portable XRF; Bronze Age pottery; provenance determination

Mit der portablen XRF werden hochdimensionale chemische Fingerabdrücke von archäologischen Objekten gemacht. Die Clusteranalyse kann angewendet werden, um homogene Gruppen von diesen Objekten zu finden. Wir schlagen hier eine Bottom-up-Variablenauswahl in der Clusteranalyse vor, die mit univariatem Clustering beginnt. Wir erwarten, dass die Clusterstruktur in einer nur kleinen Teilmenge von Variablen enthalten ist. Der Ansatz basiert auf Bootstrapping, um Cluster zu finden, die stabil sind. Bei Anwendungen in der Archäometrie können wir zeigen, dass damit ein Modell konzipiert wird, das so einfach wie möglich, aber nicht einfacher ist. Im Fall bronzezeitlicher Keramik aus Corneşti-Iarcuri haben wir herausgefunden, dass stabile Cluster auf nur drei von den insgesamt 18 Variablen basieren, nämlich auf Cl, Zr und Y.

Keywords: Clusteranalyse; Bootstrapping; Validierung; Variablenselektion; portable XRF; Bronzezeit-Keramik; Herkunftsbestimmung

Morten Hegewisch, Małgorzata Daszkiewicz und Gerwulf Schneider (eds.) | Using pXRF for the Analysis of Ancient Pottery – an Expert Workshop in Berlin 2014 | Berlin Studies of the Ancient World 75 (ISBN TODO; DOI: 10.17171/3-75) | www.edition-topoi.org

1 Introduction

Can I see where it originates solely by watching an archaeological object (marble, ceramics, glass)? Certainly not. Therefore, making a chemical fingerprint of the object under consideration is the usual starting point for solving archaeological problems such as the decision about proveniences. Herewith the objects are characterized by around 20 variables (i.e., chemical elements). Nowadays, portable XRF makes it quite easy to get chemical fingerprints. Subsequently, multivariate statistical methods such as discriminant analysis and cluster analysis (unsupervised classification) can be applied to the XRF data. They can consider many variables simultaneously. However, usually, the more variables are in the model the more instable the solution becomes. And, the higher the measurement errors the more difficult the clustering task becomes.

In clustering, many variables are considered simultaneously in order to divide a usually big set of objects into smaller groups. As a result, the objects within a cluster should be similar to each other, whereas objects from different clusters should be as dissimilar as possible to each other. That is, we are looking usually for clusters that are as homogeneous as possible with respect to some measure of similarity/distance taking into account all variables. However, in practice, there are often several masking and noisy variables without any cluster structure that make the discovery of clusters difficult and often impossible. In addition, portable XRF analysis has the drawback of increased measurement errors.

Therefore, here we propose a bottom-up variable selection in cluster analysis starting with univariate clustering, and then we are going ahead with bivariate, trivariate, and multivariate clustering. By doing so, we hope to find a stable cluster structure of interest based on a small subset of variables. For this aim, an approach for the investigation of the stability of clustering results is recommended that is based only on resampling techniques. So, it is very general and can be applied to almost all clustering algorithms. Without loss of generality, here we consider hierarchical cluster analysis methods such as the well-known *Ward*'s minimum variance method. This is mainly because of the availability of intuitive visualization techniques such as dendrograms and heat maps.

2 From univariate sorting to multivariate clustering

In the univariate case, clustering simply means that, first, the set of objects is reordered based on the measurements of a single variable, and, second, the set of total ordered objects is divided in homogeneous regions (intervals, bins). For example, archaeological objects are ordered by the concentration values of a chemical element, and then we are looking for gaps and dense regions in the ordered values to identify clusters. This is the

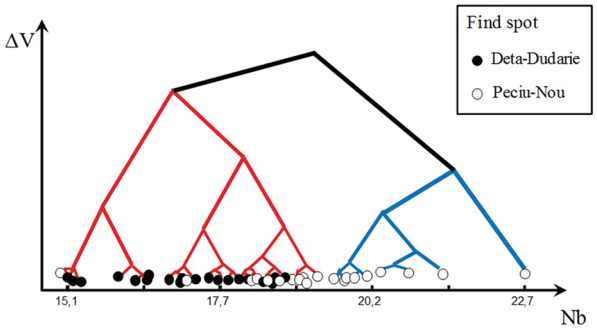

Fig. 1 Non-equidistant dendrogram of 40 measurements (in ppm) of Nb located on the real line (axis of abscissae).

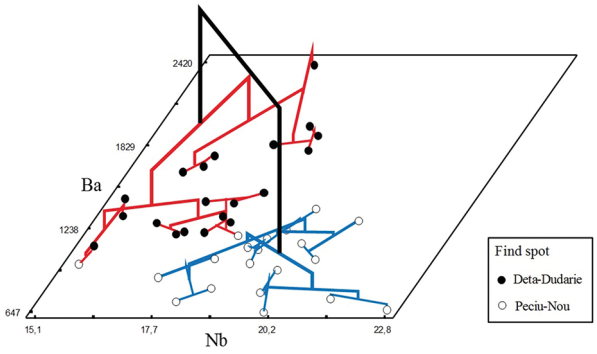

Fig. 2 Plot-dendrogram of bivariate hierarchical clustering of 40 objects.

way of sorting an archaeologist is familiar with. In high-dimensional problems, i.e., in comparison to univariate statistical analysis, the use of computers is necessary, especially when the number of objects is also high. Without loss of generality, here we consider hierarchical cluster analysis methods. This is mainly because of the availability of intuitive visualization techniques such as dendrograms (Figs. 1 and 2) and heat maps of distances. For instance, hierarchical agglomerative clustering appears self-explanatory: the corresponding binary tree (dendrogram) presents all the clusters (either disjoint or included one into the other) that were established when starting with the single objects as terminal (trivial) clusters in the process of agglomeration. It presents a complete hierarchy of partitions by cutting the dendrogram at different levels of distances ΔV between clusters.

Fig. 1 shows the univariate hierarchical clustering of $I = 40$ archaeological objects. In this case the minimum variance method of *Ward* is used.[1] This method is based on the squared Euclidean distance. These 40 objects are ceramics that were found in two different locations, namely Deta Dudarie and Peciu-Nou. These are two archaeological

1 See below and Ward 1963.

Site		Abbr.	45°y'N	21°x'E	Height a.s.l. / m	Sample size #
Corneşti	Cornet	CC				64
	Iacuri	CI				153
Hodoni Puszta		HP	54	5	100	30
Timişoara Fratelia		TF	45	14	90	50
Giroc Mezcal		GM	42	14	80	60
Peciu-Nou		PN	36	3	89	20
Voiteg Voiteni		VV	28	4	88	50
Deta Dudarie		DD	24	14	100	20

Tab. 1 Geographic information and sample sizes of the sites.

sites out of all in all eight locations of Bronze Age pottery from Corneşti Iarcuri (see Tab. 1, Fig. 3).[2] (The whole dataset of 447 objects is investigated below). In Fig. 1, the objects are represented by points that in addition contain the information of their location (total black or white filled circles). The univariate information (variable) is the content of Nb that is located on the real line (axis of abscissae), and so the approximate measurement values can be taken from the picture. Each point is a terminal node in the tree. The ordinate represents the increment of within-clusters variance ΔV (in logarithmic scale) when merging two clusters (see below for details). Obviously, univariate cluster analysis is nothing else than reordering the set of objects based on a single variable followed by dividing the total order of objects into homogeneous regions.

The dream of statisticians is a univariate setting (i.e., the simplest model) that explains the archaeological model. But, that is often a dream only, as one can see in Fig. 1 where obviously the element Nb is unable to differentiate between the two different locations. When moving to two and more variables the total order is usually lost. In addition, a scaling problem occurs when the variables are measured in different scales such as weight percent and ppm. Fig. 2 shows the dendrogram of the bivariate hierarchical *Ward*'s clustering of the 40 objects that is projected on the scatterplot of the corresponding variables Nb and Ba. Here the two groups of ceramics look much better separated as it is the case in the univariate clustering in Fig. 1. Two objects from Peciu-Nou were

2 See their contribution in this volume.

Fig. 3 Detail of the geological map of Romania with the archaeological locations.

classified into the wrong cluster. However, in the scatterplot, it is possible to divide the two different locations perfectly by a line, i.e., a linear separation without errors is possible.

Without any doubt, this small example shows that better results can be obtained by adding further variables. In general, the hope is that the separation between the different locations can be further improved by including additional variables. However, it is a theoretical hope that the more information is used the better are the statistical results and conclusions. In applications, our experience is that the model has to be chosen as simple as possible, but not simpler. That is a wide field of investigation, simply too extensive for this paper. It is an ongoing research topic.[3]

2.1 *Ward*'s hierarchical clustering in a nutshell

Without loss of generality, here we consider hierarchical cluster analysis methods, and the well-known *Ward*'s minimum variance method in more detail (see Figs. 1 and 2: dendrograms for direct reading of hierarchical clustering results). Both the latter and

3 Mucha and Bartel 2015b.

the most frequently used partitional K-means method are based on the same simplest additive Gaussian cluster analysis model.

Let a sample of I independent observations be given in R^J. The corresponding data matrix consisting of I rows and J columns (variables) is denoted by $\mathbf{X} = (x_{ij})$, where the element x_{ij} provides a value for the jth variable describing the ith observation. Observations can be archaeological objects such as ceramics, tiles or bricks. In cluster analysis, it is supposed that the set of I observations stem from at least two different subpopulations (clusters). Partitional cluster analysis such as the well-known K-means method aims at finding a partition $P(I,K) = \{C_1, C_2, \ldots, C_K\}$ of $C = \{1, 2, \ldots I\}$ for a fixed K with

$$\bigcup_{k=1}^{K} C_k = I$$

and

$$C_k \cap C_l = \emptyset, \text{for every pair } C_k \text{ and } C_l, k, l = 1, 2, \ldots, K,$$

where the clusters C_k we are looking for should be as homogeneous as possible in some sense. For instance, the sum of within-clusters sum of squares criterion (shortly: sum of squares = SS)

$$W_k = \text{tr}\left(\sum_{k=1}^{K} \mathbf{W}_k\right) \tag{1}$$

has to be minimized with respect to a partition into K clusters, where $\mathbf{W}_k$ is the sample cross- product matrix for the kth cluster C_k:

$$\mathbf{W}_k = \sum_{i \in C_k} (\mathbf{x}_i - \bar{\mathbf{x}}_k)(\mathbf{x}_i - \bar{\mathbf{x}}_k)^T \tag{2}$$

Here $\bar{\mathbf{x}}_k$ is the usual maximum likelihood estimate of expected values in cluster C_k. The SS is fundamental for the inferential statistics and the descriptive statistics. In (1), pairwise distances occur not directly in the case of a Gaussian distribution, but indirectly they are introduced via the corresponding density function.[4] It is well known that the criterion (1) can be written in the following equivalent form without the explicit specification of cluster centers (centroids) $\bar{\mathbf{x}}_k$ by

$$W_k = \sum_{k=1}^{K} \frac{1}{n_k} \sum_{i \in C_k} \sum_{\substack{h \in C_k \\ h > i}} d_{ih}, \tag{3}$$

4 Mucha and Bartel 2015b.

where

$$d_{ih} = d(\mathbf{x}_i, \mathbf{x}_h) = (\mathbf{x}_i - \mathbf{x}_h)^T (\mathbf{x}_i - \mathbf{x}_h) = \|\mathbf{x}_i - \mathbf{x}_h\|^2 \tag{4}$$

is the squared Euclidean distance between two observations i and h, and n_k is the cardinality of the cluster C_k. Therefore, and because of its more general meaning, a distance matrix $\mathbf{D} = (d_{ih})$ can be the starting point for practical cluster analysis.

There are at least two well-known clustering techniques for minimizing the sum of squares criterion (1) based on pairwise distances: the partitional *K*-means method works iteratively by exchanging observations between clusters starting from an initial partition,[5] and the hierarchical *Ward*'s method starts with $K = I$ terminal clusters $\{\mathbf{x}_i\}$ and proceeds stepwise by agglomerative grouping.[6] It is worth noting that by moving from pairwise squared Euclidean distances d_{ih} (4) to within-cluster sum of squares $w\{i, h\}$ of the two observations i and h, it holds simply: $w\{i, h\} = d_{ih}/2$. I.e., the first step of the hierarchical *Ward*'s method is the agglomeration of the two observations having the minimum Euclidean distance. As a result one gets the first ΔV value, see the ordinate in Fig. 1. In general, the increment of within-clusters variance ΔV is given by

$$\Delta V_K = W^*_{K-1} - W^*_K \tag{5}$$

when moving from K clusters to $K - 1$ cluster(s).

The advantage of using distances is that they are always fixed during the optimization of (3). This is different from (1) where the sample cross product matrices (2) and the cluster centers $\bar{\mathbf{x}}_k$ are dependent on partitioning. This advantage can make especially the validation of hierarchical clustering results by resampling techniques computationally effective (see below). Moreover, because the distance matrix $\mathbf{D} = (d_{ih})$ (4) is additive one can think to work with J distance matrices $\mathbf{D}^{(j)} = (d^{(j)}_{ih}), j = 1, 2, \ldots, J$, where $\mathbf{D} = \sum_{j=1}^{J} \mathbf{D}^{(j)}$. That's quite important from the computational point of view for our approach of variable selection in clustering that is proposed in the next section.

Usually, the partitional *K*-means method and the hierarchical *Ward*'s method find only sub-optimum solutions. The latter presents usually unique solutions. Moreover, by cutting a dendrogram at several different levels of cluster distances ΔV one gets the whole set of (nested) partitions into $K = 2, K = 3, \ldots$clusters at once (Fig. 1). The iterative solution of the *K*-means method depends on the initial partition.[7]

5 Mucha 1992.
6 Ward 1963.
7 Mucha 2009.

2.2 Bottom-up variable selection in cluster analysis

Above, in the toy data example, we started from univariate clustering before coming to the intrinsic matter: multivariate clustering. Now we propose to do this in a bottom-up fashion by adding the most informative variable to the model at each step. So, when we find the best (i.e., most stable) univariate clustering, we are going ahead by looking for the best bivariate clustering, trivariate clustering, and so on. This bottom-up variable selection in clustering stops at a set of informative variables that is usually much smaller than the set of all original variables.[8] The basic principle behind the model selection process is the investigation of the stability of clustering results by bootstrapping (simulation studies) in order

- to find an appropriate number of clusters,
- to assess the stability of each individual cluster, and
- to evaluate the degree of cluster membership of each archaeological object.

2.3 Stability of clustering results

The assessment of stability in cluster analysis is highly related to the main difficult problem of determining the number of clusters present in the data. This has been the subject of many investigations and papers considering different resampling techniques as practical tools. As already shown above, clustering techniques can find homogeneous groups of ceramics. However, cluster analysis usually presents always clusters – even in the case of no structure in the data. Moreover, hierarchical clustering presents nice dendrograms in any case containing all the clusters that are established during the process of agglomeration (see Fig. 1). Obviously, in every agglomeration step an increasing amount of information is lost. The main question is: How many clusters are there? Or, in other words, when should the agglomeration process be stopped?

Let us suppose that the cluster analysis algorithm does a good (accurate) job, i.e., it is able to reflect an appropriate model of the data. This is because otherwise the validation can give the right answer to the wrong question. The main question then will be: is there really a cluster structure in the data? And if it is the case, how many clusters are there?

Therefore, a validation of clustering results based on resampling techniques is highly recommended. This validation can be considered as a three level assessment of stability:

8 For details see Mucha and Bartel 2015a.

1. The first and most general level is to decide on the appropriate number of clusters. This decision is based on such well-known measures of correspondence between partitions such as the *Rand*'s index[9] and the *adjusted Rand*'s index R_K of Hubert and Arabie.[10]

These are pair-counting-measures[11] with maximum value equals 1.

2. The stability of each individual cluster C_k is assessed based on measures of similarity between sets,[12] e.g., the symmetric measure of *Jaccard* γ_k. From many applications we know that it makes sense to investigate the specific stability of clusters of the same clustering on the same data. One can often observe that the clusters have a quite different stability.[13] Some of them are very stable. Thus, they can be reproduced and confirmed to a high degree, for instance, by bootstrap simulations. They are homogeneous inside and well separated from each other. Moreover, sometimes they are located far away from the main body of the data like outliers. On the other side, hidden and tight neighboring clusters are more difficult to detect and they cannot be reproduced to a high degree. In order to assess the stability of a partition into K clusters, these individual stability values can be aggregated in some way to a total measure such as the averaged *Jaccard* measure γ_K. The latter is the average over all individual γ_k, $k = 1, 2, \ldots, K$.

In the third and most detailed level of validation, the reliability of the cluster membership of each individual object can be assessed.[14]

The validation of clustering results is often based on resampling techniques. There are different resampling techniques. Without loss of generality, here bootstrapping is used. The latter is resampling with replacement.[15]

2.4 Application to archaeometry: portable XRF data of ceramics

Concretely, the application of bottom-up variable selection in cluster analysis to Bronze Age pottery data is presented. The data under investigation comes from eighth archaeological sites in the Timiş district (Western Romania, see Tab. 1 and Fig. 3) and was kindly provided by Małgorzata Daszkiewicz and Berhard Heeb.[16] In detail, $I = 447$ pottery fragments were analyzed by p-ED-XRF. Altogether 18 variables were taken into account: seven oxides (SiO_2, TiO_2, Al_2O_3, Fe_2O_3, MnO, CaO, K_2O, in %) and eleven trace elements (Cl, V, Cr, Zn, Rb, Sr, Y, Zr, Nb, Ba, Pb, in ppm). (P_2O_5 was indeed measured but not used for purpose of clustering because of possible soil contamination.) Tab. 1

9 Rand 1971.
10 Hubert and Arabie 1985.
11 Mucha 2009; Mucha and Bartel 2015a.
12 Henning 2007.
13 Dolata, Mucha, and Bartel 2007; Mucha 2009; Mucha, Bartel, et al. 2015.
14 Mucha 2009.
15 Mucha 2014.
16 See their contribution in this volume.

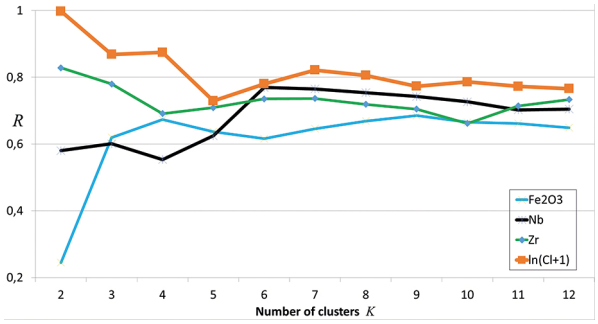

Fig. 4 The ARI R_K (average) versus the number of clusters in univariate hierarchical clustering. For $K = 2$, $K = 3$, and $K = 4$, the R_K values looks quite different for the four variables selected for presentation. For instance, the two cluster solution based on Fe_2O_3 is not stable.

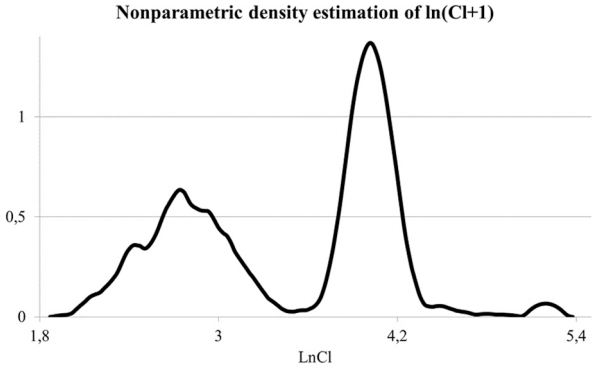

Fig. 5 Nonparametric density estimation of the most informative variable: Chlorine. Concretely, $\ln(\mathrm{Cl} + 1)$ was investigated using the bandwidth 0.15. Note: In addition, five outliers (values 5.55, 5.62, 6.49, 6.63, and 7.09) were trimmed to 5.3.

presents the geographic coordinates and the sample sizes of the eight sites. Fig. 3 shows the corresponding map.

We start with univariate clustering including investigation of stability of results. Fig. 4 shows an extract from the results of investigation of stability of univariate *Ward*'s clustering based on the adjusted *Rand*'s index (ARI) R_K. Here only the results of four out of the 18 variables were presented. For each variable, the original cluster analysis was compared with 250 bootstrap cluster analyses. Without any doubt, univariate clustering based on Cl has the highest ARI R_K value of stability, especially for $K = 2$ clusters. So, Cl is the most informative variable with respect to clustering. Fig. 5 shows the nonparametric density estimation of the transformed and trimmed variable $\ln(\mathrm{Cl} + 1)$ (as it is used in the statistical investigations because of outliers). The density estimate also clearly votes for two clusters. Without any doubt, the density of $\ln(\mathrm{Cl})$ is not the result of only one underlying Gaussian distribution. There is a very well separated, very dense region right from the gap in the middle.

As the final result of the first step of the proposed bottom-up variable selection procedure, the univariate clustering based on Cl is the most stable one. Now we are going ahead by looking for the best partner of Cl. The distance measure (4) is not scale-

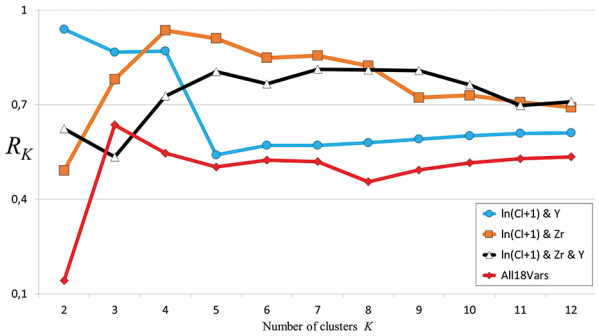

Fig. 6 The ARI R_K (average) versus the number of clusters in bivariate and multivariate hierarchical *Ward*'s clustering.

invariant. Therefore, when we are going to more than one variable the scaling problem (different scales: weight percent and ppm) has to be handled. Here, the measured values x_{ij}^* of variable j (in the case of Cl-measurements $\ln(\mathrm{Cl}+1)$ is used) were transformed proportional to the inverse of the mean $\bar{\mathrm{x}}_j^*$ simply by

$$x_{ij} = x_{ij}^* / \bar{\mathrm{x}}_j^* \qquad (i = 1, \ldots, I; j = 1, \ldots, J). \tag{6}$$

As a result, the transformed values of each variable j vary around its average value $\bar{\mathrm{x}}_j = 1$.[17] Fig. 6 shows an extract from the results of investigation of stability of bivariate *Ward*'s clustering based on the adjusted *Rand* index (ARI) R_K, namely the combinations Cl and Y, and Cl and Zr. The latter has the highest R_K value in comparison with all other $J - 1 = 17$ bivariate cluster analyses. For each pair of variables (Cl combined with one of the others), the original cluster analysis was compared with 250 bootstrap cluster analyses as before. As final result of the second step of the proposed bottom-up variable selection procedure the bivariate clustering based on Cl and Zr has the highest ARI R_K value of stability for $K = 4$ clusters.

Fig. 7 shows the estimate of the bivariate density of the (transformed and trimmed variable) $\ln(\mathrm{Cl}+1)$ and Zr. It suggests that there can be an additional cluster. This is different to the investigation of stability where R_K votes for four clusters. There is a very dense region at the top characterized by high values of Cl and low values of Zr. Another view at the estimate of the bivariate density is presented in Fig. 8. This contour plot was obtained by cutting the density at different levels.

Now we come to the next step of the proposed variable selection procedure, i.e., we are going ahead by looking for the best partner of the variables Cl and Zr. We found out that the result of the trivariate cluster analysis based on Cl, Zr and Y is the most stable among all possible $J - 2 = 16$ trivariate cluster analyses. In Fig. 6, the black line represents the corresponding ARI R_K values. Obviously, the values of stability R_K are now

17 Mucha 1992.

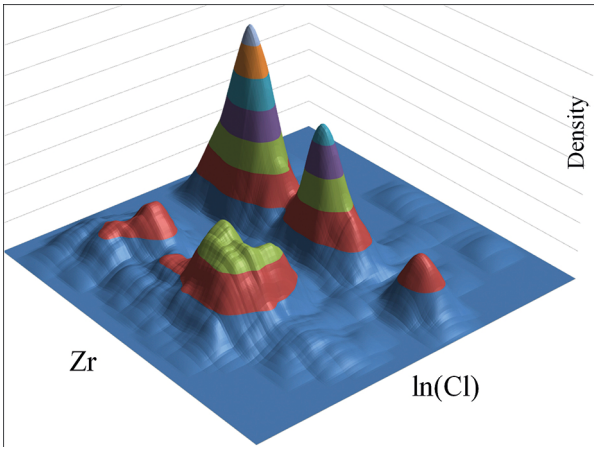

Fig. 7 Nonparametric bivariate density estimation of $\ln(\mathrm{Cl}+1)$ and Zr using the bandwidth 0.25 and 18, respectively.

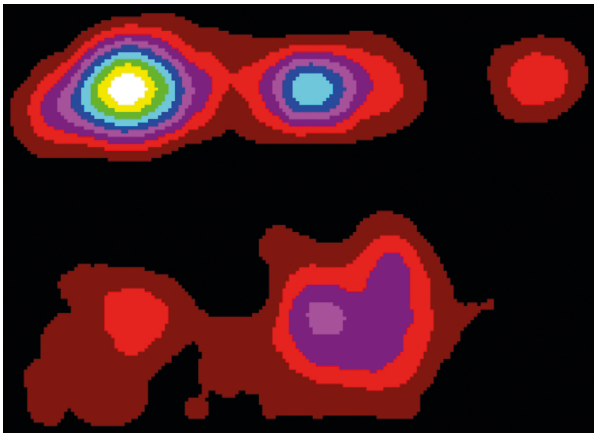

Fig. 8 Cuts at several levels of the bivariate density estimate presented in Fig. 7.

much lower than in the univariate $\{\mathrm{Cl}\}$ or bivariate $\{\mathrm{Cl}, \mathrm{Zr}\}$ setting. That means, in this application, the stability of results of clustering decreases when taking into account additional variables. However, the trivariate clustering based on $\{\mathrm{Cl}, \mathrm{Zr}, \mathrm{Y}\}$ presents stable results with low within-cluster distances as shown in Fig. 9. Here each element of the (447 x 447) distance matrix becomes a color that is 'proportional' to its distance value. For instance, the color in the first row ranges from black and dark red (very small and small distances, respectively) to yellow and white (large and very distances, respectively). In the center of the map, the dark area represents a dense cluster with very small within-cluster distances. In the heat map, the observations are ordered (1) by their cluster $C_1, C_2, \ldots, C_5$, and (2) by their first principal component value within the cluster.

As one can see by looking at the lower red line in Fig. 6, the R_K value (for $K = 2$)

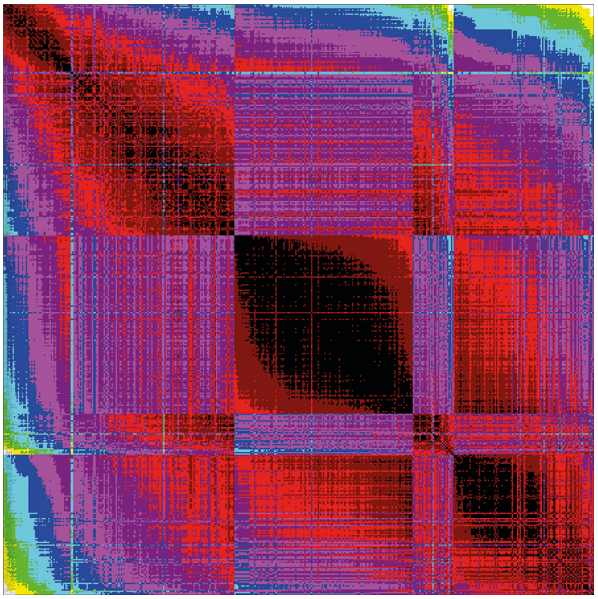

Fig. 9 Heatmap of the Euclidean distance matrix of all 447 ceramics from the eight different findspots in the Timiş district. The pairwise distances were computed based on the most informative three variables Cl, Zr and Y.

is about 0.15. That is quite low, and it means the cluster analysis is very instable when taking into account all the $J = 18$ variables. As a consequence, the very stable partition into two clusters found by univariate Cl-clustering (and the stable partition into four clusters found by bivariate Cl/Zr-clustering) can never be discovered when using all variables. That means there is no chance to find such interesting solutions that will be interpreted in detail below.

Fig. 10 summarizes the results of the bottom-up variable selection in cluster analysis. At the top, the very stable result of univariate Cl-clustering into the two clusters Cl(–) and Cl(+) is characterized by so-called sparklines (profiles) of the within-cluster average values of the transformed data (6). The symbols (–) and (+) stand for low and high Cl-values, respectively (see Fig. 5). The cluster profiles shown correspond to the sequence of variables presented at the bottom. The profile of these two clusters look quite different. The linear discriminant analysis based on all the remaining 17 variables (Cl is removed) quantifies the individual contributions of the variables by the well-known univariate F-value:[18] Y (168.76), Al_2O_3 (68.18), Nb (65.28), Sr (58.19), Rb (20.64) MnO (16.84), Pb (13.71), and Zr (10.16) are highly significant at the significance level 0.01. That is all of a sudden. From the statistical point of view, it seems that Chorine has a kind of indicator function for other chemical elements.

18 Mucha 1992.

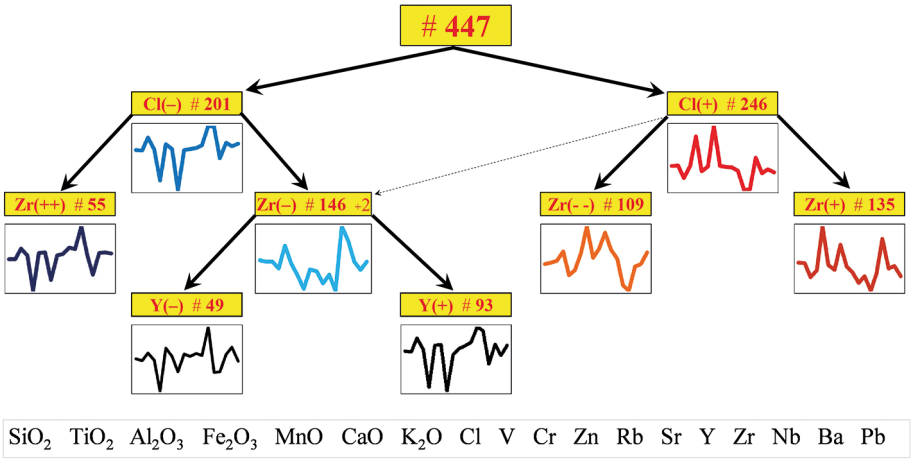

Fig. 10 Cluster tree: Visual presentation of bottom-up variable selection proposal starting with univariate clustering and followed by bivariate and trivariate clustering.

In the middle of Fig. 10, the most stable result of bivariate clustering into the four clusters Zr(++), Zr(–) (coming from cluster Cl(–)), Zr(––), and Zr(+) (coming from cluster Cl(+)), is characterized by cluster profiles. (The dotted arrow Cl(+) → Zr(–) marks a mismatch in only two observations between the univariate Cl- and the bivariate Cl/Zr-clustering.) By the way, it is a little bit surprising that Zr becomes the best partner of Cl because of its rather moderate F-value 10.16 compared to other variables, see above. Obviously, the profile of these four clusters differ among each other not as clear as in the level before. Finally, at the bottom, a special result of trivariate clustering is presented, namely the splitting of the cluster Zr(–) in the two clusters Y(+) and Y(–).

Is there an archaeological meaning of the results of cluster analysis? Before we are going to answer this question in the next section another test for statistical significance is presented. Let us look at the simplest result, the very stable two clusters of the Cl-clustering and its relation to the archaeological sites. Fig. 11 shows the corresponding contingency table. Pearson's chi-squared test can be applied to such a contingency table to evaluate how likely it is that any observed difference between the two categorical variables Cl-partition and archaeological sites arose by chance.[19] It tests whether paired observations on these two variables, expressed in the contingency table in Fig. 11, are independent of each other (i.e., the test of independence). The chi-squared test statistic of the contingency table is 226.07. It exceeds the corresponding critical value from the chi-squared distribution with 7 degrees of freedom and significance level 0.01 (= 18.48[20])

19 Mucha 1992.

20 Mucha 1992.

Count	Chlorine		
Find Spot	1(CL+)	2(CL-)	Total
Cornesti Cornet	30	34	64
Cornesti Larcuri	**120**	33	153
Deta Dudarie		**20**	20
Giroc Mezcal	2	**58**	60
Hodoni Puszta	**30**		30
Peciu Nou	2	**18**	20
Timisoara Fratelia	**50**		50
Voiteg Voiteni	12	**38**	50
Total	**246**	**201**	**447**

Fig. 11 Contingency table obtained by crossing the archaeological sides and the result of univariate Cl-clustering.

a number of times. Therefore, from the statistical point of view, the null hypothesis that the Cl-partition is independent of the variable "archaeological sites" is very clearly rejected. To summarise, so far, we found very stable cluster analysis results by the proposed bottom-up variable selection method with, in addition, interesting connections to archaeological information such as the findspots.

3 Interpretation of statistical results

It is well investigated that clay, as the main source for making pottery, can have a different composition within the same location or be very similar in different locations. Therefore, the recommendation of experts is to pay extraordinary attention to minor and trace elements.[21] Most generally, the cluster analysis results presented in the section before are in line with this because we found out that trace elements such as Cl, Zr, and Y seems to be much more important than oxides.

21 Bonizzoni et al. 2013.

In our application, the most informative variable is Cl. Where it comes from? Rice pointed out that "Salt or salt water is often added to calcareous clays or clay tempered with calcareous materials…".[22] To the best of our knowledge, a modification of clay by adding salt (NaCl) seems unlikely in our case because almost all of the 447 measurements are less than 100 ppm, but only 10 are greater than 100: 1196, 755, 656, 275, 256, 176, 132, and 110. So, we suppose other reason such as geological-geographic features.

Tab. 2 shows the crossing of the Cl-partition with both the periods and the archaeological sites. So, this table is an extension of Fig. 11 where we proofed that the Cl-partition is dependent on the variable "archaeological sites". That comes, maybe, from geological reasons which have to be verified in a future work. In fact, so far, the red line in Fig. 3 separates different geological areas, see also Fig. 12 for a comparison of the corresponding archaeological sites above and below the red line. In addition to Fig. 11, there is also a clear dependence of period and Cl-clusters: In the time period Late Bronze (LB) all ceramics found at the site "Cornesti Iarcuri" (CI) belong to Cl(+). That means theoretically, whenever a ceramic of Late Bronce is found in CI than it has with very high probability a high amount of chlorine.

What about the geographical coordinates? Are there relations to the Cl-clustering? Fig. 12 shows that there is local dependence of the clusters to a certain degree, see also the geological map in Fig. 3.

Tab. 3 shows the crossing of the four most stable clusters of the bivariate Cl-Zr-cluster analysis with both the periods and the archaeological sites. As a reminder, these four clusters are very strong connected to the univariate Cl-clustering: Each cluster is divided into two Cl-Zr-cluster (see Fig. 10). As already seen in the contingency table of Fig. 11, there is clearly no independence of clusters and sites.

To summarise, we found very stable clusters by our proposed variable selection in clustering. Without any doubt, these clusters are also significant from the statistical point of view when taking into account additional archaeological information such as location. Moreover, there seems to be geological-geographic reasons for the clusters, and thus archaeological interpretations are possible. The proposal to variable selection in clustering works without using special clustering criteria such as within-cluster or between cluster variances. This approach is based on non-parametric resampling and criteria of stability such as the ARI R_K using confusion tables.

22 Rice 1987.

Period		**MB**		**LB**		
		# 117		**# 330**		
Cluster		**Cl(+)**	**Cl(–)**	**Cl(+)**	**Cl(–)**	
		# 50	**# 67**	**# 196**	**# 134**	
	CC	**# 30** **46.9 %$_M$**	**# 34** **53.1 %$_M$**			# 64$_M$
	CI	# 20 37.7 %$_M$	**# 33** **62.3 %$_M$**	**# 100** **100 %$_L$**		# 153 = 53$_M$ + 100$_L$
Site	HP			**# 30** **100 %$_L$**		# 30$_L$
	TF			**# 50** **100 %$_L$**		# 50$_L$
	GM			# 2 3.3 %$_L$	**# 58** **96.7 %$_L$**	# 60$_L$
	PN			# 2 10.0 %$_L$	**# 18** **90.0 %$_L$**	# 20$_L$
	VV			# 12 24.0 %$_L$	**# 38** **76.0 %$_L$**	# 50$_L$
	DD				**# 20** **100 %$_L$**	# 20$_L$

Tab. 2 The result of univariate Cl-clustering vs. period and sites (MB – Middle Bronze, LB Late Bronze).

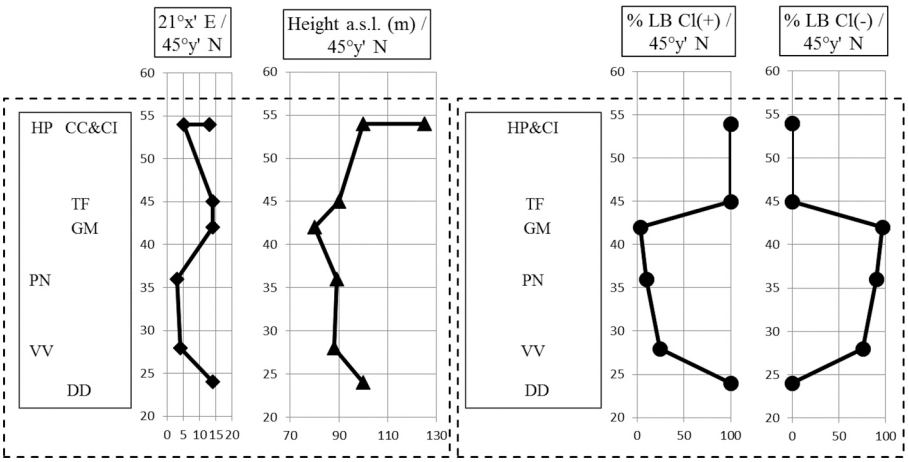

Fig. 12 The result of univariate Cl-clustering of Late Bronze (LB) samples in relation to geographical coordinates.

Cl-Cluster		**Cl(+)** **# 246**					**Cl(–)** **# 201**			
Period		**MB** **# 50**		**LB** **# 196**			**MB** **# 67**		**LB** **# 134**	
Cl/Zr-Cluster		**Zr(+)** # 44	**Zr(––)** # 6	**Zr(+)** # 91	**Zr(––)** # 103	**Zr(–)** # 2	**Zr(++)** # 53	**Zr(–)** # 14	**Zr(++)** # 2	**Zr(–)** # 132
Site	CC	**25**	5				**25**	9		
	CI	19	1	**74**	**26**		**28**	5		
	HP			**16**	**14**					
	TF				**50**					
	GM				2				2	**56**
	PN				1	1				**18**
	VV			1	10	1				**38**
	DD									**20**

Tab. 3 The result of bivariate Cl/Zr-clustering vs. period and sites (MB – Middle Bronze, LB Late Bronze).

Bibliography

Bonizzoni et al. 2013
Letizia Bonizzoni, Anna Galli, Marco Gondala, and Marco Martini. "Comparison between Xrf, Txrf, and Pxrf Analyses for Provenance Classification of Archaeological Bricks." *X-Ray Spectrometry* 42 (2013), 262–267.

Dolata, Mucha, and Bartel 2007
Jens Dolata, Hans-Joachim Mucha, and Hans-Georg Bartel. "Uncovering the Internal Structure of the Roman Brick and Tile Making in Frankfurt-Nied by Cluster Validation." In *Advances in Data Analysis*. Ed. by R. Decker and H.-J. Lenz. Berlin: Springer, 2007, 663–670.

Henning 2007
Christian Henning. "Cluster-Wise Assessment of Cluster Stability." *Computational Statistics and Data Analysis* 52 (2007), 258–271.

Hubert and Arabie 1985
Lawrence J. Hubert and Phipps Arabie. "Comparing Partitions." *Journal of Classification* 2 (1985), 193–218.

Mucha 1992
Hans-Joachim Mucha. *Clusteranalyse mit Mikrocomputern*. Berlin: Akademie-Verlag, 1992.

Mucha 2009
Hans-Joachim Mucha. "Cluscorr98 for Excel 2007: Clustering, Multivariate Visualization, and Validation." In *Classification and Clustering: Models, Software and Applications*. Ed. by H.-J. Mucha and G. Ritter. WIAS Report 26. Berlin: WIAS, 2009, 14–40.

Mucha 2014
Hans-Joachim Mucha. "Pairwise Dataclustering Accompanied by Validation and Visualization." In *German-Japanese Interchange of Data Analysis Results*. Ed. by W. Gaul, A. Geyer-Schulz, Y. Baba, and A. Okada. Studies in Classification, Data Analysis, and Knowledge Organization. Cham: Springer, 2014, 47–57.

Mucha and Bartel 2015a
Hans-Joachim Mucha and Hans-Georg Bartel. "Bottom-up Variable Selection in Cluster Analysis Using Bootstrapping: A Proposal." In *Second European Conference on Data Analysis*. Ed. by A. Wilhelm and H. Kestler. Springer, 2015, 125–135.

Mucha and Bartel 2015b
Hans-Joachim Mucha and Hans-Georg Bartel. "Resampling Techniques in Cluster Analysis: Is Subsampling Better Than Bootstrapping?" In *First European Conference on Data Analysis*. Ed. by B. Lausen, S. Krolak-Schwerdt, and M. P. Böhmer. Berlin: Springer, 2015, 113–122.

Mucha, Bartel, et al. 2015
Hans-Joachim Mucha, Hans-Georg Bartel, Jens Dolata, and Carlos Morales-Merino. "An Introduction to Clustering with Applications to Archaeometry." In *Mathematics and Archaeology*. Ed. by J. B. Barcelo and I. Bogdanonic. London: CHR Press, 2015, 190–213.

Rand 1971
William M. Rand. "Objective Criteria for the Evaluation of Clustering Methods." *Journal of the American Statistical Association* 66 (1971), 846–850.

Rice 1987
Prudence M. Rice. *Pottery Analysis – A Sourcebook*. Chicago and London: The University of Chicago Press, 1987.

Ward 1963
Jr. Ward Joe H. "Hierarchical Grouping to Optimize an Objective Function." *Journal of the American Statistical Association* 58 (1963), 236–244.

Illustration and table credits

ILLUSTRATIONS: **1–2** H.-J. Mucha and H.-G. Bartel. **3** Map created by H.-J. Much and H.-G. Bartel on the base of "Atlas geografic Unirea, Brasov, 1928, Pr.N.A.Constantinescu" from Wikimedia Commons: https://de.wikipedia.org/wiki/Datei:RomGeolActual.jpg (last visited 08.09.2020). **4–12** H.-J. Mucha and H.-G. Bartel.
TABLES: **1–3** H.-J. Mucha and H.-G. Bartel.

HANS-JOACHIM MUCHA

Hans-Joachim Mucha, Dipl.-Math. (Freiberg University of Mining and Technology); Zentrales Geologisches Institut (since 1975); Academy of Sciences of the GDR (since 1982); member of the research group 'Stochastic Algorithms and Nonparametric Statistics' of the Weierstrass Institute for Applied Analysis and Stochastics (since 1992); Chair of the Working Group 'Data Analysis and Numerical Classification' of the German Classification Society; field of research: computational statistics.

Dipl.-Math. Hans-Joachim Mucha
Weierstrass Institute for Applied Analysis and Stochastics (WIAS)
Mohrenstraße 39
10117 Berlin, Germany
E-mail: achimhj.mucha@gmail.com

HANS-GEORG BARTEL

Hans-Georg Bartel, Dr. rer. nat. 1972 and Habilitation 1985 at Humboldt University in Berlin; has been a lecturer for Physical and Theoretical Chemistry at this university since 1988. In addition to Theoretical and Mathematical Chemistry, his research fields include: History of Science, Archaeometry, Chemometrics, and Egyptology.

Dr. Hans-Georg Bartel
Department of Chemistry at
Humboldt-Universität zu Berlin
Brook-Taylor-Straße 2
12489 Berlin, Germany
E-mail: hg.bartel@yahoo.de

Marcin Baranowski, Małgorzata Daszkiewicz, Gerwulf Schneider

Chemical Analysis Using WD-XRF and p-ED-XRF and Using Macroscopic Analysis of Fabrics in Studying Moesian Sigillata

Summary

Four reference groups of Moesian Sigillata from Butovo and Pavlikeni were identified using WD-XRF analysis, thin-section studies and MGR-analysis. Published NAA results were compared. A series of 160 sherds found within the region and suspected to be Moesian sigillata were subsequently classified using pXRF measurements and macroscopic descriptions. Problems arising with pXRF measurements are discussed. The interpretation of the pXRF data was done using a combination of bivariate plots of Rb, Sr, Zr and principal component analysis. Ultimately, 129 sherds could be classified. The macroscopic classification was less reliable showing up to 45% erroneous attributions.

Keywords: WD-XRF; pXRF; multivariate; macroscopic analysis; MGR-analysis; Moesian sigillata; Butovo

Mit WD-RFA, Dünnschliffuntersuchungen und MGR-Analysen waren vier Referenzgruppen mösischer Sillata aus Butovo und Pavlikeni definiert und von Produkten von Novae und von Pontischer Sigillata unterschieden. Publizierte Analysen mit NAA wurden trotz gewisser Einschränkungen verglichen. Eine Serie von 160 als Moesische Sigillata angenommenen Scherben diente danach zur Prüfung, wie weit die Klassifizierung auch makroskopisch und mit pXRF Messungen am frischen Bruch und auf den Glanztonoberflächen möglich ist. Probleme der Messungen mit pXRF werden diskutiert. Die Interpretation der pXRF Daten erfolgte mit bivariaten Variationsdiagrammen und Hauptkomponentenanalysen. Damit ließen sich 129 Scherben zuordnen. Die makroskopische Klassifizierung war mit bis zu 45% falschen Zuordnungen weniger zuverlässig.

Keywords: WD-RFA; pRFA; multivariat; makroskopische Analyse; MGR-Analyse; Mösische Sigillata; Butovo

The paper is based on the thesis of Marcin Baranowski, who wishes to thank to his adviser Prof. Dr. Piotr Dycek. The samples were given by Paolina Vladkova from the Museum at

Morten Hegewisch, Małgorzata Daszkiewicz und Gerwulf Schneider (eds.) | Using pXRF for the Analysis of Ancient Pottery – an Expert Workshop in Berlin 2014 | Berlin Studies of the Ancient World 75 (ISBN TODO; DOI: 10.17171/3-75) | www.edition-topoi.org

Veliko Tirnovo, from excavations at Novae by Piotr Dycek, and to a large part from a survey by Dr. Sven Conrad, to whom we are very much indebted for his kind help. The laboratory work was made at ARCHEA in Warsaw and we would like to thank all co-workers. The WD-XRF measurements were made in Deutsches GeoForschungsZentrum GFZ in Potsdam by courtesy and help from, of Dr. Anja Schleicher and Mrs. Andrea Gottsche.

1 Introduction

The aim of the present paper is to present the reference groups for Moesian sigillata and in the same time to test the possibilities of non-destructive analysis to attribute finds to their true places of production. It testes two methods: macroscopic classification and chemical analysis using portable X-ray fluorescence (pXRF). The study, however, is based on laboratory analysis of samples taken from the sherds combining geochemical, technological and mineralogical methods. These were used to establish reference groups for the production centers for sigillata (red gloss pottery) at Butovo and Pavlikeni in modern Bulgaria[1] and for the probable production of red slipped fine wares at the Roman castrum Novae. Production at Butovo and Palikeni started around the middle of the 2nd century and continued until the middle of the 3rd century. Kilns for pottery have been found at Butovo, Pavlikeni and Hotnica (Fig. 1). The sites are situated in an area which in Roman times was under the administration of Nicopolis ad Istrum. The nearby hills are rich in deposits of good quality clay which to this day provide the raw materials used at a local brickworks at Butovo. For Novae, a group of sigillata is assumed to be locally produced which is clearly distinguished from the Butovo/Pavlikeni groups and which chemically resembles local bricks from Novae. Kilns for fine wares, however, were not discovered yet at Novae.

Five groups of Moesian sigillata in two papers had been distinguished using wavelength-dispersive X-ray fluorescence (WD-XRF) and MGR-analysis.[2] The groups are called BRG 1 (Butovo), PRG 1, PRG 2, and PRG 3 (Pavlikeni), and Novae. The mean chemical composition of the relevant reference groups using WD-XRF, including all available analyses, is compared in Tab. 1.

Chemically the groups do not differ very much and are also similar to the major group of North Pontic sigillata. The differences of typical samples of the reference

1 Sultov 1985.

2 Daszkiewicz, Schneider, and Bobryk 2006; Daszkiewicz and Schneider 2007.

groups after refiring at 1200°C (MGR-analysis) [3] is shown in Fig. 2. The groups were confirmed with fewer samples by thin-section studies and detailed macroscopic description.

The first part of our study is looking at a first series of sherds securely attributed using combined laboratory methods. The second part is the classification of a larger series of samples collected as supposed Moesian Sigillata but with unknown attribution. These attributions had to be done only by using macroscopic description and analyses by pXRF.

2 Methods and samples

2.1 Thin-section studies

Thin-sections have been used to confirm the grouping but not to classify the whole series. The differences in micro-fabrics can clearly be seen (Figs. 3, 4 and 5). All fabrics show silty clay without additional temper. Mica seems to be less in samples from Novae which on the other hand are characterized by typical microfossils (foraminifera) characterizing a very different clay. This is also the case for sample BM022 what chemically is classified to PRG 3. Obviously, this attribution is not possible looking at the microfabric. The amount of quartz silt is highest in PRG 1 and lowest in PRG 2. PRG 3 is made from obviously different clay with many tiny iron-rich aggregates.

2.2 Macroscopic analysis

Non-destructive attribution of finds using macroscopic analysis of fabrics was compared to laboratory analyses results for the first series of sherds. Examples of the macroscopically distinguished fabrics at cut sections are shown in Fig. 6. The quality of the slip[4] differs also very much. Fig. 7 shows a collation of macro-photographs of the surfaces of samples attributed to the reference groups. The red slip of the samples belonging to the Novae Reference Group is of much poorer quality than those of samples from groups BRG 1 or PRG 1 and 3. It can also be seen that samples representing group BRG 1 are characterized by the best quality red slip.

Macroscopic classification of each sample was carried out prior to their analysis by WD-XRF and pXRF. It is based on the visual examination of sherds, usually conducted

3 Daszkiewicz and Schneider 2001; Daszkiewicz 2014; Daszkiewicz 2017.

4 The term slip here is kept even if this for some good quality sherds could be called gloss, describing a glossy slip made by very fine levigation of the clay as in sigillata of the best quality (Arezzo, La Graufesenque).

with the unassisted eye or using a magnifying glass (occasionally a binocular microscope) with a maximum magnification of 10times. Thus, the ceramic fabric is described without the help of any laboratory procedures and descriptions can be written either in the field or later during post-processing. When conducting this analysis the following diagnostic features were taken into account: color, firing atmosphere, temper, pores, texture, compactness, fresh fracture appearance, hardness, durability and later changes. The results of macroscopic pottery analysis carried out on samples securely classified by laboratory methods are presented in Tab. 2. Samples from PRG 1 are characterized by pore sizes of 0.2–0.4 mm and by a granular, earthy fresh fracture. In contrast, samples from PRG 3 are characterized by the size of their non-plastic inclusion grains (0.1–0.3 mm) which are well-sorted grains and in larger amounts. Samples from BRG 1 are characterized by the size of their non-plastic inclusions (grains 0.1–0.2 mm) and by an earthy fresh fracture.

2.3 Laboratory methods

Laboratory methods are called such methods which use laboratory instruments for chemical, mineralogical or technological analysis to determine the composition of the body and/or the way how the vessel was made.[5] Such analysis presents information on provenance and technology which may be interpreted in terms of cultural and economic history and in history of technology. Generally, a sample must be taken from the object. The necessary sample size depends on the questions to be answered and can be as small as about 150 milligram of powder necessary for chemical and phase analysis. Small fragments of up to five gram are needed for combined analysis including MGR-analysis and a thin-section study. Restricted sample sizes and costs for laboratory analysis prevent that a very large number of samples can be analyzed. On the other hand, the number of samples selected for analysis, depending on the heterogeneity of the assemblage, should not be too small.[6] The use of the more or less non-destructive analysis of the chemical composition of sherds by pXRF is only possible with important restrictions.

2.4 Analysed samples

A first series of finds from Butovo, Pavlikeni and several other places within the region was classified using MGR-analysis and chemical analysis by WD-XRF. These analyses served as a basis to securely attribute the sherds of Moesian Sigillata to their reference groups. Some additional samples were included to check if they could be classified (e.g.

5 Daszkiewicz 2014; Daszkiewicz and Schneider 2014. 6 Daszkiewicz 1995.

BM035 attributed to Novae). The assignment of the reference groups to their geographical places of production was made looking at samples from the kiln sites at Butovo and Pavlikeni. Most of the analysed sherds, however, are finds from various places within the region and classified by laboratory analysis and macroscopic description. Further sherds classified by WD-XRF and/or MGR-analysis were added to this first series of 56 samples and all were used as a basis to check the possibilities of analyses by pXRF. Thereafter further 104 sherds had to be classified using their macroscopic classification together with pXRF analysis (Tab. 3). The true attribution may be by MGR-analysis and WD-XRF which in all cases correspond.

2.5 Definition of reference groups

Reference groups are groups of analysed samples with known attribution serving to be compared to non-attributed samples. Reference groups could be of different quality. If a reference group comprises analyzed finds in an excavated potter's workshop, as unfired pottery, potter's tools, molds, and true kiln wasters, we can be sure about the local composition. Less secure attributions will be if only arguments on the geographical attribution could be gained from geological information e.g. from characteristic rock fragments or minerals detected in thin section or from a typical geochemical characteristic e.g. in contents of Cr and Ni. A reference group could also represent an archaeologically defined ware (shape, decor) or just a homogeneous chemical group to which analyzed samples may be attributed without knowing the geographical attribution.

The reference groups of the known workshops in Pavlikeni and Butovo are not very strong because only very few finds from kilns have been available for laboratory analysis. The original reference group Butovo (BRG 1) comprises four samples from the kiln site, including one waster, together with other finds from Butovo and sherds found in Pavlikeni, Hotnica, Iatrus, Novae, and Nikopolis at Istrum. The nine samples analyzed from the kiln site at Pavlikeni represent three compositional groups. The groups PRG 1 and PRG 3 each comprise also two amphorae assumed to be local products thus confirming the local workshops. Two samples from a kiln in Pavlikeni villa represent group PRG 2 which differs in MGR-analysis, in thin-section and chemically from all other groups. Only two samples found at other sites, however, chemically were attributed to this group. The chemical reference groups thus were now established including all samples with the same composition found within the region. The basis thus is much enlarged and attributions to the four groups of Moesian Sigillata can be made more securely.

Already Ivelin Kuleff and Rumiana Djingova[7] had analysed 26 samples from exca-

7 Kuleff and Djingova 1996.

vations in Pavlikeni and Butovo using NAA. After multivariate analysis a group of eight samples including three kiln wasters by them have been regarded as a reference group for Pavlikeni villa. From the 24 elements determined by NAA seven are also determined by us using WD-XRF. This will be discussed in a later chapter.

2.6 Evaluation of pXRF measurements

All measurements were carried out using a Niton XL3t 900S GOLDD portable X-ray analyzer. Measuring time is 30 sec for each of the four filters, without using He. The calibration was made using twelve own standards prepared from fired clay samples and ancient ceramics. Samples were measured in a sample changer and are checked by repeated measuring of a monitor sample. After measuring the original table of results must first be checked for reliability of all data. For a secure interpretation automatic averaging should only be used after eliminating deviating values. This could be done first by comparing the results of the three (or more) repeated measurement of the same sample but should also be done by checking the resulting groups e.g. by using bivariate diagrams to detect outliers in one or more elements of a sample. These problems make the interpretation of data received by pXRF much more laborious than of the more reliable WD-XRF results of analyzed powder.

It turned out that in our archaeological ceramic samples some elements showed abnormal high concentration levels which should be below detection limits of the instrument as U, Bi, Hg, Cd. Those certainly wrong numbers would not to have be regarded at all if not other elements seemed to be involved as mainly Ba. Sometimes the wrong measurements are connected with certain samples (more often with measurements on cut sections than on fresh breaks) and they also appear when measurements were repeated, but not always. In any case, it seems that it is worth to check all measured data (e.g. for U) before this whole measurement is included in the average. Not eliminating such wrong data may lead to wrong classifications. This was considered in our choice of elements used for interpretation of the data (see below).

Another test which should be done is for too low values of Al (and Si), mostly connected with the distance of the fresh fracture to the detector. Such low values sometimes indicate also outlying data of other elements. Detected from 25 samples, pXRF measurements on cut sections nearly always have higher sums of major elements than measurements on a fresh break (geometric effect). It is worth to check the sum of the calculated oxides and eliminate measurements with sums below 75% and above 95% (calculated without Mg, Na and l.o.i.). In our experience Al seems only to be stable and reaching a reliable value after about five hours of measurements with the machine which exceeds a normal warming up time. A normalization of the data to a constant sum seems not to make sense.

We always use averages of three measurements for each sample after checking the individual data (instead using an automatic average). We did not use the medians. For the above discussed reasons some measurements were repeated and then a new average calculated.

Measurements of the same sample BM004 during several sessions is discussed in Tab. 4 to demonstrate the problems. The wrong average (BM004-b) of the first three measurements (which in the first measurement showed 61 ppm U what, however, at this time was not recognized as important) and the good values from the second session some minutes later (BM004-b) resulted in a different attribution of the sample by PCA (see the two pale red triangles in Fig. 23). The measurements on the sherds outer surface on a spot without slip (BM004a) and on a cut section (BM004c) deviated also because of wrong measurements showing U. In the latter case removing outliers before averaging would have removed the good values of the third measurement as outliers because the other two measurements are similar. The third series of four measurements 50 minutes later seems to be o.k. if we delete the outlying one measurement with high U which showed 214 ppm Cr. However, in the corrected mean b 2 the value of Cr is systematically too low. The repeating of the measurements ten months later (average b 3), all showed U correctly as LOD (lower limit of detection), gave reproducible results if the first two deviating measurements are not taken into account. So the average of the last three measurements seems to be the most secure and results in a correct attribution to group BRG 1 by PCA.

3 Results

3.1 Comparing reference groups using WD-XRF

In this paper the focus is on sigillata produced in Butovo and Pavlikeni. These products, however, must also be distinguished from sigillata produced in Novae[8] and also must be compared to North Pontic sigillata. Looking at the means and standard deviations not all regarded reference groups seem to be chemically easily distinguishable (Tab. 1). For Pontic sigillata A (reference groups PS 1 and PS 2) the geographical attribution is still unknown but their distinction from products of Butovo, Pavlikeni, and Novae is important because they may have been distributed within the same region. Pontic sigillata C because of high Mg, Cr and Ni differs from other Pontic sigillata and must have been produced in a geologically very different area. Chersonesian sigillata (reference group PS 4 of the north Pontic sigillata) was made in the SW-Crimea. For Pontic sigillata only

8 Daszkiewicz, Schneider, and Bobryk 2006.

analyses by WD-XRF are available whereas the groups of Moesian sigillata are characterized also by MGR-analysis and by a limited number of thin-sections. Comparison with sigillata produced in Roman Dacia as well as the problem of multivariate attributions discusses a later paper by Daszkiewicz et al.[9]

All reference groups were checked using multivariate methods of the chemical data. For the multivariate calculations the concentrations of the oxides of Si, Ti, Al, Fe, Mn, Mg, Na, K, and the elements V, Cr, Ni, Zn, Rb, Sr, and Zr have been used. P and Ba have been omitted because these elements may depend on alteration effects during burial. The generally low concentrations of Cu, Y, Nb, La, Ce and Pb are determined with less precision and therefore have not been used. Not all groups were clearly distinguished in a single diagram after principal component analysis (PCA) or discriminant analysis (DA). When, however, only few groups were compared the distinctions are clearer. This was proved for the distinction of Pontic sigillata PS 1 and PS 2 and for the Moesian groups BRG 1, PRG 1, PRG 3 and for Novae. Only the two samples of group PRG 2, defined by MGR-analysis are not unequivocally attributed. As an example for the distinction of the various groups Fig. 8 shows the results of PCA of the Moesian groups and Pontic sigillata PS 1. In the diagram the finds from Butovo/Pavlikeni are marked to be distinguished from attributed samples found at other sites. The distinction of Moesian sigillata from North Pontic sigillata PS 1 and PS 2 is clearer when discriminant analysis is applied (Fig. 9). The multivariate distinction of the reference groups of Moesian sigillata and Novae shows Fig. 10.

3.2 Chemical classification of sigillata from Butovo and Pavlikeni

Novae and north Pontic sigillata will not be further regarded. Analysis by WD-XRF was made of the new samples collected by Sven Conrad and Marcin Baranowski (Tab. 5) which were combined with the already published data.[10] By MGR-analysis have been classified 32 of this series and 12 samples without WD-XRF analysis. All samples were also classified macroscopically.

As a first step the WD-XRF data underwent multivariate cluster analysis. The resulting dendrogram (Fig. 11) is based on Euclidean distances using the logarithms of the concentration values of fifteen elements (the same as used for PCA). The dendrogram confirmed the groups detected by PCA except group 2 (PRG 2) which here may be regarded as a subgroup of group 4 (BRG 1). This coincidence with group 4 was already shown by PCA in Fig. 8 whilst discriminant analysis (Fig. 10) separated the two samples BM2554 and BM2559 from this group. BM007 in the dendrogram is shown as

9 Daszkiewicz, Schneider, Baranowski, et al. 2018.

10 Daszkiewicz, Schneider, and Bobryk 2006; Daszkiewicz and Schneider 2007.

not belonging to any group. According PCA or DA, however, the most probable group for this sample is group 1 (PRG 1). The aberrant classification probably is due to its low Ca content (Tab. 5). Four samples (BM022, BM035, BM037, and BM329) are not attributed to one of the reference groups of Butovo or Pavlikeni and further regarded as unknown. A second cluster analysis using calculated scores instead of the logarithms of the original values and using Wards method yielded a similar result, however, with BM007 belonging to group 1. The samples without attributions by Wards's method have now been integrated into the groups.

To verify the differing results after numerous dendrograms and analyses by PCA and DA it is indispensible to regard the original compositional data including all significant elements either univariate in the original table or in a series of bivariate diagrams. Regarding possible secondary alteration effects for the classification we did not include P and Ba. Elements which within our series of analyses did not show any tendencies to distinguish groups will be not discussed further (Na, Ni, Cu, Nb, La, Ce, and Pb). One of the most significant elements is Rb. It was therefore taken in all diagrams as Y-axes and correlated with all other more or less diagnostic elements. The first diagram Si vs. Rb (Fig. 12) distinguishes Butovo from three groups of Pavlikeni. Sample BM007 here appears as an outlier like in the dendrogram (Fig. 11). The four samples of PRG 2 are clearly separated from other Pavlikeni groups and certainly made from different material. This will show also the following diagrams even if group PRG 2 not always was clearly separated using multivariate analysis. The groups can also be recognized more or less clear in Fig. 13 (Ti) and Fig. 14 (Al). Rb is correlated with Al and also, as expected, with K (Fig. 15). The latter diagram also illustrates the different ratio of Rb/K of the Novae group compared to the groups of Butovo and Pavlikeni indicating geochemically different provenance regions. In the same diagram are also included the analysis results of NAA by Ivelin Kuleff.[11] which will be discussed in an extra chapter. Sample BM2529 attributed by MGR-analysis to PRG 1 is an outlier in Fig. 15. By PCA and DA nevertheless it is attributed to PRG 1. For a secure attribution of this single sample we have to wait for more analysed samples to decide if this composition represents another yet not determined group (an analytical error of WD-XRF for K and Rb can be excluded). In Fig. 15 all unknown samples (empty circles) may be attributed to Novae. This, however, is not the case regarding Fig. 16 or Fig. 10 where only BM035 may be securely attributed. For the other samples bivariate diagrams using other elements do not distinguish Novae from Butovo or Pavlikeni and so could not confirm nor contradict their attribution.

Besides samples BM2529 and BM035 some other samples are less clearly connected to the groups to which they should belong according MGR-analysis. These samples are marked in some diagrams. Sample BM007 of group PRG 1 is an outlier with a lower Ca

11 Kuleff and Djingova 1996.

content (Fig. 17) connected with a higher Si content. Both elements, however, generally are showing large variations within the same clay deposit and thus are less significant for provenance determination than other elements. Their influence on grouping, however, is large and this may result in wrong attribution by multivariate cluster analysis. In Fig. 18 showing Cr vs. Rb the samples of PRG 1 and PRG 3 differ from samples of BRG 1. In this diagram are again included the NAA data from Kuleff and Djingova.[12] Their eight samples of local pottery from Pavlikeni correspond well to our reference groups PRG 1 and/or PRG 3. Five other samples with high Rb and Cr match our group BRG 1.

The elements which are measured by WD-XRF as well as with sufficient precision by pXRF are Rb, Sr, and Zr. Therefore, the next four diagrams show the results of WD-XRF (Figs. 19, 20) and of pXRF (Figs. 21, 22) for direct comparison. By WD-XRF the groups are separated more or less clearly but using all three elements makes a clear distinction possible, e.g. sample BM226 in Fig. 19 clearly belonging to of PRG 3 would be misclassified only using Fig. 20. The deviations, however, are less than 10 ppm and thus little more than the precision of WD-XRF. The combination of Rb, Sr and Zr allows a characterisation of BRG 1, PRG 1 and PRG 3 (PRG 2 may still be regarded as a very preliminary group as long as further analyses are missing).

Figs. 21 and 22 show the analysis results of pXRF for Rb, Sr, and Zr. The groups are less clearly separated than with WD-XRF because of a much larger variation due to the more or less non-destructive analysis on fresh fractures instead of homogenized and more representative powder samples taken from the body of sherds.

3.3 Comparison with published data by I. Kuleff

Chemical analyses results of pottery from Butovo and Pavlikeni using NAA[13] and ICP-OES[14] were compared to our data. In the first paper 26 samples of finds from Pavlikeni Villa and Butovo, including three wasters from Pavlikeni Villa, had been submitted to cluster analysis. Of the 24 elements determined only Ce, Co, Cr, Cs, Eu, Fe, Hf, La, Lu, Sc, Sm, Th, Yb were used to create a dendrogram. This resulted in four groups. The major group included the three wasters and further five samples found at Pavlikeni. This major group therefore should represent the production of the products of Pavlikeni villa. It was not written why the elements Na, K and Rb have not been used in the calculation, elements which could well be determined by NAA.[15] Thanks to the raw data given in their tab. 2 we could compare the results of the elements determined by NAA and by WD-XRF (Fe, Na, K, Cr, Rb, Ba, and Ce). This showed that the eight samples of cluster 1 (black triangles in Figs. 15 and 18) match quite well our reference

12 Kuleff and Djingova 1996.
13 Kuleff and Djingova 1996.
14 Kuleff, Djingova, and Kabakchieva 1999.
15 Schneider and Mommsen 2009.

groups of PRG 1 and/or PRG 3 but they do not match our two samples from Pavlikeni Villa (PRG 2). Seven samples with Rb > 150 ppm and K between 3 and 4% K_2O (Fig. 15) may be attributed to Butovo (Kuleff clusters 3 and 4) but, on the other hand, for most of these samples Fe is too low. One sample of Kuleff cluster 1 in spite of his multivariate attribution deviates which much too high Fe (7.55% Fe_2O_3). It cannot be excluded that the published individual analysis results may be wrong for some elements which is certainly the case at least for some values of K and Rb, the latter varying between 18 and 332 ppm (outside our diagrams). This may also be true for the Cr-values below 90 ppm (Fig. 18). In a second paper Kuleff et al. (1999) had clustered ICP-OES analyses of 36 samples from finds at Oescus and Novae, unfortunately without publishing the raw data. Of the 18 elements published as mean concentrations (see Tab. 1) only 14 can be compared to our results (Si, Na, K and Rb have not been determined by ICP-OES). The mean of cluster 3, tab. 4[16] was believed to represent products of Pavlikeni and/or Butovo, however, it deviates systematically by too low Al, Ca, Sr, Zr, Ba and too high Cr and Ni (Tab. 1). Nevertheless, taking into account the very large standard deviations of the means of their group 3 this group may be correlated with all our groups of Tab. 1 (maybe except Ca and Sr). The discussion shows that the inclusion of published data needs control of the interlaboratory comparability through exchange of samples which should be analysed by all involved labs.

3.4 Results and interpretation of pXRF-measurements

Measurements by pXRF for every sample were made on three different spots of fresh fractures and the averages calculated. So each analysis used for further treatment represents the average of three measurements. Of some sherds measurements have also been made on cut sections or on parts of cleaned surfaces which were uncovered by a slip (outside or inside). Quite large differences after comparing the results of these measurements are obvious but did not appear to be systematically. Some analyses results e.g. with too low sums of the major elements were deleted and measurements were repeated. As an example of repeated measurements sample BM004 was already discussed. For the following interpretation only the measurements on fresh fractures were used (in two cases these were not done and measurements on cut surfaces were taken instead).

In a first step only the 56 samples already classified by WD-XRF and/or MGR-analysis were regarded as a basis for the later classification of the larger series of 104 samples which only were analysed by pXRF and macroscopic description. This will be discussed as a second step.

16 Kuleff, Djingova, and Kabakchieva 1999.

A first approach to the grouping of the pXRF data was cluster analysis using the same conditions as for the dendrogram of the WD-XRF data in Fig. 11 but without the elements Na and Mg. Nine out of 56 analyses results by pXRF were misclassified corresponding to 16%. Several other dendrograms (Euclidian distances of logarithms, average linkage) were made omitting the less precisely measured elements or using a different multivariate procedure (scores, Ward's method). The resulting dendrograms yielded more or less differing results for some samples but generally did not reduce the number of misclassified samples.

Our next approach was done using a series of bivariate diagrams as was done with the WD-XRF data in Figs. 12–20. The variation of the pXRF data, however, was so large that differences between groups could not be seen except for Rb, Sr, and Zr. The diagrams Rb/Sr (Fig. 21) and Rb/Zr (Fig. 22) show a more or less clear separation of the groups except for the two samples of PRG 2 which will be not regarded in the following. The larger variations of the data compared to the data from WD-XRF make secure attributions more difficult as e.g. sample BM240 shows which deviates only by 10 ppm Rb from the value analysed by WD-XRF. This is hardly more than the precision of the methods. A first possibility to prove outliers not belonging to Butovo/Pavlikeni was by looking at the table of all data. Taking the limits of Figs. 14 and 15, as not matching are regarded all samples with Rb less than 110 ppm, all samples with Sr lower than 150 ppm or higher than 650 ppm, and all samples with Zr outside the range between 150 ppm and 250 ppm (the possibility of EXCEL of sorting data in columns here was a great help).

As a third approach a multivariate classification was made by PCA using the eight elements Ti, Fe, Ca, K, Cr, Rb, Sr, and Zr which were determined by WD-XRF and securely enough by pXRF (Fig. 23). The groups are clearly distinguished regarding the data received by WD-XRF as well as those by pXRF. In spite of a thorough calibration of pXRF using 12 standards analysed by WD-XRF a slight systematic shift between the two data sets can be observed, i.e. the pXRF data moved somewhat towards the lower left corner in the diagram. The shift between pXRF and WD-XRF data can also be seen in the measurements of the four unknown samples measured by both methods, however, for the two samples of PRG 2 the tendency is opposite. BM035 in the middle between groups according MGR-analysis belongs to the reference group Novae. Samples BM022 (see also Fig. 5) and BM037 in spite of their multivariate similarities to PRG 3 do not belong to PRG 3 according MGR-analysis.

The shift is the same for sample BM004 (indicated by a pale red square respectively a pale red rhomb), however, one of two measurements of BM004 is clearly misclassified. It is given here as an example of the limited reliability of some pXRF measurements (this case was already discussed in more detail with Tab. 4). The first (wrong) measurement of BM004 is clearly attributed to group PRG 1 what is wrong when the results of MGR-

analysis and WD-XRF are considered as reliable. This led to repeating the measurement (and to discover that not only outliers but also U must be regarded). The repeated measurement led to a correct attribution. Of course, this presents no problem when the attribution is known but may limit the reliability of attributions.

Keeping all this in mind, we tried to attribute a next series of 104 samples without data from WD-XRF or MGR-analysis to their places of origin using all pXRF data for PCA (Fig. 24). If we agree that the fields presented by the securely attributed samples (diagrams Figs. 14–19), in Fig. 24 indicated as triangles, would also be valid for the non-attributed samples, we can classify the majority of the samples to the three established reference groups BRG 1, PRG 1 and PRG 3. This attribution by PCA then must also satisfy the diagrams Figs. 25 and 26. In several cases the comparison of the three diagrams required several changes of the original classification making the procedure quite tedious. A few examples shall be given. Sample BM271 by PCA clearly attributed to BRG 1 has too high Sr, and sample BM244 has too low Zr. Sample BM313 by PCA attributed to PRG 3 has to low Zr. The original measurements of the three samples do not show any indication that something could be wrong. The three samples therefore have been attributed with question marks.

The outlying values of Rb, Sr, Zr however, must not always be just outlying measurements as e.g. the very high value of 259 ppm Rb in sample BM243 was confirmed by WD-XRF with 257 ppm (by PCA it cannot be attributed to any group). Using the table of the original analysis, results all very aberrant data were checked and then these samples were considered to belong to unknown groups. Of course, the large coefficients of variation of some elements have to be taken into account. The consequence is that some samples with outlying concentrations of one or more elements in reality could be members of the Butovo/Pavlikeni groups and that some other samples could have been wrongly attributed to the reference groups. But this could only be proved by control analyses of samples using MGR- analysis or WD-XRF.

Regarding CaO two outlying groups could be recognized, one with high Ca (CaO > 14.7%) and low Ti and K contents (TiO_2 < 0.6% and K_2O < 2.5%). This relatively homogeneous group X (five brown rhombs in Fig. 24) certainly represents a yet unknown provenance. On the other hand, the samples with very low calcium contents (CaO < 4.2% and Sr < 200 ppm, five yellow rombs) must be interpreted as belonging to three different yet unknown provenance groups. Six samples also included in the first series with unknown attributions (empty circles) lie within the fields of the three Moesian sigillata groups, but as discussed already, cannot be attributed to Butovo or Pavlikeni (the Novae group has not been analysed using pXRF). Finally, we must consider at least 19 out of the altogether 160 samples measured by pXRF as not belonging to the Butovo/Pavlikeni reference groups. The final attributions of all samples are included in the list of all analysed samples in the sixth column PCA/RbSrZr (Tab. 3).

3.5 Non-destructive pXRF measurements on the slipped surface

A series of well-preserved sherds were analysed by measuring on the slipped surface without any preparation besides cleaning with a brush. This procedure is the only possibility if whole preserved vessels of sigillata must be analysed without making a fresh break for taking a sample. The previous attributions using pXRF measurements at fresh breaks have been used to check the attributions of the slip measurements in bivariate diagrams for Rb, Sr, and Zr (Figs. 27, 28).

The classification using cluster analysis and PCA was less effective. Compared to analysis results of the body (pXRF of fresh fractures, WD-XRF of powders) a systematic difference in the concentration values of the slip is observed which is enriched in e.g. Al and K and depleted in Ca (this can also be seen for sample BM004 with Tab. 4). When regarding the bi-plots Figs. 27 and 28 most of the samples seem to be classified correctly. The samples with deviating attributions are BM004, BM011, BM313, and BM358, and also BM317 and BM2519 with Rb below 110 ppm. Two of them (BM004, BM313) showed already problems in attribution by measurements on fresh fractures (Figs. 23, 25, and 26).

Looking at the bi-plots with the already attributed samples in different colours presents a too optimistic picture. In reality we do not know the attributions (respective colours in the diagram) and we must attribute samples using simple rules. Then we could attribute all samples with Rb 142–170 ppm to BRG 1 and all samples with Rb 115–190 to PRG 1 or PRG 3. The distinction of the two Pavlikeni groups could best be done by Sr. Then Sr 300–700 ppm means PRG 3 and Zr should be 140–190 ppm using the distinguishing line in Fig. 28. Samples outside these frames cannot securely be attributed to one of the three groups. Accepting these criteria seven samples would be misclassified. This means about 15% of the samples are wrongly attributed if we regard the classification with measurements at fresh breaks as correct. The results are included in Tab. 3.

4 Conclusions

Based on MGR-analyses and analyses by WD-XRF, backed by a small series of thin-sections, the compositional groups of Moesian sigillata established earlier have been confirmed by new analyses. The clearly attributed samples were used to develop a system of macroscopic classification, and also to check if measurements by pXRF lead to the same classification result as analyses by WD-XRF. The reference groups of Butovo (BRG 1) and Pavlikeni (PRG 1, PRG 2, PRG 3) chemically and in thin-sections are similar and in fabrics mainly distinguished by different size and amount of quartz grains

as a natural temper. This also show chemically the SiO_2 contents. On the other hand, MGR-analysis and minor- and trace element composition (e.g. Rb) show that the clay matrix used had been also somewhat different. Thus, four different clays had been used at Butovo/Palikeni but from our limited number of samples from kilns it is not possible to tell if the various clays had been used at both neighbored sites because sherds of different chemical attribution have been found at both sites. It is possible to distinguish the Butovo/Pavlikeni groups securely from products at Novae and from North-Pontic sigillata. These latter groups, however, have not been included in the tests using pXRF measurements and macroscopic classification.

Previous analyses by Kuleff and co-workers using NAA and ICP-OES were considered taking into account the limited number of elements which can be compared and a much larger analytical variation of their data. Their group from Pavlikeni villa (corresponding to PRG 1 and/or PRG 3) including three kiln wasters seem to confirm our analyses.

Our first series of 56 analyses using secure classification methods showed some discrepancies with macroscopic description and pXRF measurements. Up to about 15% of the samples have been misclassified, not regarding obviously wrong data. Those were found when the three measurements were averaged without checking for non-explained outlying measurements, for too low or too high sums, and for non-sense concentration values of elements as high levels of Hg or U in pottery. Mostly this may be corrected by repeating the measurement but, of course, before it must be recognized that something went wrong. An example was discussed. At the end the interpretation and repeating measurements took much more time than analysis of samples by WD-XRF.

For the interpretation of pXRF data a combination of bivariate diagrams of Rb, Sr and Zr as the most precisely elements determined by pXRF and PCA with eight elements was used. Cluster analysis by average linkage or Ward's method was also applied to check the grouping. Here however, as with PCA or DA, the table with the original values or a series of bivariate diagrams must be checked to be sure that single outlying elements do not disturb the multivariate classification. Such elements could be Ca or also extraordinary high values e.g. of Zn originating possibly from contamination during burial. Alteration effects may also change other concentration values, a reason why fresh fractures should be measured rather than surfaces or old fractures. Cluster analysis using Ward's method tends to include samples into a group which not always can be confirmed in the original data. This means that the non-attributed samples in the original table erroneously appeared as members of established groups (our example showed 14 out of 160 samples as wrongly clustered).

To summarize, the evaluation of the chemical data needs carefully proving of the original values. This is easier with WD-XRF data where normally at least analytical errors can be neglected but it is tedious work when using pXRF data where numbers could be

wrong or at least very imprecise. This limits also the number of usable elements of pXRF measurements to about eight or ten.

The application of the results of the first part of the study classifying a series of 104 samples of supposed Moesian sigillata only using pXRF measurements must consider the above discussed statements. Nevertheless, most of the analyzed samples could be attributed to the reference groups of Butovo or Pavlikeni. Some samples may represent yet unknown reference groups and imports from outside the region. Attribution of samples to Novae were not checked because the few distinguishing elements concluded from WD-XRF data were not sufficient precisely analyzed by pXRF.

The chemical classification by pXRF of the 149 samples with BM-numbers, most received from a survey collection of Sven Conrad, resulted in 66 samples belonging to BRG 1, 24 samples to PRG 1, and 37 samples to PRG 3. Five samples can be classified as a group X with low Ca, and three samples with high Ca as group Y of unknown provenances. Besides one sample attributed to Novae by WD-XRF and one clear import with high Ti further 13 samples are still with unknown attribution. The results were compared to the macroscopic classification which attributes 116 samples to Butovo and 37 samples to Pavlikeni (of those only 8 samples to PRG 1). Looking only at the first series of samples confirmed by secure methods (BM004-59) 32 macroscopic attributions were correct and 7 wrong (18%). From the second series only based on pXRF results and not confirmed by secure methods (BM100-366) were 61 correct and 49 wrong (45%). Even taking into account that some of the pXRF attributions were not correct it seems that the macroscopic classification does not give very reliable results.

Non-destructive analysis by pXRF on surfaces with well-preserved red slip (gloss), without making a fresh fracture, was tested with a series of 47 sherds. The data evaluation is best done again using bivariate diagrams of Rb, Sr and Zr. In the diagrams the securely attributed samples can be taken as frames for the attribution to BRG 1, PRG 1 and PRG 3. Seven samples because of unexplained false measurement results were incorrectly or not been classified. This corresponds to about 15%.

Chemical analysis is a powerful tool for the determination of provenances of ceramics but it is based on precision and accuracy of the data. This makes a big difference between analyses of sample powders (e.g. WD-XRF) and of measurements by pXRF. Generally, we have to regard several limitations. The first is that even clear attribution to a chemical reference group does not mean that this must be true as e.g. sample BM022 showed for which a thin-section proved that it is certainly not belonging to the chemical group PRG 3 to which it chemically could securely be attributed. Such aspects have generally been discussed by Daszkiewicz.[17] The second limitation is data interpretation using multivariate cluster analysis (dendrograms), principal component analysis or

17 Daszkiewicz, Schneider, and Bobryk 2012; Daszkiewicz 2014.

discriminant analysis even of precisely and accurately determined chemical data of representative powder samples e.g. by WD-XRF because samples not belonging to any of the reference groups may be falsely attributed if not all relevant reference groups have been included.[18] Furthermore the classification depends on the table of the original analysis results. All elements in the table therefore have to be checked univariate for outliers not explained by possible analytical errors or by alterations effects. What to do with an outlier in only one significant element as Rb measured by WD-XRF and pXRF as e.g. sample BM243? The search for outliers is even more important when data gained by pXRF are used where unexplained outliers are quite common. If not every sample is repeated until the data are stable we must count on many wrong attributions even with fine pottery like Roman sigillata. Using macroscopic classification or pXRF measurements the experience showed that of about ten attributed samples eight or nine may be o.k. but up to two are not correctly attributed, but we do not know which ones.

18 Schneider, Hoffmann, and Wirz 1979.

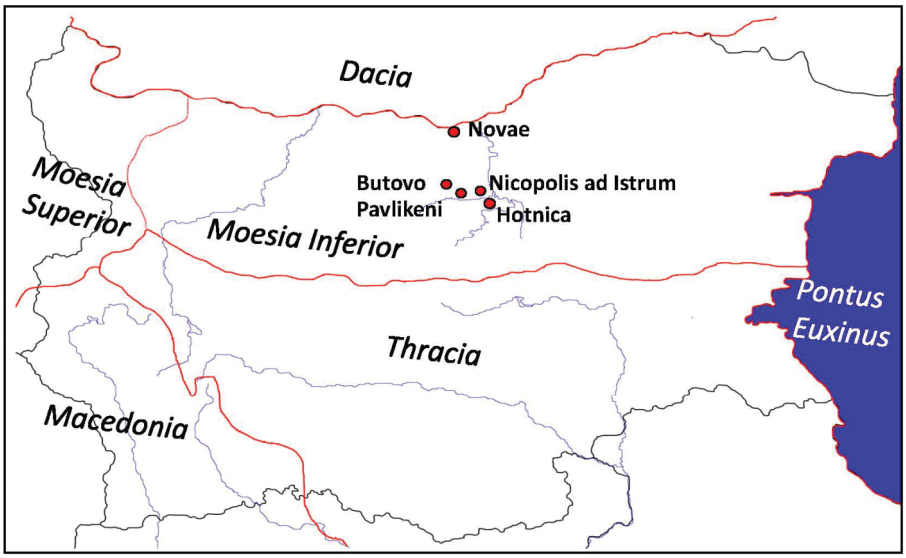

Fig. 1 Map of ceramic production centres in Moesia.

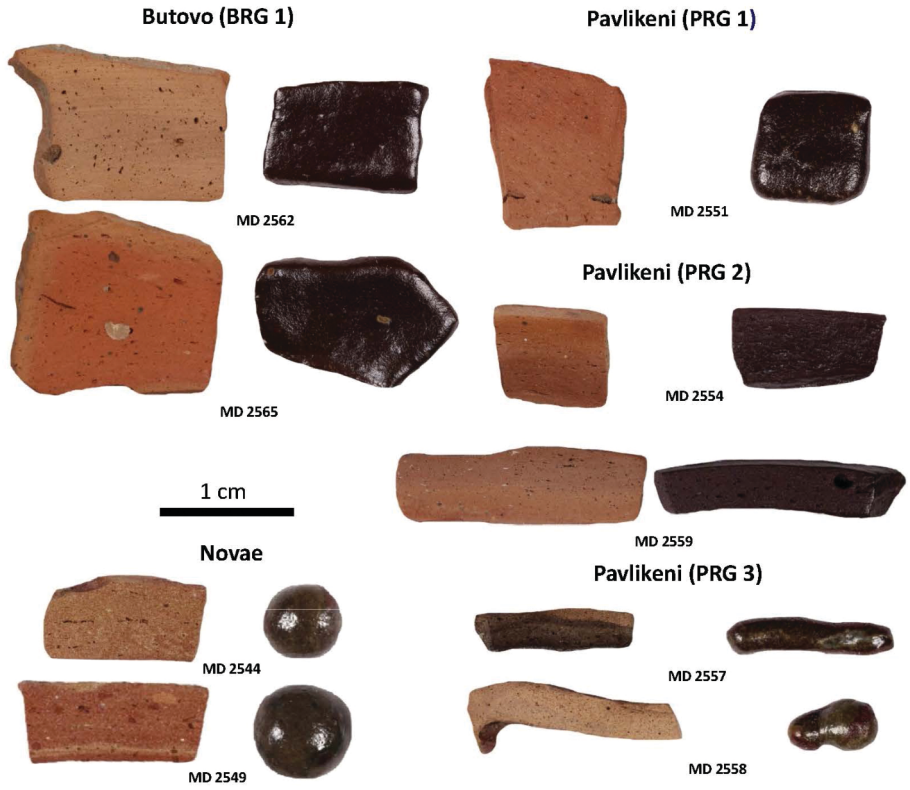

Fig. 2 MGR-analysis of typical examples from the Moesian reference groups, left side = original fragments, right side = fragments after refiring at 1200°C.

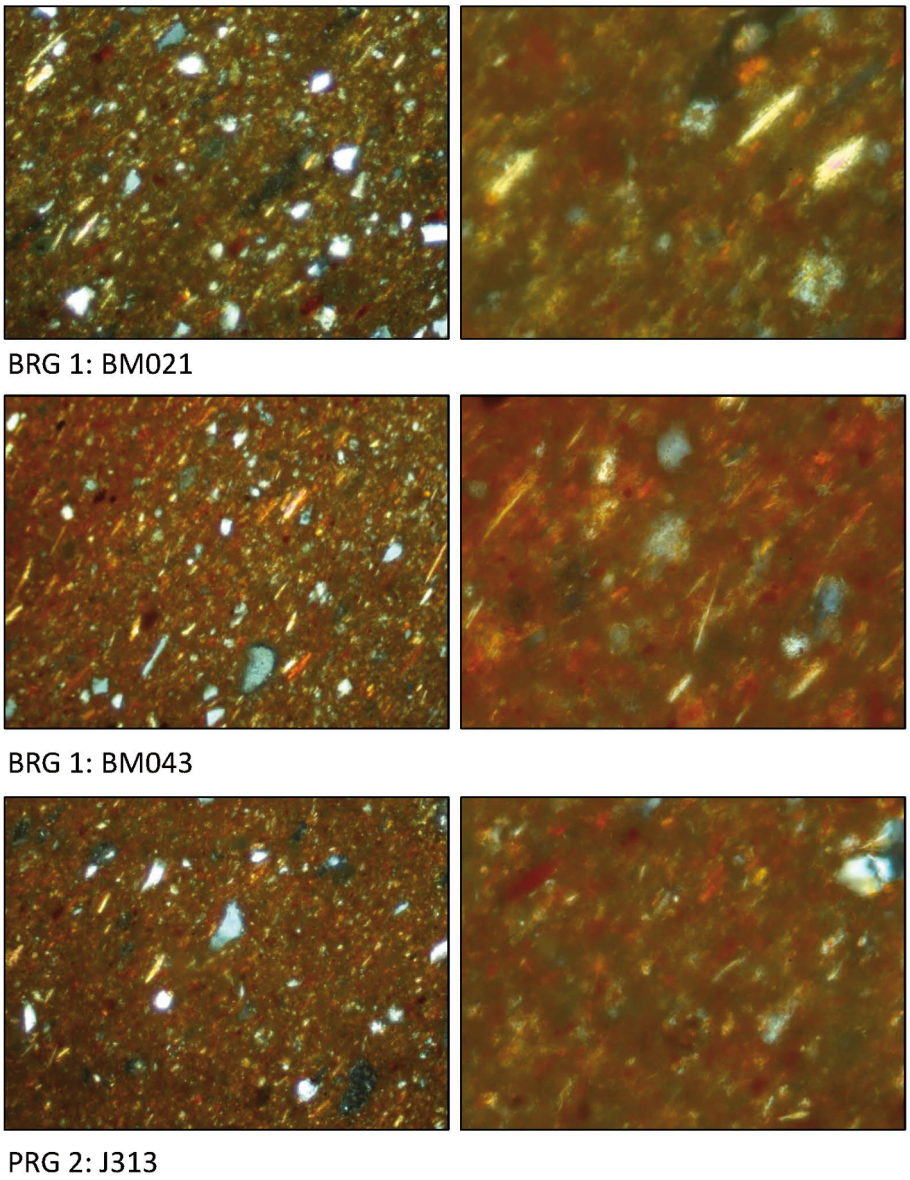

Fig. 3 Photomicrographs of typical thin-sections of Moesian sigillata from BRG 1 (samples BM021, BM043) and from PRG 2 (sample J313), XPL, width of field left side: 0.7 mm, right side: 0.17 mm.

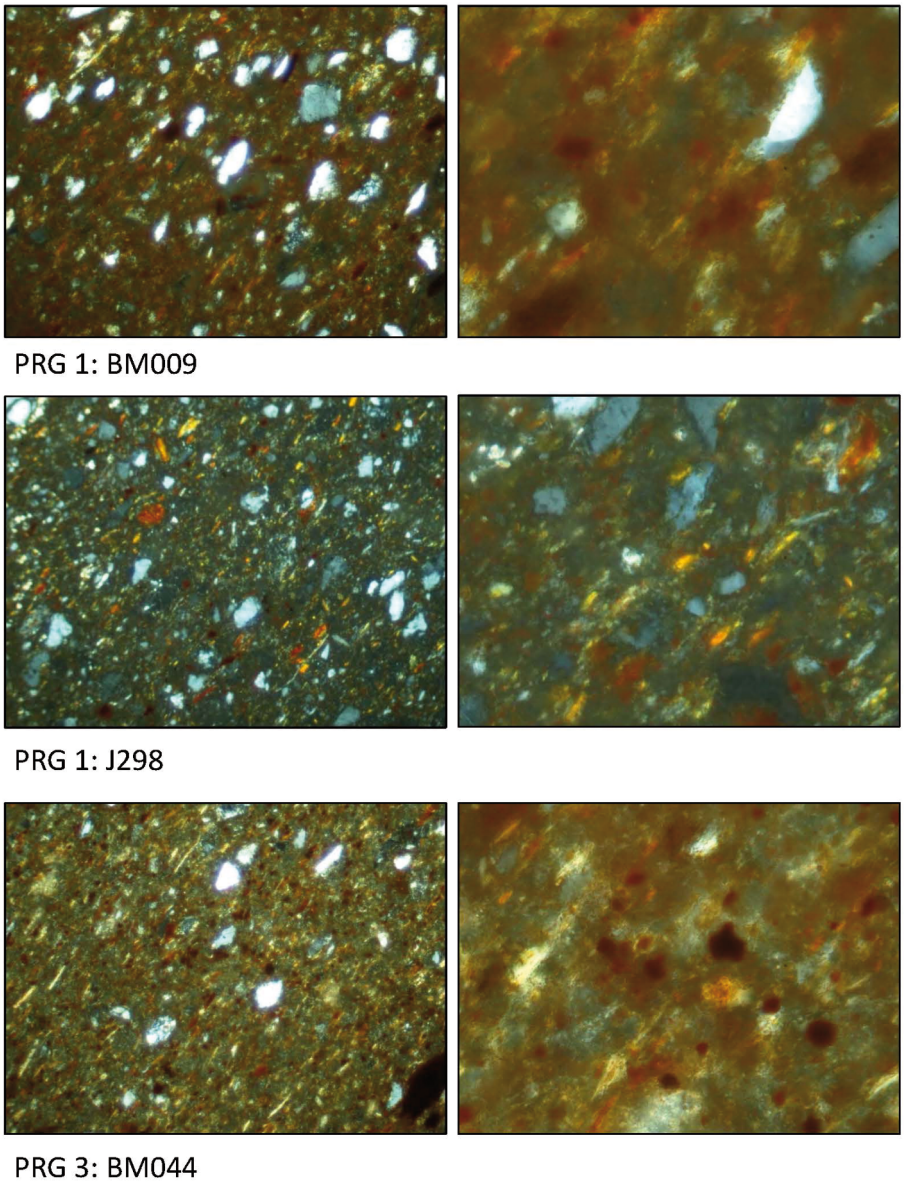

Fig. 4 Photomicrographs of typical thin-sections of Moesian sigillata from PRG 1 (samples BM009, BM298) and from PRG 3 (sample BM044), XPL, width of field left side: 0.7 mm, right side: 0.17 mm.

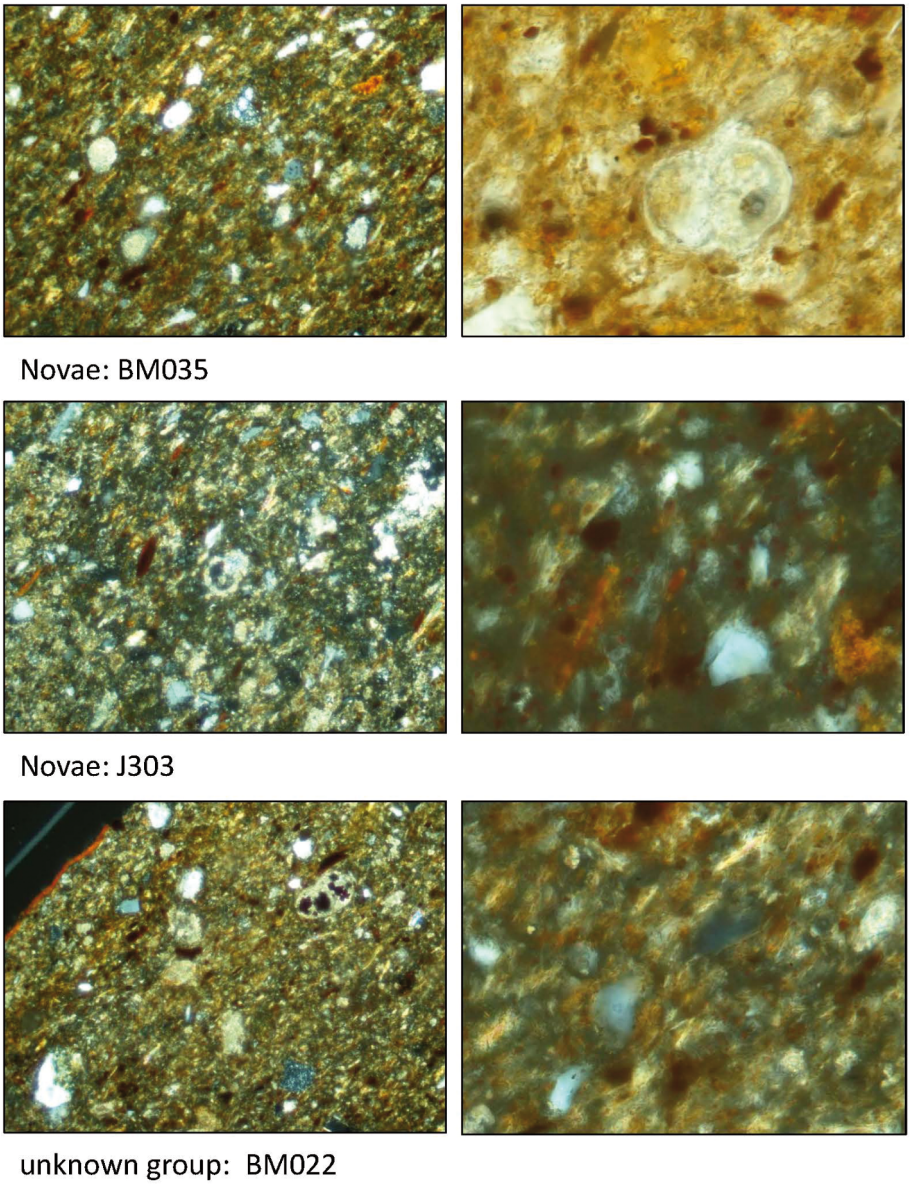

Fig. 5 Photomicrographs of typical thin-sections of sigillata from Novae (samples BM035, J303) and a sample with unknown attribution (BM022), XPL, width of field left side: 0.7 mm, right side: 0.17 mm.

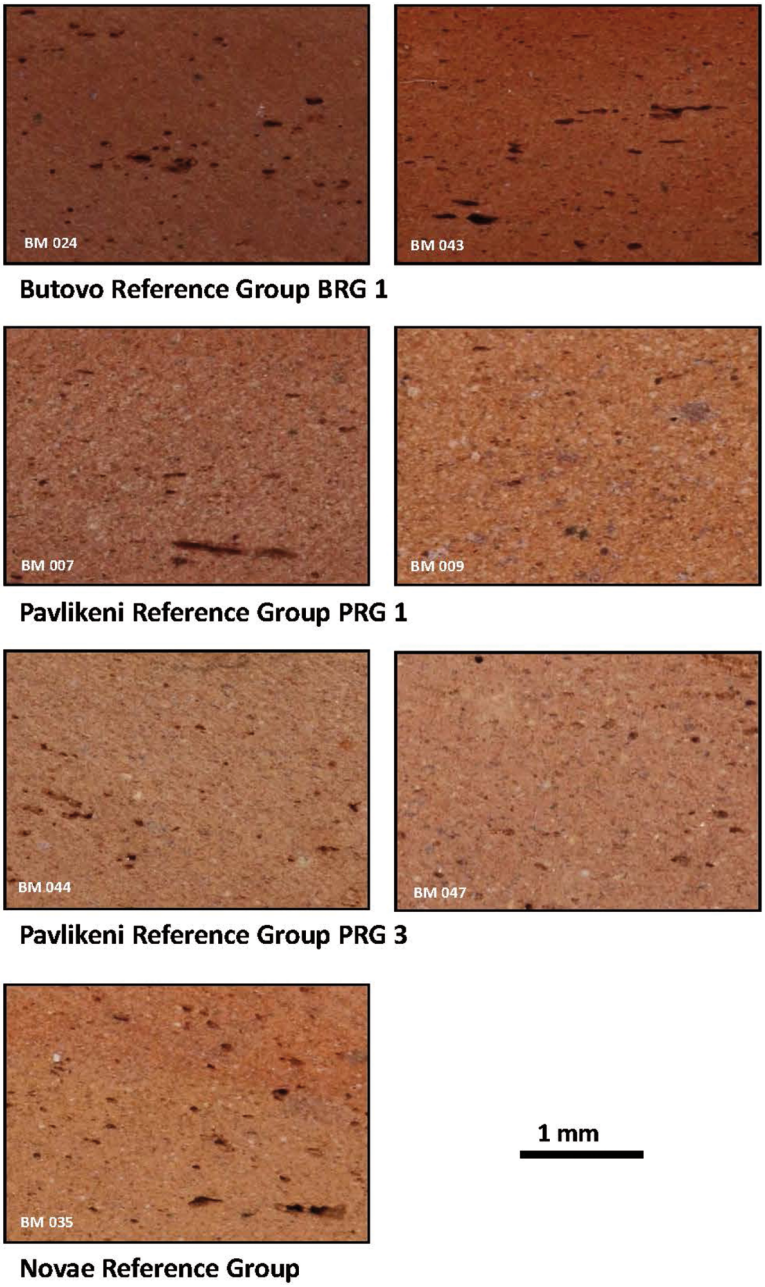

Fig. 6 Macroscopic images of cut sections of typical samples of the reference groups.

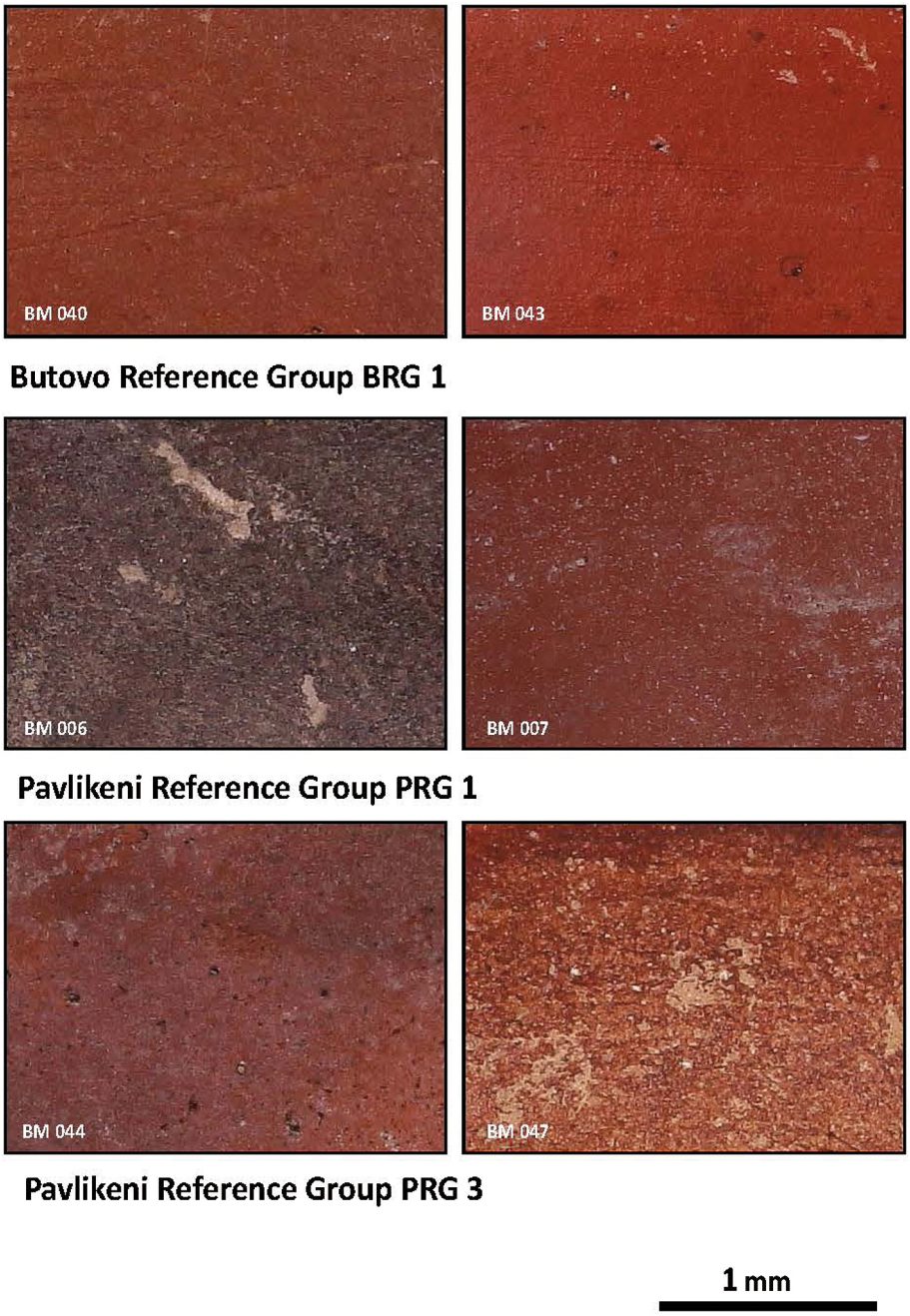

Fig. 7 Macrophotos of the slipped surfaces of typical sherds from the reference groups BRG 1, PRG 1, and PRG 3, XPL (BM035 right side PPL).

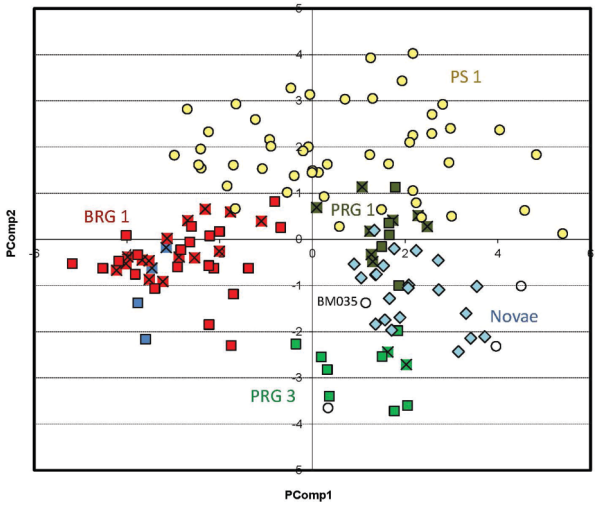

Fig. 8 Principal component analysis (PCA) of WD-XRF data of groups of Moesian sigillata, Novae and of north Pontic sigillata PS 1 (using concentration values of SiO_2, TiO_2, Al_2O_3, Fe_2O_3, MnO, MgO, CaO, Na_2O, K_2O, V, Cr, Ni, Zn, Rb, Sr, and Zr). Moesian sigillata BRG 1 = red squares, PRG 1 = dark olive squares, PRG 2 = blue squares, PRG 3 = green squares; Novae = pale blue rhombs; Pontic sigillata PS 1 = yellow circles, non-attributed samples = empty circles; reference samples from Butovo and Pavlikeni are marked with a cross, the others are finds attributed to reference groups by MGR-analysis and WD-XRF.

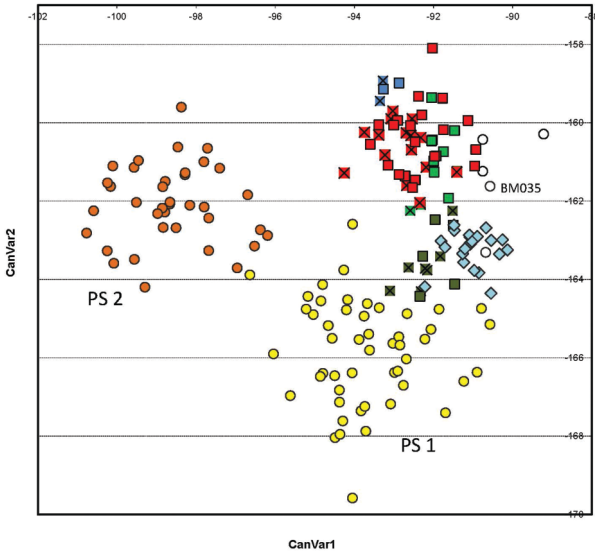

Fig. 9 Discriminant analysis using scores of the same elemental data as in Fig. 8 but including Pontic sigillata PS 2 (= brown circles, other symbols as in Fig. 8).

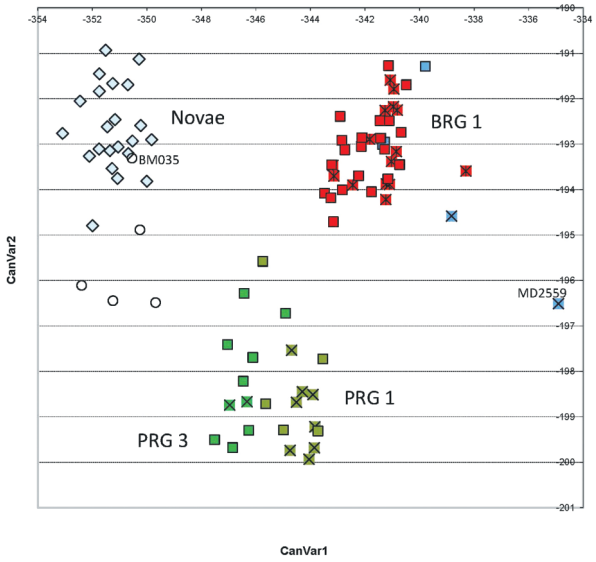

Fig. 10 Discriminant analysis of the three groups of Moesian sigillata and of Novae (Symbols as in Fig. 8).

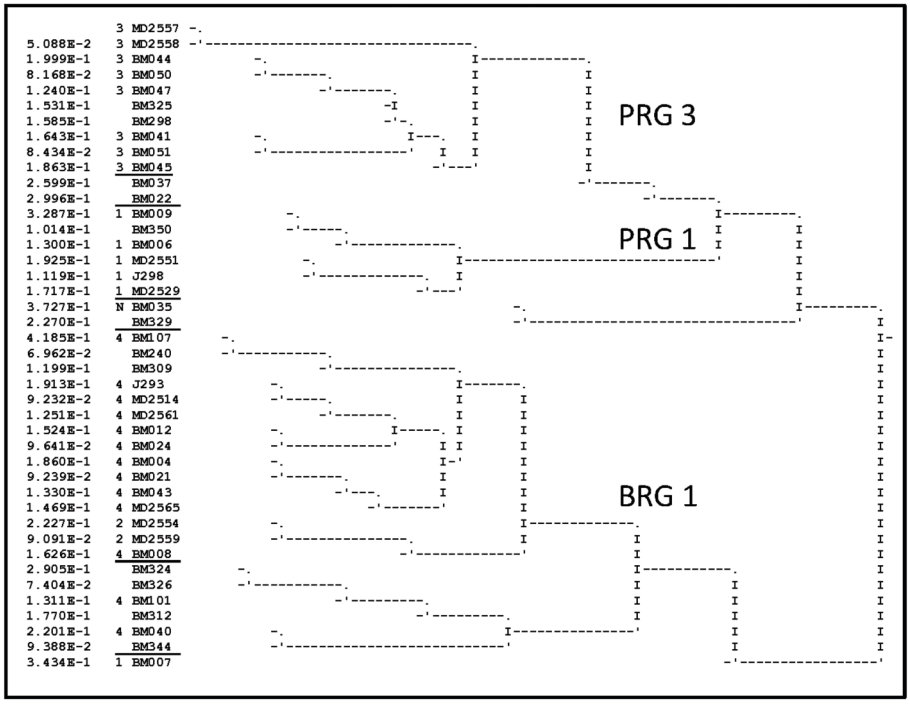

Fig. 11 Dendrogram of WD-XRF data of 42 samples of Moesian sigillata (Euclidean distances of logged data of SiO_2, TiO_2, Al_2O_3, Fe_2O_3, MnO, MgO, CaO, Na_2O, K_2O, V, Cr, Ni, Rb, Sr, Zr, Zn; average linkage). Column 1: Euclidean distances, column 2: group attributions by MGR-analysis, column 3: sample nos.

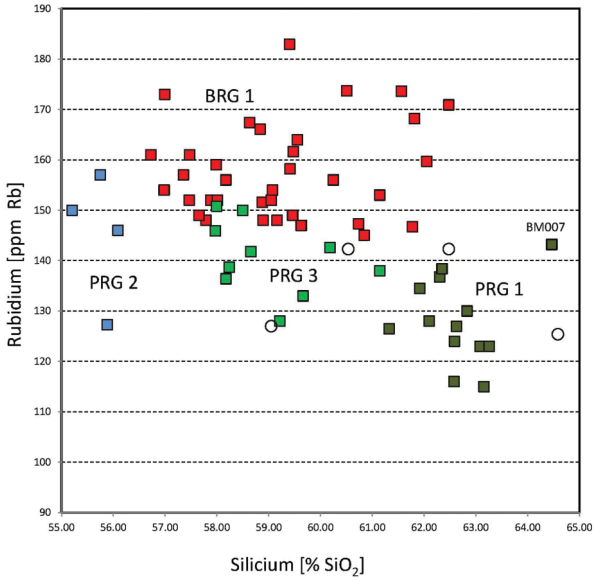

Fig. 12 Bivariate diagram Silicium/Rubidium (analyses by WD-XRF): BRG 1 = red squares, PRG 1 = dark olive squares, PRG 2 = blue squares, PRG 3 = green squares, non-attributed = empty circles.

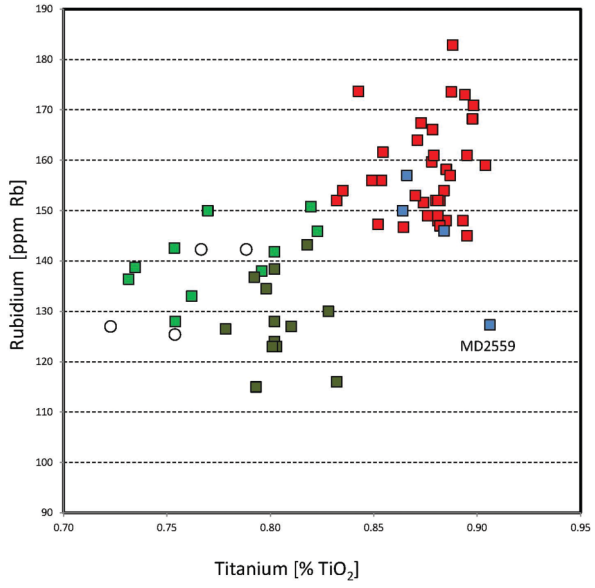

Fig. 13 Bivariate diagram Titanium/Rubidium (analyses by WD-XRF): symbols as in Fig. 12.

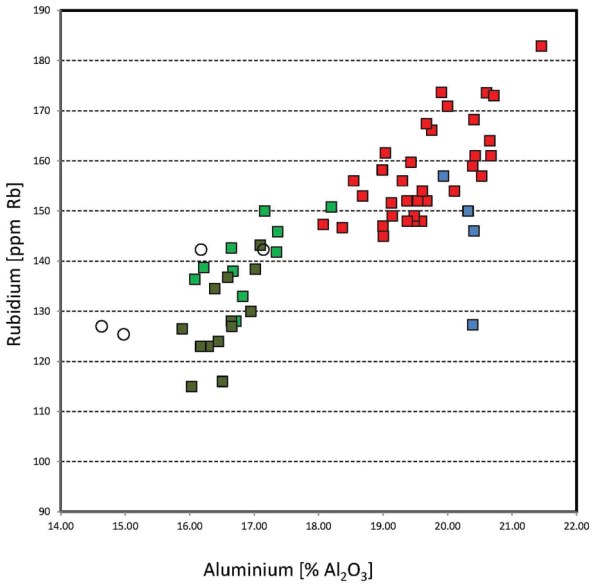

Fig. 14 Bivariate diagram Aluminium/Rubidium (analyses by WD-XRF): symbols as in Fig. 12.

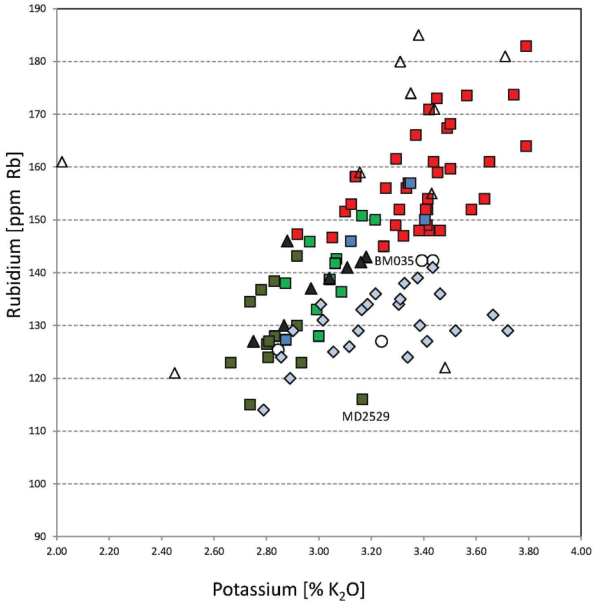

Fig. 15 Bivariate diagram Potassium/Rubidium (analyses by WD-XRF): pale blue rhombs = Novae, other symbols as in Fig. 12. Data by Kuleff/Djingova 1996: black triangles = major group of eight samples attributed by Kuleff and Djingova 1996 to Pavlikeni, empty triangles = other data by Kuleff and Djingova 1996 (five analyses are outside the frame).

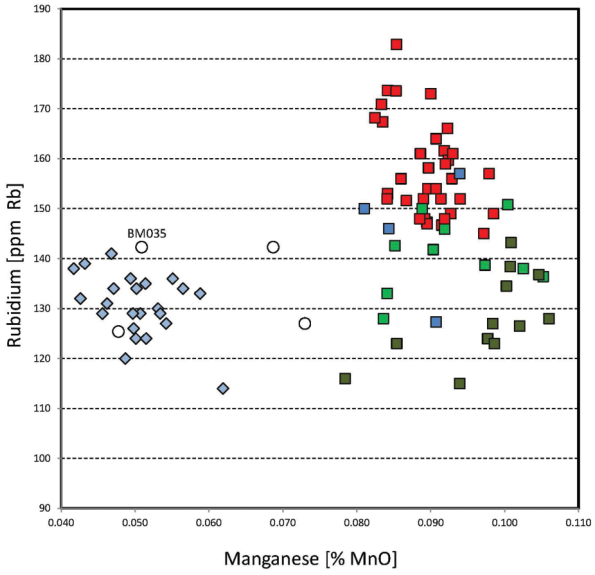

Fig. 16 Bivariate diagram Manganese/Rubidium (analyses by WD-XRF): symbols as in Fig. 15.

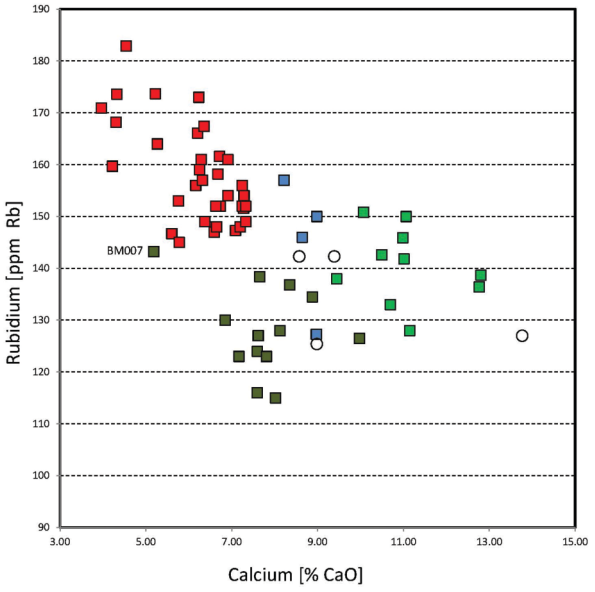

Fig. 17 Bivariate diagram Calcium/Rubidium (analyses by WD-XRF): symbols as in Fig. 15.

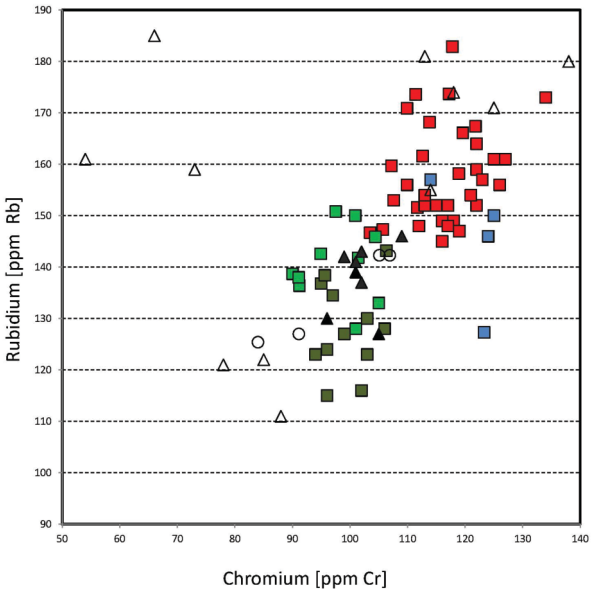

Fig. 18 Bivariate diagram Chromium/Rubidium (analyses by WD-XRF): symbols as in Fig. 15.

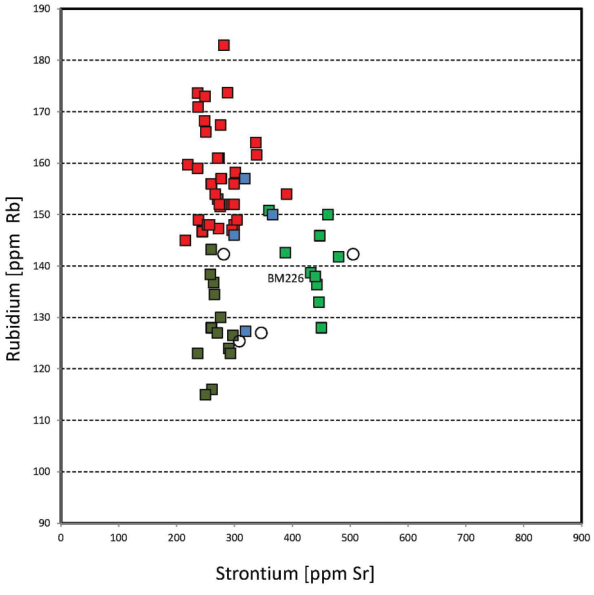

Fig. 19 Bivariate diagram Strontium/Rubidium (analyses by WD-XRF): symbols as in Fig. 15.

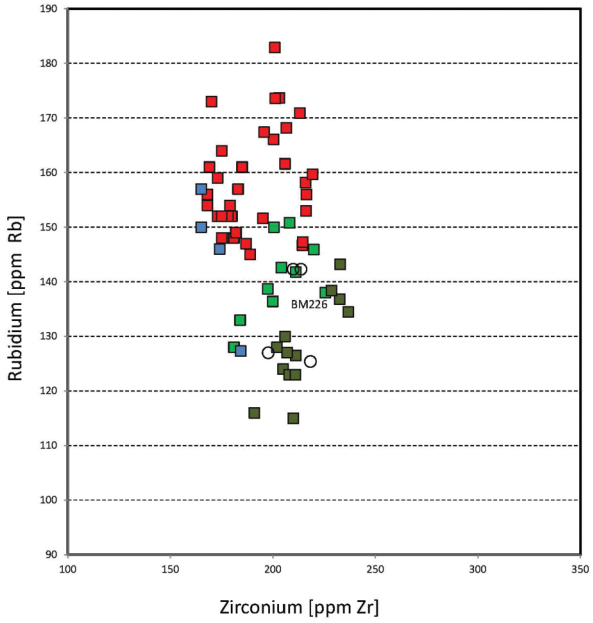

Fig. 20 Bivariate diagram Zirconium/Rubidium (analyses by WD-XRF): symbols as in Fig. 15.

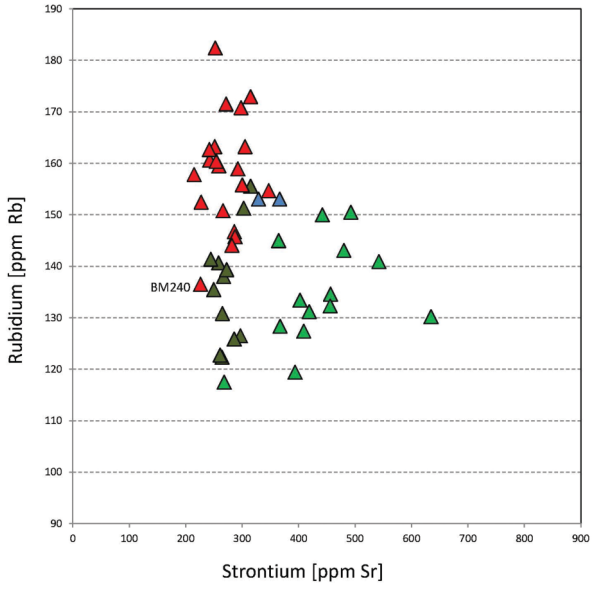

Fig. 21 Bivariate diagram Strontium/Rubidium (analyses exclusively by pXRF (every triangle represents the average of three measurements on fresh fracture): colors as in Fig. 15.

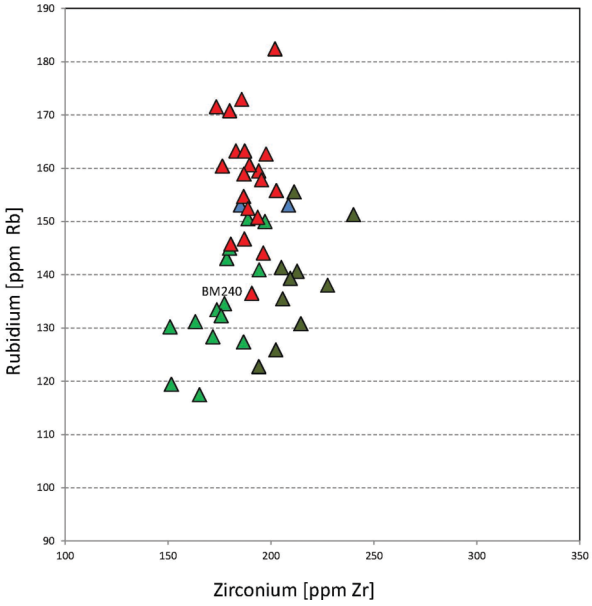

Fig. 22 Bivariate diagram Zirconium/Rubidium (analyses exclusively by pXRF (every triangle represents the average of three measurements on fresh fracture): symbols as in Fig. 21.

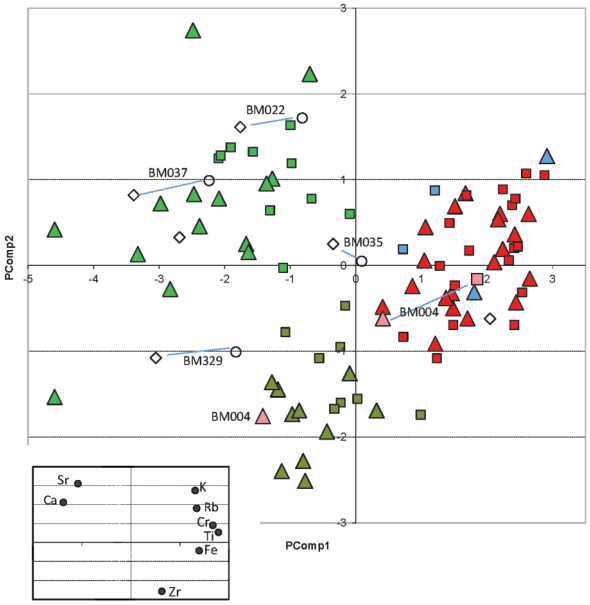

Fig. 23 PCA of WD-XRF and pXRF data of Moesian sigillata (elements used Ti, Fe, Ca, K, Cr, Rb, Sr, Zr): squares and circles = WD-XRF, triangles and rhombs = pXRF, colors as in Fig. 21, differing results of sample BM004 are marked with pale red colors.

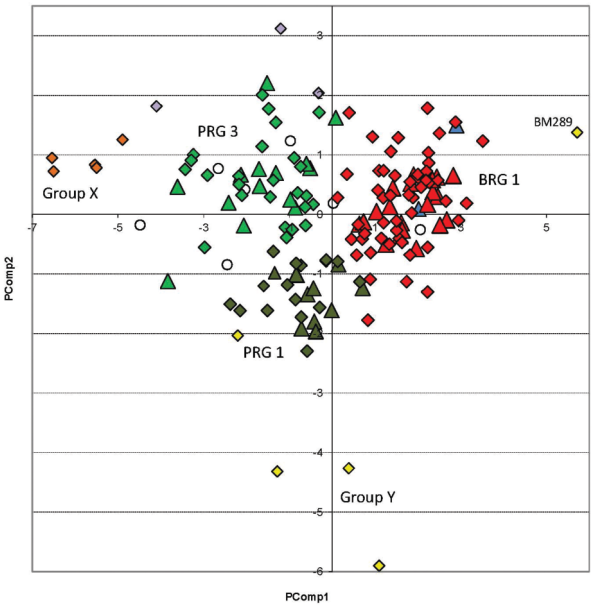

Fig. 24 PCA of all samples using exclusively pXRF (every point represents the average of three measurements on a fresh break): triangles = pXRF of samples confirmed by other methods, rhombs = samples attributed to groups by pXRF (brown = calcareous samples of group X, yellow = non-calcareous samples, violet = three samples with extremely high Strontium contents, other colors as in Fig. 21.

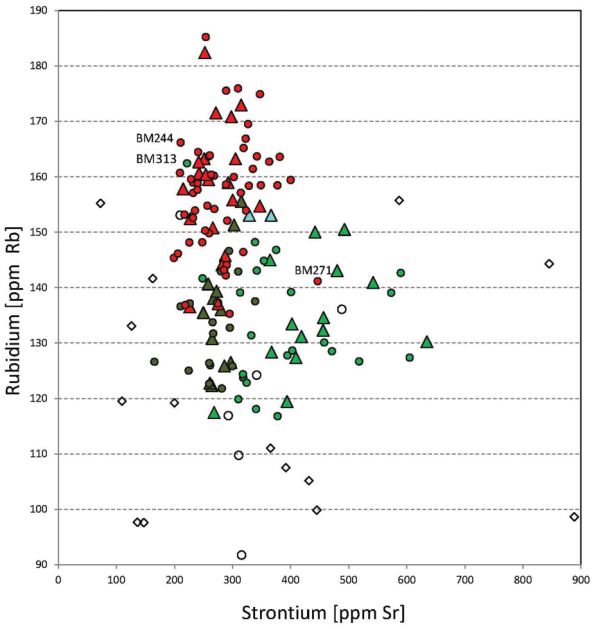

Fig. 25 Bivariate diagram Strontium/Rubidium of pXRF measurements: triangles as in fig. 21, circles = samples attributed using results of PCA in fig. 24 (BM271, BM244 and BM313 are erroneously classified by PCA), empty rhombs and empty circles = samples not attributed to the three Moesian groups by PCA.

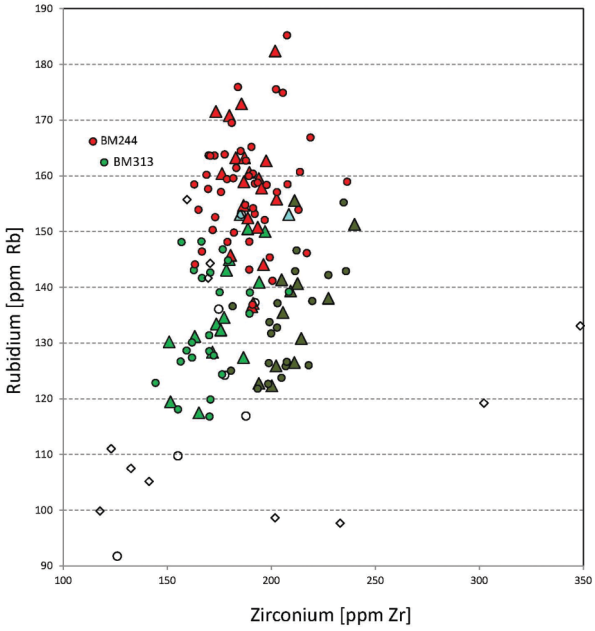

Fig. 26 Bivariate diagram Zirconium/Rubidium of pXRF measurements (symbols as in Fig. 25).

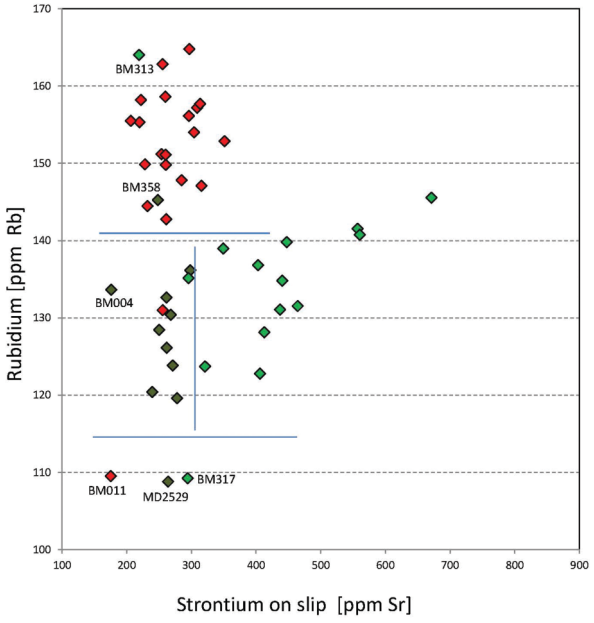

Fig. 27 Bivariate diagram Strontium/Rubidium of pXRF measurements on slipped surfaces (symbols as in Fig. 25).

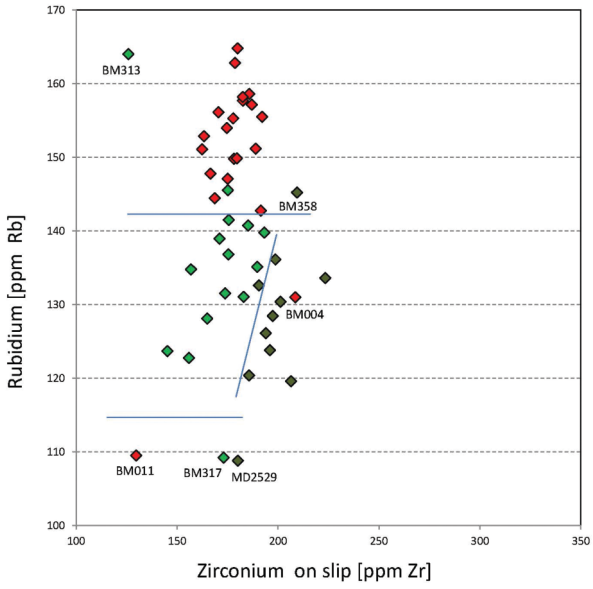

Fig. 28 Bivariate diagram Zirconium/Rubidium of pXRF measurements on slipped surfaces (symbols as in Fig. 25).

Reference group	SiO_2	TiO_2	Al_2O_3	Fe_2O_3	MnO	MgO	CaO	Na_2O	K_2O	P_2O_5	V	Cr	Ni	(Cu)	Zn	Rb	Sr	Y	Zr	(Nb)	Ba	(Ce)	(Pb)	l.o.i.
	% by weight										ppm													%
Pontic Sigillata:																								
PS 1 (n=52)	**65.13**	**0.860**	**16.79**	**6.27**	**0.078**	**1.99**	**4.76**	**1.05**	**2.90**	**0.173**	**120**	**110**	**58**	**45**	**103**	**130**	**234**	**28**	**186**	**16**	**508**	**67**	**21**	**1.92**
std ±	2.38	0.050	1.27	0.62	0.027	0.33	1.45	0.16	0.23	0.055	13	12	8	14	13	12	58	3	20	3	104	12	6	0.77
cv [%] ±	3.7	5.8	7.6	9.9	34.7	16.8	30.4	14.8	7.8	32.0	10.7	11.3	13.5	30.1	12.7	9.3	24.6	10.8	10.6	17.7	20.6	18.6	28.7	39.9
PS 2 (n=39)	**57.16**	**0.839**	**18.00**	**7.35**	**0.100**	**3.01**	**9.15**	**1.24**	**2.94**	**0.205**	**138**	**147**	**85**	**50**	**96**	**124**	**364**	**26**	**148**	**14**	**419**	**68**	**17**	**2.53**
std ±	2.57	0.047	1.38	0.46	0.034	0.30	2.72	0.15	0.22	0.180	17	15	10	10	14	16	70	3	18	3	76	12	11	1.47
cv [%] ±	4.5	5.6	7.6	6.3	33.8	10.0	29.7	12.3	7.6	87.7	12.0	9.9	11.6	19.8	14.3	13.0	19.3	11.7	12.5	20.4	18.2	17.9	61.9	58.3
Pavlikeni:																								
PRG 1 (n=13)	**62.66**	**0.805**	**16.51**	**6.22**	**0.098**	**1.94**	**7.75**	**0.94**	**2.84**	**0.213**	**120**	**99**	**53**	**33**	**94**	**128**	**268**	**26**	**214**	**14**	**385**	**76**	**23**	**2.28**
std ±	0.76	0.015	0.37	0.15	0.009	0.09	1.10	0.15	0.12	0.070	10	4	6	10	6	8	17	4	14	2	50	10	6	1.17
cv [%] ±	1.2	1.8	2.2	2.4	8.8	4.6	14.2	15.8	4.4	32.7	8.0	4.1	10.5	30.8	6.8	6.6	6.5	15.3	6.6	13.0	13.1	13.1	24.5	51.3
PRG 2 (n=4)	**55.64**	**0.878**	**20.35**	**7.04**	**0.087**	**2.86**	**8.68**	**1.01**	**3.19**	**0.173**	**149**	**122**	**61**	**37**	**113**	**144**	**323**	**30**	**171**	**15**	**419**	**92**	**27**	**1.34**
std ±	0.37	0.017	0.33	0.10	0.006	0.34	0.34	0.09	0.24	0.004	4	5	4	2	5	14	30	2	7	0	18	4	2	0.31
cv [%] ±	0.7	1.9	1.6	1.4	6.5	11.8	3.9	9.1	7.5	2.0	2.5	4.3	5.9	6.5	4.8	9.9	9.3	7.3	4.1	0.0	4.2	4.6	6.4	23.2
PRG 3 (n=12)	**59.17**	**0.769**	**16.58**	**5.90**	**0.088**	**2.12**	**11.29**	**0.73**	**3.05**	**0.292**	**121**	**97**	**56**	**39**	**95**	**138**	**427**	**22**	**202**	**14**	**424**	**68**	**22**	**4.26**
std ±	1.17	0.034	0.98	0.31	0.015	0.22	1.23	0.09	0.12	0.078	11	5	7	10	5	9	41	4	13	1	62	10	5	1.44
cv [%] ±	2.0	4.4	5.9	5.2	16.7	10.2	10.9	12.7	4.0	26.6	9.0	5.6	12.5	24.5	5.4	6.4	9.5	16.6	6.4	6.0	14.5	15.3	24.6	33.8
Kuleff et al. 1996, 1999:																								
cluster 1 (NAA)				**5.66**				**0.94**	**3.00**			**102**				**138**					**410**	**70**		
cluster 3 (ICP)	***mean***	**0.80**	**14.49**	**5.95**	**0.081**	**2.79**	**4.97**				**137**	**168**	**138**	**46**			**194**		**149**		**280**	**81**		
cluster 3 (ICP)	*std* ±	0.08	4.06	0.77	0.012	0.71	0.77				16	66	54	20			47		37		80	28		
Butovo:																								
BRG 1 (n=37)	**59.15**	**0.875**	**19.60**	**6.71**	**0.090**	**2.62**	**6.34**	**0.96**	**3.40**	**0.218**	**145**	**117**	**63**	**42**	**108**	**157**	**276**	**27**	**189**	**15**	**436**	**81**	**24**	**1.54**
std ±	1.57	0.019	0.77	0.40	0.004	0.33	1.12	0.12	0.20	0.074	13	6	6	13	8	10	37	4	17	1	56	9	6	0.74
cv [%] ±	2.6	2.1	3.9	5.9	4.6	12.8	17.6	12.3	5.8	34.0	8.7	5.6	9.1	29.8	7.4	6.4	13.5	14.3	8.9	6.2	12.8	11.1	24.9	47.8
Novae:																								
Novae (n=23)	**62.31**	**0.788**	**15.97**	**5.50**	**0.050**	**2.04**	**8.79**	**0.94**	**3.27**	**0.335**	**126**	**99**	**47**	**31**	**111**	**131**	**306**	**25**	**190**	**14**	**372**	**71**	**32**	**2.92**
std ±	1.05	0.019	0.56	0.17	0.004	0.09	1.46	0.09	0.24	0.107	10	8	5	9	15	6	42	2	7	2	24	9	20	1.23
cv [%] ±	1.7	2.4	3.5	3.1	8.903	4.3	16.6	9.1	7.2	32.0	7.8	8.2	9.8	29.4	13.8	4.5	13.8	6.1	3.9	12.3	6.4	12.5	64.0	42.1

Tab. 1 Averages and standard deviations of analyses by WD-XRF of reference groups of North Pontic and Moesian sigillata (samples ignited at 900°C, l.o.i = loss on ignition), and published data by Kuleff and Djingova 1996 and Kuleff, Djingova, and Kabakchieva 1999.

Sample No.	Non-plastic inclusions						
	color	shape	roundness	size [mm] main	size [mm] isolated	volume %	sorting
PRG 1							
BM 007	ecru, white, shiny	very spherical	well-rounded	0.1-0.2		5%	very well-sorted
BM 009	grey, white, shiny	very spherical	well-rounded	0.1		5%	very well-sorted
BM 006	ecru, grey, shiny	very spherical	well-rounded	0.1-0.2		5%	very well-sorted
PRG 3							
BM 041	ecru, grey, shiny	very spherical	well-rounded	0.1-0.2		10%	well-sorted
BM 045	white, grey, ecru, shiny	very spherical	rounded	0.1-0.2	1	15%	moderately sorted
BM 051	ecru, grey, brown, shiny	very spherical	rounded	0.1-0.2		10%	well-sorted
BM 044	white, grey, brown	very spherical	rounded	0.1-0.3		10%	well-sorted
BM 047	white, grey, ecru, brown	very spherical	rounded	0.1-0.3		20%	well-sorted
BM 050	white, grey, brown, shiny	very spherical	well-rounded	0.1-0.3		10%	well-sorted
BRG 1							
BM 004	grey, ecru, brown, shiny	very spherical	well-rounded	0.1-0.2		5%	very well-sorted
BM 008	ecru, grey, shiny	very spherical	well-rounded	0.1-0.2		5%	very well-sorted
BM 012	ecru, shiny	very spherical	well-rounded	0.1-0.2		2.5%	very well-sorted
BM 021	white, grey, ecru, red	very spherical	well-rounded	0.1-0.2		10%	well-sorted
BM 024	grey, white, shiny	very spherical	well-rounded	0.1-0.2	0.3	10%	very well-sorted
BM 040	white, grey, ecru, shiny	very spherical	well-rounded	0.1-0.2		10%	well-sorted
BM 043	white, ecru, grey, shiny	very spherical	rounded	0.1-0.2		10%	well-sorted
unknown							
BM 022	grey, white, brown, ecru	very spherical	rounded	0.1-0.2		20%	moderately sorted
BM 037	white, grey, red, shiny	very spherical	rounded	0.1-0.2		20%	well-sorted

Sample No.	Appearance			Pores			
	Texture	in fresh fracture	Compactness	size [mm] main	size [mm] isolated	pattern	shape
PRG 1							
BM 007	dense with few pores	granular-earthy	good	0.2-0.4	1.8	random	elongated, bubbles
BM 009	dense with few pores	granular-earthy	good	0.2-0.4	1.2	random	elongated
BM 006	dense with few pores	granular-earthy	good	0.2-0.4	1.9	random	bubbles
PRG 3							
BM 041	dense with a lot of pores	granular-earthy	good	0.1-0.4	0.8-1.1	random	elongated, bubbles
BM 045	dense with few pores	earthy	good	0.1-0.5		random	elongated
BM 051	dense with few pores	granular-earthy	good	0.1-0.4	1.1	random	elongated, bubbles
BM 044	dense with few pores	earthy	good	0.1-0.4		random	elongated, bubbles
BM 047	dense with a lot of pores	earthy	good	0.1-0.3	0.7-1.0	random	elongated, bubbles
BM 050	dense with few pores	earthy	good	0.3-1.0		random	elongated, bubbles
BRG 1							
BM 004	dense with few pores	earthy	good	0.2-0.5	1.0-1.2	random	elongated, bubbles
BM 008	dense with few pores	earthy	good	0.2-0.4		random	elongated, bubbles
BM 012	dense with a lot of pores	earthy	good	0.2-0.7		random	bubbles, elongated
BM 021	dense with few pores	earthy	good	0.1-0.4		random	elongated, bubbles
BM 024	dense with few pores	earthy	good	0.2-0.5	1.1	random	elongated
BM 040	dense with a lot of pores	earthy	good	0.1-0.5	1	random	elongated
BM 043	dense with few pores	earthy	good	0.1-0.4		random	elongated
unknown							
BM 022	dense with few pores	earthy	good	0.1-0.6	2	random	elongated
BM 037	dense with few pores	earthy	good	0.2-1.0		random	elongated

Tab. 2 Macroscopic classification of typical samples of Moesian sigillata (non-plastic inclusions, appearance of the fresh fractures, and pores).

Find spot	Lab.-No.	MGR-analysis	WD-XRF	Thin-section	pXRF PCA/RbSrZr	pXRF Dendrg	archaeolog. attribution macroscopic	archaeolog. attribution typological
Butovo (kiln)	J293	BRG 1	BRG 1		BRG 1	BRG 1	BRG 1	
Pavlikeni villa (kiln)	J298	PRG 1	PRG 1	PRG 1	PRG 1	PRG 1	PRG 1	
Novae	MD2514	BRG 1	BRG 1		BRG 1	BRG 1	BRG 1	
	MD2529	PRG 1	PRG 1		PRG 1	PRG 1	PRG 1	
	MD2551	PRG 1	PRG 1		PRG 1	PRG 1	PRG 1	
Pavlikeni	MD2554	PRG 2	PRG 2		PRG 2	BRG 1		
	MD2557	PRG 3	PRG 3		PRG 3	PRG 3	PRG 3	
	MD2558	PRG 3	PRG 3		PRG 3	PRG 3	PRG 3	
	MD2559	PRG 2	PRG 2		PRG 2	BRG 1		
	MD2561	BRG 1	BRG 1		BRG 1	BRG 1	BRG 1	
Butovo	MD2565	BRG 1	BRG 1		BRG 1	BRG 1	BRG 1	
Pavlikeni	BM004	BRG 1	BRG 1		BRG 1	PRG 1	BRG 1	Butovo
	BM005	PRG 1			PRG 1	PRG 1	PRG 3	
Butovo	BM006	PRG 1	PRG 1		PRG 1	PRG 1	PRG 1	
	BM007	PRG 1	PRG 1		PRG 1	PRG 1	PRG 1	Pavlikeni
	BM008	BRG 1	BRG 1		BRG 1	BRG 1	BRG 1	
	BM009	PRG 1	PRG 1	PRG 1	PRG 1	PRG 1	PRG 1	Pavlikeni
Hotnica	BM011	BRG 1			BRG 1	BRG 1	BRG 1	
	BM012	BRG 1	BRG 1		BRG 1	BRG 1	BRG 1	Butovo
Pavlikeni	BM017	PRG 1			PRG 1	PRG 1	BRG 1	
	BM020	BRG 1			PRG 1	PRG 1	PRG 3	
Novae	BM021	BRG 1	BRG 1	BRG 1	BRG 1	BRG 1	BRG 1	Butovo
	BM022	unkown	unknown	unknown	unknown	PRG 3	PRG 3	
	BM024	BRG 1	BRG 1		BRG 1	BRG 1	BRG 1	Butovo
	BM026	Novae			unknown	PRG 3	PRG 3	
	BM031	unknown			unknown	BRG 1	BRG 1	
	BM035	Novae	Novae		Novae	PRG 3	Novae	
	BM036	PRG 3			PRG 3	PRG 3	PRG 3	
	BM037	unkown	unknown	unknown	unknown	PRG 3	PRG 3	
	BM040	BRG 1	BRG 1		BRG 1	BRG 1	BRG 1	Butovo
Nikopolis	BM041	PRG 3	PRG 3		PRG 3	–	PRG 1	
	BM043	BRG 1	BRG 1	BRG 1	BRG 1	BRG 1	BRG 1	Butovo
	BM044	PRG 3	PRG 3	PRG 3	PRG 3	PRG 3	PRG 3	
	BM045	PRG 3	PRG 3		PRG 3	PRG 3	PRG 3	Pavlikeni
	BM046	PRG 3			PRG 3	PRG 3	PRG 3	
	BM047	PRG 3	PRG 3		PRG 3	PRG 3	PRG 3	Pavlikeni
	BM050	PRG 3	PRG 3		PRG 3	PRG 3	PRG 3	
	BM051	PRG 3	PRG 3		PRG 3	PRG 3	PRG 3	
	BM054	Novae			unknown	PRG 3	BRG 1	
	BM056	PRG 3			PRG 3	PRG 3	PRG 3	
	BM057	PRG 3			PRG 3	PRG 3	PRG 3	
	BM059	PRG 3			PRG 3	PRG 3	PRG 3	
Butovo	BM100				BRG 1	BRG 1	BRG 1	
	BM101	BRG 1	BRG 1		BRG 1	BRG 1	BRG 1	
	BM102				BRG 1	BRG 1	BRG 1	
	BM103				BRG 1	BRG 1	BRG 1	
	BM104				BRG 1	BRG 1	BRG 1	
	BM105				BRG 1	BRG 1	BRG 1	
	BM106				BRG 1	BRG 1	BRG 1	
	BM107	BRG 1	BRG 1		BRG 1	BRG 1	BRG 1	
	BM108				BRG 1	BRG 1	BRG 1	
	BM109				BRG 1	PRG 3	BRG 1	
Stäklen, Novae canabe	BM200				PRG 3	PRG 3	BRG 1	
	BM201				BRG 1	BRG 1	BRG 1	
	BM202				PRG 3	PRG 3	BRG 1	

Tab. 3 List of analysed samples, methods used for attribution. Final results for all samples in column PCA/RbSrZr (combined result from PCA and bivariate diagrams).

Find spot	Lab.-No.	MGR-analysis	WD-XRF	Thin-section	pXRF PCA/RbSrZr	pXRF Dendrg	archaelog. attribution macroscopic	archaelog. attribution typological
Manastirski trap	**BM206**				BRG 1	BRG 1	BRG 1	
Dălboki dol	**BM234**				PRG 3	PRG 3	BRG 1	BRG/PRG
	BM235				PRG 1	PRG 1	BRG 1	Pavlikeni
Ostrite mogili (near Novae)	**BM236**				BRG 1	BRG 1	BRG 1	
	BM237				PRG 3	PRG 3	BRG 1	
	BM238				BRG 1	BRG 1	BRG 1	
	BM239				PRG 3	PRG 3	BRG 1	
	BM240		BRG 1		BRG 1	BRG 1	BRG 1	
	BM241				unknown	–	BRG 1	
	BM242				PRG 1	PRG 3	BRG 1	
	BM243		Lezoux		unknown	PRG 3	BRG 1	
	BM244				BRG 1 ?	PRG 3	BRG 1	
	BM245				PRG 1	PRG 1	PRG 3	PRG/BRG
	BM246				BRG 1	BRG 1	BRG 1	Butovo
	BM247				BRG 1	BRG 1	BRG 1	Butovo
	BM248				PRG 3	PRG 3	BRG 1	Butovo
	BM249				PRG 1	PRG 3	BRG 1	Butovo
	BM250				BRG 1	BRG 1	BRG 1	Butovo
	BM251				BRG 1	BRG 1	BRG 1	
	BM252				BRG 1	PRG 3	BRG 1	
	BM253				BRG 1	BRG 1	BRG 1	
	BM255				BRG 1	BRG 1	BRG 1	Pavlikeni
	BM257				BRG 1	BRG 1	BRG 1	PRG/BRG
	BM258				BRG 1	BRG 1	BRG 1	
Livadite	**BM264**				PRG 3	PRG 3	BRG 1	
Selište	**BM270**				PRG 3	PRG 3	PRG 3	
	BM271				BRG 1 ?	PRG 3	PRG 3	
West of Hadžidimitrovo	**BM272**				PRG 3	PRG 3	PRG 3	
	BM273				PRG 3	PRG 3	BRG 1	
Zad Lozjata	**BM284**				PRG 3	PRG 3	BRG 1	
	BM285				PRG 1	PRG 3	PRG 3	
	BM286				PRG 1	PRG 3	PRG 3	
	BM287		PRG 1		PRG 1	PRG 1	BRG 1	
	BM288				BRG 1	PRG 1	BRG 1	
	BM289				unknown	BRG 1	BRG 1	
	BM290				BRG 1	BRG 1	BRG 1	
Erloolu	**BM291**				BRG 1	BRG 1	BRG 1	
	BM292				BRG 1	BRG 1	BRG 1	Butovo
	BM293				BRG 1	BRG 1	BRG 1	Butovo
	BM294				BRG 1	BRG 1	BRG 1	
	BM295				PRG 1	PRG 3	BRG 1	
	BM296				PRG 3	PRG 3	PRG 3	
	BM297				BRG 1	BRG 1	BRG 1	
	BM298		PRG 3		PRG 3	PRG 3	PRG 3	PRG/BRG
Popinca	**BM299**				PRG 3	PRG 3	BRG 1	
	BM300				BRG 1	BRG 1	BRG 1	
	BM301				BRG 1	BRG 1	BRG 1	
	BM302				PRG 1	PRG 1	PRG 1	
	BM303				BRG 1	BRG 1	BRG 1	
	BM304				BRG 1	BRG 1	BRG 1	
	BM305				BRG 1	BRG 1	BRG 1	Butovo
	BM306				PRG 3	PRG 3	BRG 1	Butovo
	BM307				BRG 1	BRG 1	BRG 1	
	BM308				PRG 1	PRG 3	BRG 1	
Latinski grobišta	**BM309**		BRG 1		BRG 1	PRG 1	BRG 1	PRG/BRG

Tab. 3 (Continued) List of analysed samples, methods used for attribution. Final results for all samples in column PCA/RbSrZr (combined result from PCA and bivariate diagrams).

Find spot	Lab.-No.	MGR-analysis	WD-XRF	Thin-section	pXRF		archaelog. attribution	
					PCA/RbSrZr	Dendrg	macroscopic	typological
Sazantalăk; Pčelina	BM310				group X	unknown	BRG 1	
	BM311				BRG 1	BRG 1	BRG 1	PRG/BRG
	BM312		BRG 1		BRG 1	BRG 1	BRG 1	PRG/BRG
	BM313				PRG 3 ?	PRG 3	BRG 1	
	BM314				group X	unknown	BRG 1	PRG/BRG
	BM315				PRG 3	PRG 3	BRG 1	BRG/PRG
	BM316				BRG 1	BRG 1	BRG 1	Butovo
	BM317				PRG 3	PRG 3	BRG 1	
Brjastovete	BM318				BRG 1	PRG 1		
	BM319				BRG 1	BRG 1	BRG 1	BRG/PRG
Gatevska mogila; Zad grobištata	BM321				BRG 1	BRG 1	BRG 1	
	BM322				PRG 1	PRG 1	BRG 1	PRG/BRG
	BM323				group X	unknown	PRG 3	PRG/BRG
	BM324		BRG 1		BRG 1	BRG 1	BRG 1	PRG/BRG
	BM325		PRG 3		PRG 3	PRG 3	PRG 3	PRG/BRG
	BM326		BRG 1		BRG 1	BRG 1	BRG 1	
Drakite	BM327				group X	unknown	BRG 1	
	BM328				PRG 3	PRG 3	BRG 1	
Dolna Studena	BM329		unknown		unknown	PRG 3	BRG 1	Butovo
valley Pavelsko dere	BM330				PRG 3	PRG 3	BRG 1	
	BM331				BRG 1	BRG 1	BRG 1	
	BM332				PRG 3	PRG 3	BRG 1	Butovo
	BM333				PRG 1	PRG 3	BRG 1	
Gradište	BM335				group X	unknown	BRG 1	
Dermenjolu	BM338				BRG 1	BRG 1	BRG 1	
Nicopolis, near agora	BM342				unknown	PRG 3	BRG 1	
	BM343				PRG 3	PRG 3	BRG 1	
	BM344		BRG 1		BRG 1	BRG 1	BRG 1	
	BM345				unknown	PRG 3	PRG 3	
	BM346				BRG 1	BRG 1	BRG 1	
	BM347				PRG 3	PRG 3	BRG 1	
	BM348				PRG 3	PRG 3	BRG 1	
	BM349				unknown	PRG 3	BRG 1	
	BM350		PRG 1		PRG 1	PRG 1	BRG 1	
Novae	BM351				BRG 1	BRG 1	BRG 1	
	BM352				BRG 1	BRG 1	BRG 1	
	BM353				PRG 1	PRG 1	BRG 1	
	BM354				BRG 1	BRG 1	BRG 1	
	BM355				PRG 1	PRG 1	BRG 1	
	BM356				BRG 1	BRG 1	BRG 1	
Butovo	BM357				BRG 1	PRG 1	BRG 1	
Hotnica	BM358				PRG 1	PRG 1	BRG 1	
	BM359				group Y	group Y		
	BM360				group Y	group Y		
	BM361				BRG 1	PRG 1	BRG 1	
Bjala Cerkva	BM362				PRG 1	PRG 1	BRG 1	
	BM363				PRG 3	PRG 3	BRG 1	
	BM364				PRG 1	PRG 1	PRG 1	
	BM365				group Y	group Y	BRG 1	
	BM366				unknown	PRG 3		

Tab. 3 (Continued) List of analysed samples, methods used for attribution. Final results for all samples in column PCA/RbSrZr (combined result from PCA and bivariate diagrams).

Time	SAMPLE	TiO_2	Fe_2O_3	CaO	K_2O	Cr	Rb	Sr	Zr	Ba
	WD-XRF	**0.885**	**6.84**	**6.68**	**3.14**	**119**	**158**	**302**	**216**	**462**
10.5.13 17:07	BM004-b *	0.76	6.8	8.4	2.62	93	136	263	210	318
10.5.13 17:09	BM004-b	0.64	6.1	7.8	2.25	92	128	259	204	389
10.5.13 17:11	BM004-b	0.70	5.9	7.8	2.40	101	123	238	192	418
mean	**b 1 (n = 3)**	**0.70**	**6.2**	**8.0**	**2.42**	**95**	**129**	**253**	**202**	**375**
10.5.13 17:14	BM004-a *	1.01	8.7	8.7	3.30	161	155	305	254	< LOD
10.5.13 17:17	BM004-c *	1.01	8.7	8.7	3.35	156	147	311	246	82
10.5.13 17:19	BM004-c *	0.95	8.1	8.1	3.12	136	146	290	234	< LOD
10.5.13 17:22	BM004-c	0.71	7.1	6.5	2.50	104	146	273	226	429
mean	**c (n = 3)**	**0.92**	**7.9**	**7.8**	**2.99**	**132**	**147**	**292**	**235**	**256**
10.5.13 17:24	BM004-s	0.81	6.7	4.7	3.93	176	131	249	205	277
10.5.13 17:27	BM004-s *	*1.10*	6.9	4.5	*4.26*	*131*	130	268	209	*192*
10.5.13 17:30	BM004-s	0.79	6.6	5.6	3.68	217	132	250	212	285
	s (n=3)	**0.90**	**6.7**	**4.9**	**3.95**	**175**	**131**	**256**	**208**	**251**
10.5.15 17:56	BM004-b	0.70	7.9	5.2	2.32	77	157	302	209	509
10.5.15 17:59	BM004-b	0.68	6.9	5.1	2.30	81	141	273	190	601
10.5.15 18:01	BM004-b *	1.19	*8.9*	*7.8*	*2.87*	*214*	*155*	*320*	*211*	*208*
10.5.15 18:04	BM004-b	0.70	7.5	5.1	2.28	69	143	283	189	451
mean	**b 2 (n=3)**	**0.70**	**7.4**	**5.1**	**2.30**	**76**	**147**	**286**	**196**	**521**
1.8.15 12:45	BM004-b +	0.87	7.2	6.2	2.87	*173*	136	281	185	*417*
1.8.15 12:48	BM004-b +	0.68	6.8	*9.0*	*2.40*	125	*129*	*291*	178	471
1.8.15 12:53	BM004-b	0.76	6.4	6.3	2.67	122	134	280	186	517
1.8.15 12:55	BM004-b	0.73	6.4	5.7	2.59	112	136	273	175	506
1.8.15 12:58	BM004-b	0.76	6.6	6.1	2.57	139	134	275	170	488
mean	**b 3 (n = 3)**	**0.75**	**6.5**	**6.8**	**2.56**	**125**	**133**	**280**	**177**	**495**
variation		0.64-1.19	5.9-8.9	5.1-9.0	2.25-3.35	69-214	123-157	238-320	170-254	82-601
best values	mean (n = 8)	0.71	6.7	6.1	2.42	99	137	273	189	485
	± std	0.04	0.7	1.1	0.16	24	10	19	13	66
measurement	± 1 SIGMA	0.01	0.03	0.03	0.03	13	3	2	2	35
monitor sample	**± std (1 year)**	**0.02**	**0.05**	**0.10**	**0.02**	**8**	**3**	***5***	**4**	**34**

Tab. 4 Example of repeated measurements of sample BM004 by pXRF showing large variations in Ti, Fe, Ca, K, Cr, Rb, Sr, Zr, and Ba. The first line shows analyses by WD-XRF, other lines show repeated measurements by pXRF on fresh fractures b, cut sections c, and on slip s. Sample numbers marked with * showed extremely high U, samples numbers marked with + gave unexplained wrong results, aberrant results are in italics. The variation of the measurements (excluding the measurements on slip) is very large. The average of the best values for measurement at fresh breaks and their standard deviation are calculated and the latter compared to the 1 Sigma range (error of measurement shown by the machine) and to the long-term precision of repeated measurements of a ceramic monitor sample with cut surface.

Sample No.	SiO_2	TiO_2	Al_2O_3	Fe_2O_3	MnO	MgO	CaO	Na_2O	K_2O	P_2O_5	V	Cr	Ni	(Cu)	Zn	Rb	Sr	(Y)	Zr	(Nb)	Ba	(Ce)	(Pb)	l.o.i.	total
	% by weight										ppm													%	%
Pavlikeni (PRG 1)																									
BM006	61.92	0.798	16.39	6.19	0.100	2.03	8.88	0.80	2.74	0.147	142	97	59	34	89	135	265	23	237	14	316	57	13	0.01	99.76
BM007	64.46	0.818	17.09	6.48	0.101	1.84	5.18	0.95	2.92	0.161	114	105	63	47	167	143	260	19	233	14	471	67	17	1.09	99.89
BM009	62.30	0.792	16.59	6.26	0.105	1.94	8.35	0.73	2.78	0.155	124	96	61	138	109	137	264	19	233	15	315	70	20	3.65	100.10
BM287	61.32	0.778	15.88	6.05	0.102	2.05	9.97	0.77	2.80	0.268	121	96	56	29	97	127	297	30	211	18	402	67	19	4.60	101.07
BM350	62.34	0.802	17.02	6.33	0.101	1.97	7.65	0.76	2.83	0.186	110	96	57	36	94	138	258	23	229	16	353	68	20	2.09	99.76
Pavlikeni (PRG 3)																									
BM041	58.24	0.735	16.22	5.87	0.097	2.05	12.81	0.66	3.04	0.287	108	90	58	35	97	139	432	19	198	13	378	74	20	4.66	99.65
BM044	58.49	0.770	17.16	6.04	0.089	2.09	11.06	0.68	3.21	0.402	133	101	63	42	102	150	461	17	201	13	466	81	27	4.70	100.16
BM045	57.97	0.823	17.36	6.11	0.092	2.71	10.98	0.74	2.97	0.247	105	104	63	46	100	146	447	23	220	15	459	71	28	4.41	100.15
BM047	60.18	0.753	16.64	5.71	0.085	2.08	10.49	0.70	3.07	0.285	122	95	62	54	97	143	388	19	204	13	403	61	26	4.13	99.80
BM050	58.65	0.802	17.34	6.20	0.090	1.88	11.01	0.72	3.06	0.236	143	101	64	54	97	142	480	22	211	13	400	83	20	5.77	99.63
BM051	58.17	0.731	16.08	5.93	0.105	2.04	12.76	0.65	3.09	0.431	126	91	57	40	90	136	442	20	200	13	417	60	16	5.46	99.81
BM298	61.14	0.796	16.67	6.04	0.103	1.99	9.44	0.72	2.87	0.228	111	91	57	39	97	138	440	23	226	15	464	66	15	2.75	100.01
BM325	58.00	0.820	18.20	6.45	0.100	2.28	10.07	0.74	3.16	0.180	128	98	59	35	97	151	360	22	208	13	387	54	19	2.70	100.10
Butovo (BRG 1)																									
BM004	59.41	0.885	18.99	6.84	0.090	2.79	6.68	0.93	3.14	0.254	131	119	71	58	108	158	302	21	216	15	462	65	17	1.17	100.07
BM008	58.88	0.874	19.13	6.82	0.087	2.46	7.28	1.22	3.10	0.166	152	112	71	67	112	152	275	23	195	17	462	80	13	2.08	100.07
BM012	58.83	0.878	19.75	7.07	0.092	2.78	6.21	0.83	3.37	0.188	145	120	74	46	111	166	250	23	200	14	415	76	20	1.06	99.73
BM021	60.25	0.854	18.54	6.61	0.093	3.10	6.16	0.83	3.25	0.316	131	110	67	65	107	156	299	23	216	15	442	87	26	2.06	99.89
BM024	58.63	0.873	19.67	6.97	0.084	2.74	6.35	0.89	3.49	0.292	152	122	69	61	125	167	276	24	196	15	493	99	24	1.58	100.34
BM040	60.51	0.843	19.90	6.12	0.084	2.39	5.22	0.97	3.74	0.231	148	117	73	68	104	174	288	23	203	14	400	75	37	1.17	100.74
BM043	58.63	0.873	19.67	6.97	0.084	2.74	6.35	0.89	3.49	0.292	152	122	69	61	125	167	276	24	196	15	493	99	24	1.74	100.19
BM101	62.05	0.878	19.43	6.51	0.092	2.24	4.22	0.89	3.50	0.182	129	107	66	41	100	160	219	22	219	15	396	72	28	1.06	100.02
BM107	61.14	0.870	18.68	6.54	0.084	2.61	5.76	0.99	3.12	0.201	119	108	61	35	101	153	271	24	216	14	430	71	19	1.26	100.11
BM240	61.77	0.864	18.36	6.47	0.092	2.55	5.60	1.04	3.05	0.197	121	104	62	30	101	147	244	23	214	15	606	80	20	2.58	99.84
BM309	60.73	0.852	18.07	6.33	0.089	2.68	7.09	1.06	2.92	0.173	130	106	59	36	98	147	272	23	215	14	389	85	21	1.36	99.84
BM312	61.56	0.887	20.60	6.12	0.085	2.13	4.33	0.56	3.56	0.160	130	111	68	40	107	174	236	22	201	15	536	76	24	1.55	99.99
BM324	62.47	0.898	20.00	6.24	0.083	2.00	3.96	0.73	3.44	0.166	144	110	66	44	106	171	237	25	213	16	499	66	22	1.36	99.91
BM326	61.81	0.898	20.41	5.89	0.082	2.09	4.31	0.80	3.50	0.209	140	114	68	48	110	168	248	25	207	15	436	74	24	2.70	99.74
BM344	59.40	0.888	21.45	6.22	0.085	2.45	4.54	1.04	3.79	0.135	158	118	73	70	112	183	281	22	201	15	399	75	29	0.82	99.90
Novae																									
BM035	62.48	0.788	16.18	5.55	0.051	1.96	8.57	0.69	3.39	0.354	141	105	62	46	107	142	281	21	214	12	359	69	21	3.30	99.96
unknown																									
BM022	60.53	0.767	17.14	5.58	0.069	2.02	9.39	0.68	3.43	0.385	153	107	57	67	142	142	505	21	210	15	468	62	27	5.06	100.20
BM037	59.05	0.723	14.63	5.39	0.073	2.29	13.76	0.59	3.24	0.254	116	91	53	38	84	127	346	15	198	15	575	55	17	7.34	100.04
BM329	54.01	0.733	21.17	5.49	0.089	1.30	13.37	0.12	3.33	0.409	81	79	41	19	142	257	387	34	148	17	427	93	54	2.69	99.90
Lezoux																									
BM243	64.58	0.754	14.97	4.98	0.048	1.86	8.98	0.76	2.84	0.218	110	84	50	20	93	125	308	18	218	13	386	50	18	3.99	99.93

Tab. 5 Results of analyses by WD-XRF of 54 samples used in this study and attributions to provenance groups (samples ignited at 900°C, major elements normalized to a constant sum of 100%, original totals are given, l.o.i = loss on ignition).

Bibliography

Daszkiewicz 1995
Małgorzata Daszkiewicz. "Ein Vorschlag zur Klassifizierung keramischer Massenfunde unter stufenweiser Anwendung einfacher und aufwendiger Untersuchungsmethoden." In *Archäometrie and Denkmalpflege, Kurzberichte 1995*. Ed. by A. Hauptmann, Th. Rehren, and Ü. Yalçın. Bochum: Deutsches Bergbau-Museum, 1995, 75–77.

Daszkiewicz 2014
Małgorzata Daszkiewicz. "Ancient Pottery in the Laboratory – Principles of Archaeological Investigations of Provenance and Technology." *Novensia* 25 (2014), 177–197.

Daszkiewicz 2017
Małgorzata Daszkiewicz. "Sections "Re-firing", "Reconstruction the Original Firing Process by Re-firing", "Raw Material Classification Using MGR-Analysis", and "MGR-Analysis Data Reporting"." In *The Oxford Handbook of Archaeological Ceramic Analysis*. Ed. by A. Hunt. Oxford University Press, 2017, 496–502.

Daszkiewicz and Schneider 2001
Małgorzata Daszkiewicz and Gerwulf Schneider. "Klassifizierung von Keramik durch Nachbrennen von Scherben." *Zeitschrift für Schweizerische Archäologie und Kunstgeschichte* 58 (2001), 25–32.

Daszkiewicz and Schneider 2007
Małgorzata Daszkiewicz and Gerwulf Schneider. "Naturwissenschaftliche Untersuchungen kaiserzeitlicher und spätantiker Keramik aus Iatrus." In *Iatrus-Krivina. Befestigung und frühmittelalterliche Siedlung an der Unteren Donau, Band VI: Ergebnisse der Ausgrabungen 1992–2000*. Ed. by G. von Bülow. Limesforschungen. Mainz: Philipp von Zabern, 2007, 467–482.

Daszkiewicz and Schneider 2014
Małgorzata Daszkiewicz and Gerwulf Schneider. "Analysis of Chemical Composition of Ancient Ceramics." *Novensia* 25 (2014), 199–206.

Daszkiewicz, Schneider, Baranowski, et al. 2018
Małgorzata Daszkiewicz, Gerwulf Schneider, Marcin Baranowski, Dávid Petrut, Viorica Rusu-Bolindeț, and Nicoleta Man. "Moesian and Dacian Sigillata – Exploring Regional Patterns. A Methodological Approach Using Chemical Analysis by WD-XRF and p-ED-XRF." *RCRFActa* 45 (2018), 541–549.

Daszkiewicz, Schneider, and Bobryk 2006
Małgorzata Daszkiewicz, Gerwulf Schneider, and Ewa Bobryk. "Some Aspects of Composition, Technology and Functional Properties of Roman and Early Byzantine Pottery from Novae (Bulgaria)." In *Ceramic Tableware and Kitchenware of the 3rd–6th century from Novae (Northern Bulgaria)*. Ed. by J. Klenina. Poznan: Uniwersytet im. A. Mickiewicza w Poznaniu, 2006, 189–214.

Daszkiewicz, Schneider, and Bobryk 2012
Małgorzata Daszkiewicz, Gerwulf Schneider, and Ewa Bobryk. "Wozu brauchen wir kombinierte Methoden für Keramikanalysen." In *Archäometrie und Denkmalpflege 2012. Jahrestagung an der Eberhard-Karls-Universität Tübingen*. Ed. by F. Schlütter, S. Greiff, and M. Prange. Metalla Sonderheft 5. Bochum: Deutsches Bergbau-Museum, 2012, 160–162.

Kuleff and Djingova 1996
Ivelin Kuleff and Rumiana Djingova. "Chemical Profile of the Pottery Production in the Ceramic Centre near Nicopolis ad Istrum." *Analytical Laboratory* 5 (1996), 238–244.

Kuleff, Djingova, and Kabakchieva 1999
Ivelin Kuleff, Rumiana Djingova, and Gergana Kabakchieva. "On the Origin of the Roman Pottery from Moesia Inferior (North Bulgaria)." *Archaeologia Bulgarica* 3 (1999), 29–38.

Schneider, Hoffmann, and Wirz 1979
Gerwulf Schneider, Bettina Hoffmann, and Erwin Wirz. "Significance and Dependability of Reference Groups for Chemical Determinations of Provenance of Ceramic Artifacts." *Archaeo-Physika* 10 (1979), 269–283.

Schneider and Mommsen 2009
Gerwulf Schneider and Hans Mommsen. "Eastern Sigillata C von Pergamon und Çandarlı (Türkei)." In *Archäometrie und Denkmalpflege – Kurzberichte 2009. Jahrestagung in München*. Ed. by A. Hauptmann and H. Stege. Metalla Sonderheft 2. Bochum: Deutsches Bergbau-Museum, 2009, 223–225.

Sultov 1985
Bogdan Sultov. *Ceramic Production on the Territory of Nicopolis ad Istrum (2nd–4th Century)*. Vol. 1. Terra Antiqua Balcanica. Centrum Historiae, 1985.

Illustration and table credits

ILLUSTRATIONS: **1** M. Baranowski. **2** M. Daszkiewicz; Macrophotos: M. Baranowski. **3–5** G. Schneider. **6–7** M. Baranowski. **8–28** G. Schneider. **TABLES:** **1** G. Schneider. **2–4** M. Baranowski. **5** G. Schneider.

MARCIN BARANOWSKI

Marcin Baranowski, MA Warsaw 2009, PhD Warsaw University 2018 in Humanities (thesis on Moesian Sigillata from Butovo and Pavlikeni). His specialization is macroscopic classification of ceramic fabrics and macrophotography. He worked at excavations at Risan (Montenegro), Novae (Bulgaria), and Stepanki (Poland).

Dr. Marcin Baranowski
ul. Dygasinkiego 27b
01-603 Warszawa, Poland
E-mail: bmjj@02.pl

MAŁGORZATA DASZKIEWICZ

Małgorzata Daszkiewicz, MA Warsaw 1979 in Physical Geography, PhD Warsaw University 1993 in Humanities. Since 1994 she has worked in collaboration with *AG Archäometrie* FU Berlin. Formerly a part-time employee at TOPOI, she is currently an associated member of the Institute for Prehistoric Archaeology FU Berlin and also runs ARCHEA, a laboratory in Warsaw for archaeometric analysis and research. Her main research interests are determining the technology and provenance of archaeological ceramics and devising techniques for the classification of bulk ceramic finds.

Dr. Małgorzata Daszkiewicz
Freie Universität Berlin
Institut für Prähistorische Archäologie
Fabeckstraße 23–25
14195 Berlin, Germany
and
ARCHEA
ul. Ogrodowa 8m95
00-896 Warszawa, Poland
E-mail: m.dasz@wp.pl

GERWULF SCHNEIDER

Gerwulf Schneider (Dr.rer.nat. 1968, habilitation 1979, both at Freie Universität Berlin) was a research associate at Excellence Cluster Topoi and now at the Insitute of Prehistoric Archaeology at FU Berlin. Since 1975 his main focus has been on chemical and mineralogical analysis of archaeological ceramics. His research focusses on Roman pottery in Germany, Hellenistic to Late Antique pottery in the Mediterranean region, and on pottery in Europe, Mesopotamia and Sudan. Schneider is a member of the German Archaeological Institute and of various archaeometric societies.

Dr. Gerwulf Schneider
Freie Universität Berlin
Institut für Prähistorische Archäologie
Fabeckstraße 23–25
14195 Berlin, Germany
E-mail: schnarch@zedat.fu-berlin.de

Antonia Höhne (ehemals Hofmann)

Evaluation and Calibration of the p-ED-XRF Analyser "Tracer" (Co. Bruker) for Classifying Pottery from the Middle Euphrates in Comparison with WD-XRF-Results

Summary

In this article the results of the evaluation of pXRF with regard to the limits and possibilities of reconstructing economic processes will be presented. Analysis data acquired using WD-XRF showed that, for pottery from the middle Euphrates Valley, only chemical signatures partly specific to find spot could be worked out, which likely can be traced back to the geochemical conditions in the area of study. The measuring inaccuracy of pXRF, determined using comparisons with WD-XRF data, interferes with the chemical differentiability of the material.

Keywords: p-ED-XRF; WD-XRF; Middle Euphrates; ceramics; survey; evaluation; Ubaid Period until Early Iron Age

In diesem Beitrag werden die Ergebnisse der Evaluierung der portablen energiedispersiven Röntgenfluoreszenzanalyse (p-ED-RFA) im Hinblick auf Möglichkeiten und Grenzen der Rekonstruktion ökonomischer Prozesse vorgestellt. Analysedaten, die mit Hilfe der WD-RFA gewonnen wurden, konnten zeigen, dass für Keramik aus dem mittleren Euphrattal nur bedingt fundstellenspezifische chemische Signaturen herausgearbeitet werden können, was auf die geochemischen Voraussetzungen im Arbeitsgebiet zurückzuführen sein dürfte. Die Messungenauigkeiten der p-ED-RFA, die im Vergleich mit WD-RFA-Daten herausgearbeitet wurden, beeinträchtigen zudem die chemische Differenzierbarkeit des Materials.

Keywords: p-ED-RFA; WD-RFA; mittlerer Euphrat; Keramiksurvey; Evaluierung; Ubaid- bis frühe Eisenzeit

Morten Hegewisch, Małgorzata Daszkiewicz und Gerwulf Schneider (eds.) | Using pXRF for the Analysis of Ancient Pottery – an Expert Workshop in Berlin 2014 | Berlin Studies of the Ancient World 75 (ISBN TODO; DOI: 10.17171/3-75) | www.edition-topoi.org

1 Introduction

Within the scope of this project,[1] whose partial results will be presented in this paper, the question was raised as to what extent a pottery complex from a comprehensive ground survey can be differentiated with help from portable energy-dispersive x-ray fluorescence (p-ED-XRF) as well as the documentation of technological characteristics in order to give a conclusion on the development of the system of production and distribution of early societies. This overarching issue will be explored using a case study whose material basis is composed of approx. 2,500 pottery fragments, collected from a total of 187 findspots between the years 1983-1984 during a survey of a ca. 150 km section of the Middle Euphrates Valley in Syria (Fig. 1).[2]

The focus of the investigation is on the pottery[3] dating from the Chalcolithic to the Iron Age, though the pottery fragments on hand demonstrate a very diverse chronological distribution (Fig. 2).

For every time slice – and, with the help of multiple time slices – the material will undergo a synchronic and diachronic (respectively) comparison, particularly with regard to the applicability of p-ED-XRF with reference to the research question.

Pottery can be classified and characterized through chemical and technological analyses (e.g. the generation of a 'fingerprint' of pottery belonging to a given settlement), through which at best the identification of production localities is made possible. In the present case of the processed, decontextualized survey finds, the premise is assumed that the majority of the pottery was produced locally within a settlement with identical or similar characteristics (statistical provenance). Through this, the identification of 'foreign material' – and, ideally, through the comparison of pottery originating from settlements in the area of study, a reconstruction of its distribution – should be possible. In this paper it will be discussed whether the p-ED-XRF can afford the chemical characterization of the pottery or whether other methods should be consulted for statistical analysis in order to sufficiently differentiate the material.

1 Project A-6-3-1 of the Excellence Cluster Topoi.

2 Two preliminary reports of the survey as well as reports of the excavation in Tall Bi'a have thus far been published: Kohlmeyer 1984; Kohlmeyer 1986; Strommenger and Kohlmeyer 1998. The find material is stored at the Hochschule für Technik und Wirtschaft Berlin.

3 The material almost exclusively concerns diagnostic sherds, 90% of which are represented by rim sherds.

2 Evaluation of p-ED-XRF

2.1 Random sample selection and device calibration

An evaluation of the p-ED-XRF[4] to assess the methods used was carried out initially according to Helfert and Böhme.[5] A random sample of 64 pottery fragments was used as the groundwork for this as well as for the evaluation of the database documentation system and the comparison of the p-ED-XRF values with those acquired though the data measurements with WD-XRF. These fragments are composed of generally well-preserved diagnostic rim fragments, presumably locally-used, originating from 16 find-spots, which also possess a wide spatial and chronological distribution within this area of study (Tab. 1).

In order to conduct comparisons with more precisely measured values, the random samples were analysed using wavelength dispersive x-ray fluorescence (WD-XRF).[6] The WD-XRF data are valid for samples ignited at 900°C and must be recalculated to not ignited samples[7] for comparison with p-ED-XRF data[8]. These data were systemically

4 In this case, the Tracer III-SD from Co. Bruker was used. Technical details: Detector: 10mm²XFlash® SDD; peltier cooled; typical resolution 145 eV at 200,000 cps; X-raytube: Rh target; max voltage 40 kV; filter changer: manual filter for optimum flexibility; 4 filterkit supplied; Vacuum pump attachment: Yes. Allows for enhanced light element sensitivity (Source: http://pdf.directindustry.com/pdf/bruker-handheld-xrf-spectrometry/tracer-iii-sd-specification-sheet/60556-178247.html; last accessed 08.07.2019).

5 Cf. Helfert and Böhme 2010.

6 For further technical details and sample preparation, see: Daszkiewicz and Schneider 2011, 31. The preparation was done by ARCHEA, Warsaw. Measurements using a PANalyticon AXIOS spectrometer were done at the Helmholtz-Zentrum Potsdam, Deutsches GeoForschungsZentrum GFZ, Sektion 4.2, Anorganische und Isotopengeochemie (courtesy of Anja Schleicher).

7 The oxide percent of the main elements are usually normalized according to a constant sum of 100%, whereby the loss of ignition is considered, because the powder samples are heated to 900°C before the measurement. These normalized measurement values can be retroactively converted back to a dry basis in order to be able to compare with the p-ED-XRF values. For this purpose, the normalized main element oxides are multiplied by 100 minus the 'loss on ignition' and afterwards devided by 100%. Thus, e.g. SiO_2 (normalized) * (100 – l.o.i.) / 100% = SiO_2 (not ignited).

8 All analysis data, which form the basis of what is discussed in this article (but cannot be displayed in this article due to limited space), can be viewed via the following URL: https://refubium.fu-berlin.de/handle/fub188/29666. The data is permanently stored in the repository of the Freie Universität Berlin and is available under the following DOI: http://dx.doi.org/10.17169/refubium-29410. Table description: Upper part of the table – analysis results of the WD-XRF (normalized). Lower part of the table – comparison of the results of WD-XRF (oxides of major elements for comparison calculated for not ignited samples) with the results of the p-ED-XRF devices (Tracer and, where available, Niton). The analysis results are sorted according to individual fragment numbers ("number of fragment"), which in turn is made up of the find-spot number and a continuous number. "total" = sum of oxides (in %) of the original measurement before the normalization of the WD-XRF values. "l.o.i." = loss on ignition. "n.m." = not measured. For the sake of completeness, the elements affected with larger measurement errors in WD-XRF were also listed (elements in brackets). Ce is empirically affected with large measurement errors in the Niton measurements. The elements Se, Ag, Cd, Sn, Sb, Au, Hg, Hi and U were, indeed, measured with the

compared with analyses carried out by the p-ED-XRF device (Tracer). Here it was shown that the factory-calibrations for the p-ED-XRF device, based on certified geochemical reference materials (CRM's)[9], were insufficient for a quantitative pottery analysis. Only after a recalibration of the device using specially prepared pottery standards[10] did the values of the p-ED-XRF more clearly approach those of the WD-XRF device.

2.2 Determination of optimal measurement time

Two different measuring parameters[11] are used to gather the light and heavy elements for the quantitative pottery analysis using the Tracer III-SD. Six fragments[12] from the random sample were used to determine the optimal measurement time, each measured in the same place (planed/flat, even break) for 60, 120, 180, 240 and 300 seconds. First, the element values of the six fragments per measurement time were averaged. An average value from the five measurement times was then calculated per element, which functioned as a reference value for the ensuing evaluation. Finally, the values of the individual measurement times were set in relation to this average value in order to find out at which measurement time the least deviance from the average of the analysis data are recorded. An optimal measurement time of 180 seconds was found for the light elements and an optimal measurement time of 120 seconds was found for the heavy elements. These results were considered in the determination of the measurement parameters for the recalibration and in further evaluation steps.

2.3 Effects of sample preparation and representativity of individual measurements

In order to evaluate the method of sample preparation and measurement representativity of an individual pottery fragment, five fragments[13] from the random sample were each measured once on the exterior and interior surface as well as in three other places: each on an old, new[14] and planed[15] break. This produced eleven measurements per frag-

Niton device, but remained below "LOD" ("limit of detection") and therefore are not listed in the table.

9 The following CRM's were used: 1633a, 2704, 8407, BCR no141, BCR no144, G 11, GM, GNA, GSD 12, GSDM, GSS 5, NBS 1646, SARM 6.

10 The ceramic standards prepared for calibration of the p-ED-XRF analyzers by Daszkiewicz and Schneider are composed of fired clay (lab.-nos. 429, 3253, F951, MD3993, MD4001, MD4026, and O270) and samples cut to have smooth surfaces from ancient very fine pottery (lab.-nos. 5915, G255, G256, G296 (not used in case of Tracer), and G299).

11 Light elements: 15 kV, 55 µA, filter blue (Polytetrafluoroethylene film), vacuum; heavy elements: 40 kV, 25 µA, red filter (12mil Al + 1mil Ti + 1mil Cu; 1mil = $2.54^{*}10^{-2}$mm).

12 Individual fragment numbers: 1_01, 40.3_01, 45_02, 51_02, 61_03, 106_02.

13 Individual fragment numbers: 45_02, 106_02, 46_11, 50_03 and 51_02.

14 Made using a mosaic cutting pincer.

15 Made using a hand-grinding device with cylindrical, diamond-grinding attachment.

ment, which were carried out using the two different measurement parameters. The average value from the five fragments at 100% per element were normalized and the percentage difference to the WD-XRF value (not ignited) was calculated for better data comparability of the individual elements. The average percentage deviance from WD-XRF value from the average value of the eleven measurements of the five fragments is presented in Table 2.

Here, especially Al, Ca, K, P, Ni, Ba and Pb stand out with over 20% deviation. Aside from the differences relative to the WD-XRF data, it becomes apparent from Figure 3 that, for most elements, the values of the planed break lie quite close together, so that the representativity of the measurements with respect to the mean value of the eleven measurements is ensured.

Within the measurement values of the fresh breaks, outliers are frequently visible, so that a lower representativity can be expected from the measurement of fresh breaks. In contrast, the values of the exterior and interior surfaces possess the most deviation from the average value of the eleven measurements. For this and for the greater deviations of the three values of the old and new breaks, distances between the measurement window and the sample surely play a role which originates through the method of sample preparation (see small graphic in Fig. 3).

2.4 Measurement precision

The same five fragments were measured five times consecutively in the same place and the variation coefficient was calculated (in %) in order to determine the precision of measurement. For the elements Al, Mg, Cu, Nb and Pb, the variation coefficient was found to be clearly over 4%. For comparison, the variation coefficients (in %) for the WD-XRF and the p-ED-XRF "Niton"[16] device, used in the Topoi research group A-6, are sheduled in Table 3.

2.5 Comparison of the WD-XRF measurements with those of the p-ED-XRF analysers "Tracer" and "Niton"

For the sake of completeness, what follows are the average values from the measurement of 41 fragments from the random sample[17] using the Tracer compared to the average

16 Technical data: Niton XL3t 900S GOLDD+ XRF analyzer from Thermo Scientific; Au-Anode; calibration (for measurements in "miningCu/Zn" mode, measurements in %) with 12 pottery standards manufactured by the Schneider/Daszkiewicz research group (courtesy of F. Kutz and G. Schneider).

17 Individual fragment numbers: 1_01, 1_02, 1_03, 106_01, 106_02, 106_03, 118_01, 16.5_01, 16.8_01, 16.8_02, 16.8_03, 20_01, 20_02, 20_03, 40.3_01, 45_02, 45_03, 45_05, 45_06, 45_08, 46_02, 46_05, 46_08, 46_09, 46_10, 46_11, 46_12, 5_01, 5_02, 5_03, 50_01, 50_02, 51_01, 51_02, 51_03, 61_01, 61_02, 64_02, 64_03, 87.1_02, 87.1_03.

values from measurements using the Niton[18] and the WD-XRF values calculated for non-ignited samples (Tabs. 4–5).

Hereby it becomes clear that the Niton device captured not only more main and trace elements as the Tracer device, but the measurement data showed lower deviations relative to the WD-XRF values.

The main elements Si, Al, Mg and P were not captured in the measurements of the Tracer in order to reduce the measurement time to half. Also because, as shown in the following section of this article, except for Mg, they are not essentially contributing to the differentiation of the Euphrates material. To this is added the relatively large measurement inaccuracy (measurement precision and measurement accuracy) of these elements.

3 Chemical differentiation of the ceramic material in comparison with WD-XRF and p-ED-XRF

In order to be able to assess whether or not the WD-XRF data on its own is suitable to sufficiently differentiate the ceramic material, the values of all measured elements were collected together in a box plot diagram (Fig. 4).

The values were normalized to 100% in order to achieve comparability of the data variation. Presented in grey are the minimal and maximal values of the data series. In comparison, it becomes obvious that the main elements Si, Ti, Al and Fe and the trace element Zr do not contribute substantially to the differentiation. P was not taken into account from the beginning, as the values can be influenced by contamination (alteration during burial).[19] The elements Cu, Nb, La, Ce, Pb, Th, Co, Ga, Nd and Sc also were not used for multi-element analysis, as they either exhibit too low absolute ppm-values and/or were measured with a lower accuracy.[20]

Cluster analysis[21] on the remaining elements reveals that ten clusters can be differentiated from each other (Fig. 5).

In this case, the 10-cluster solution was used, although the "Elbow Criterion"[22] produces a 3-cluster solution, which was permuted in the following figures using different

18 The fragments were measured using the "mining Cu/Zn" mode; measuring spot 8mm; total measuring time 120s (filter: main, 30s, low 30s, high 30s, light 30s); value outputs in %; without Helium; measurement of 3 places on planed break per fragment.

19 See e.g. Schneider 2017.

20 The elements shown in parenthesis were determined with lower accuracy in WD-XRF-measurements (courtesy of G. Schneider, 16.7.2014).

21 Software: PAST 2; algorithm: Ward's method. In this case, 43 additional fragments from the Middle Bronze Age from two sites, 0 and 46, located east of the study area were incorporated in the cluster analysis, of which 36 fragments were interpreted as imports (bottle-shaped pottery), originating from a considerable distance.

22 In accordance to Backhaus et al. 2011, 436–438.

colors. Clusters 1, 2 and 3 form a group, which differentiates itself early on from the remaining clusters; Clusters 4 and 5 differentiate themselves as a group again from Clusters 6-10. The clusters, again, can be divided according to the corresponding time slices and their range within the study area can be mapped (Figs. 6 and 7).

The synopsis of both representations allows the recognition of interesting tendencies, despite the meagre data pool: Clusters 7–10 are located in almost all time slices and simultaneously distributed evenly throughout the entire area of study. A new group appears in the Uruk Period (Cluster 4), initially limited to the east of the area of study, which is recorded in Clusters 4 and 5 in the Early Bronze Age in the entire area of study. For the Middle Bronze Age, data from only two settlements in the eastern part of the work area exist. Despite this, however, it is interesting that the chemical groups (Clusters 1, 2 and 3), which considerably set themselves apart from the other chemical groups and appear exclusively in ceramic samples from the Middle Bronze Age arise in both the local and suspected imported ware, whereas the 'bottles', presumed to be imported, reveal both the chemical signature of the 'new' groups as well as the chemical signature appearing in all the time slices. This suggests that it is not about imports, but rather the exploitation of new raw material sources or the application of entirely new recipes. During the Late Bronze and Iron Ages Clusters 7–10 are distributed relatively evenly over the entire area of study.

According to the WD-XRF data with regard to the size of the area of study, the ceramic material differentiates only roughly and merely tendencies can be revealed. Settlement-specific chemical signatures ('fingerprints') cannot be worked out by means of the pottery material of this area of study using WD-XRF data. The data pool could be significantly increased with the application of p-ED-XRF, but, on the basis of the preconditions here in the Middle Euphrates Valley, the chemical differentiability would be only marginally possible; the larger potential measurement error in particular would further distort the image.

This can already be seen in the random sample data: projecting the clusters determined by the p-ED-XRF data on the cluster analysis of the WD-XRF data, most clusters cannot be reproduced (Fig. 8).

Hardly any comparable clusters are formed, although the elements possess relatively high measurement inaccuracies (see Fig. 4) were not included at all in the statistical analysis.

4 Conclusions and prospects

Sufficient examples are known in which pottery groupings can initially be reproduced via laboratory analysis with help from p-ED-XRF, even for narrower regions[23], up to *intra-site* differentiation[24]. In the case of the Middle Euphrates area of study, the geochemical preconditions for a corresponding fine differentiation of the ceramic material within the scope of the processing time are not given. The possibility of expanding the working area would on the one hand go beyond the geographical scope of the investigation and, on the other hand, would prove ineffective for the goal of answering the research question. Instead, new investigative opportunities will be sought in order to adequately characterize and classify the material from the Middle Euphrates Valley.

Therefore, in order to achieve a spatial and chronological differentiation of the investigated ceramic material concerning the reconstruction of production and distribution in the area of study, morphological, technological and likewise metric variables of the pottery will be incorporated in future investigations. A database[25] has already been created containing detailed input possibilities for the acquisition of technological characteristics of the individual fragments as well as complete information on handwritten survey documentation, which could serve as a solid basis. Porousness and type, size, form, distribution and amount of temper will be seen as decisive variables for the grouping of the ceramic material. For this, new statistical methods for mutual analysis of metric, ordinal and nominal data in the database should be tested.[26] Furthermore, scientific analysis (MGR analysis[27] and ceramic petrography analysis on thin sections) will be carried out and their results incorporated into those of the analysis of the technological characteristics within the statistical evaluation.

Using statistical methods, verified changes in the range of the chemical and technological groups and alterations in diversity of the ceramic assemblages should allow

23 See e.g. Behrendt and Mielke 2013.

24 See e.g. the "Cornești-Iarcuri" project: Bernhard Heeb, Małgorzata Daszkiewicz, Gerwulf Schneider, Andrei Bălărie, and Alexandru Szentnmiklosi. "Household Production and Wider Connections – Analysis of Bronze Age Pottery Found in the Romanian Banat". In *Approaching Economic Spaces: Methods and Interpretation in Archaeometric Ceramic Analysis*. Eds. by M. Meyer. Berlin Studies of the Ancient World 64. Berlin: Edition Topoi, in press. See also the contribution by Daszkiewicz, Schneider, Heeb and Bălărie in this volume.

25 The Access Database was created according to the base work from Schneider 1989 and Rice 2005.

26 Possible methods of analysis might be the Bayes classifier for nominal data, correspondence analysis for the use of clusters and, for the XRF values, methods based on machine learning and M-Anova. For the representation of similarities and dissimilarities between settlements, network analysis and GIS analysis present themselves as possible candidates (information courtesy of Martin Hinz, Univ. Kiel, from 25.4.2014).
Concerning the subject data-mining and machine learning see in addition: Hörr 2011; Hörr, Lindinger, and Brunnett 2009; Zweig 2012.

27 Matrix Grouping by Refiring analysis for the classification of pottery on the basis of clay matric. For more information on this, see Daszkiewicz and Schneider 2011, 17.

conclusions regarding the intensification of trade and exchange and the organization of ceramic production (e.g. from the degree of craftwork specialization). Additionally, for the interpretation of analysis results with regard to the economic processes, the comparison of settlement patterns and the analysis data from time slice to time slice will be carefully considered. Considering the poor amount of data on settlement patterns in the area of study itself, results from surveys from the neighbouring areas should be brought in for comparison.[28]

28 Cf. Kühne 1974–1977; Kühne 1978–1979; Bernbeck 1993; Wilkinson et al. 2012; Ricci 2013.

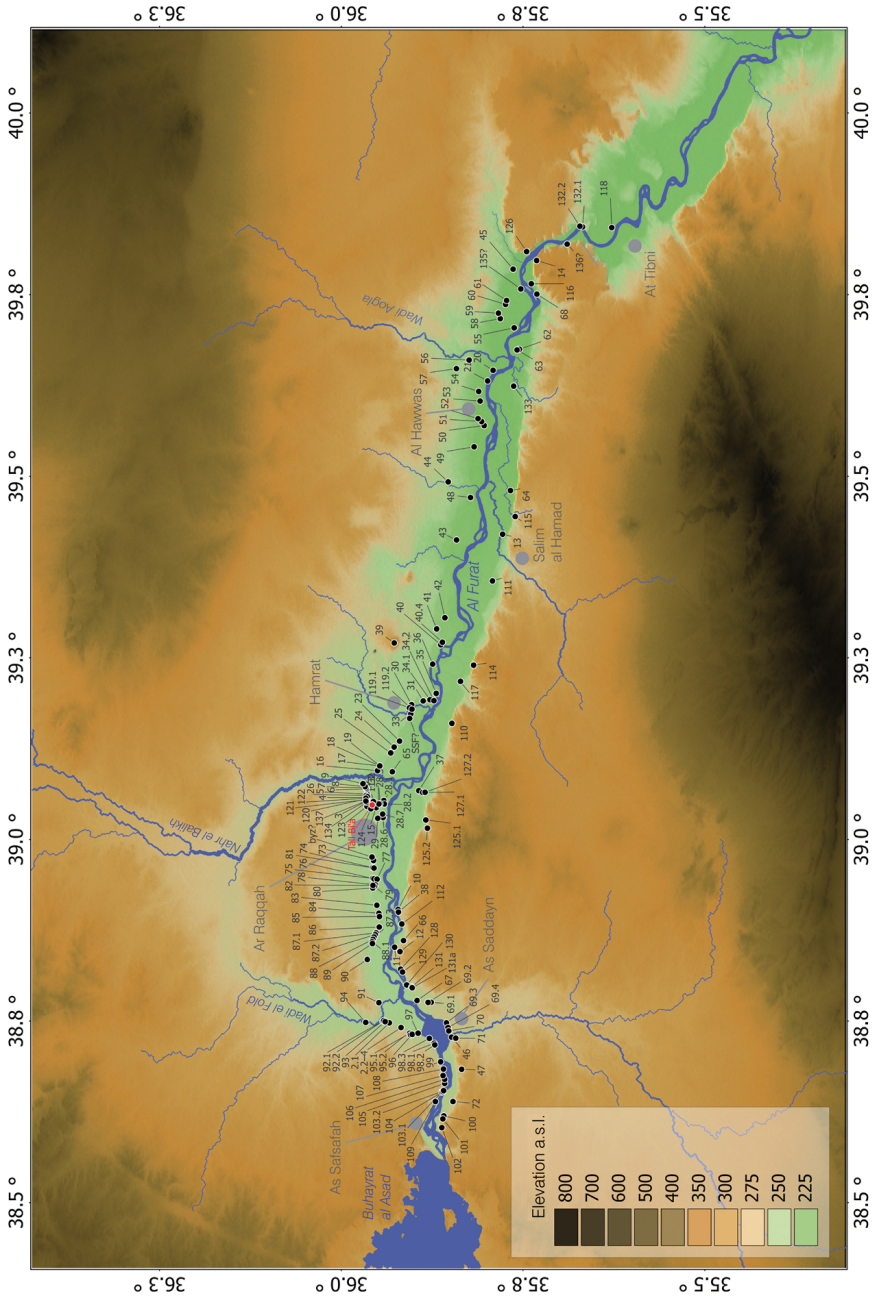

Fig. 1 Map of all sites from the surveys of the years 1983-84 in the Middle Euphrates Valley (SRTM data used as basis for the map).

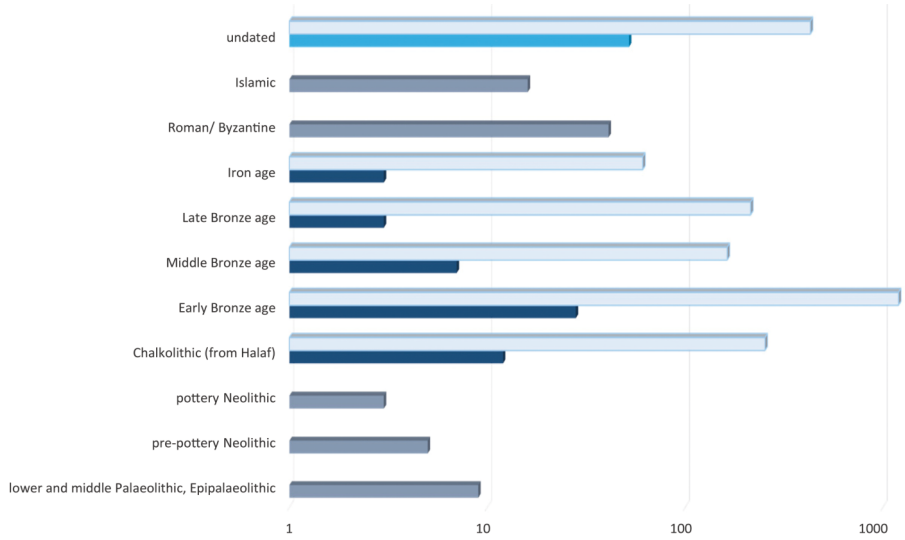

Fig. 2 Overview of the present ceramic material of the project; mid-blue and dark blue: number of sites (according to documentation), dark blue: time frame processed in the project; light blue: number of pottery fragments of the processed time frame (according to artifact drawings).

Time Period	Find-spot Numbers	Number of Fragments
Chalcolithic	16	3
Ubaid Period	51, 61, 87.1	9
Uruk Period	1, 25, 45, 99	12
Early Bronze Age	5, 16, 40, 45, 46, 64, 106	21
Middle Bronze Age (Bottles)	46, (0)	5, (43)
Late Bronze Age	45, 46	5
Iron Age	20, 50, 118	9

Tab. 1 Assembly of pottery fragments from the random sample, classified according to find-spot numbers and chronology.

SiO_2	8.1	Cr	-9.6
TiO_2	-5.4	Ni	-25.2
Al_2O_3	21.9	Cu	-6.1
Fe_2O_3	-10.3	Zn	-0.6
MnO	1.1	Rb	-5.8
MgO	6.5	Sr	-5.7
CaO	-23.1	Y	6.2
K_2O	20.2	Zr	-9.2
P_2O_5	22.5	Nb	9.7
		Ba	25.1
		Pb	29.8

Tab. 2 Average percentage deviation of the average value of all 11 measurements of 5 pottery fragments from the WD-XRF (non-ignited samples) value.

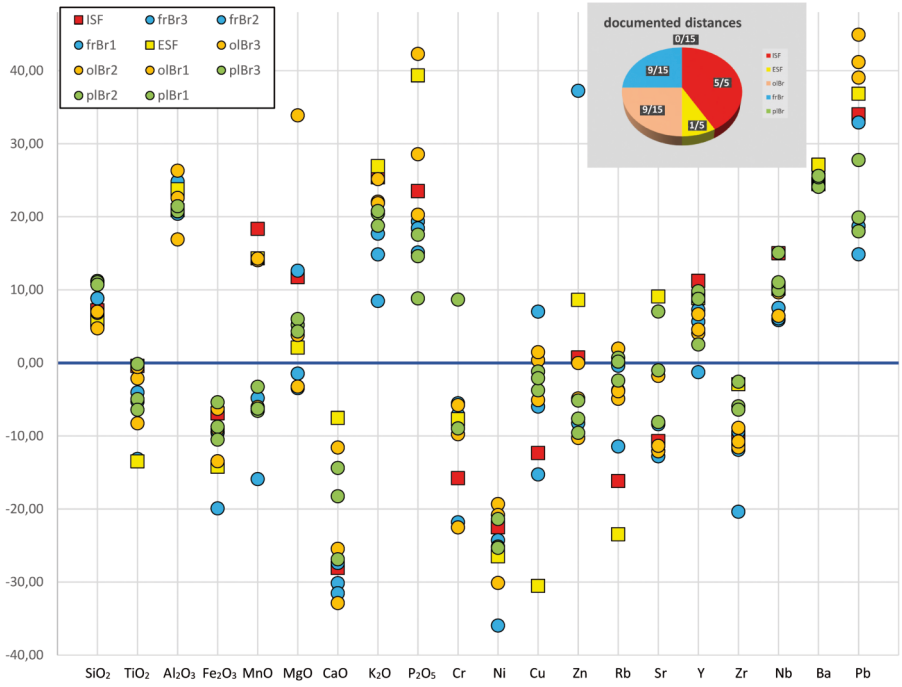

Fig. 3 Influence from sample preparation; representativity of measurements on different surfaces; values of the Tracer measurement normalized to 100% and compared to the WD-XRF non-ignited sample values (difference in relative %)); ISF = interior surface, ESF = exterior surface, olBr = old break, frBr = fresh break, plBr = planed break; smaller graphic, upper right: number of cases in which a distance between the pottery and Tracer's measurement window was documented.

	SiO_2	TiO_2	Al_2O_3	Fe_2O_3	MnO	MgO	CaO	K_2O	P_2O_5	V	Cr	Ni	Cu	Zn	Rb	Sr	Y	Zr	Nb	Ba	Ce	Pb
Tracer Fr. 1	2.0	2.2	5.3	0.2	2.9	20.2	0.5	3.6	3.6	n.m.	4.6	1.5	8.2	2.5	1.4	0.8	4.2	0.8	2.1	0.8	n.m.	27.3
Tracer Fr. 2	2.5	1.6	6.2	0.1	2.2	39.4	0.6	2.3	1.3	n.m.	1.0	1.0	7.5	0.7	1.2	0.4	3.4	0.7	7.9	1.5	n.m.	10.3
Tracer Fr. 3	1.2	1.9	4.3	0.1	1.6	18.5	0.7	2.8	2.0	n.m.	5.5	1.9	9.5	1.1	1.2	0.5	3.3	0.8	8.4	0.6	n.m.	12.0
Tracer Fr. 4	0.7	1.5	1.7	0.1	1.1	14.2	0.4	2.6	0.9	n.m.	4.2	1.7	6.0	4.4	1.1	0.5	3.9	0.4	3.0	0.6	n.m.	20.0
Tracer Fr. 5	1.4	1.5	3.2	0.2	1.9	21.1	0.5	4.4	3.3	n.m.	2.8	2.0	5.3	3.3	2.3	0.5	5.1	0.8	4.8	1.5	n.m.	10.3
Tracer average v.	**1.6**	**1.7**	**4.1**	**0.1**	**1.9**	**22.7**	**0.6**	**3.1**	**2.2**	**n.m.**	**3.6**	**1.6**	**7.3**	**2.4**	**1.4**	**0.5**	**4.0**	**0.7**	**5.2**	**1.0**	**n.m.**	**16.0**
Niton	**3.7**	**0.7**	**6.2**	**0.5**	**2**	**n/a**	**2.2**	**1.5**	**85.0**	**8**	**7.3**	**3.5**	**10.4**	**3.8**	**2.3**	**1.5**	**3.3**	**1.3**	**5.9**	**4.6**	**2.5**	**n/a**
WD-XRF	**0.3**	**0.9**	**0.4**	**0.9**	**1.5**	**n/a**	**1.7**	**1.1**	**1.9**	**2.7**	**2.0**	**2.0**	**6.7**	**2.0**	**1.8**	**1.2**	**2.7**	**1.3**	**4.4**	**2.1**	**5.5**	**n/a**

Tab. 3 Comparison of the measurement precision of WD-XRF and the p-ED-XRF devices Niton and Tacer (variation coefficients in %); n.m. = not measured, n/a = not available. Source values for Niton: Reproducibility of individual measurement, 10x repetition on standard sample G296 (Schneider and Daszkiewicz 2010, 111). Source values for WD-XRF: Long-term reproducibility from Schneider and Daszkiewicz 2010, 111.

	SiO_2	TiO_2	Al_2O_3	Fe_2O_3	MnO	MgO	CaO	Na_2O	K_2O	P_2O_5
Niton	47.64	0.73	13.65	7.08	0.13	5.39	14.67	n.m.	2.09	0.40
Tracer	n.m.	0.77	n.m.	6.74	0.13	n.m.	11.19	n.m.	2.67	n.m.
WD-XRF	50.08	0.80	13.30	7.33	0.13	5.81	14.68	1.40	2.03	0.30

Tab. 4 Comparison of the measurement values (in %) of the three XRF devices, average values from 41 pottery fragments; marked in grey are the measurement values of the p-ED-XRF which are closest to those of the WD-XRF; n.m. = not measured.

	S	Cl	Sc	V	Cr	Co	Ni	Cu	Zn	Ga	As
Niton	1199	296	n.m.	138	284	n.m.	188	11	82	n.m.	1
Tracer	n.m.	n.m.	n.m.	n.m.	329	n.m.	191	42	74	n.m.	n.m.
WD-XRF	1220	n.m.	23	132	385	30	244	48	83	16	n.m.

Tab. 5 Comparison of the measurement values (in ppm) of the three XRF devices, average values from 41 pottery fragments; marked in grey are the measurement values of the p-ED-XRF which are closest to those of the WD-XRF; n.m. = not measured.

	Rb	Sr	Y	Zr	Nb	Ba	La	Ce	Nd	Pb	Th
Niton	53	529	21	127	n.m.	507	n.m.	94	n.m.	n.m.	n.m.
Tracer	52	515	23	168	13	469	n.m.	n.m.	n.m.	13	n.m.
WD-XRF	53	577	21	181	12	417	16	45	25	8	9

Tab. 5 (Continued) Comparison of the measurement values (in ppm) of the three XRF devices, average values from 41 pottery fragments; marked in grey are the measurement values of the p-ED-XRF which are closest to those of the WD-XRF; n.m. = not measured.

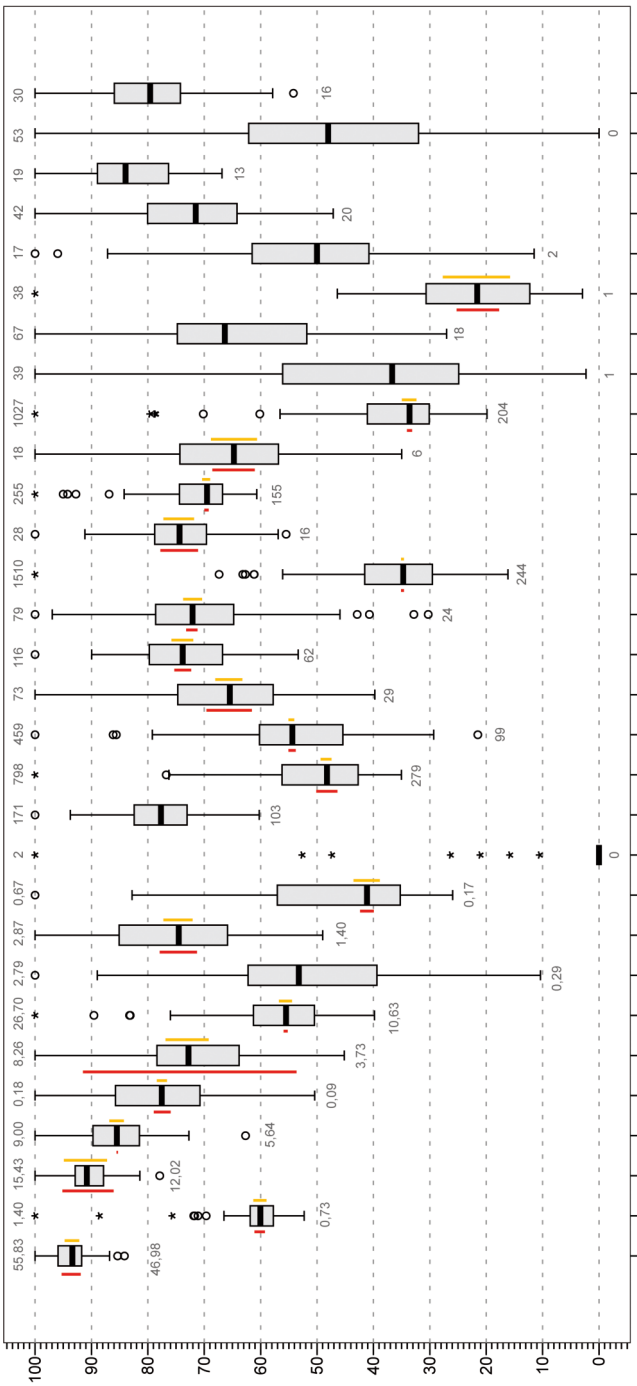

Fig. 4 Boxplot diagram of WD-XRF data (ignited samples, oxides normalized to 100%) as well as measurement precision (red, in relative %) from the p-ED-XRF Tracer device and the measurement inaccuracy ('average deviation' of actual value from target value) in relative % (orange); numbers in grey, minimum and maximum of absolute measurement values in % and ppm.

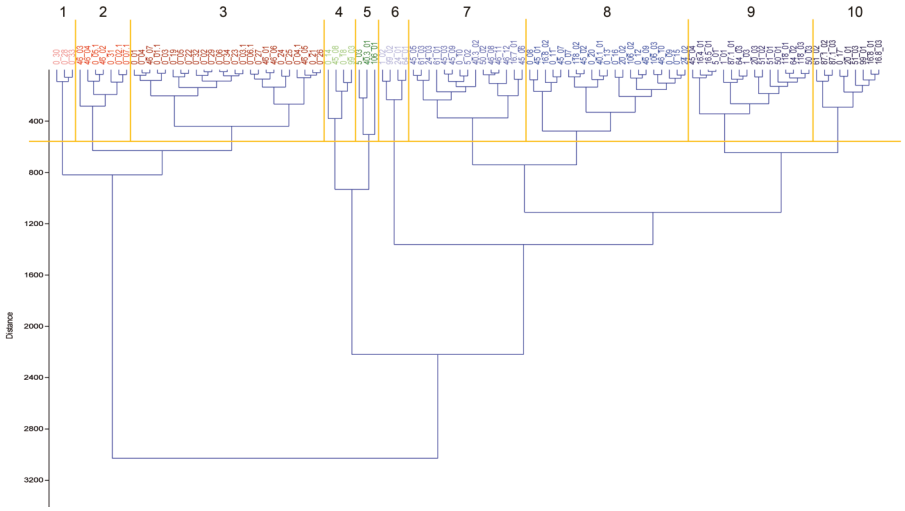

Fig. 5 Cluster analysis of the WD-XRF data (ignited samples); application of elements Mn, Mg, Ca, Na, K, V, Cr, Ni, Zn, Rb, Sr, Y, Ba. 10-Cluster solution drawn in and colored.

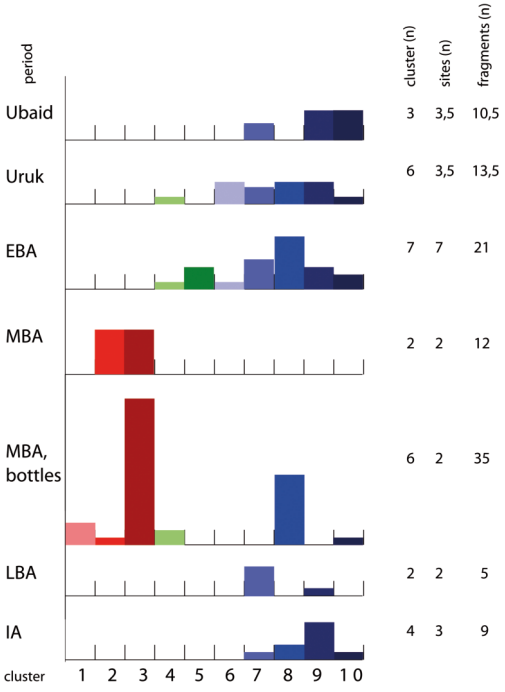

Fig. 6 Clusters (WD-XRF, ignited samples) plotted according to time slice.

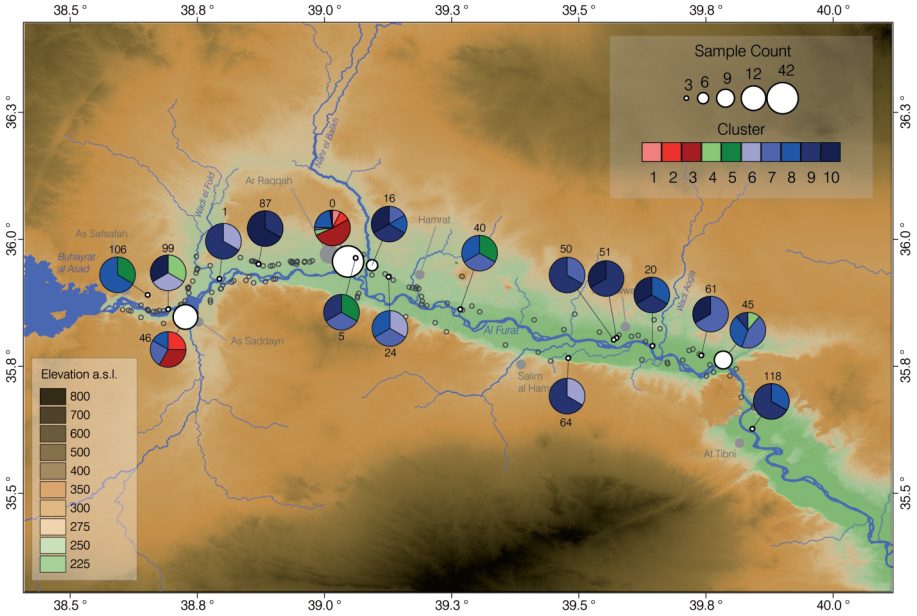

Fig. 7 Mapping of Clusters (WD-XRF, ignited samples) from all time slices in the area of study.

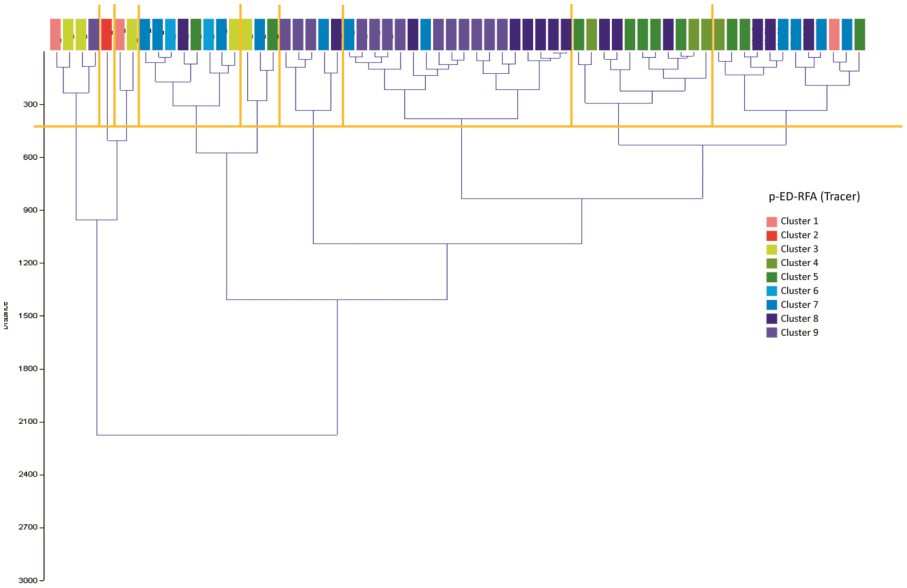

Fig. 8 Projection of 9 p-ED-XRF clusters onto the WD-XRF dendrogram (cluster analysis WD-XRF with mapping in of the 9 cluster subdivisions; application of the elements Mn, Ca, K, Cr, Ni, Zn, Rb, Sr, Y, Ba (without Find-spot 0); 9-cluster solution of the p-ED-XRF (application of the same elements and samples) mapped on, cluster colors were chosen in correspondence with their similarities.

Bibliography

Backhaus et al. 2011
Klaus Backhaus, Bernd Erichson, Wulff Plinke, and Rolf Weiber. *Multivariate Analysemethoden. Eine anwendungsorientierte Einführung*. Berlin and Heidelberg: Springer, 2011.

Behrendt and Mielke 2013
Sonja Behrendt and Dirk Paul Mielke. "Probleme und Perspektiven archäometrischer Untersuchungen großer Keramikmengen – Ein Projektbericht." In *Naturwissenschaftliche Analysen vor- und frühgeschichtlicher Keramik III. Methoden, Anwendungsbereiche, Auswertungsmöglichkeiten*. Ed. by Britta Ramminger, Stilborg Ole, and Helfert Markus. Bonn: Habelt, 2013, 93–121.

Bernbeck 1993
Reinhard Bernbeck. *Steppe als Kulturlandschaft. Das 'Ağığ-Gebiet vom Neolithikum bis zur islamischen Zeit. Mit Beiträgen von P. Pfälzner*. Vol. 1. Berliner Beiträge zum Vorderen Orient, Ausgrabungen. Berlin: Dietrich Reimer, 1993.

Daszkiewicz and Schneider 2011
Małgorzata Daszkiewicz and Gerwulf Schneider. "Archäokeramologische Klassifizierung am Beispiel Kaiserzeitlicher Drehscheibenkeramik aus Brandenburg." In *Drehscheibentöpferei im Barbaricum. Technologietransfer und Professionalisierung eines Handwerks am Rande des Römischen Imperiums, Akten der Internationalen Tagung in Bonn vom 11. bis 14. Juni 2009*. Ed. by J. Bemmann, Hegewisch M., M. Meyer, and M. Schmauder. Bonn: Institut für Vor- und Frühgeschichtliche Archäologie, 2011, 15–31.

Helfert and Böhme 2010
Markus Helfert and Dieter Böhme. "Herkunftsbestimmung von römischer Keramik mittels portabler energiedispersiver Röntgenfluoreszenzanalyse (P-ED-RFA). Erste Ergebnisse einer anwendungsbezogenen Teststudie." In *Naturwissenschaftliche Analysen vor- und frühgeschichtlicher Keramik I. Methoden, Anwendungsbereiche, Auswertungsmöglichkeiten*. Ed. by B. Ramminger and O. Stilborg. Univforsch. Prähist. Arch. 238. Bonn: Habelt, 2010, 11–30.

Hörr 2011
Christian Hörr. *Algorithmen zur automatisierten Dokumentation und Klassifikation archäologischer Gefäße*. Dissertation. Chemnitz: Universitätsverlag der TU Chemnitz, 2011.

Hörr, Lindinger, and Brunnett 2009
Christian Hörr, Elisabeth Lindinger, and Guido Brunnett. "New Paradigms for Automated Classification of Pottery." *Chemnitzer Informatik-Berichte* CSR-09-06 (2009), 1–15.

Kohlmeyer 1984
Kay Kohlmeyer. "Euphrat-Survey – Die mit Mitteln der Gerda Henkel Stiftung durchgeführte archäologische Geländebegehung im syrischen Euphrattal." *Mitteilungen der Deutschen Orient Gesellschaft* 116 (1984), 95–118.

Kohlmeyer 1986
Kay Kohlmeyer. "Euphrat-Survey 1984. Zweiter Vorbericht über die mit Mitteln der Gerda Henkel Stiftung durchgeführte archäologische Geländebegehung im syrischen Euphrattal." *Mitteilungen der Deutschen Orient Gesellschaft* 118 (1986), 51–66.

Kühne 1974–1977
Hartmut Kühne. "Zur historischen Geographie am Unteren Ḫābūr. Vorläufiger Bericht über eine archäologische Geländebegehung." *Archiv für Orientforschung* 25 (1974–1977), 249–255.

Kühne 1978–1979
Hartmut Kühne. "Zur historischen Geographie am Unteren Ḫābūr. Zweiter, vorläufiger Bericht über eine archäologische Geländebegehung." *Archiv für Orientforschung* 26 (1978–1979), 181–195.

Ricci 2013
Andrea Ricci. *An Archaeological Lanscape Study oft he Birecik-Carchemish Region (Middle Euphrates River Valley) during the 5th, 4th and 3rd Millenium BC*. Dissertation. Kiel: Christian-Albrechts-Universität Kiel, 2013.

Rice 2005
Prudence M. Rice. *Pottery Analysis. A Sourcebook*. Chicago and London: University of Chicago Press, 2005.

Schneider 1989
Gerwulf Schneider. "Naturwissenschaftliche Kriterien und Verfahren zur Beschreibung von Keramik. Diskussionsergebnisse der Projektgruppe Keramik im Arbeitskreis Archäometrie in der Fachgruppe Analytische Chemie der Gesellschaft Deutscher Chemiker." *Acta Praehistorica et Archaeologica* 21 (1989), 7–39.

Schneider 2017
Gerwulf Schneider. "Mineralogical and Chemical Alteration." In *Oxford Handbook of Archaeological Ceramic Analysis*. Ed. by A. Hunt. Oxford: Oxford University Press, 2017, 162–180.

Schneider and Daszkiewicz 2010
Gerwulf Schneider and Małgorzata Daszkiewicz. "Testmessungen mit einem tragbaren Gerät für energiedispersive Röntgenfluoreszenz (p-XRF) zur Bestimmung der chemischen Zusammensetzung archäologischer Keramik." In *Archäometrie und Denkmalpflege. Jahrestagung im Deutschen Bergbau-Museum Bochum*. Ed. by O. Hahn, A. Hauptmann, D. Modarressi-Tehrani, and M. Prange. Metalla Sonderheft 3. Deutschen Bergbau-Museum, 2010, 110–112.

Strommenger and Kohlmeyer 1998
Eva Strommenger and Kay Kohlmeyer. *Tall Bi'a / Tuttul – I. Die altorientalischen Bestattungen*. Vol. 96. WVDOG (Wissenschaftliche Veröffentlichungen der Deutschen Orient-Gesellschaft). Saarbrücken: Saarbrücker, 1998.

Wilkinson et al. 2012
Tony J. Wilkinson, Nikolaos Galiatsatos, Dan Lawrence, Andrea Ricci, Rob Dunford, and Philip Graham. "Late Chalcolithic and Early Bronze Age Landscapes of Settlement and Mobility in the Middle Euphrates: A Reassessment." *Levant* 44 (2) (2012), 139–185.

Zweig 2012
Zachi Zweig. "Using Data Mining Techniques for the Analysis of Pottery from Tell es-Safi/Gath." In *Tell es-Safi/Gath I: the 1996–2005 Seasons, Part 1: Text*. Ed. by A. M. Meier. Ägypten und Altes Testament 69. Wiesbaden: Harrassowitz, 2012, 429–453.

Illustration and table credits

ILLUSTRATIONS: **1–8** A. Höhne (ehemals Hofmann). **TABLES:** **1–5** A. Höhne (ehemals Hofmann).

ANTONIA HÖHNE (EHEMALS HOFMANN)

Antonia Höhne studied restoration of archaeological cultural heritage at the University of Applied Sciences Berlin (HTW). Since 2012, in context of her doctoral project in cooperation with Freie Universität Berlin and HTW, she has been working on the differentiability of survey ceramics from Syria using the p-ED-XRF in addition to the record of technological features in order to provide information on the development of production and distribution systems of former societies.

Dipl.-Rest. (FH) Antonia Höhne (ehemals Hofmann)
Hochschule für Technik und Wirtschaft Berlin
Fachbereich Gestaltung und Kultur
Konservierung und Restaurierung/
Grabungstechnik
Wilhelminenhofstraße 75A
12459 Berlin, Germany
E-mail: antonia.hofmann@htw-berlin.de

Toni Walter, Marc Fellinger

Portable X-Ray Fluorescence in Archaeometry

Summary

This article expresses the authors' positions on various problems in archaeometry. It discusses the nature of matrix effects, the properties of SiO_2 samples containing iron or iron and nickel, and how these are corrected using fundamental parameter (FP) algorithms. In addition, it presents the analysis programs Mining, Soil, and Test All Geo; addresses the significance of the balance value in the Mining program; and discusses some factors that influence measurement results, such as moisture. It also addresses the question of when the use of helium is advisable.

Keywords: Niton XL3t; measuring programs; matrix effect; error; Helium

In diesem Artikel wird zu unterschiedlichen archäometrischen Problemfeldern Stellung genommen. Es wird thematisiert, was Matrixeffekte sind, wie sich SiO_2 Proben mit Eisengehalt bzw. mit Eisen und Nickel verhalten und wie die Korrektur mittels Fundamentalparameter (FP)-Algorithmus erfolgt. Vorgestellt werden ferner die Messprogramme „Minerals", „Soil" und „Test all GEO", die Bedeutung der Balance im Messprogramm „Minerals", außerdem Einflüsse auf die Messergebnisse wie etwa Feuchte. Darüber hinaus wird verdeutlicht, wann der Einsatz von Helium sinnvoll ist.

Keywords: Niton XL3t; Messprogramme; Matrix Effekt; Fehler; Helium

Morten Hegewisch, Małgorzata Daszkiewicz und Gerwulf Schneider (eds.) | Using pXRF for the Analysis of Ancient Pottery – an Expert Workshop in Berlin 2014 | Berlin Studies of the Ancient World 75 (ISBN TODO; DOI: 10.17171/3-75) | www.edition-topoi.org

1 Introduction

In the past few years, portable x-ray fluorescence has become an established geochemical technique in the field archaeometry. The possibility of obtaining information about the elemental composition of a sample quickly and, for the most part, without involving elaborate sample preparation offers great advantages:

- a very large number of samples can be analyzed within an extremely short period of time;
- samples can be analyzed on site; waiting periods and transportation logistics are eliminated;
- samples can be analyzed without destructive sample preparation / extremely little effort is involved in sample preparation and
- the individual costs of measurements are negligibly small.

In order to make best use of these advantages in practice, it is helpful to have a good understanding of the physics and technology involved. The following questions arose during the archaeometry conference in Berlin:

1. What are matrix effects and what influence do they have on the results of measurements?
2. How do the analysis programs Mining, Soil and Test All Geo of the Niton XL3t differ from one another? Which program is appropriate for what sample form? What is "balance" and what is its significance for measurement results?
3. What must one pay attention to when preparing samples? (Influence on measurement results)

These questions are discussed below with a focus on using portable EDXRF systems effectively and obtaining the best possible measurement results with them. The focus in this regard is on the portable Niton XL3t XRF Analyzer.

2 What are matrix effects?

So-called matrix effects are generated in a sample during x-ray fluorescence analysis. The term refers to physical effects stemming from the composition of a sample that influences the measurement result. The number of matrix effects that are possible is enormous, and it would be nearly impossible to describe them in a short text. Nonetheless, we will address one very relevant example, inter-element excitation, in order to cast

some light on this important topic.

As most researchers know, with portable XRF the sample is excited with x-rays, and the elements being investigated emit their characteristic spectral lines in the x-ray range. Since every element is particularly effectively excited by a certain range of energy (the so-called absorption edges), the lines characteristic of certain elements necessarily lie in energy ranges that are associated with additional excitation of other elements also present in the sample. This effect is especially strong between elements that are two atomic numbers apart, such as nickel and iron. To explain the influence this has on the analysis, we will present two different situations here.

2.1 Example 1 – SiO_2 sample containing iron

In this first example, we assume that the goal is to determine the iron content in a ferrous mineral that contains iron only in SiO_2. We further assume that the instrument has been calibrated in advance using reference samples appropriate for Fe in SiO_2 in the concentration range of interest. During the analysis, the iron atoms are solely excited by the primary radiation from the analyzer causing them to emit their characteristic spectral lines, while the detector records the intensity. Thanks to the calibration, the intensity measured can be used to arrive at the Fe concentration.

2.2 Example 2 – SiO_2 sample containing iron and nickel

In the second example, the system being investigated contains both iron and nickel. Again, the goal is to determine the iron content in this Fe-Ni-SiO_2 matrix. As is the case in example 1, all of the iron atoms are excited and emit their characteristic spectral lines; the same holds true for the nickel atoms. The characteristic spectral lines emitted by the nickel atoms are in an energy range within which iron atoms are very effectively excited. In other words, the characteristic x-ray energy of the nickel functions as a source of excitation, thus triggering additional x-ray fluorescence in the iron atoms. In this measurement, a higher Fe intensity will reach the detector given the same degree of excitation by the primary radiation while Ni signal is absorbed by the iron atoms. If no correction is performed, iron would be over- and nickel underquantified in this case.

2.3 Correction through fundamental parameters – FP algorithm

In the examples described above, one example of a matrix effect, the influence of the elementary composition of the sample on the measurement signal, was explained. A procedure known as a fundamental parameter correction (FP correction) is employed to allow researchers to make optimal use of the advantages of x-ray fluorescence as a

fast, on-site method of element analysis. This involves the application of knowledge of the principles of physics through mathematical formulas in complex correction algorithms with the aim of eliminating, to the greatest extent possible, the distortion effects mentioned. This approach considerably reduces the number of reference samples necessary, since in a purely empirical procedure, one would have to reproduce each of the interelement effects individually.

3 The analysis programs Mining, Soil and Test All Geo

3.1 Mining analysis program

In order to arrive at usable results quickly, the Niton XL3t has a variety of analysis programs available depending on requirements.

The Mining analysis program is optimized for determining the elemental contents in a SiO_2 matrix. To reflect the specific demands associated with varying element contents, the FP algorithm is an essential part of the Mining analysis program. This algorithm makes it possible to obtain values that approximate the actual element contents of a sample as closely as possible even if the sample is completely unknown and differs from the reference standards used to calibrate the instrument. Due to the nearly infinite number of matrices that one might encounter in the field, the first step involves a semi-quantitative determination. If trueness of the results is of great significance, a matrix adjustment can be undertaken quite easily on site using appropriate samples of known content. Such an adjustment involves the analysis with the Niton instrument of a suitable set of samples containing a known content of the element in the concentration range of interest and the generation of a new linear slope and intersection with the y-axis (linear regression). A CD or USB stick with software from analyticon contains the tool "correct calc", which is intended to enable the simple calculation of these values. In this manner, one can derive up to 20 adjustments from the basic calibration, which will be available on the analyzer.

3.2 The significance of the "Balance" value in the Mining analysis program

The x-ray fluorescence analysis technique is generally subject to a natural, physical limitation with respect to the light elements. This limitation stems in part from the fact that the x-ray fluorescence effect, i.e. the emission of characteristic, measurable x-ray quanta, becomes weaker with decreasing atomic numbers. In addition, the energy of the spectral line emitted by an element also decreases with decreasing atomic numbers. As a result, more and more of these energies are absorbed by the matrix, by the air present

in the beam path and ultimately by the detector window. This means that sodium is the lightest element that can still be detected with portable systems, which, for reasons of geometry, basically function in an energy dispersive manner. In the quantification, magnesium is the lightest element calculated in the Mining analysis program.

The Mining analysis program operates with 100% scaling. This is of great significance for the robustness of the method in the field. Therefore, in order to arrive at a correct quantification of the measurable elements in an SiO_2 matrix, it is essential to know the proportion of non-detectable elements within the sample. This relates chiefly to oxygen; if the sample contains a high proportion of organic material, then carbon and hydrogen are also at issue. So-called Compton scattering makes it possible to estimate the sum of all non-measurable elements of lower atomic numbers, because the Compton scattering is dependent on the density of the sample. The analyzer always displays the sum in the analysis as "Balance" or "Bal." For this purpose, the Compton peak of the silver tubes Ag Kα line is evaluated. This procedure always takes place in the main filter, which is basically the first in each measurement If the composition of the sample differs greatly from the SiO_2 matrix of the NIST standard used for the basic calibration, it will affect the balance value and thus the quantification of all the elements in the sample. For example, a higher moisture content would introduce a massive quantity of the scattering light elements H and O to the matrix, causing an increase in the balance relative to the dry substance. Accordingly, all the measurable elements present would be represented at lower concentrations relative to those in the dry substance.

3.3 Soil analysis program

The focus in the Soil program is on the analysis of extremely low concentrations, in the range of a maximum of 1%, within a SiO_2 matrix, associated with the desire to have the lowest possible limits of detection. An example of a typical use for this program is the analysis of heavy metal pollution in soils. The fact that it operates without FP correction thus constitutes a significant feature of the Soil program. As discussed above, the FP correction serves to eliminate, to a great extent, the distortion of the measurement results by interelement effects (e.g. secondary excitation/absorption), the intensity of which increases with increasing concentrations of the relevant elements in the sample. The mathematical correction routine also results in an increase in the limits of detection for the elements. When the concentration of the elements are in the range of hundreds of ppm, for instance, then the interelement effects are negligible. Without unnecessary FP correction, the smallest possible limits of detection can be attained. Conversely, the absence of the mathematical correction routine means that the Soil program is not suitable for concentration ranges of >1%. As concentrations increase, interelement effects would result in an ever-greater distortion of the results. The Mining program would be

the correct choice in this case.

The Soil program also takes a different approach to dealing with the non-measurable elements. While the Mining program treats the Compton intensity generated like one element (Balance/Bal) and integrates it in its 100% scaling, the Soil program performs a Compton normalization. All element intensities are placed in relation to the Compton intensity, i.e., divided by it. In this way, the Soil program automatically achieves a bulk density correction.

To sum up, the two programs, Soil and Mining, complement one another due to their different functionalities. While the Mining program with its FP correction algorithm is the most versatile program over varying SiO_2 matrices of all concentration ranges, providing at least approximations as results and capable of adjustment if necessary, the Soil program presents a solution for quantification of elements in the ppm range in simple SiO_2 matrices.

3.4 Test All Geo analysis program

The Test All Geo mode combines both approaches, Mining and Soil, within one analysis. In this context, Test All Geo checks the concentration ranges, inter element effects and line overlaps for all elements present and then selects the best approach for each of the elements. In this mode, concentrations are displayed in an integrated analysis, in which elements calculated with the Soil program are shown in ppm, and those calculated in the Mining program are shown as percentages.

4 Influences on the analysis results

4.1 Influence of moisture

In an earlier section, the balance value in the Mining program was described as depicting the sum of all of the light elements. In this context, a high moisture content introduces a massive quantity of the scattering light elements H and O to the matrix. This results in an increase in the balance value for the moist sample, causing all of the measurable elements to be represented within the framework of the 100% scaling with concentrations that are too low.

4.2 Influence of the distance between sample and detector

As it travels from the excited spot to the detector, the characteristic x-ray radiation is subject to the inverse square law. This means that its intensity decreases in proportion

with the square of the distance. As an approximation the following can be accepted. Assuming the x-ray tube anode sits 2 cm behind the front panel, then the intensity of the excitation would be reduced to one fourth if the distance between the front panel and the measured object is 2 cm (i.e. the distance is doubled). The characteristic radiation's path from the excited measured surface to the detector further reduces the intensity to one sixteenth. This is a theoretical observation related to a perfect point source of radiation, but it shows how great an impact the distance to the sample has on the measurement signal. Added to that are the effects of absorption of the signal by the air, which negatively affect the measurement of the low-energy lines of the light elements (Mg, Al, Si, P, S) when the distance to the sample is lengthened. Reference samples are therefore placed in direct contact with the front panel for the calibration.

4.3 When is helium flushing advisable

Even when the analyzer is in direct contact with the sample, the air present in the measurement window still absorbs measurable radiation. While this has no noticeable impact for elements that have higher atomic numbers (≥Ti), with the lighter elements Mg, Al, Si, P and S one sees a marked attenuation of the intensity. If concentrations of >~1% are being measured (this depends on the makeup of the matrix as a whole and must be tested on a case by case basis), then the signal stands out clearly from the detector background and basically a straightforward quantification in air atmosphere is possible. When concentrations are very low, the measurement signal is completely lost in the detector background. In this situation, one can increase the intensity of the signal reaching the detector from light elements, and thus lower their detection limit, by flushing the volume between the measurement window film and the detector with less-absorbent helium. As a result, small concentrations of light elements can be made measurable. Even at concentrations that can be measured without helium purging, helium purging significantly improves the signal-to-noise ratio and thus the achievable precision. Starting from the element titanium upwards no signal improvement is recognizable and a helium flush thus ineffective. Since helium flushing is recorded as an independent calibration, it is important to ensure that the correct helium setting (He:on/He:off) is used. In the current XL5 device, that was launched in 2017, the performance of the light elements is achieved elsewhere. The combination of a strong excitation side with a 5 W tube and a greatly shortened detection path make helium flushing and therefore extra equipment superfluous. As a result, an excellent performance of the light elements is permanently available.

4.4 On obtaining "true" measurement results

One frequently asked question related to portable x-ray fluorescence analysis is that of accuracy. In this context, one should understand the concept of accuracy as a combination of "trueness" and precision. Precision here is determined by the measurement time per filter and can be described as a count-statistics-based error contribution to measurement uncertainty. Precision is shown for each element in the right-hand column of the instrument display under 2 σ. The trueness of the results is produced by the calibration. As mentioned above, due to the many possible matrices, the Mining analysis program undergoes a basic calibration using SiO_2 NIST standards, and daughter calibrations can be derived from this original calibration using appropriate reference samples of known content.

To achieve the maximum possible trueness, all sources of error must be considered and weighted. In this context, the total error (F_{ges}) is made up of the sum total of all the individual errors ($F_{1\ldots n}$) associated with the characteristics of the method.

$$F_{\text{ges}} = \sqrt{F_1^2 + F_2^2 + \ldots + F_n^2}$$

– Inhomogeneity (F_I) of the sample usually represents the greatest source of error. Depending on the method, the first µm or mm of the sample surface right at the beam spot contributes directly to the result and, depending on the degree of inhomogeneity, is not representative of the sample as a whole. To minimize this source of error, the recommended procedure is to measure at multiple sites of the sample and then calculate the mean values, or to grind up the sample. While grinding is a more time-consuming method, it is also substantially more effective. In archaeometry in particular, it is appropriate to mention layer systems in this context. This refers, for instance, to applications on substrates (glazes), in connection with which only a purely qualitative observation of the layer structure (elements contained in the layer, and elements contained in the substrate, depending on the thickness of the layer) is reasonable. A quantitative consideration regarding the total composition would result in an overquantification of the application for the reasons mentioned above.

– The moisture content of the sample (F_F) has the effect of boosting the balance value. This causes all the measurable elements to be underquantified. Samples must be dried in order to obtain measuring results suitable for comparisons. In addition, it should be noted that in moist samples, the light elements, first and foremost magnesium, are barely measurable, if at all, due to absorption. Helium purging is not effective here because the signal path is already blocked in the sample.

– Varying matrix density / matrix density greatly different from that of the references (F_D) results in absorptions of the elements and affects the balance value. The measurable elements are thus over- or under-quantified accordingly.

– The more the specific matrix differs from the SiO_2 NIST references used for the calibration, the more the results may differ from the actual contents due to matrix effects (F_M). To minimize these errors, researchers should, as mentioned above, derive measurement value adjustments from the basic calibration.

This list in no way attempts to be exhaustive, but it conveys an overview of the main sources of error (F_H).

$$F_H = \sqrt{F_I^2 + F_F^2 + F_D^2 + F_M^2 (+F_x^2)}$$

In order to use portable x-ray fluorescence as a fast method of analysis on site, researchers should perform an overall assessment of the sample with respect to these criteria. Having assessed the sample and weighed the sources of error, appropriate steps to minimize those errors can be taken. Even if it is not possible to prepare the sample in a manner that addresses these criteria, the researcher will have gained an awareness of the degree of accuracy permitted by the object under consideration based on physical and technical factors.

Used sensibly, portable x-ray fluorescence represents a fast and flexible addition to the established laboratory analyses.

TONI WALTER

Toni Walter is a sales engineer and technical consultant for portable x-ray fluorescence at analyticon instruments gmbh. He received his BA in process engineering from Frankfurt University of Applied Science in 2011 and then joined Analyticon as a trainer for portable XRF. He specializes in the area of industrial applications and is a lecturer at his former university. Additionally, he conducts feasibility studies and consults clients on archaeometrical applications.

Toni Walter
analyticon instruments gbmh
Dieselstr. 18
61191 Rosbach v. d. H., Germany
E-mail: t.walter@analyticon.eu

MARC FELLINGER

Marc Fellinger has worked for more than 10 years as an application specialist for portable XRF and LIBS at analyticon instruments gbmh. His deep understanding of analytical requirements results from his long experience in developing customer-specific applications. He combines physical knowledge with expertise in instrumental construction and the components, details, and software of XRF instruments, allowing him to explain complicated things with ease for instrument users.

Marc Fellinger
analyticon instruments gbmh
Dieselstr. 18
61191 Rosbach v. d. H., Germany
E- mail: m.fellinger@analyticon.eu

Małgorzata Daszkiewicz and Gerwulf Schneider
with a contribution by Bernhard Heeb and Andrei Bălărie

Using Portable Energy-Dispersive XRF Analyzer in the Analysis of Ancient Ceramics – a Case Study Based on Bronze Age Pottery from the Banat Region, Romania

Summary

Bronze Age pottery fragments from the Banat region (recovered from the following sites: Corneşti-Iarcuri, Corneşti-Cornet, Timişoara-Fratelia, Deta-Dudarie, Giroc-Mezcal, Peciu Nou, Voiteni-Voitec) dated to between the 19th and 11th century BC were subjected to archaeometric analysis. This article presents the results of chemical analysis by portable energy-dispersive X-ray fluorescence (pXRF) and wavelength-dispersive X-ray fluorescence (WD-XRF) regarding tests of precision and accuracy, as well as the results of MGR-analysis, thin-section studies and analysis of some aspects of the technological process.

Keywords: Bronze Age pottery; Banat; archaeometry; pXRF; WD-XRF; MGR-analysis

Bronzezeitliche Keramikscherben aus der rumänischen Banatregion (von folgenden Fundorten: Corneşti-Iarcuri, Corneşti-Cornet, Timişoara-Fratelia, Deta-Dudarie, Giroc-Mezcal, Peciu Nou, Voiteni-Voitec), datiert zwischen dem 19. und 11. Jh. v. Chr., wurden archäometrisch analysiert. Der Beitrag präsentiert sowohl die Ergebnisse der chemischen Analysen mit pRFA und WD-RFA, einschließlich von Tests zur Präzision und Richtigkeit, als auch Vergleiche mit den Ergebnissen von MGR-Analysen, Dünnschliffuntersuchungen und Analysen einiger technologischer Aspekte.

Keywords: Bronzezeit; Keramik; Banat; Archäometrie; pRFA; WD-RFA; MGR-Analyse

Morten Hegewisch, Małgorzata Daszkiewicz und Gerwulf Schneider (eds.) | Using pXRF for the Analysis of Ancient Pottery – an Expert Workshop in Berlin 2014 | Berlin Studies of the Ancient World 75 (ISBN TODO; DOI: 10.17171/3-75) | www.edition-topoi.org

1 Introduction

For over twenty years now the team of M. Daszkiewicz, E. Bobryk and G. Schneider has been using a standard package of analyses for investigating the provenance of ancient ceramics. It includes the analysis of chemical composition, mineralogical and petrographic composition, analysis of physical and mechanical ceramic properties, as well as the estimation of firing temperature and atmosphere and an assessment of functional properties. Comprehensive analysis of this type can provide insights into the provenance of ceramic raw materials and into the technology of ceramic production. Studying ceramic technology is important because differences in know-how are not only indicative of the level of technological knowledge within a given culture or period, but they can also reflect the transfer of technological knowledge at the level of individuals (e.g. a potter migrates and starts making stylistically local ceramic vessels in his new location using local raw materials, but employing the technology already known to him). Furthermore, geological factors may have dictated that potters based at different pottery production centres used the same clay as well as the same non-plastic raw materials to make ceramic bodies. In this scenario it is only technological analysis that has the potential to identify individual production centres.

The methods used in a standard package are: MGR-analysis, chemical analysis by WD-XRF, thin-section studies and an estimation of physical ceramic properties (apparent density, open porosity and water absorption).[1]

MGR-analysis (Matrix Group by Refiring) is used in order to determine the composition of the ceramic matrix. Matrix types can be identified using this analytical method because of the fact that the thermal behaviour of the plastic components during firing is governed by their chemical and phase composition.[2] After the sherds are refired at a higher temperature than their original firing temperature, i.e. once the effects caused by the original firing temperature and conditions are 'removed', the colour, shade and appearance of the matrix relate to the chemical and phase composition of the plastic part of the body. MGR-analysis allows pottery assemblages to be divided into groups of sherds made of the same plastic raw material. Two variants of MGR-analysis can be used: abridged MGR-analysis, in which samples are fired at 1100, 1150 and 1200°C, or full MGR-analysis, which includes additional refiring at 400, 700, 800, 900 and 1000°C. Abridged analysis is only used for provenance studies, while full analysis also allows for an estimation of the original firing temperature.

Chemical analysis of sherds is used to determine the chemical composition of both the plastic and non-plastic ingredients of the pottery fabric. This analysis enables the

1 For a full description of methods see Appendix.

2 Daszkiewicz and Schneider 2001; Daszkiewicz 2014; Daszkiewicz and Maritan 2017.

quantity of major and trace elements in the body to be established, revealing the geochemical characteristics of the raw materials used, although the phases in which individual elements occur cannot be determined[3] (giving the major elements as oxides[4] is standard procedure in geochemistry when presenting the results of chemical analysis).

The main aim of thin-section studies is to identify the mineralogical-petrographic content and grain size distribution of the non-plastic (clastic) components of the body. Thin-section analysis can provide only very general information about the matrix owing to the resolution of the microscope, the size of the clay minerals making up the plastic part of the body and the fact that they undergo transformation when fired.

When using three analytical methods in provenance studies, pottery groups are determined independently using: MGR analysis, chemical analysis and thin-section studies. Each of these methods yields a different type of classification (matrix groups, geochemical groups and clastic material groups respectively). Collectively, these three types of classification allow provenance groups to be established, which not only highlight differences in chemical composition but can also demonstrate what these differences are associated with (e.g. ceramic vessels belonging to two different groups, such as tableware and kitchenware, may be locally produced using the same clay with the addition of different tempers depending on the intended function of the vessel).

The physical ceramic properties (apparent density, open porosity and water absorption) of the original pottery fragments are also evaluated. Physical ceramic properties depend on the type of raw material from which a vessel was made, the temperature at which it was fired, how it was formed, and in particular on the method used to de-air the ceramic body, which is very individual to each potter (de-airing is a very time-consuming process and as such is less susceptible to random problems). If we have products made of the same ceramic body, formed using the same technique, thoroughly dried and fired at the same temperature, their porosity will be entirely dependent on how well the ceramic body was de-aired.[5] The more poorly de-aired the ceramic body, the greater the pottery's porosity and commensurate degree of water absorption, and the lower its apparent density.

A *step by step* strategy is adopted for provenance analysis, allowing for a reduction in the number of analyses carried out. An estimation is made of the physical ceramic

3 For example, Ca content identified by chemical analysis may be attributable to, for example, inclusions of calcite or dolomite or calcium silicates, or may occur exclusively in clay fraction in the matrix.

4 Si = silicon, calculated as SiO_2; Al = aluminium, calculated as Al_2O_3; Ti = titanium, calculated as TiO_2; Fe = iron, total iron calculated as Fe_2O_3; Mn = manganese, calculated as MnO; Mg = magnesium calculated as MgO; Ca = calcium calculated as CaO; Na = sodium calculated as Na_2O; K = potassium calculated as K_2O; P = phosphorus calculated as P_2O_5.

5 If the products differ only in firing temperature, when they are refired at a temperature higher than the original firing temperature they will exhibit the same porosity and density. Therefore, it is best to assess physical ceramic properties on original samples and samples after refiring at 1200°C.

properties of all samples selected by archaeologists for laboratory analysis, and all samples undergo MGR-analysis, the results being used as the basis for raw material and technological classification, after which samples representing each group are taken for chemical analysis and for examination in thin-section.

When dealing with very large numbers of samples a variation of this strategy can be applied in order to significantly reduce the costs of analysis.[6] This *down–up sampling classification* strategy can be used to classify pottery. In this procedure individual analyses are carried out consecutively; however, the number of samples chosen for each subsequent analysis is restricted based on the results of the preceding analysis (down). Thus far, when employing this strategy, MGR-analysis has always been the first method used by the authors. All samples are subjected to MGR-analysis, and when this has been completed only those samples that represent individual MGR-groups are chosen for chemical analysis. Once the results of chemical analysis have been obtained, the samples are reclassified and then selected fragments are chosen for thin-section studies and technological analysis. When this has been completed, it is possible to identify all of the analysed potsherds (up) using macroscopic descriptions of the pottery fabrics. Thus, it is only after comprehensive laboratory analyses have been completed that a macroscopic study should be carried out to identify macroscopic diagnostic parameters typical of the groups determined by laboratory analysis. Subsequently, a catalogue of reference fabrics can be created for individual groups.

Where among this sequence of analyses and classification strategies should chemical analysis using a portable ED-X-ray fluorescence analyser (pXRF) be positioned? Does the fact that pXRF provides a relatively swift and cheap means of performing multiple measurements to determine the chemical composition of ancient ceramics provide an opportunity to revolutionise currently used analytical models? Will using this analytical technique eliminate the need for multi-tiered classification, meaning that all of the samples on which MGR-analysis is done can be analysed using pXRF and thus dispensing with the need to select samples for chemical analysis using a technique such as WD-XRF?

Berendt et al. demonstrated that using only pXRF to try and determine provenance resulted in 10–45% of samples (c.10–20% in the case of fine wares) being misclassified.[7] Thus, given that potentially as many as half of the samples could be incorrectly classified, it is recommended that this technique should be used in conjunction with more precise laboratory methods such as those included in the *down-up* sampling strategy. In other words, when planning a project involving the use of pXRF it must be remembered that chemical analysis by WD-XRF, NAA and ICP-MS cannot be replaced by pXRF in provenance studies. Likewise, the limitations associated with the use of pXRF, in particular

6 This strategy draws out the length of time required for analyses, however it significantly reduces their cost.

7 Behrendt, Mielke, and Mecking 2012.

when analysing coarsely tempered pottery, must be taken into account when writing up the results of analysis carried out using this technique.[8] Furthermore, as outlined earlier, chemical analysis represents an important but limited part of the analysis of archaeological pottery, hence the use of pXRF cannot completely eliminate MGR-analysis and thin-section studies from the suite of analyses used in provenance studies.

Bearing in mind the scope and limitations of chemical analysis by pXRF, the authors submit that the use of MGR-analysis in the *down-up* classification strategy can be preceded by classification based on chemical composition analysis using the pXRF technique, thus increasing the number of analysed samples. This new model of tiered analysis was tested on sherds of Bronze Age pottery from the Banat region. Laboratory analyses were carried out on a total of 447 pottery fragments. The chemical composition of all of these fragments was initially assessed using pXRF; this was followed by MGR-analysis, chemical analysis by WD-XRF, thin-section studies, estimation of physical ceramic properties and estimation of the original firing temperature. All analyses were carried out by the authors as part of a project conducted at the Freie Universität Berlin by the Excellence Cluster Topoi 2, Research area A – Spatial Environment; A-6 Economic Space.

2 Archaeological background

by B. Heeb and A. Bălărie

Iarcuri is the largest Bronze Age settlement in Europe. The true extent of this fortified site was unknown until the end of the 20th century. It was not until 1972 that military aerial photos revealed the existence of a fourth 16 km-long rampart surrounding the three inner rings. This means that the site consists of four earth-filled wooden ramparts with a total length of more than 33 km, encompassing an area of over 17.5 km^2 (Fig. 1). Since the end of the 19th century, the date of the site has been the subject of intense and sometimes controversial discussions. Some of the first theories put forward an Avar origin.[9] However, during the course of the first excavations, carried out in 1932 and 1939 by the universities of Cluj and Bucureşti, a late Bronze Age date was put forward for the first time.[10] The outbreak of WWII interrupted further research for decades. It was not until 2006 that work resumed when the West-University of Timişoara undertook a small-scale magnetic survey. A year later, the Muzeul Banatului and the Johann Wolfgang Goethe-Universität Frankfurt/Main undertook excavations for the first time after nearly

8 Schneider and Daszkiewicz 2010, Daszkiewicz and Schneider 2011, Daszkiewicz and Schneider 2012; Behrendt, Mielke, and Mecking 2012.

9 Pech 1877.

10 Medeleţ 1993.

70 years. In 2009, the University of Exeter and the Museum für Vor- und Frühgeschichte Berlin joined the project.[11] To date seventeen trenches have been excavated and around 250 ha have been covered by magnetic survey and systematic field walking (Fig. 2). So far, more than 100 000 sherds (Copper Age, Middle Bronze Age, and predominantly Late Bronze Age) have been collected by field walking or uncovered in the trenches.

Archaeometric analyses focused on Middle and Late Bronze Age pottery from the Iarcuri site (Rings I and II), Middle Bronze Age pottery from the Corneşti-Cornet site, and Late Bronze Age pottery from five other sites in the Banat region (Timişoara-Fratelia, Deta-Dudarie, Giroc-Mezcal, Peciu Nou, Voiteni-Voitec). In cultural terms, we are dealing with the Vattina and Cruceni-Belegiş-Culture of this region, dated to between the 19th and 11th century BC.

Vattina pottery is one of the hardest and best-fired wares from the Middle Bronze Age in southeast Europe. Its colour is mostly yellow-brownish or, in the later phase, blackish. The fine ware often shows a polished surface and has a very fine slip.[12] The most typical shapes of the Vattina group are the so-called kantharos bowls with two pulled up handles, bowls with ansa-lunata- or ansa-cornuta-handles, hanging vessels with a lid, twin vessels, 'Röhrenfußschüsseln', pyraunoi, as well as spherical and biconical vessels.[13] Typical ornamentation consists of grooves, mostly in singular, double or threefold lines on the upper part, forming arched garlands. The ornamentation is very varied, including triangles, geared doubled lines, circles and spirals.[14]

The Vattina culture existed from the end of Bz A until the end of Bz B (in Iarcuri only the later phase is represented). During the same period, Bronze Age tell settlements also vanish and the Vattina culture is followed by the Cruceni-Belegiš culture.[15]

The typical vessel shapes of the Cruceni-Belegiš culture are spherical and biconical amphoras, bowls, cups without handles, twin vessels and pyraunois. Colours range from bright brownish and greyish to blackish.[16] This is often linked to the chronology of the vessels. The Cruceni-Belegiš culture can be divided into three main phases (I – III). The first phase is characterized by ornamentation techniques such as grooves, pseudo-cord impressions and in some cases vertical and oblique cannelures on the body. They suggest a continuation of Vattina traditions. Phase I covers the period from Bz B and Bz C.

In the second phase cannelures become characteristic and the rim of the bowls starts being curved inwards. The colour is now mostly greyish-blackish, which points to not-oxidising firing conditions. Phase II covers the period from Bz D to the first half of Ha A1.

11 Szentmiklosi et al. 2011.
12 Bóna 1975, 181.
13 Bóna 1975, 182–183; Bogdanović 1996, 99–100; Gogâltan 2004, 84, 137–151.
14 Bóna 1975, 181; Gogâltan 2004, 84, 137–151.
15 Bóna 1975, 186–187; Gogâltan 2004, 81–82.
16 Vranić 2002, 187; Szentmiklosi 2009, 167.

The biconical amphoras with low bodies, cannelure garlands on the neck and turban motifs on the body are typical elements of the third phase. Bowls with incurved rims, which are mostly faceted, are also typical. Phase III dates to the second half of Ha A1 to Ha A2, which coincides with the end of this culture.[17]

The analysed ceramic material from Iarcuri was found during fieldwalking surveys between 2008 and 2014. The sherds from the other sites are mostly from excavations and, therefore, stratified. The material from Iarcuri is not stratified. For the analyses, only pieces which had been securely identified as dating to the Middle or Late Bronze Age were chosen by optical parameters (shape, ornamentation, ware).

3 Results of pXRF tests

The chemical composition of all 447 ceramic sherds was determined by pXRF. Readings were taken with a Niton XRF analyser (XL3t 900S GOLDD RF-Analyser, MINING software, 50 kV, Ag anode). The instrument was calibrated on twelve ceramic reference samples analysed by WD-XRF, which were prepared in the form of round discs fired at 900°C by G. Schneider and M. Daszkiewicz. Measurements were performed without helium, in a sample chamber, with an 8-mm measuring spot and a measurement time of 120 seconds (30 seconds per filter). The measurement surface of each of the 447 pottery fragments was prepared by creating a fresh fracture using pliers with a cutting surface made of tungsten carbide. Subsequently, three measurements were taken at three different spots on the prepared fresh fracture surface of each sample. In addition, a series of extra measurements was performed on a dozen samples in order to test the precision of analysis and the accuracy of analysis. The criterion for selecting samples for these tests was the size of the ceramic sherds (unfortunately, most of the 447 pottery fragments were not big enough to use for all test measurements).

In this project, the total precision of analysis, which is affected by several errors, was tested. These tests examined the following:

- precision of sampling (sampling error connected with non-homogeneity of measured samples),
- preparation error (precision of preparing the sample, personal error),
- precision of measurement.

17 Gumă 1993, 180; Szentmiklosi 2009, 80.

It should be remembered that the so-called preparation error plus the measurement error should be less than ~ ⅓ of the sampling error because in this situation analysis precision is mainly associated only with the non-homogeneity of the analysed ceramic sherd.

$$S_a^2 = S_s^2 + S_p^2 + S_m^2$$

where: Sa = analysis precision; Ss = sampling precision; Sp = preparation precision; Sm = measurement precision. If the preparation error plus the measurement error is greater than ~ ⅓, groups cannot be correctly identified nor can pottery sherds from various vessels be recognised because the preparation error and measurement error make up too great a proportion of the analysis error (!). This means that, in the case of ancient pottery, chemical analysis must be carried out with high precision.

Errors stemming from sampling have the biggest impact on analysis precision; this error is particularly large in the case of coarse ware pottery, especially where the temper is poorly sorted and/or grains of temper are not homogeneously distributed within the matrix. When analysing ancient pottery there is actually no way to minimise this error (it must be borne in mind that the smaller the sample taken for analysis, the larger the sampling error).

The preparation error was tested by having two people both performing the measurements and creating the fresh fractures. Measurements were also performed on surfaces that had been prepared for measurement by cutting with a diamond-coated blade.

Precision of measurement was improved by measuring a monitor sample and was tested by repeating measurements of the same sample after certain periods.

Tests were also conducted to assess the impact on measurement results caused by the fact that pXRF analysis was carried out on original pottery fragments, i.e. air-dry samples. To this end, prior to measurement the samples were fired at 900°C in the same conditions as samples prepared for analysis by WD-XRF (the authors perform measurements by WD-XRF on samples after determining loss on ignition at 900°C). All tests were conducted on samples removed by the same method from one pottery fragment.

Accuracy of measurement was tested by measurement of reference materials and was additionally tested by comparing the results of pXRF measurements with the results of WD-XRF measurements carried out on the same ceramic sherd.

Figure 3 shows sampling precision, i.e. the minimum, maximum and average value of the coefficient of variation (cv%)[18] calculated for individual samples from measurements taken on three different surface spots of a fresh fracture.

This figure does not show results for: Na, La and Th, as they are not measured; for Mg and S because they were not detected; and for S, Cl, Ni, Cu, Sn, Ce and Th, which were mostly not detected. These calculations relate to 446 samples. One sample

18 Throughout this article cv% refers to 1σ.

was disregarded because only two measurements were taken from it (due to the small surface of the fresh fracture). The average sampling precision is relatively good, and lower than that expected given the experiences of Berendt et al. (2012) regarding coarse-tempered sherds (but not with grog). It is less than 5% for Si, Ti, Fe, K, Rb, Sr and Zr. Average sampling precision above 10% was only noted for Mn, P, Cl, Cr and Pb, hence for elements (except Cr) whose non-homogenous distribution within the matrix is recognised. Relatively large differences in sample precision were observed for individual samples: for example, for Ti precision of sampling ranges from less than 1% to 28.7% (average cv% = 3.6%), however, the number of samples in which sampling precision was greater than 10% is small (2.2% of all samples). Of the total number of 446 sherds the percentage of samples in which sampling precision was greater than 10% for individual elements is small (up to 17%), with the exception of Mn, P, Cr, Nb, Ba and Pb (Fig. 4).

Surprisingly good sampling precision was noted for coarse-tempered sherds, despite the non-homogeneous distribution of inclusions. Grains of coarse sand size and gravel size are easily macroscopically visible in these sherds (Fig. 5), and with an 8 mm measurement spot these should produce an increase in sampling precision. Thus, the observed correlation, or rather its absence, must be linked to the type of inclusions. Structural-textural MGR-analysis[19] revealed that gravel-size grains represent grog consisting of crushed pottery made from the same plastic raw material as the vessel to which it was added. Figure 6 shows fragments of grog and clay lumps[20] which exhibit the same thermal behaviour after firing at 1150°C as the matrix of the analysed sherd. The results of thin-section studies also leave no doubt that the grog and clay lumps and the sherd represent the same ceramic body; in some samples some clay aggregates are also visible (Fig. 7). Figure 8 shows the precision of sampling for samples containing 30%[21] non-plastic inclusions of various grain sizes. Samples marked with diamonds are those in which only grains of 0.1–0.5 mm (red diamond) or 0.1–1.0 mm were observed; other samples also featured grains in very coarse sand fraction and gravel fraction (triangles). Inclusions of gravel-size grains do not significantly improve sampling precision (except when determining Mn and P contents); in this case it is the type of inclusions rather than their size which has the greatest impact on sampling precision.

19 For a description of this method see appendix.

20 Clay lumps = particles of the same clay as that used to make the ceramic body, clay aggregates = particles of a different clay than that used to make the ceramic body. Clay lumps may have resulted from the clay being inadequately broken down or they may represent fragments of crushed, unfired vessels (hence, actually clay and not grog), e.g. misshapen vessels or ones that became deformed during the drying process. Experiments have shown that the distinction between grog, clay lumps and unfired 'grog' is not always clear. In consequence, the authors often use the term 'grog/lump'.

21 Estimating the percentage of non-plastic components was based on the visual examination of sherds, using a binocular microscope at a maximum magnification of 10x and reference cards (AGI data sheets 1982).

The next procedure was multivariate cluster analysis[22] (using the average value from three measurements) investigating the concentration of elements usually taken into consideration by the authors in this type of analysis. Experience in the comparison of chemical data shows that two samples are identical (i.e. the differences are within the limits of precision) if they yield matching levels of all analysed and significant elements (e.g. not including phosphorus).[23] In this instance, cluster analysis was carried out using Euclidean distance and average linkage aggregative clustering of a distance, and logarithmic transformation of data; the elements used were: Si, Ti, Al, Fe, Mg, Ca, K, V, Cr, Rb, Sr, Y, Zr, Nb and Ba. Based on the results of this analysis and analysis of pXRF data using the finger method,[24] 170 samples were selected for MGR-analysis (abridged MGR-analysis). When this had been completed, MGR-groups were compared with chemical clusters and 103 samples were selected for chemical analysis by WD-XRF. Having obtained the results of chemical analysis by WD-XRF. Having obtained the results of chemical analysis by WD-XRF, a Student's t-test for paired data was performed for individual elements determined in 103 samples in order to verify at the 0.01 significance level the hypothesis that element concentrations determined by pXRF (on fresh fractures of air-dry samples) differ from those determined by WD-XRF. The results of the t-test confirm that the type of analytical technique used has a significant impact on determining the concentrations of individual elements, except for Fe and Cr. After these results further tests were undertaken.

The first test examined personal error. The results of the test revealed that this error had a very significant impact on the total precision of analysis. Comparisons were made of the average values of a given element, calculated using three measurements taken from identically prepared surface measurement spots (both individuals made a fresh fracture using the same tool), with measurements being performed in the same conditions. The individuals performing the measurements were not told that they were taking part in a test. Analysis results vary greatly for specific elements, with up to two-fold differences being noted in the concentrations of some of them (Al, Cl). However, in the case of Si, Ti, Fe, K, Rb and Zr average personal error was almost the same as average sampling error calculated for 446 samples. For the remaining elements, except Al and Ba, personal error was lower than average sampling error (Fig. 9). Figure 10 shows the differences in the average value of individual elements for two samples (the analysis results of one of the two people performing the measurements were normalised to 1 – red line in figure).

22 All multivariate clusters a*nalysis,* discriminant analysis and principal components analysis *were carried out using* the SYSTEM Package on licence from the *Weierstrass Institute for Applied Analysis and Stochastics, Leibniz Institute in Forschungsverbund Berlin e.V.*

23 This is the basis of provenance studies and is done by WD-XRF, NAA or ICP-MS yielding data on 25 to 30 elements with good precision (e.g. Schneider and Mommsen 2009). Multivariate cluster analysis based on fewer than about 15 elements may produce erroneous provenance groups.

24 Or 'by eye' as it is sometimes referred to.

Only the results of determining Sr content show minimal deviations; similar results were obtained by both individuals for Ti and Rb levels. In the case of two individuals, personal error was not a systematic error that can be corrected by a specific factor. This test revealed that measurements by pXRF are subject to greater personal error than, for example, preparations carried out in the laboratory for WD-XRF. It would be optimal to have one person performing all of the measurements for one project.

The precision of measurement of these two individuals was also tested. In this particular instance, an F-test revealed that there are no differences in variances between the precision of measurements (P = 99%) performed by these two individuals for most elements. Personal error only has a statistically significant impact in the determination of Si content, with a significance level of 0.05 in the case of Zr content (Fig. 11). Additional tests were carried out to assess the impact of personal error on the accuracy of analysis. Comparisons were made of the differences between results obtained by different individuals, the results obtained by WD-XRF for ignited samples (Fig. 12), and the results recalculated to a dry basis. There are quite significant differences in accuracy between individual measurements, though these are only statistically significant (P = 99%) in the determination of Si, Ti and Al levels (Fig. 11).

The precision and accuracy of different sample preparation methods were also tested. Analysis by pXRF was carried out on:

- fresh fractures,
- fresh fractures of samples refired at 900°C,
- fresh fractures of samples refired at 1000°C,
- cut surfaces,
- cut surfaces of samples refired at 900°C,
- cut surfaces of samples refired at 1000°C.

These tests revealed that measurements performed on cut surfaces yielded far better precision than on fresh fractures. The precision of measurements on fresh fractures improved when samples were ignited at 900°C before measurement; for measurements on cut surfaces the difference was much smaller (Fig. 12). It was examined whether these differences were statistically significant. The results are presented in Figure 13. The F-test tested the hypothesis that there are no differences in variances between measurements performed on differently prepared samples. In the case of the pottery analysed

for this project[25] there is a 99% probability that the difference in variances between measurements on original samples and samples ignited at 900°C is not statistically significant, which is applicable to measurements performed on fresh fractures as well as on cut surfaces. With samples ignited at 1000°C there is a 99% probability that the difference is not statistically significant for measurements performed on a cut surface, but for those performed on the surface of a fresh fracture it is significant for concentrations of Si, Al, Ca and K, as well as for Ti and Mn at a significance level of $\alpha = 0.05$. In contrast, comparing the results of measurements performed on fresh fractures and cut surfaces of original samples (air-dry) revealed that there were statistically significant differences (P = 99%) in determining Si, Ca and P contents, as well as Ti, Al, Fe and K contents, with P = 95%.

In order to assess the precision of measurement and eliminate problems associated with the variable geometry of samples, which are encountered when performing three measurements on three different spots, precision was also tested by measuring the same place every 30 minutes over a period of 8 hours (Tab. 1). The error of measurement for these 16 measurements is lower than the error for the average of three measurements per sample, except Mn. K. Cr, Zn, Rb, Nb and Pb, differences of less than 10% are noted only in the estimation of Al content, with differences of more than 100% being recorded for estimations of Mn, Cr, Rb and Nb contents. It means the results of this test show that the variable geometry of samples has a very strong influence on the precision of the determination of Si, Ca, P, V, Sr, Y and Zr and strong influence on the determination of Ti, Al and Fe contents. Precision of the determination of Mn, K, Cr, Zn, Rb, Nb and Pb contents is less connected with geometry of samples.

Of the total number of 447 ceramic sherds analysed by pXRF, 103 also underwent chemical analysis by WD-XRF (for the principles of selecting samples for analysis by WD-XRF – see below under the heading 'Results of down-up classification'), the results of which were used to test accuracy. The accuracy of analysis by pXRF on the surface of a fresh fracture (air-dry samples) was tested by comparison with the WD-XRF data. The results of WD-XRF, recalculated to a dry basis, were compared with the average from three pXRF measurements taken on various spots. The average relative difference for results obtained using these two techniques is less than 5% for Fe and Rb content and in the range of 5–10% for levels of Ti, K, Cr, Zn, Sr and Nb. Large differences were noted in the accuracy of analysis among individual samples, for example the accuracy of determining Cr content ranged from less than 1% to 25% (Fig. 14). The number of samples for which individual elements were determined with an accuracy worse than 10% ranges from 98 samples in the case of Si to two samples in the case of Fe (Fig. 15).

25 It must be stressed that these are not general conclusions valid for all types of pottery; they are only valid conclusions for the pottery examined as part of this project.

Figure 16 shows the minimum and maximum accuracy of pXRF analysis (n = 103), as well as the minimum and maximum precision of averages calculated from the standard deviation for each of the three measurements (cv% of precision of three measurements divided by √3; n = 446). This collated data reveals that maximum values are below 20% for only five elements: Ti, Fe, K, Zn and Rb. The number of samples with accuracy worse than 10% was lowest for the determination of Fe content and highest for Si, Al, P, V and P (over 90% of all samples). The number of samples for which the concentrations of four elements (Ti, Fe, K, Rb) were determined with accuracy and precision of averages worse than 10% does not exceed 18% of all samples (Fig. 15).

Comparing the impact of various sample preparation methods on the accuracy of pXRF analysis results revealed a much greater error when measurements were performed on the surface of a fresh fracture rather than on a cut surface. Moreover, the accuracy of analysis is considerably improved by performing measurements on ignited samples. The elements most sensitive to differences in the preparation of samples for analysis by pXRF are: Si, Ti, Al, Fe, Mn, Zr, Nb and Pb. The results of an F-test showed that statistically significant differences (P = 99%) affected a small number of elements: Si, Al, Zr, Nb and Pb. This relates to comparisons made between the results obtained from pXRF measurements and the results of analysis by WD-XRF recalculated to dry basis. When comparing the results of analysis carried out on samples after loss on ignition, as expected, the differences between variances increased (Fig. 17).

Regardless of special tests, standard procedure involves assessing the accuracy of measurement by measuring reference samples. A very fine ware ceramic cylindrical briquette (φ = 2 cm, h = 0.5 cm) with parallel flat bases is used as a monitor sample for routine measurements. The measurements are performed on one of the polished base surfaces of the cylinder, positioning the sample centrally in the measurement window. A measurement is taken at the beginning and the end of each measurement session, and additional measurements are made if the session lasts for several hours. Table 2 presents the average of the results of 147 measurements performed on the monitor sample from March 2013 to November 2015. Measurement repeatability by pXRF is too poor compared to the acceptable by authors range for WD-XRF measurements, except for the determination of Fe, Ca, K, Rb, Sr and Zr contents, but the accuracy[26] is acceptable for most elements except Al, Mn, Ca, Mg, V, Ni, Zn, Ce and Pb. Of the 147 measurements, Mg content was only determined in five instances (in WD-XRF measurements MgO = 2.9%), Ni content in 33 instances (in WD-XRF – 71 ppm) and Ce content in 22 instances (in WD-XRF – 82 ppm).

26 The average of 147 measurements performed using pXRF on the monitor sample was compared with WD-XRF data for this sample recalculated to dry basis.

The results of the tests revealed that in the case of the project on 'pottery from the Banat region' it is sufficient to limit pXRF analysis to measurements performed on the surface of fresh fractures of air-dry samples. The impact of time-consuming processes such as the preparation of a smooth cut surface and ignition of samples in order to improve precision and accuracy of analysis is only statistically significant in determining the concentrations of very few elements (Si, Al, Ca, P). However, this impact is not significant enough to warrant the use of these procedures in routine measurements of pottery from the Banat region because even if they are performed they will not yield results which are sufficiently precise and accurate to use them as the basis for defining reference groups and making inferences about provenance. A significant obstacle to using pXRF measurements in provenance studies is the fact that determining concentrations of Mg, Ni and Ce is problematic and Na content is not determined at all. Imprecisely determining Mg content and not determining Na content may lead to significant errors in establishing provenance.[27] In view of the fact the Na (and mostly also Mg) content of the sample is not determined and because the original sum of the major elements in pXRF measurements is usually less than 90%, the authors contend that the content of major elements should not be normalised to a constant sum of 100%.

In measurements performed by pXRF the authors accepted: average accuracy < 10% for major and trace elements, average precision better than 5% for major elements and average precision of up to 10% for important trace elements and not lower than 20% for other trace elements.

By accepting these criteria for pottery fragments from the Banat region it was found that measurements on fresh fractures (air-dry samples) allowed levels of

- Ti, Fe, K, Cr, Zn, Rb, Sr and Nb to be determined with good average accuracy and good average precision;
- Ca, Zr and Ba to be determined with good average precision, but not so good accuracy;
- Si and Y to be determined with good average precision and poor accuracy;
- Al to be determined with good average precision and very poor accuracy;
- Mn, P and Pb to be determined with poor average precision and poor accuracy.

27 See for example Daszkiewicz, Dyczek, et al. 2007.

It should be emphasised that average accuracy was better than 10% for eight of the elements listed above, but maximum values of accuracy, except for Fe, fell to 15%–20%, falling to over 20% for Cr, Sr and Nb.[28]

No element concentration was determined with a precision (average coefficient of variation) better than 2% as is the case for analysis carried out by the authors using WD-XRF for major elements (except Na). Trace element concentrations of V, Cr, Ni, Zn, Rb, Sr, Y, Zr, and Ba were determined by WD-XRF with long-term precision (measurement and preparation) ranging up to 3%, and for Nb, Cu and Ce up to 6% (for trace elements at very low concentrations it may rise up to 15–20%, and up to 30% for Th).

4 Results of down-up classification

The next stage of the study focused on pottery sherds from Corneşti-Iarcuri. One hundred fragments of Middle Bronze Age pottery from this site were submitted for analysis (50 samples each from Ring I and Ring II) together with 53 ceramic sherds dated to the Late Bronze Age (23 samples from Ring I and 30 from Ring II). Comprehensive analysis was carried out on all 153 ceramic fragments using a *down-up* classification strategy in which selection for laboratory analysis was not only based on macroscopic examination of fabrics (as had been the practice hitherto) but also on the results of chemical analysis by pXRF (Fig. 18). The results of these analyses were used as the basis for selecting 76 pottery fragments for MGR-analysis. The thermal behaviour of each sample refired at three temperatures (1100°C, 1150°C and 1200°C) was taken into account when defining different MGR-groups. Definitive classification was based on thermal behaviour at 1200°C. Figure 19 shows examples of various MGR-groups. If samples display the same appearance (e.g. in figure 19 samples MD540 and MD620 have an over-fired[29] matrix type, samples MD542 and MD544 have an over-melted[30] matrix type), colour and shade after refiring at 1200°C this indicates that they were made using the same plastic raw material. All ceramic samples belonging to the same MGR-group were made of the same clay – a non-calcareous clay coloured by iron compounds. MGR-analysis results enabled 36 groups to be defined; they represent groups of greatest similarity in the plastic material used. These groups can be combined into major MGR-groups based on similarities in thermal behaviour. It is interesting that none of the Middle Bronze Age (MBA) sherds

28 The accuracy of WD-XRF analysis carried out by the authors is tested by analysing international reference samples and by exchange of samples with other laboratories; for major elements, except Na, it is below 5%. For sodium and most trace elements it is between 5 and 10 relative per cent, and up to 30% for Nb, La, Ce, Th and Pb

29 Over-fired (ovF): the sample changes in shape, bloating, however, does not occur nor does the surface of the sample become over-melted.

30 The surface of the sample becomes over-melted and its edges slightly rounded.

belong to the same MGR-group as the Late Bronze Age (LBA) pottery. In the case of both periods, pottery found in Ring I was made from a different clay than that found in Ring II. Only MBA pottery has two MGR-groups represented both in Ring I and in Ring II (Fig. 20). Most MGR-groups are represented by just one ceramic fragment (the term 'group' is used even when groups are each represented by only a single sample[31]); the most numerously represented are MGR-groups 3, 7 and 14. Macroscopic examination of samples before and after refiring indicates different recipes (formula = matrix in vol.% / non-plastic ingredients in vol.%) but the same type of non-plastic ingredients – no intentional mineral or organic temper is observed, only clay lumps/aggregates or grog of the same composition as the sherd (with isolated examples of grog of a different composition). Therefore, samples which belong to the same MGR-group ought to have the same chemical composition (Fig. 19).

After classification based on the results of MGR-analysis, 60 samples were chosen for chemical analysis by WD-XRF (it is important to emphasise that individual MGR-groups can only be sorted into groups of the same geochemical parameters on condition that chemical analysis is carried out with good precision and accuracy). The table in figure 19 presents the results of chemical analysis by WD-XRF for the refired samples shown in that figure. Samples attributed to the same MGR-group (MGR-groups 3 and 7) differ only negligibly in their chemical composition.

In Figure 21 MGR-groups have been grouped by similarity in chemical composition: MGR-groups with the same geochemical characteristics are framed in violet (major MGR-groups 101 and 102). Pottery fragments belonging to these MGR-groups can be deemed to represent local wares produced on-site. It is not only the quantity of these sherds (70% of all samples subjected to MGR-analysis) which suggests that they represent local pottery, but also their similarity to clays sampled from the immediate vicinity of the site at Corneşti-Iarcuri.[32] Four samples attributed to different MGR-groups (framed in green, Fig. 21) most probably represent pottery made at regional workshops or locally at Corneşti-Iarcuri using different clays than those used in mainstream pottery production.

Sherds attributed to major MGR-group 201, characterised by higher concentrations of Al, Fe, V, Cr, Zn and Rb and much lower levels of Si and Zr than noted in the local ware group, were identified as regional wares. The term 'regional wares' is warranted by the fact that sherds of similar chemical composition have also been found at other LBA sites (Timişoara-Fratelia, Deta-Dudarie, Giroc-Mezcal, Hodoni Pusta, Peciu Nou,

31 It is unlikely that only a single vessel was made from one ceramic body, hence it is assumed that the sample submitted by archaeologists for analysis represents a group of vessels made from the same material. It is for this reason that the term 'group' is used even in relation to those groups which are represented solely by one sample.

32 A total of 43 raw materials were sampled; analysis is ongoing.

Voiteni-Voitec). Ceramic fragments attributed to this group at Corneşti-Iarcuri were only noted in the LBA horizon; there were none among the MBA pottery discovered at Corneşti-Iarcuri or the MBA pottery found at Corneşti-Cornet. Only one sample of similar geochemical characteristics was found in the MBA horizon at Corneşti-Iarcuri, but this sample belonged to major MGR-Group 202. Five samples representing different MGR-groups were classified as extra-regional wares (e.g. Fig. 21, sample MD553).

Table 3 presents the results of chemical analysis by WD-XRF of samples attributed to major MGR-groups 101 and 102. The chemical composition of these groups differs only negligibly; the greatest difference is in Ca content (average concentration: 1.89% and 2.23% respectively), but this is an element for which the cv% also amounts to 23.4 and 29.6 respectively. Large differences in Mn and P levels are also noted (the presence of P in the sherd is linked to the alteration effect; there is a less than 0.5% content of this element in the local clay). The major MGR-groups 101 and 102 can jointly be considered as the reference group for local wares produced on-site at Corneşti-Iarcuri because the compositional variation between these groups is smaller than the differences within each group.

The five samples representing major MGR-groups 301, 401, 501 and 601[33] were most probably made within the region.

The dendrogram shown in Figure 22 represents the results of multivariate cluster analysis based on the results of chemical analysis by WD-XRF. Analysis was done using Euclidean distance and average linkage aggregative clustering of a distance, logarithmic transformation of data, and the elements used were: Si, Ti, Al, Fe, Mn, Mg, Ca, Na, K, V, Cr, Ni, Zn, Rb, Sr, Y, Zr and Nb. The groups generated by this analysis are consistent with the major MGR-groups, with the exception of samples attributed to major MGR-group Imp5 (sample MD605). This sample belongs to the same cluster as the regional wares (major MGR-group 201), hence to a cluster comprising samples with a low Zr content in comparison with other samples; however, it differs from these samples in its thermal behaviour and it is characterised by much lower levels of Ti, Al, Fe, Cr and Zr. Figure 23a shows the results of PCA (the same elements were used as in the dendrogram), which also corroborate the close correlation between MGR-groups and chemical composition. In PCA, sample MD605 is isolated and does not fall into any group.

An assessment of physical ceramic properties (open porosity, water absorption and apparent density) was carried out on the same sherds that had undergone MGR-analysis. The open porosity value for most samples ranges from 25% to 35% (with four exceptions

33 In the case of the sample attributed to MGR-group 601, refiring could only be carried out on the powder left after this sample had been prepared for chemical analysis, therefore, this group has been omitted from the table in figure 20, while in the dendrograms shown in Figures 22, 25 and 26 the number of this MGR-group is shown in italics.

below and one above these values). There is no correlation between these results and either dating or chemical groups (Fig. 24).

Next, twelve samples were selected for further analyses (analyses listed in Figure 18) in order to determine their original firing temperature (Teq[34]). These samples had originally been fired at 700–800°C or 800–900°C. Two of the twelve analysed samples had been exposed briefly to a higher temperature, i.e. the outer portion of the vessel wall shows evidence of having been exposed to a higher temperature than the middle and inner portions (this could be linked both to the original firing process and to secondary contact with fire). In one sample this effect is also observed on the inner part of the vessel wall. The grey areas visible in fresh fracture are related to unburnt organic matter (this is indicated by the results of TG-DTG-DTA analysis – an exothermic peak can be seen which is associated with a loss of mass within the temperature range for the combustion of organic matter).

After the 'down' part of the down-up strategy had been completed for pottery sherds from Corneşti-Iarcuri, work began on the 'up' part. In this instance, as well as selecting the diagnostic parameters of macroscopic fabric descriptions that correlated best with the results of laboratory analysis, the correlation between clusters arising from the results of pXRF and WD-XRF was also assessed. To this end multivariate cluster analysis was carried out on 60 samples which had undergone chemical analysis both by pXRF and by WD-XRF. All cluster analyses were performed using Euclidean distance and average linkage aggregative clustering of a distance, logarithmic transformation of data; the results of analysis by WD-XRF were recalculated to dry basis. Figure 25 shows a dendrogram of elements whose concentrations were determined using both techniques (elements used: Si, Ti, Al, Fe, Mn, Ca, K, V, Cr, Zn, Rb, Sr, Y, Zr and Nb). In this case, as predicted, clusters are related to the technique used. The only exceptions are samples of pottery identified as extra-regional groups Imp 1, 3 and 4 (Fig. 25, third cluster, marked in grey) and extra-regional samples from group Imp 2 (last two clusters, Fig. 25). Next, multivariate cluster analysis was performed using only elements which, based on test results, were deemed to have been determined by pXRF with good average accuracy and good average precision (Ti, Fe, K, Cr, Zn, Rb, Sr and Nb) as well as Zr, which was determined with good average precision, but not so good accuracy. Zr was included because of the significant differences in its content between local groups and the regional group. The difference in Zr content between these groups is much greater than 2 sigma level. As can be seen in Figure 26, when elements which were well-determined by pXRF are used, there is no observable division into clusters associated with the technique used for the analysis. Extra-regional wares are, as previously, well distinguished by pXRF. In the case of local and regional wares, these samples are separated into large clusters

34 Teq = equivalent original firing temperature.

regardless of the determination technique. However, a division into results produced by pXRF and WD-XRF are still visible within these clusters. This means that applying multivariate cluster analysis to data obtained by pXRF using elements determined with good average accuracy and good average precision can identify major groups and can very clearly distinguish samples with a markedly different chemical composition. PCA performed on the pXRF results using the same good determined elements also shows the same general divisions as for WD-XRF (Figs. 23a and 23b).

However, cluster analysis (the results of which are shown in the form of a dendrogram in Fig. 26), shows that the results of analysis by pXRF and WD-XRF for individual samples are not always side-by-side. Table 4 shows examples of analysis results for samples that appear side-by-side in the dendrogram (MD541) and for remote samples – sample MD573 features in the first cluster (yellow) according to data obtained by pXRF and in cluster 2 (green) according to data obtained by WD-XRF. Comparison of individual samples from Cornești-Iarcuri is subject to an error of 13.3% (which falls within the error range described by Berendt et al.[35]). This applies to multivariate cluster analysis performed using elements determined by pXRF with good precision and accuracy.

Because the first stage of analysis in the *down* part of the classification of 447 ceramic sherds consisted of chemical composition analysis by pXRF, all of the groups defined based on this analysis had to be verified in the *up* part of the classification. The first assessment of analysis results obtained by pXRF examined a group of sherds distinguished by having higher levels of Y than noted in other samples. Figure 27 shows the results of analysis by pXRF (triangles) and by WD-XRF (rectangles), Y versus Zr content and Y versus Rb content. In both instances, three groups can be seen in the pXRF results: local, regional and a group of samples with a higher concentration of Y. This last group does not exist in the results obtained using the WD-XRF technique. This group is visible not only in bivariate diagrams, but also in PCA if Y content is also taken into consideration as well as elements determined with good precision and good accuracy (Fig. 28). The Y-group only exists in the results of analysis by pXRF. The Y content of these samples determined by WD-XRF does not deviate from the Y content of the remaining samples. Figure 29 shows bivariate diagrams of Fe versus Cr, Ti, Zn, Rb, K and Zr. Only the local group and the regional group of wares can be seen in each of these diagrams. When using chemical composition analysis by pXRF as the basis for classification in a down-up strategy, it is important to remember that the initial clusters must be verified in the 'up' part of the classification using only well-determined elements (which do not have to be the same for each project, as demonstrated by the analyses carried out by the authors).

Results obtained by pXRF using elements determined with good average precision (Ti, Fe, K, Cr, Zn, Rb, Sr, Zr and Nb) for all 446 samples were the subject of multivari-

35 Behrendt, Mielke, and Mecking 2012.

ate cluster analysis, PCA and bivariate diagrams. Figure 30 shows Zr content versus K content (as K_2O). The group of samples representing pottery with a regional distribution (wares noted at sites in Corneşti-Iarcuri, Timişoara-Fratelia, Deta-Dudarie, Giroc-Mezcal, Hodoni Pusta, Peciu Nou and Voiteni-Voitec) is clearly distinguishable. In the case of local pottery, there is an evident tendency associated with the location of these sites. Further analysis of pottery and raw materials from these sites is ongoing.

5 Conclusions concerning analysis by pXRF

Tests revealed that chemical composition analysis using the pXRF technique yields very good results when integrated with a *down-up* classification strategy. Using MGR-analysis should be preceded by classification based on chemical composition analysis using the pXRF technique. However, a small pilot series should first be carried out to establish which elements in the given project are determined with good precision and accuracy. Checks should also be made to assess whether the size, number and type of non-plastic inclusions in the sherd mean that performing this type of analysis would be subject to a large error (e.g. the 45% error described by Berendt et al.,[36] which could result in practically every other pottery fragment being incorrectly classified).

Using pXRF to determine chemical composition of pottery from the Banat region enables pottery to be grouped in the same major clusters as WD-XRF (but only elements determined with good precision and accuracy should be taken into account when defining groups); however, it should be emphasised that pXRF results cannot be used to define the composition of reference groups on which precise provenance analysis is based.

Tests conducted on samples from the Banat region show that pXRF measurements do not have to be performed on cut surfaces or on ignited samples; measurements taken on the surface of a fresh fracture of an air-dry sample are sufficient.

It is important to take personal error into consideration, hence to limit, if possible, the number of individuals performing measurements (personal error is much greater in measurements by pXRF than it is in analysis by WD-XRF).

6 Conclusions concerning pottery from the Banat region

It was confirmed that pottery made at a single production centre was present at sites in Timişoara-Fratelia, Deta-Dudarie, Giroc-Mezcal, Hodoni Pusta, Peciu Nou, Voiteni-

36 Behrendt, Mielke, and Mecking 2012.

Voitec and Corneşti-Iarcuri.

Each site features pottery which does not appear at any of the other sites – local wares made at the given site.

At Corneşti-Iarcuri MBA and LBA pottery is characterised by the same technology, but there is no continuity in raw material use. Local wares produced on-site, regional wares and single products probably from outside the region were all represented at this site.

7 Description of methods used

7.1 MGR-analysis

Four thin slices were cut from each sample in a plane at right angles to the vessel's main axis. One of these sections was left as an indicator of the sample's original appearance, whilst the remaining three were refired, each one at a different temperature, in a Carbolite electric laboratory resistance furnace using the standard procedure. Firing was carried out at the following temperatures: 1100°, 1150° and 1200°C in air, static (this means without air flow), at a heating rate of 200°C/h and a soaking time of 1h at the peak temperature, and cooled at a cooling rate of 5°C/min to 500°C, followed by cooling with the kiln for 1 hour. They were subsequently removed from the kiln and left to continue cooling until they reached room temperature. The fragments were then glued on to paper and a photograph was taken with a macro lens for each slice.

7.2 Textural-structural MGR-analysis

One thin slice was cut from each sample in a plane at right angles to the vessel's main axis. Each slice was photographed using reflected light microscopy and then refired at the following temperatures: 400, 600, 700, 800, 900, 1000, 1100, 1150 and 1200°C. Firing conditions were the same as those earlier described for MGR-analysis. The fragment was photographed (focusing on the same spot on the sample's surface) after each refiring.

7.3 Chemical analysis

In this instance, chemical analysis by WD-XRF (Wavelength-dispersive X-ray fluorescence) was used to determine the content of major elements, including phosphorus and a rough estimation of sulphur and chlorine. Total iron was calculated as Fe_2O_3. Samples were prepared by pulverising fragments weighing *c.* 2g (sample size was determined by the number and size of the non-plastic components), having first removed

their surfaces and cleaned the remaining fragments with distilled water in an ultrasonic device. The resulting powders were ignited at 900°C (heating rate 200°C/h, soaking time 1h), melted with a lithium-borate mixture (Merck Spectromelt A12) and cast into small discs for measurement. This data is, therefore, valid for ignited samples but, with the ignition losses given, may be recalculated to a dry basis. Major elements are calculated as oxides. For easier comparison these are normalised to a constant sum of 100%. The precision of analysis for major elements is below 2%, this rise to a maximum of 6% for sodium and trace elements (for very low contents it rises up 20%). Accuracy was tested by analysing international reference samples and by exchange of samples with other laboratories. For major elements in standard reference samples the maximal deviation mostly is below 5% and for sodium and trace elements (except La, Ce, Nb, Pb, Th) below 10%. Accuracy was tested by analysing international reference samples and by exchange of samples with other laboratories. For major elements in standard reference samples the maximal deviation mostly is below 5% and for sodium and trace elements (except La, Ce, Nb, Pb) below 10%.

Preparation of samples for analysis was carried out by M. Daszkiewicz in ARCHEA, measurement using a PANnalytical AXIOS XRF-spectrometer and the calibration of Arbeitsgruppe Archaeometrie by Gerwulf Schneider (Freie Universität Berlin) and Anja Schleicher (Helmholtz-Zentrum Potsdam, Deutsches Geo-ForschungsZentrum GFZ, Sektion 4.2, Anorganische und Isotopengeochemie).

7.4 Thin-sections

Thin-sections were studied under a polarising microscope to provide some information on the matrix (the amount of information gleaned being dictated by the resolution of the microscope), primarily to estimate the composition and distribution of non-plastic inclusions.

7.5 Physical ceramic properties

Physical ceramic properties (apparent density, open porosity, water absorption) estimated by hydrostatic weighing can be carried out on original pottery fragments. Individual values were calculated using one of three measurements: mass of sample immersed in water, mass of moist sample weighed in air, mass of dry sample.

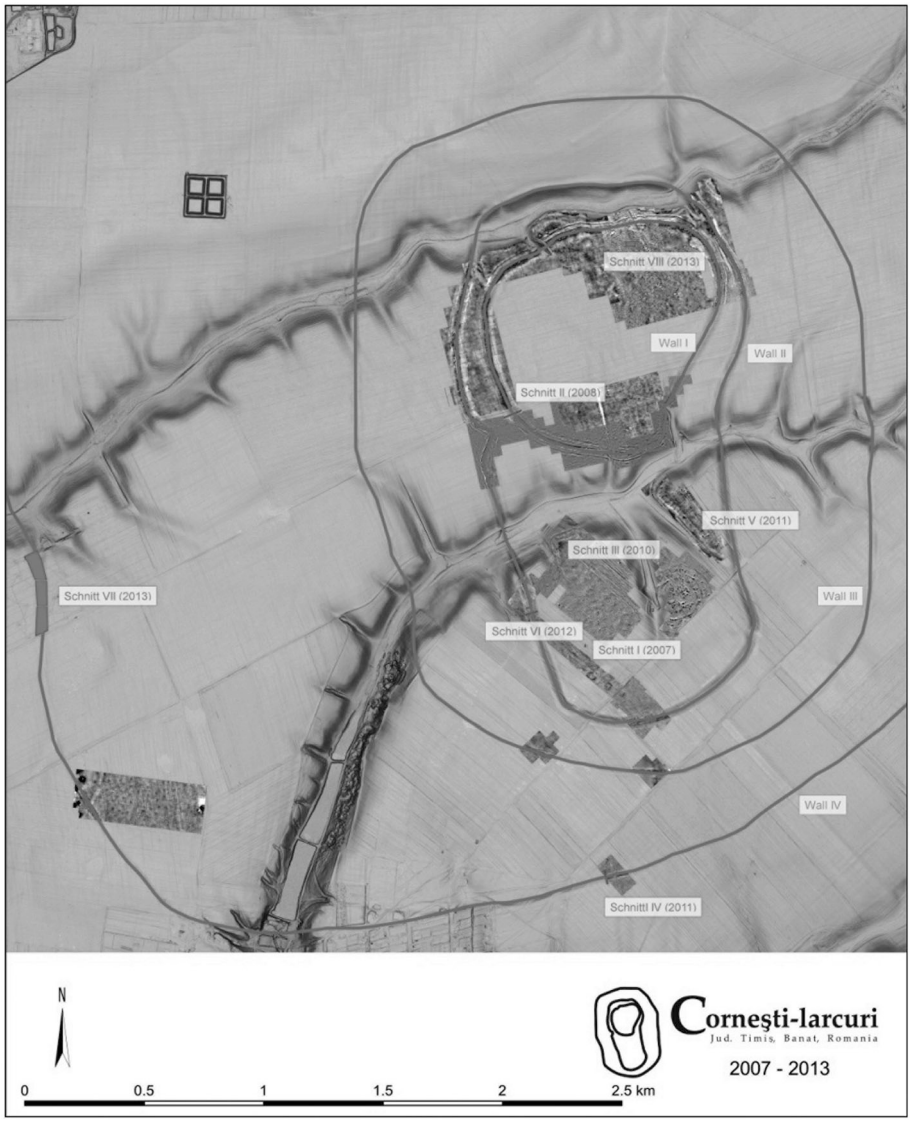

Fig. 1 Corneşti-Iarcuri, four earth-filled wooden ramparts with a total length of more than 33 km, encompassing an area of over 17 km^2.

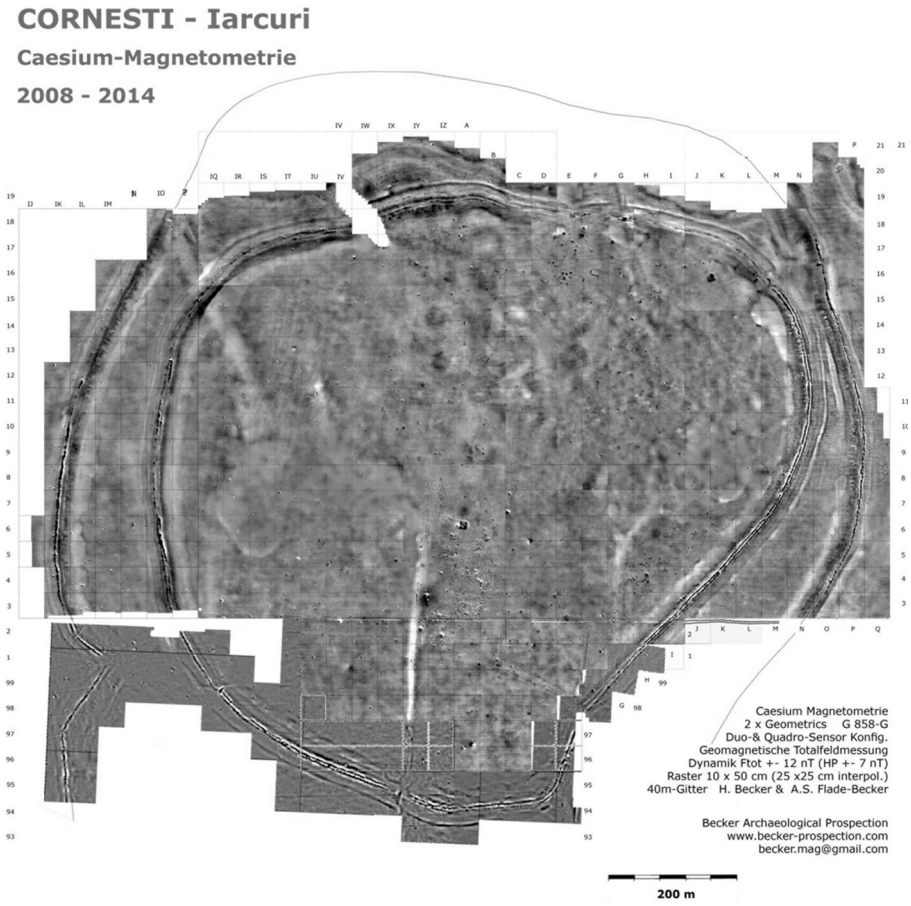

Fig. 2 Cornești-Iarcuri, area covered by magnetic survey and systematic field walking.

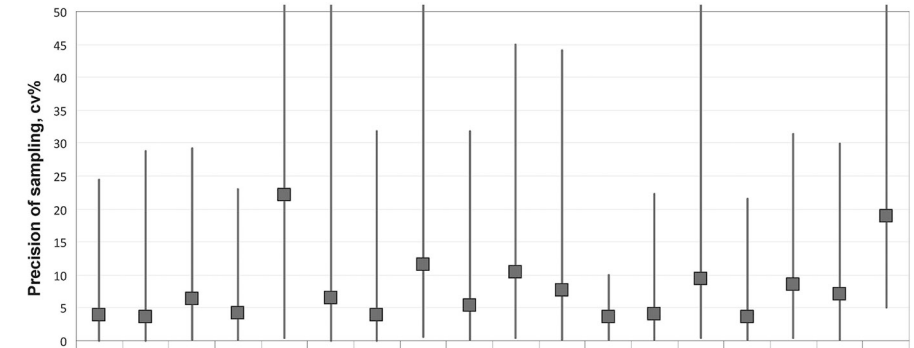

	SiO_2	TiO_2	Al_2O_3	Fe_2O_3	MnO	CaO	K_2O	P_2O_5	V	Cr	Zn	Rb	Sr	Y	Zr	Nb	Ba	Pb
max	24.4	28.7	29.2	23.0	175.1	85.5	31.8	76.7	31.8	44.9	44.1	9.9	22.2	64.4	21.5	31.3	29.9	65.4
min	0.02	0.07	0.11	0.15	0.37	0.07	0.02	0.57	0.20	0.40	0.20	0.20	0.20	0.50	0.10	0.40	0.10	5.00
average	3.8	3.6	6.4	4.2	22.1	6.6	3.8	11.6	5.4	10.4	7.6	3.6	4.0	9.4	3.6	8.6	7.1	19.0

Fig. 3 Sampling precision (analysis by pXRF). The minimum, maximum and average value of the coefficient of variation (cv%) calculated for individual samples (n = 446) from measurements taken on three different spots on the surface of a fresh fracture.

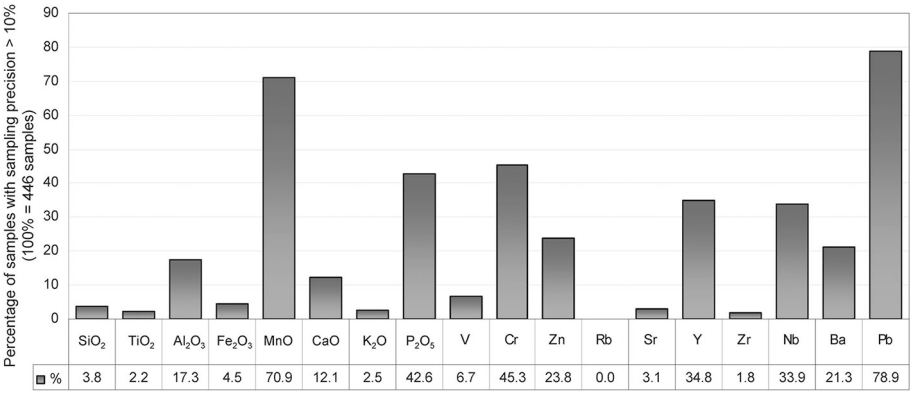

	SiO_2	TiO_2	Al_2O_3	Fe_2O_3	MnO	CaO	K_2O	P_2O_5	V	Cr	Zn	Rb	Sr	Y	Zr	Nb	Ba	Pb
%	3.8	2.2	17.3	4.5	70.9	12.1	2.5	42.6	6.7	45.3	23.8	0.0	3.1	34.8	1.8	33.9	21.3	78.9

Fig. 4 The percentage of samples in which sampling precision (analysis by pXRF) for individual elements was greater than 10%.

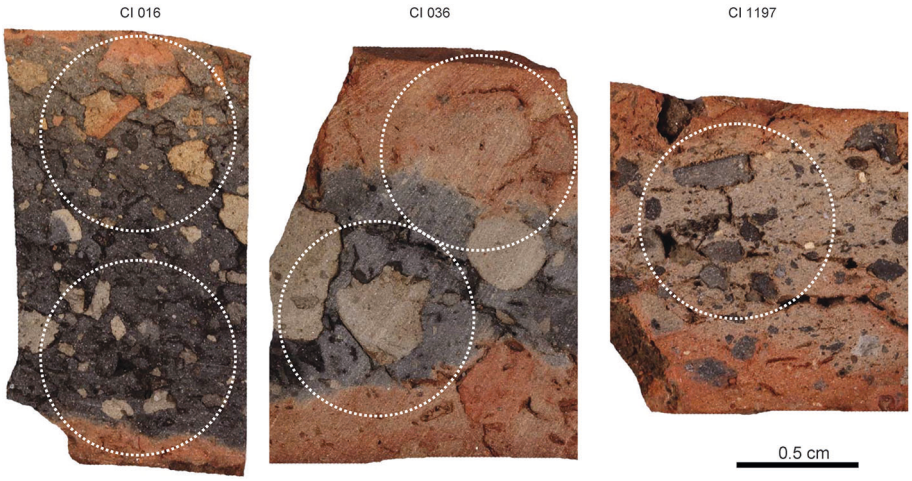

Fig. 5 Pottery fragments found in Cornești-Iarcuri. Cut-sections: grains of coarse-sand size and gravel size are macroscopically visible in the matrix. The dashed line delineates an 8 mm measurement spot used in pXRF analysis.

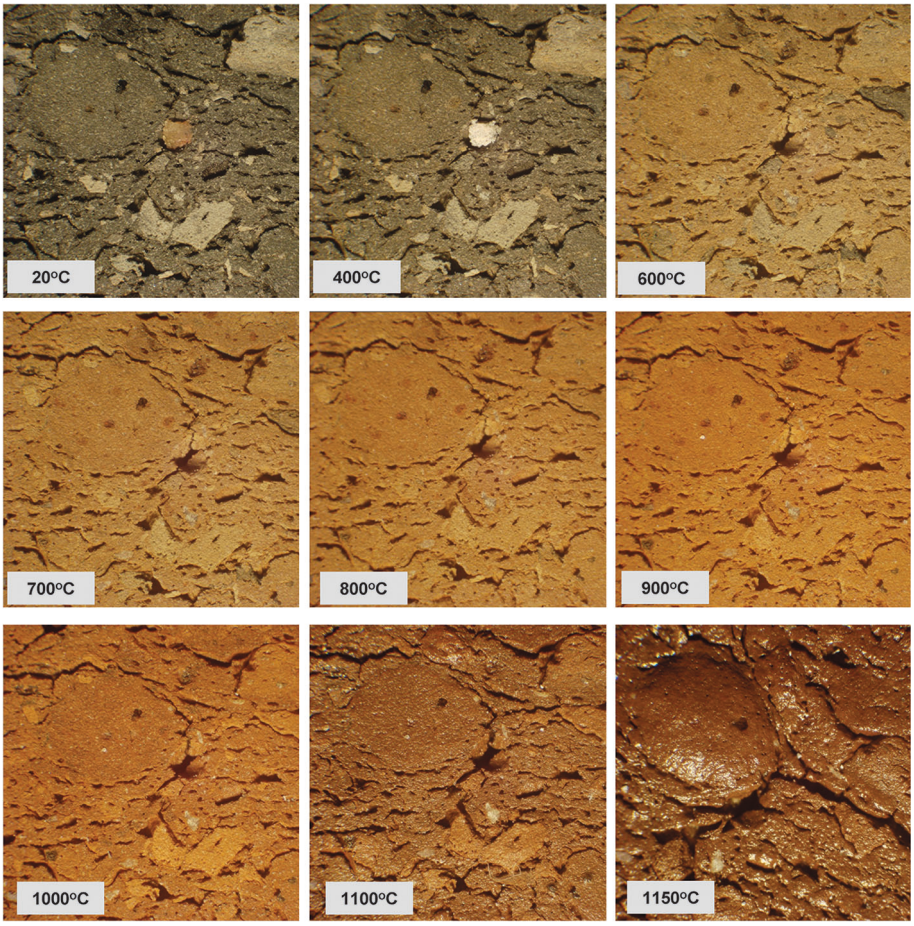

Fig. 6 Pottery fragment found in Cornești-Iarcuri (CI1193). Results of structural-textural MGR-analysis. Fragments of grog and clay lumps exhibit the same thermal behaviour after firing at 1150°C as the matrix of the analysed sherd.

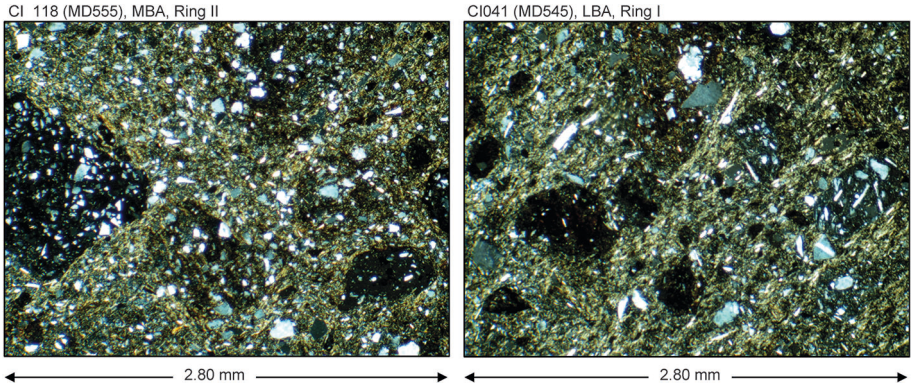

Fig. 7 Pottery fragments found in Cornești-Iarcuri (CI041, MD545). Grog, clay lumps and clay aggregates visible in the matrix. Thin-section, microphotos, XPL.

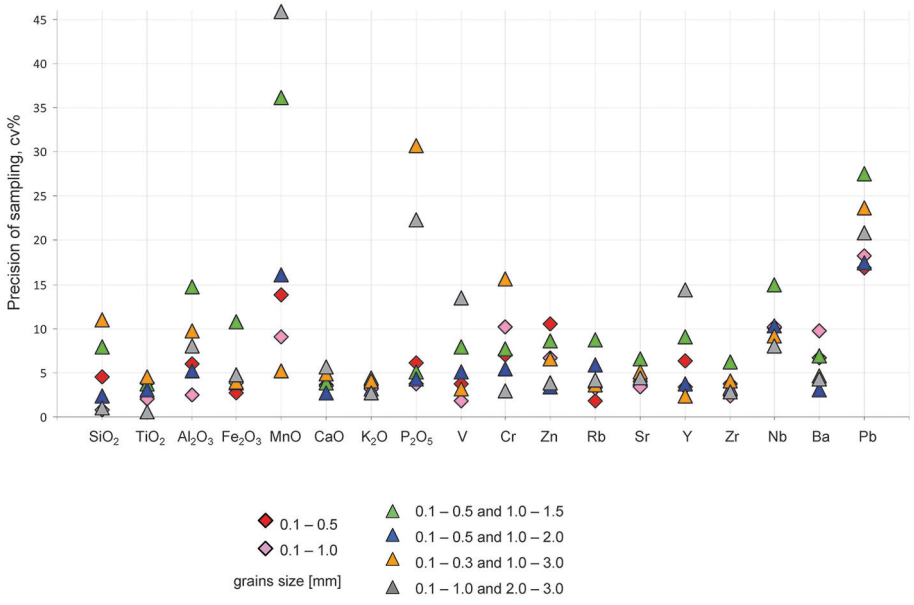

Fig. 8 Sampling precision, analysis by pXRF, averages of coefficients of variation (calculated as averages from cv for three measurements per sample) for samples containing 30% non-plastic inclusions of various grain sizes.

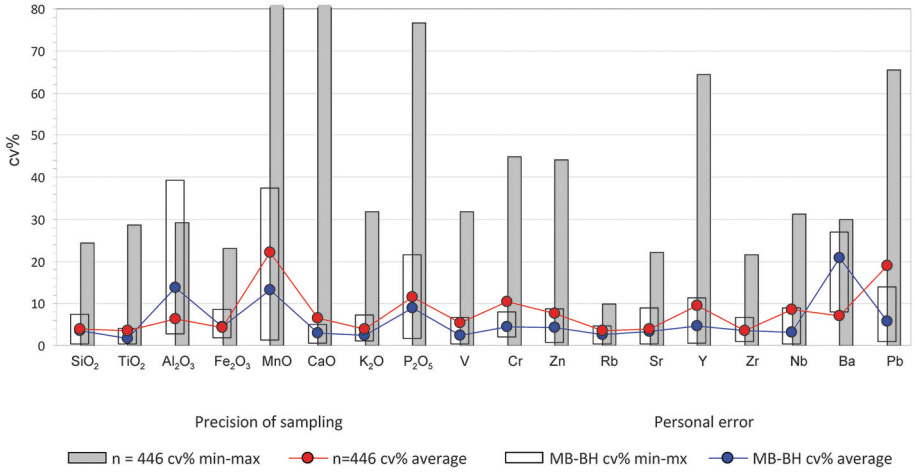

Fig. 9 Personal error and sampling error, minimum, maximum and average cv%. Except for Al and Ba, average personal error is lower than average sampling error.

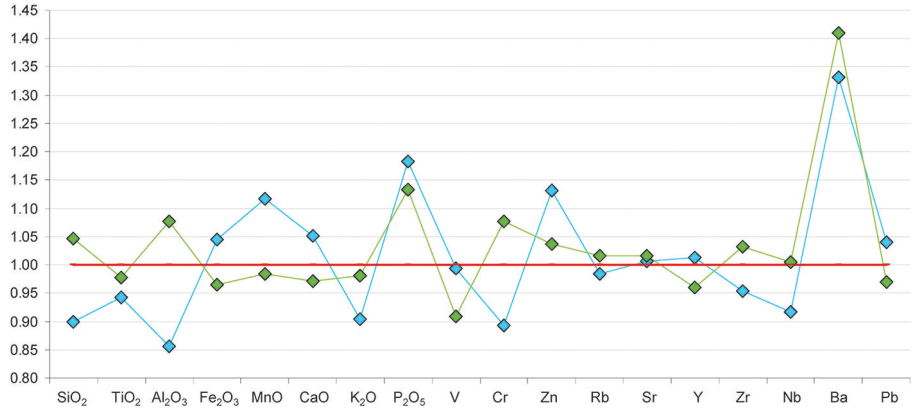

Fig. 10 Example of personal error. The differences in the average value of individual elements for two samples measured by pXRF by two persons. The results of one person's measurements were normalised to 1 (red line) and compared with the results of measurements performed by the other person (squares).

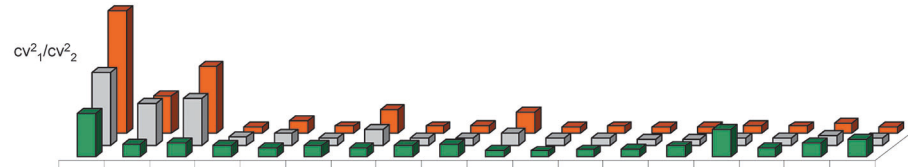

	SiO_2	TiO_2	Al_2O_3	Fe_2O_3	MnO	CaO	K_2O	P_2O_5	V	Cr	Zn	Rb	Sr	Y	Zr	Nb	Ba	Pb
prec.	7.5	2.2	2.3	1.9	1.6	1.9	1.5	2.0	2.2	1.1	1.0	1.2	1.3	1.8	4.6	1.5	2.3	3.0
-l.o.i.	12.4	7.2	8.0	1.4	1.9	1.2	2.8	1.2	1.3	2.0	1.2	1.1	1.0	1.1	1.2	1.3	1.6	1.1
+l.o.i.	30.4	6.3	11.4	1.2	2.1	1.2	4.1	1.2	1.3	3.5	1.0	1.2	1.0	1.2	1.3	1.2	1.6	1.1

Fig. 11 F-test results. Statistical significance of personal error: differences in the precision of sampling and accuracy were tested for pXRF measurements performed by two persons: precision of sampling (green bars) and accuracy calculated as the difference in pXRF results in relation to the results of chemical analysis using the WD-XRF technique on ignited samples (grey bars, -l.o.i) and results recalculated to dry basis (red bars, +l.o.i.).

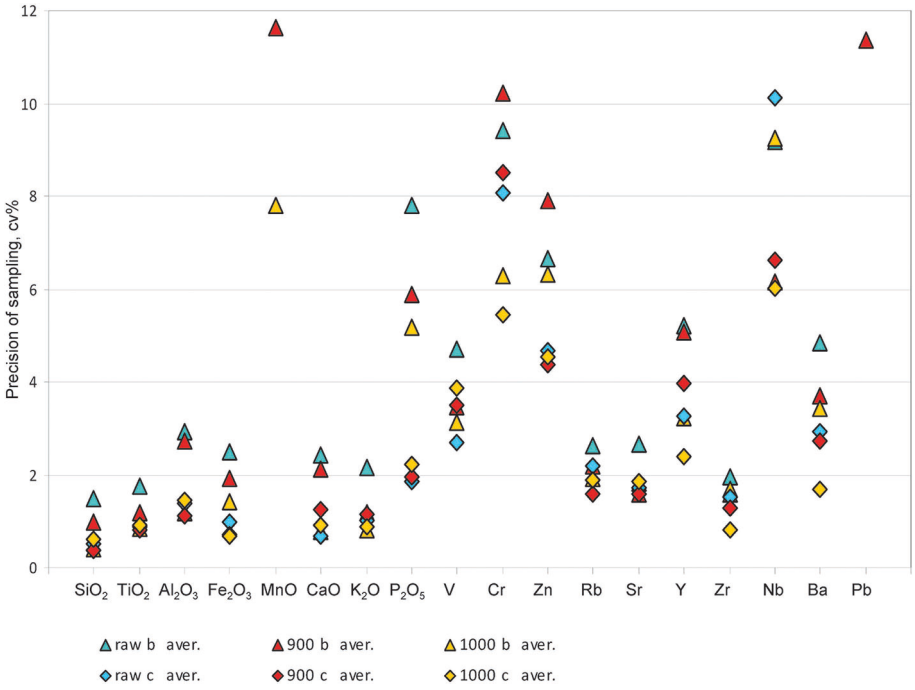

Fig. 12 Preparation error. Differences in average precision associated with measurements taken by pXRF on variously prepared samples. raw = original air-dry sample, b = fresh fracture, c = cut surface, 900 = sample refired at 900°C, 1000 = sample refired at 1000°C. All elements were determined with poorer precision when measurements were taken on fresh fracture surfaces.

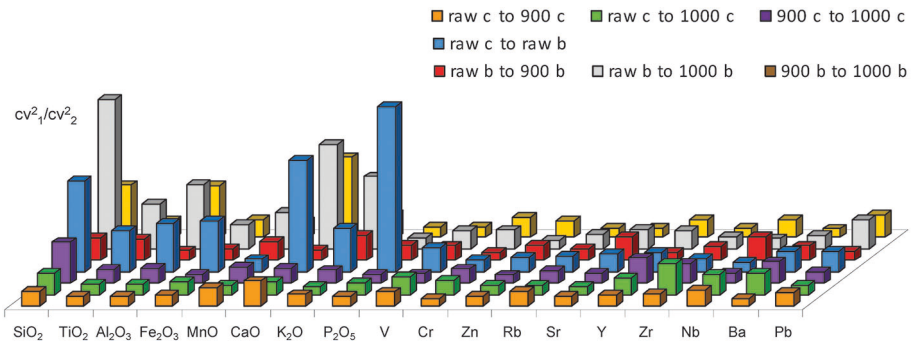

Fig. 13 Preparation error, results of F-test. Test of significance of the difference in results of measurements performed by pXRF on fresh fracture surfaces (b) and on saw-cut surfaces cut (c) of air-dry samples (raw) and samples ignited at 900°C (900) and 1000°C (1000).

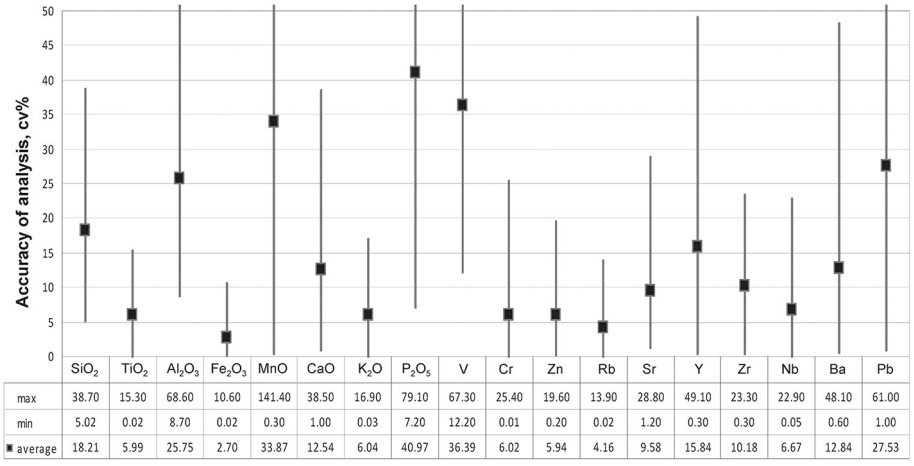

	SiO_2	TiO_2	Al_2O_3	Fe_2O_3	MnO	CaO	K_2O	P_2O_5	V	Cr	Zn	Rb	Sr	Y	Zr	Nb	Ba	Pb
max	38.70	15.30	68.60	10.60	141.40	38.50	16.90	79.10	67.30	25.40	19.60	13.90	28.80	49.10	23.30	22.90	48.10	61.00
min	5.02	0.02	8.70	0.02	0.30	1.00	0.03	7.20	12.20	0.01	0.20	0.02	1.20	0.30	0.30	0.05	0.60	1.00
average	18.21	5.99	25.75	2.70	33.87	12.54	6.04	40.97	36.39	6.02	5.94	4.16	9.58	15.84	10.18	6.67	12.84	27.53

Fig. 14 Maximum, minimum and average accuracy of analysis by pXRF tested as the difference between the results of measurements taken by pXRF on fresh fracture surfaces (air-dry samples) and the results of chemical analysis by WD-XRF (recalculated to dry basis) of the same samples (n = 103).

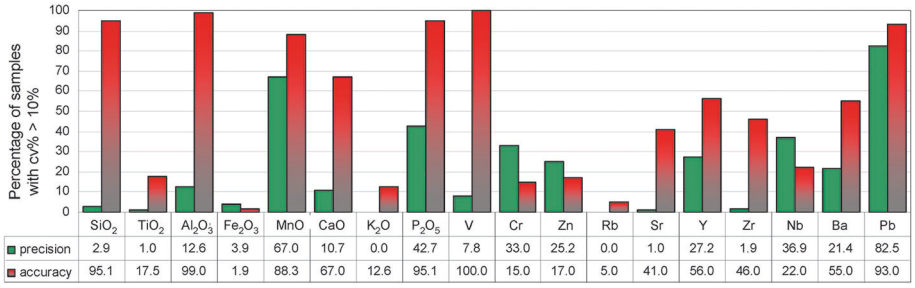

	SiO_2	TiO_2	Al_2O_3	Fe_2O_3	MnO	CaO	K_2O	P_2O_5	V	Cr	Zn	Rb	Sr	Y	Zr	Nb	Ba	Pb
precision	2.9	1.0	12.6	3.9	67.0	10.7	0.0	42.7	7.8	33.0	25.2	0.0	1.0	27.2	1.9	36.9	21.4	82.5
accuracy	95.1	17.5	99.0	1.9	88.3	67.0	12.6	95.1	100.0	15.0	17.0	5.0	41.0	56.0	46.0	22.0	55.0	93.0

Fig. 15 The percentage of samples with accuracy of analysis and precision of measurement (precision of average from three measurements) of less than 10% (measurement by pXRF on fresh fracture surfaces of air-dry samples).

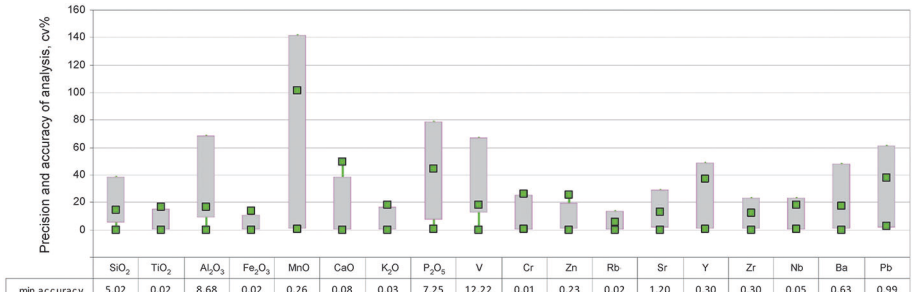

	SiO_2	TiO_2	Al_2O_3	Fe_2O_3	MnO	CaO	K_2O	P_2O_5	V	Cr	Zn	Rb	Sr	Y	Zr	Nb	Ba	Pb
min accuracy	5.02	0.02	8.68	0.02	0.26	0.08	0.03	7.25	12.22	0.01	0.23	0.02	1.20	0.30	0.30	0.05	0.63	0.99
min precision	0.01	0.04	0.06	0.09	0.21	0.04	0.01	0.33	0.12	0.23	0.12	0.12	0.12	0.29	0.06	0.23	0.06	2.89
max precision	14.13	16.59	16.87	13.32	101.21	49.43	18.37	44.34	18.38	25.95	25.49	5.72	12.83	37.23	12.43	18.09	17.28	37.80
max accuracy	38.70	15.33	68.56	10.61	141.42	38.54	16.91	79.07	67.33	25.35	19.61	13.88	28.81	49.15	23.29	22.87	48.11	60.95

Fig. 16 The minimum and maximum accuracy of pXRF analysis calculated from comparison with the results of WD-XRF analysis (n = 103), as well as the minimum and maximum precision of averages calculated from the standard deviation for each of the three measurements (cv% of precision of three measurements divided by √3; n = 446). Measurements by pXRF on fresh fracture surfaces of air-dry samples.

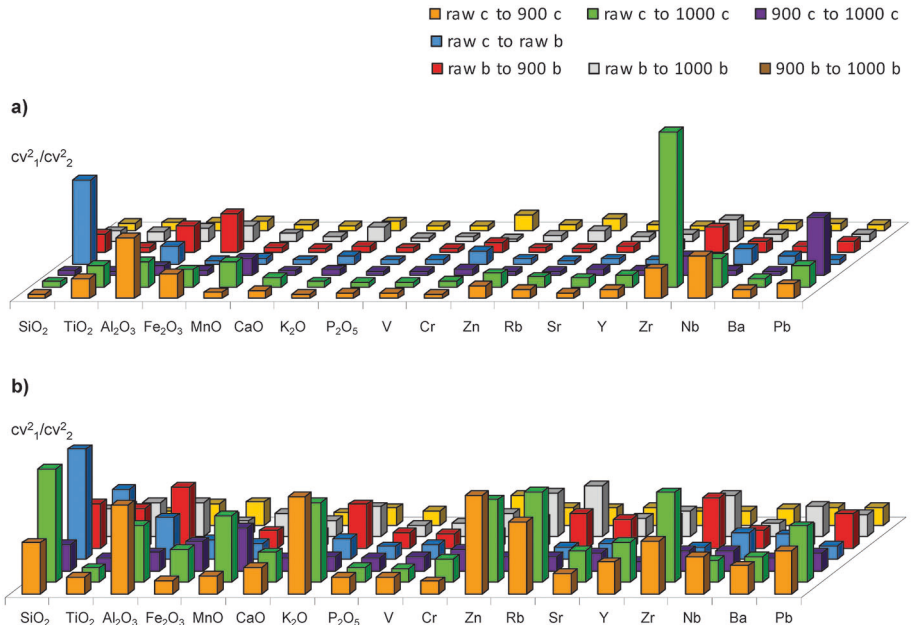

Fig. 17 Accuracy of analysis, results of F-test. Test of significance of the differences in accuracy of analysis by pXRF measurements taken on fresh fracture surfaces (b) and on saw-cut surfaces (c) of air-dry samples (raw) and samples ignited at 900°C (900) and 1000°C (1000). Accuracy was tested by comparing with the results of analysis by WD-XRF of the same samples. a = data of WD-XRF recalculated to dry basis, b = data of WD-XRF valid for ignited samples, major elements normalised to constant sum of 100%.

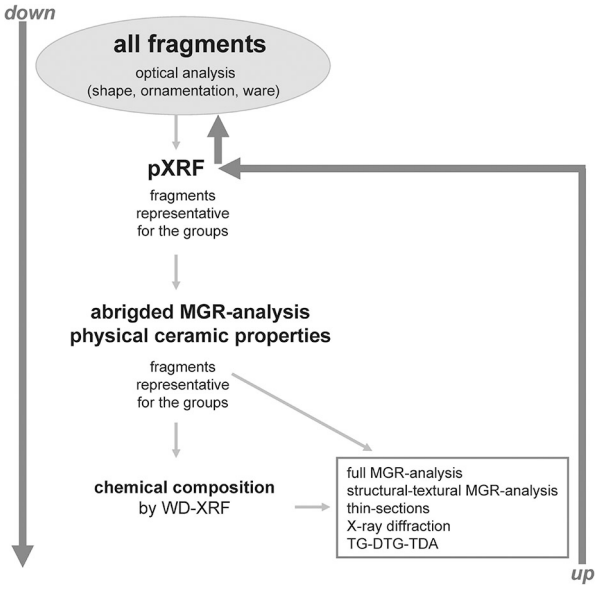

Fig. 18 Schematic diagram of comprehensive analysis of ceramic fragments using a *down-up* classification strategy in which selection for laboratory analysis was not only based on optical analysis (as had been the practice hitherto) but also on the results of chemical analysis by pXRF.

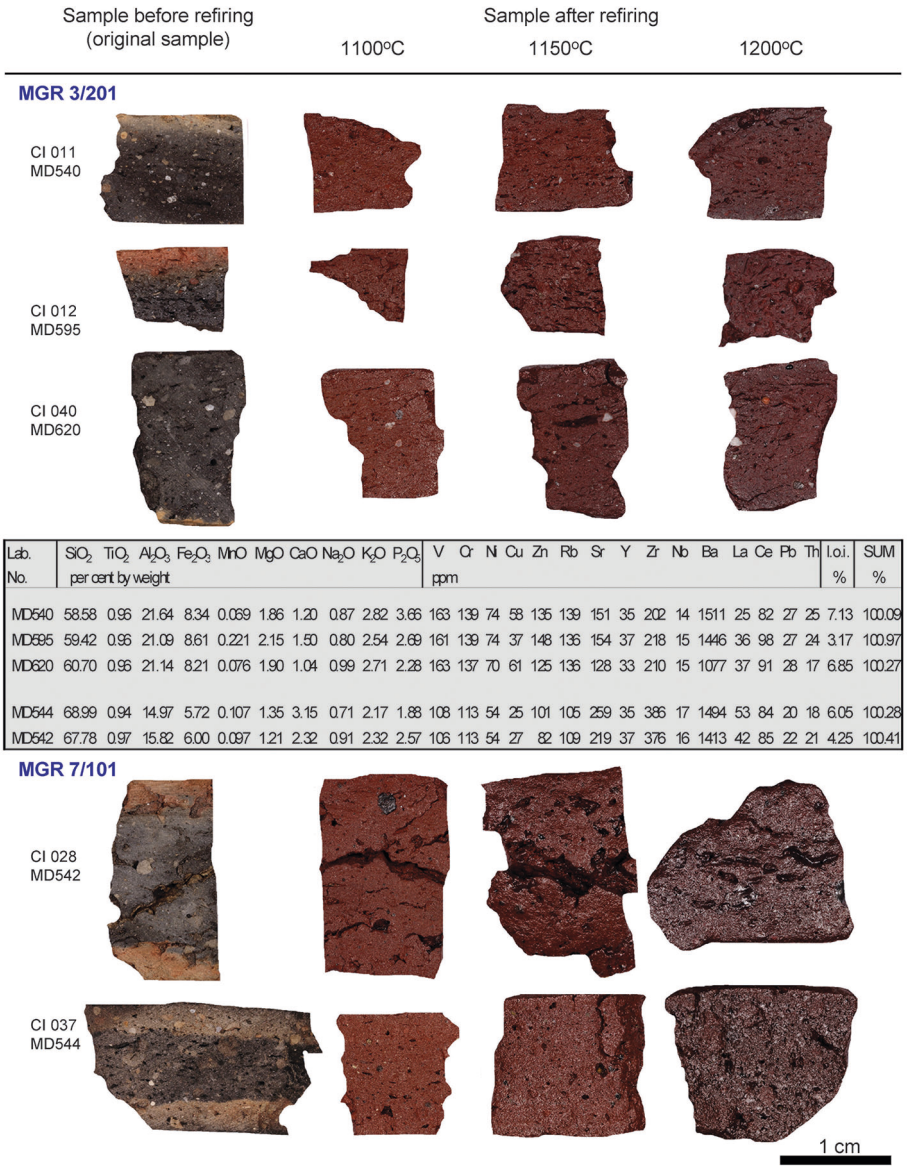

Lab. No.	SiO_2	TiO_2	Al_2O_3	Fe_2O_3	MnO	MgO	CaO	Na_2O	K_2O	P_2O_5	V	Cr	Ni	Cu	Zn	Rb	Sr	Y	Zr	Nb	Ba	La	Ce	Pb	Th	l.o.i.	SUM
	per cent by weight										ppm															%	%
MD540	58.58	0.96	21.64	8.34	0.089	1.86	1.20	0.87	2.82	3.66	163	139	74	58	135	139	151	35	202	14	1511	25	82	27	25	7.13	100.09
MD595	59.42	0.96	21.09	8.61	0.221	2.15	1.50	0.80	2.54	2.69	161	139	74	37	148	136	154	37	218	15	1446	36	98	27	24	3.17	100.97
MD620	60.70	0.96	21.14	8.21	0.076	1.90	1.04	0.99	2.71	2.28	163	137	70	61	125	136	128	33	210	15	1077	37	91	28	17	6.85	100.27
MD544	68.99	0.94	14.97	5.72	0.107	1.35	3.15	0.71	2.17	1.88	108	113	54	25	101	105	259	35	386	17	1494	53	84	20	18	6.05	100.28
MD542	67.78	0.97	15.82	6.00	0.097	1.21	2.32	0.91	2.32	2.57	105	113	54	27	82	109	219	37	376	16	1413	42	85	22	21	4.25	100.41

Fig. 19 Pottery fragments found in Cornești-Iarcuri. Samples before and after refiring at 1100, 1150 and 1200°C. Samples representing MGR-groups 3/201 and 7/101 together with results of chemical analysis by WD-XRF. Samples exhibiting the same thermal behaviour (the same MGR-group) have the same chemical composition.

Major MGR group	MGR-group	Dating / finding spot: LBA Ring I	LBA Ring II	MBA Ring I	MBA Ring II	Provenance (by chemical analysis)
		number of samples				
101	6	3				local wares produced on-site
101	7 a.v.	5				
101	11 a.v.	2				
101	14 a.v.		13			
101	17		1			
101	18 a.v.		4			
101	21		1			
101	27 a.v.			1	3	
101	25				2	
102	29			2		
102	31				1	
102	32 a.v.			2	1	
102	33				2	
102	34				1	
103	22		1			
104	4	2				
104	20 a.v.		2			
105	9	1				
105	24				1	
106	35	1				
106	36	1				
201	3	6				regional (pottery present at seven sites)
201	5	3				
201	8	1				
201	12	1				
201	13	1				
201	15		1			
202	28			1		regional
301	10	1				local? regional?
401	30				2	
501	23				1	
Imp 1	1	1				extra-regional
Imp 2	2	1				
Imp 3	19		1			
Imp 4	26				1	
Imp 5	16		1			

Fig. 20 Pottery fragments found in Cornești-Iarcuri for which MGR-analysis was carried out. Numbers of samples attributed to individual MGR-groups and major MGR-groups divided into MBA pottery and LBA pottery and find location (Ring I and Ring II). Provenance of individual MGR-groups (local, regional, extra-regional) determined by chemical analysis.

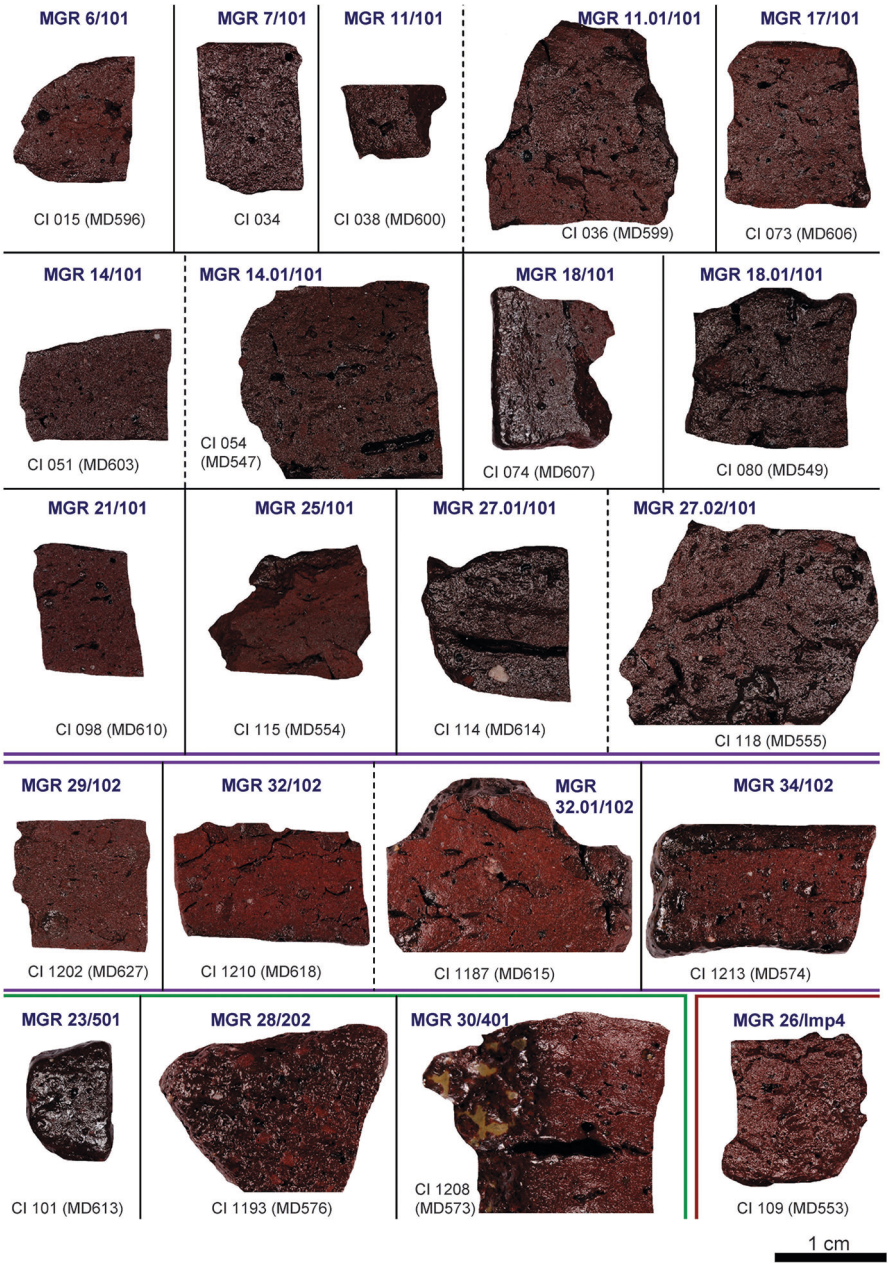

Fig. 21 Pottery fragments found in Cornești-Iarcuri: samples after refiring at 1200°C. Samples attributed to major MGR-groups 101 and 102 represent local wares made at Cornești-Iarcuri. Wares made at regional workshops: major MGR-groups 202, 401, 501. Extra-regional wares: Imp4 (macro photos by M. Baranowski).

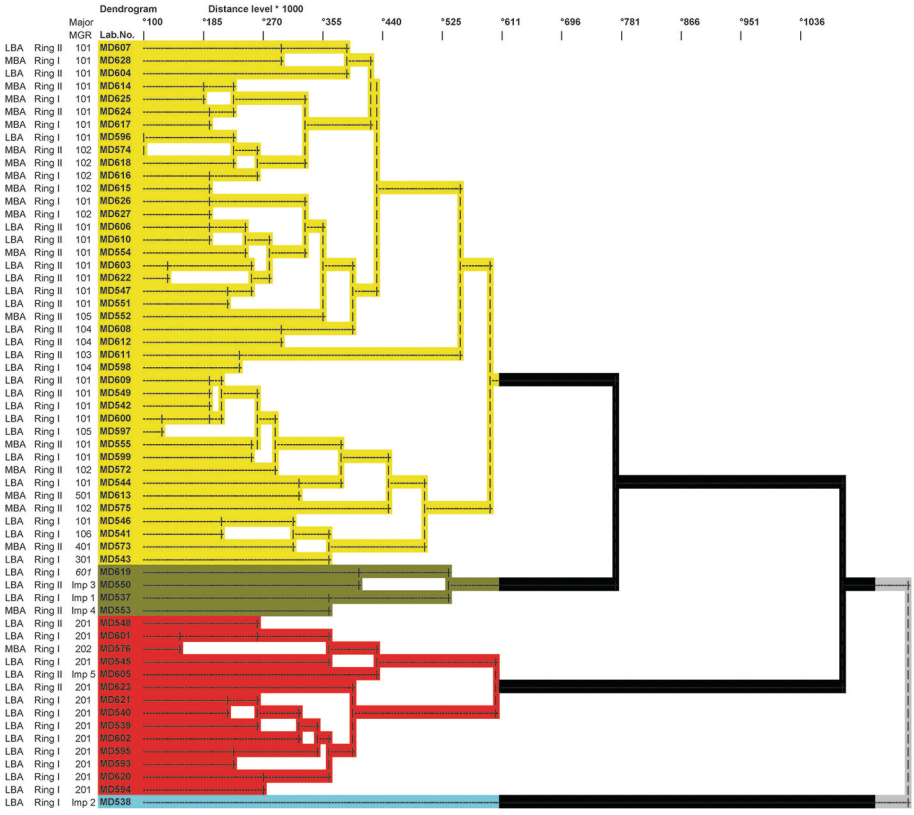

Fig. 22 Pottery fragments found in Cornești-Iarcuri. The results of multivariate cluster analysis by WD-XRF presented in the form of a dendrogram. Analysis was done using Euclidean distance and average linkage aggregative clustering of a distance, logarithmic transformation of data, and the elements used were: Si, Ti, Al, Fe, Mn, Mg, Ca, Na, K, V, Cr, Ni, Zn, Rb, Sr, Y, Zr and Nb.

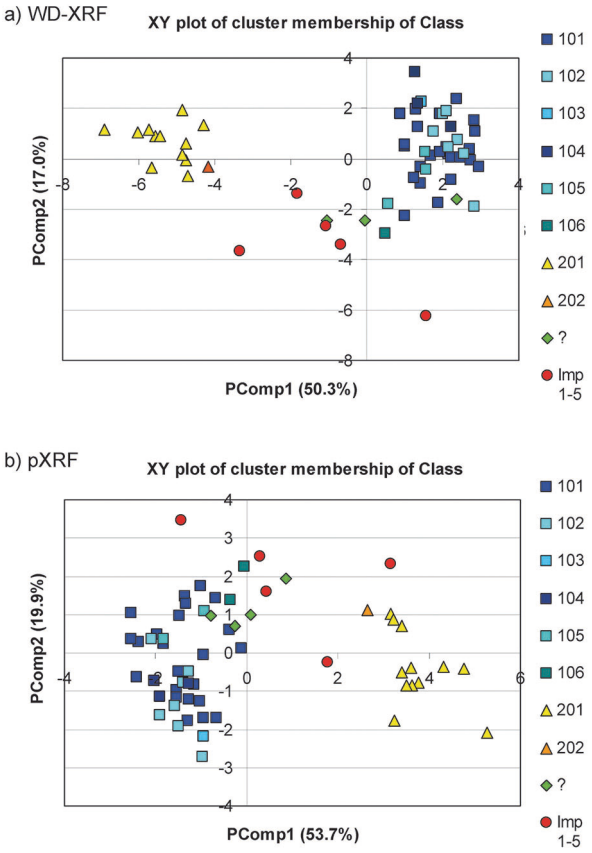

Fig. 23 Pottery fragments found in Corneşti-Iarcuri. Results of PCA. a = PCA using contents of: Si, Ti, Al, Fe, Mn, Mg, Ca, Na, K, V, Cr, Ni, Zn, Rb, Sr, Y, Zr and Nb based on WD-XRF data of ignited samples, major elements normalised to 100%. b = PCA using contents of: Ti, Fe, K, Cr, Zn, Rb, Sr, Zr and Nb based on pXRF data, measurements taken on the fresh fracture surface of air-dry samples.

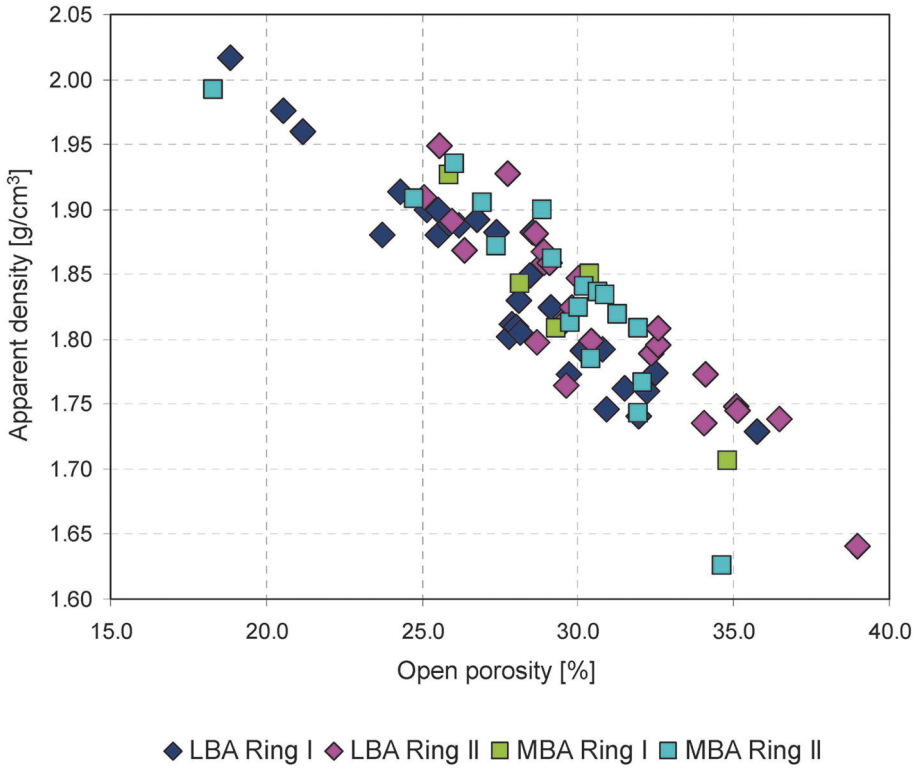

Fig. 24 Pottery fragments found in Cornești-Iarcuri. Apparent density values versus values of open porosity.

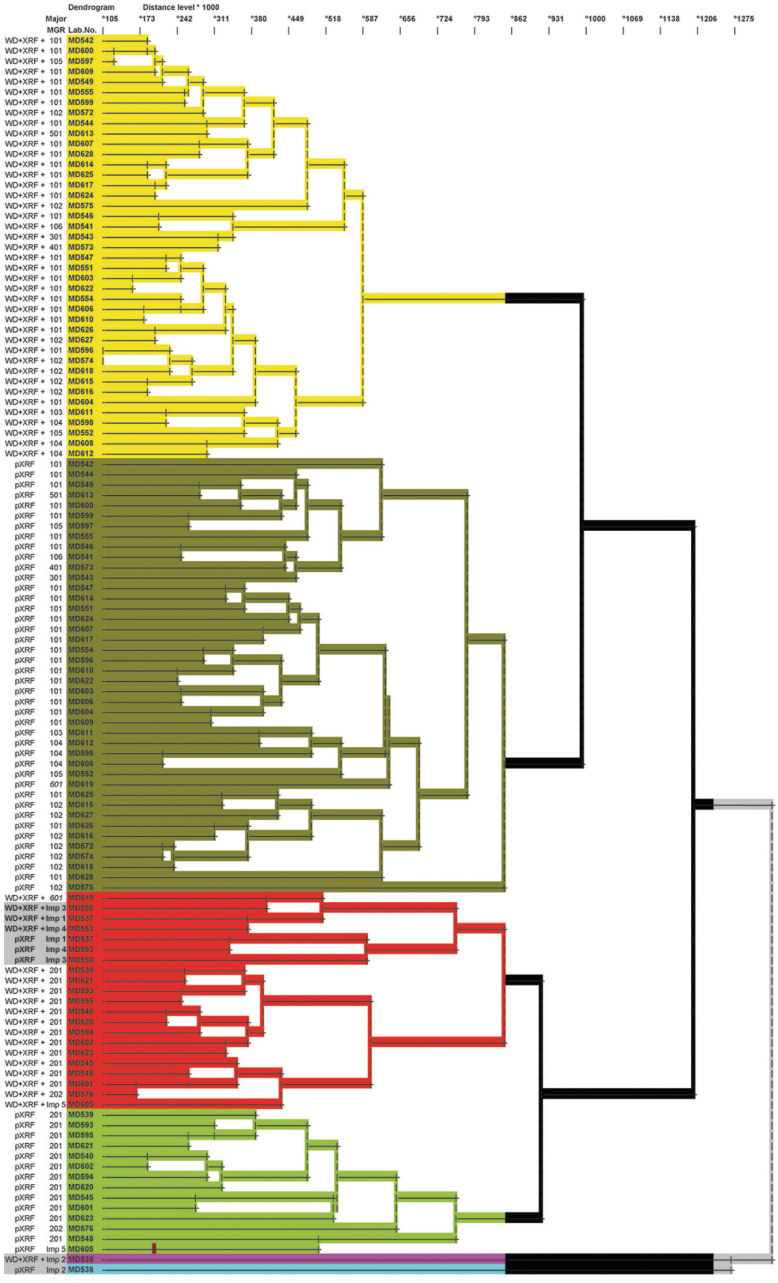

Fig. 25 Pottery fragments found in Corneşti-Iarcuri. The results of multivariate cluster analysis by WD-XRF and by pXRF (Euclidean distance and average linkage aggregative clustering of a distance, logarithmic transformation of data), used elements whose concentrations were determined using both techniques (Si, Ti, Al, Fe, Mn, Ca, K, V, Cr, Zn, Rb, Sr, Y, Zr and Nb). Clusters are related to the technique used, except for the samples of pottery identified as extra-regional groups Imp 1, 3 and 4 Imp 2.

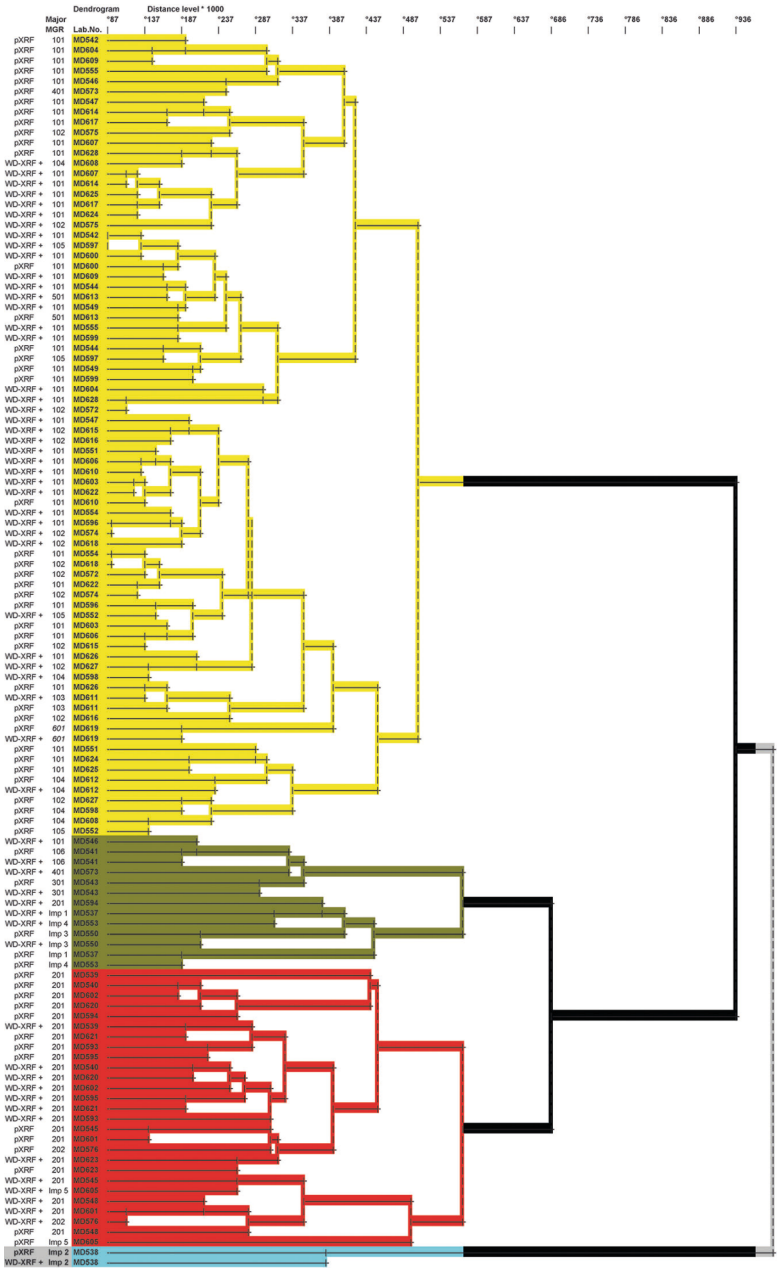

Fig. 26 Pottery fragments found in Cornești-Iarcuri. The results of multivariate cluster analysis by WD-XRF and by pXRF (Euclidean distance and average linkage aggregative clustering of a distance, logarithmic transformation of data), used elements whose contents were determined by pXRF with good precision and accuracy (Ti, Fe, K, Cr, Zn, Rb, Sr and Nb), and additionally Zr.

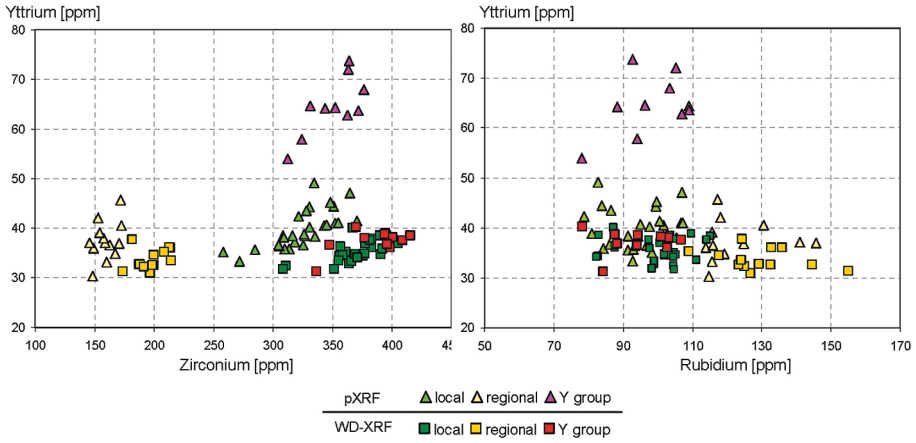

Fig. 27 Pottery fragments found in Cornești-Iarcuri, except for extra-regional samples. Bivariate diagrams of Y content versus Zr (left side) and Rb (right side). The results of pXRF analysis (triangles) highlight a group of samples distinguished by their Y content; this group does not emerge from the results of WD-XRF analysis (squares).

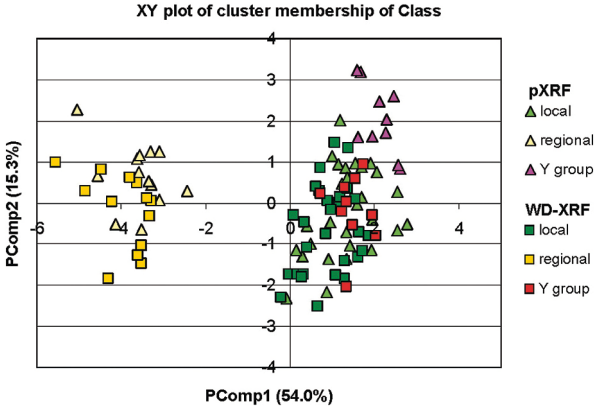

Fig. 28 Pottery fragments found in Cornești-Iarcuri, except for extra-regional samples. Results of PCA using elements whose contents were determined by pXRF with good precision and accuracy, and additionally Y.

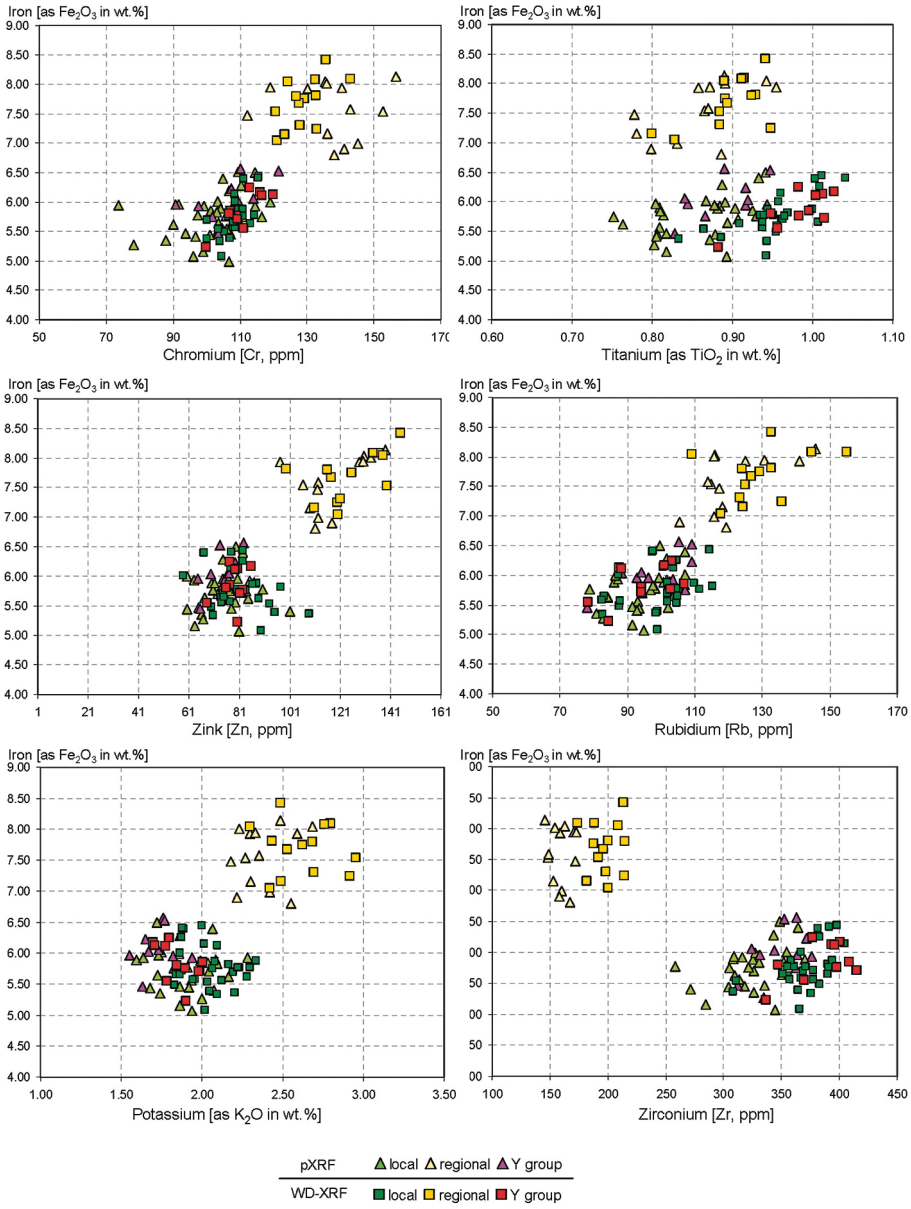

Fig. 29 Pottery fragments found in Cornești-Iarcuri, except for extra-regional samples. Bivariate diagrams of contents of Fe versus: Cr, Ti, Zn, Rb, K and Zr. The results of analysis by pXRF (triangles) and analysis by WD-XRF (squares) are similar (division into local pottery and pottery with a regional distribution), regardless of the differences between pXRF and WD-XRF visible, for example, within the local group in the diagram of Fe versus Ti.

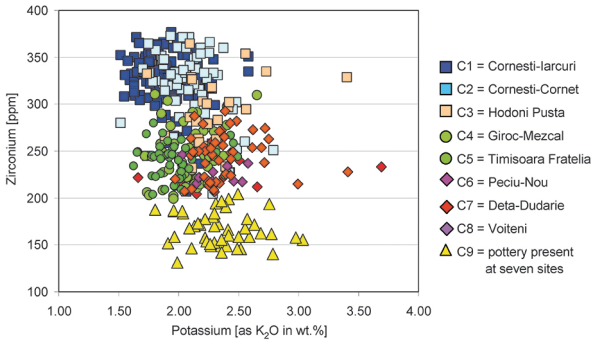

Fig. 30 446 pottery fragments found in the Banat region. Bivariate diagram of Zr content versus K content (as K_2O). Yellow triangles = pottery with a regional distribution (wares noted at sites in Cornești-Iarcuri, Timişoara-Fratelia, Deta-Dudarie, Giroc-Mezcal, Hodoni Pusta, Peciu Nou and Voiteni-Voitec).

Sample MD599 (CI036)	SiO_2 % by weight	TiO_2	Al_2O_3	Fe_2O_3	MnO	CaO	K_2O	P_2O_5	V ppm	Cr	Zn	Rb	Sr	Y	Zr	Nb	Ba	Pb
	pXRF measurements on the same spot of cut surface (every 30 minutes)																	
	65.34	0.946	13.01	5.73	0.055	1.44	1.93	0.58	181	104	71	102	175	43	366	18	857	14
	65.95	0.964	13.19	5.76	0.050	1.45	1.94	0.56	195	105	82	102	178	43	365	18	802	13
	65.77	0.950	13.17	5.76	0.063	1.48	1.91	0.57	187	121	74	100	177	44	371	17	889	13
	65.83	0.937	13.33	5.76	0.054	1.48	1.96	0.55	195	137	71	102	176	43	368	21	848	16
	66.08	0.956	13.01	5.72	0.056	1.46	1.99	0.57	181	111	73	104	176	40	368	20	897	12
	66.19	0.948	13.26	5.73	0.067	1.47	1.97	0.55	202	113	63	100	174	43	368	20	906	15
	66.18	0.959	13.38	5.70	0.064	1.46	1.96	0.57	184	123	66	101	174	46	369	16	805	15
	66.03	0.960	12.99	5.75	0.056	1.46	1.99	0.57	176	132	79	102	175	44	372	17	822	13
	65.58	0.956	13.04	5.71	0.055	1.47	1.97	0.53	182	104	70	105	178	43	361	19	836	15
	66.46	0.959	13.55	5.84	0.061	1.46	1.96	0.58	192	97	70	100	176	45	371	19	841	14
	66.29	0.972	13.22	5.78	0.053	1.47	1.97	0.57	181	126	76	102	181	41	368	19	880	15
	65.92	0.964	13.19	5.74	0.055	1.49	1.98	0.56	192	119	68	105	173	44	368	17	879	16
	66.14	0.948	13.20	5.73	0.056	1.49	1.97	0.57	181	134	70	99	173	44	370	20	838	16
	65.77	0.967	13.18	5.74	0.049	1.48	1.95	0.56	191	117	73	105	175	40	370	20	805	10
	66.11	0.957	13.26	5.74	0.056	1.45	1.99	0.55	175	111	72	97	178	41	371	18	841	17
	65.98	0.952	13.50	5.73	0.055	1.47	1.95	0.59	190	127	66	100	171	43	367	16	867	15
mean	65.98	0.956	13.22	5.75	0.057	1.47	1.96	0.56	187	118	71	101	176	43	368	19	851	14
std ±	0.28	0.009	0.16	0.03	0.005	0.01	0.02	0.01	8	12	5	2	2	2	3	2	33	2
cv%	**0.42**	**0.94**	**1.23**	**0.55**	**8.55**	**0.94**	**1.16**	**2.55**	**4.1**	**10.0**	**6.7**	**2.3**	**1.4**	**4.0**	**0.8**	**8.5**	**3.9**	**11.9**
	precision calculated from measurements on three different spots on fresh fracture of the same sample CI036																	
cv%	**1.08**	**1.07**	**1.36**	**0.66**	**4.20**	**3.27**	**0.88**	**11.83**	**6.3**	**3.1**	**4.2**	**0.6**	**2.7**	**8.0**	**2.0**	**3.2**	**6.4**	**9.9**
	precision calculated from measurements on three different spots on fresh fractures (n = 591)																	
cv% (aver.)	**4.30**	**3.91**	**7.12**	**4.41**	**21.22**	**7.01**	**4.10**	**10.60**	**5.9**	**10.4**	**7.6**	**3.8**	**4.2**	**9.0**	**3.6**	**8.3**	**6.9**	**18.3**

Tab. 1 Results of pXRF measurements on sample MD599: test of influence of geometry of samples on the precision of analysis. Difference between error of measurement calculated for 16 measurements on the same place (every 30 minutes) and error calculated from three measurements per sample on three different spots of a fresh fracture.

G296	SiO_2	TiO_2	Al_2O_3	Fe_2O_3	MnO	MgO	CaO	K_2O	P_2O_5	V	Cr	Ni	Cu	Zn	Rb	Sr	Y	Zr	Nb	Ba	Ce	Pb
	% by weight									ppm												
pXRF: monitor sample (G296), 147 measurements from March 2013 to November 2015 (polished surface)																						
aver	**61.47**	**0.79**	**17.04**	**5.72**	**0.029**	**0.89**	**2.83**	**3.20**	**0.34**	**153**	**147**	**42**	**32**	**222**	**186**	**147**	**27**	**123**	**18**	**518**	**124**	**23.15**
STD	2.14	0.02	0.95	0.04	0.006	0.22	0.02	0.03	0.03	9	11	5	9	16	3	2	2	2	1	32	26	3.51
cv%	3.5	2.1	5.6	0.7	21.4	24.5	0.9	0.9	8.9	6.1	7.7	11.2	27.0	7.0	1.9	1.5	9.1	1.9	8.0	6.3	21.4	15.1
WD-XRF, data calculated to dry basis																						
G296	62.14	0.75	19.10	5.51	0.041	2.30	3.09	3.20	0.31	135	140	71	27	123	172	144	30	122	17	480	82	18.41
accuracy of pXRF measurements of monitor sample																						
pXRF	61.47	0.79	17.04	5.72	0.029	0.89	2.83	3.20	0.34	153	147	42	32	222	186	147	27	123	18	518	124	23.15
WD-XRF	62.14	0.75	19.10	5.51	0.041	2.30	3.09	3.20	0.31	135	140	71	27	123	172	144	30	122	17	480	82	18.41
difference %	1.1	4.7	10.7	3.9	29.7	61.3	8.5	0.2	6.4	14.0	5.2	41.5	18.3	80.1	8.1	1.8	10.4	0.7	0.4	8.0	50.8	25.7

Tab. 2 Long-term precision (March 2013–November 2015) calculated as the difference between the average of 147 pXRF measurements of monitor samples and the results of WD-XRF calculated to dry basis.

	SiO_2	TiO_2	Al_2O_3	Fe_2O_3	MnO	MgO	CaO	Na_2O	K_2O	P_2O_5	V	Cr	Ni	(Cu)	Zn	Rb	Sr	Y	Zr	(Nb)	Ba	(La)	(Ce)	(Pb)	(Th)	l.o.i.	SUM
	% by weight										ppm															%	%
	local groups																										
	major MGR-group 101, n=23																										
aver.	**68.04**	**1.00**	**15.93**	**5.97**	**0.107**	**1.21**	**1.91**	**0.77**	**2.14**	**2.92**	**108**	**114**	**52**	**27**	**84**	**102**	**186**	**38**	**395**	**18**	**1691**	**43**	**94**	**22**	**22**	**4.34**	**100.14**
STD	1.18	0.03	0.48	0.26	0.033	0.13	0.45	0.14	0.17	1.2	7	4	6	5	8	11	35	2	17	1	329	9	10	2	2	1.02	0.31
cv%	1.7	3.2	3.0	4.4	31.0	11.0	23.6	17.9	7.8	40.5	6.2	3.6	11.8	19.5	9.6	10.4	18.7	6.0	4.4	6.3	19.4	20.5	10.6	9.4	10.7	23.5	0.3
	major MGR-group 102, n=7																										
aver.	**68.07**	**1.01**	**16.09**	**6.10**	**0.106**	**1.30**	**2.23**	**0.64**	**1.92**	**2.54**	**108**	**114**	**47**	**21**	**82**	**101**	**166**	**38**	**395**	**18**	**1305**	**44**	**95**	**23**	**22**	**3.54**	**99.84**
STD	0.78	0.04	0.56	0.29	0.035	0.06	0.66	0.12	0.12	0.65	6	5	3	4	4	8	27	2	25	2	204	8	7	1	2	1.26	0.40
cv%	1.1	3.5	3.5	4.8	32.9	4.7	29.6	19.3	6.1	25.5	5.8	4.4	6.0	18.8	4.5	7.8	16.3	5.3	6.3	9.0	15.6	18.2	7.5	5.2	9.0	35.6	0.4
	regional pottery																										
	major MGR-group 201, n=12																										
aver.	**59.31**	**0.94**	**21.14**	**8.10**	**0.093**	**1.85**	**1.46**	**0.84**	**2.76**	**3.51**	**161**	**136**	**67**	**52**	**132**	**137**	**168**	**36**	**207**	**15**	**1722**	**39**	**83**	**25**	**23**	**5.38**	**100.12**
STD	1.73	0.04	0.56	0.38	0.046	0.22	0.31	0.08	0.23	1.30	6	6	9	9	13	12	38	2	12	1	642	7	9	1	3	1.44	0.39
cv%	2.9	4.5	2.6	4.6	49.1	11.7	21.2	10.1	8.4	37.0	3.8	4.4	13.9	17.3	9.9	8.8	22.7	5.8	6.0	8.6	37.3	18.1	10.3	5.5	12.6	26.8	0.4

Tab. 3 Results of chemical analysis by WD-XRF, analysis of ignited samples, major elements normalised to 100% (preparation of melted, ignited samples by M. Daszkiewicz ARCHEA, measurements with an AXIOS spectrometer by A. Schleicher and G. Schneider in GFZ Potsdam).

Chemical analysis	Lab. No.	TiO_2	Fe_2O_3	K_2O	Cr	Zn	Rb	Sr	Zr	Nb
		wt.%			ppm					
pXRF	MD541	0.81	5.41	2.07	97	101	93	184	272	13
WD-XRF -l.o.i.	MD541	0.83	5.37	2.20	100	108	98	194	309	14
pXRF	MD611	0.94	6.49	1.72	115	79	100	94	348	18
WD-XRF -l.o.i.	MD611	1.01	6.26	1.87	113	82	105	102	383	18
pXRF	MD619	0.75	5.45	2.22	96	84	121	122	319	18
WD-XRF -l.o.i.	MD619	0.87	5.51	2.41	103	90	122	128	326	16
pXRF	MD573	0.80	5.22	2.30	98	86	114	157	246	17
WD-XRF -l.o.i.	MD573	0.89	5.55	2.66	106	100	128	186	295	14

Tab. 4 Results of chemical analysis by pXRF and WD-XRF (calculated to dry basis). Examples of analysis results for samples that appear side-by-side in the dendrogram presented in figure 26 (MD541, MD611, MD619) and for remote samples – sample MD573 features in the first cluster (yellow) according to data obtained by pXRF and in cluster 2 (green) according to data obtained by WD-XRF.

Bibliography

Behrendt, Mielke, and Mecking 2012
Sonja Behrendt, Dirk Paul Mielke, and Oliver Mecking. "Die portable Röntgenfloureszenzanalyse (P–RFA) in der Keramikforschung: Grundlagen und Potenzial." *Restaurierung und Archäologie* (2012), 93–110.

Bogdanović 1996
Milenko Bogdanović. "The Yugoslav Danube and the Neighboring Regions in the 2nd Millenium B.C." In Belgrad-Vršac: Serbian Academy of Sciences and Arts Institute for Balkan Studies, 1996. Chap. Mittelserbien in der Bronzezeit und die Vattina-Kultur, 97–108.

Bóna 1975
István Bóna. *Die Mittlere Bronzezeit Ungarens und ihre Südlichen Beziehungen*. Budapest: Akadémiai Kiadó, 1975.

Daszkiewicz 2014
Małgorzata Daszkiewicz. "Ancient Pottery in the Laboratory – Principles of Archaeoceramological Investigations of Provenance and Technology." *Novensia* 25 (2014), 177–197.

Daszkiewicz, Dyczek, et al. 2007
Małgorzata Daszkiewicz, Piotr Dyczek, Gerwulf Schneider, and Ewa Bobryk. "Preliminary Results of Archaeometric Analysis of Amphorae and Gnathia-Type Pottery from Risan, Montenegro," in *Archaeometric and Archaeological Approaches to Ceramics (Papers Presented at EMAC'05, 8th European Meeting on Ancient Ceramics, Lyon 2005)*. Ed. by S. Y. Waksman. BAR International Series 1691. Oxford: Archaeopress, 2007, 85–93.

Daszkiewicz and Maritan 2017
Małgorzata Daszkiewicz and Lara Maritan. "Experimental Firing and Re-firing." In *The Oxford Handbook of Archaeological Ceramic Analysis*. Ed. by A. Hunt. Oxford: Oxford University Press, 2017, 487–508.

Daszkiewicz and Schneider 2001
Małgorzata Daszkiewicz and Gerwulf Schneider. "Klassifizierung von Keramik durch Nachbrennen von Scherben." *Zeitschrift für Schweizerische Archäologie und Kunstgeschichte* 58 (2001), 25–32.

Daszkiewicz and Schneider 2011
Małgorzata Daszkiewicz and Gerwulf Schneider. "Archäokeramologische Klassifizierung am Beispiel kaiserzeitlicher Drehscheibenkeramik aus Brandenburg." In *Drehscheibentöpferei im Barbaricum – Technologietransfer und Professionalisierung eines Handwerks am Rande des Römischen Imperiums*. Ed. by J. Bemmann, M. Hegewisch, M. Meyer, and M. Schmauder. Vol. 13. Bonner Beiträge zur Vor– und Frühgeschichtlichen Archäologie. Bonn: Institut für Vor- und Frühgeschichtliche Archäologie der Rheinischen Friedrich-Wilhelms-Universität Bonn, 2011, 17–33.

Daszkiewicz and Schneider 2012
Małgorzata Daszkiewicz and Gerwulf Schneider. "Archäometrie und Denkmalpflege, Metalla SH 5." In ed. by F. Schlütter, S. Greiff, and M. Prange. Bochum: Eberhard–Karls–Universität Tübingen, 2012. Chap. Möglichkeiten und Grenzen zerstörungsfreier Analysen von Keramik mit pXRF, 167–170.

Gogâltan 2004
Florin Gogâltan. "Bronzul mijlociu în Banat. Opinii privind Grupul Corneşti–Crvenka." In *Festschrift für Florin Medelet*. Timisoara: Editura MIRTON Timisoara, 2004, 79–153.

Gumă 1993
Marian Gumă. *Civilizaţia primei epoci a fierului în sud-vestul României*. Vol. 4. Bibliotheca Thracologica. Bucureşti: S. C. Melior Trading SRL, 1993.

Medeleţ 1993
Florin Medeleţ. "În legătură cu fortificaţia de pământ de la Corneşti (comuna Orţişoara, judeţul Timiş)." *Analele Banatului Arheologie Istorie* II (1993), 119–150.

Pech 1877
Josef Pech. "A zsádanyi avar telepek Temesvármégyében." *Történelmi és Régészeti Értesitö* III.2 (1877), 49–59.

Schneider and Daszkiewicz 2010
Gerwulf Schneider and Małgorzata Daszkiewicz. "Archäometrie und Denkmalpflege, Metalla SH 3." In ed. by O. Hahn, A. Hauptmann, D. Modarressi-Tehrani, and M. Prange. Bochum: Deutsches Bergbaumuseum Bochum, 2010. Chap. Testmessungen mit einem tragbaren Gerät für energiedispersive Röntgenfluoreszenz (P-XRF) zur Bestimmung der chemischen Zusammensetzung archäologischer Keramik, 110–112.

Schneider and Mommsen 2009
Gerwulf Schneider and Hans Mommsen. "Eastern Sigillata C von Pergamon und Çandarlı (Türkei)." In *Archäometrie und Denkmalpflege – Kurzberichte 2009. Jahrestagung in München*. Ed. by A. Hauptmann and H. Stege. Metalla Sonderheft 2. Bochum: Deutsches Bergbau-Museum, 2009, 223–225.

Szentmiklosi 2009
Alexandru Szentmiklosi. "Aezările culturii Cruceni-Belegis în Banat." PhD thesis. 2009.

Szentmiklosi et al. 2011
Alexandru Szentmiklosi, Bernhard S. Heeb, Julia Heeb, Anthony Harding, Rüdiger Krause, and Helmut Becker. "Corneşti-Iarcuri – A Bronze Age Town in the Romanian Banat?" *Antiquity* 85.329 (2011), 819–838.

Vranić 2002
Svetlana Vranić. *Belegiš, Stojića Gumno – nekropola spaljenih pokojnika Belegiš. Stojića Gumno – A Necropolis of Cremation Burials*. Beograd: Muzej Grada Beograda, 2002.

Illustration and table credits

ILLUSTRATIONS: **1–2** B. Heeb. **3–4** M. Daszkiewicz. **5** M. Daszkiewicz / H. Baranowska. **6** M. Daszkiewicz/ E. Bobrink. **7** G. Schneider. **8–17** M. Daszkiewicz / H. Baranowska. **18** M. Daszkiewicz. **19–30** M. Daszkiewicz / H. Baranowska.
TABLES: **1–4** M. Daszkiewicz / G. Schneider.

MAŁGORZATA DASZKIEWICZ

Małgorzata Daszkiewicz, MA Warsaw 1979 in Physical Geography, PhD Warsaw University 1993 in Humanities. Since 1994 she has worked in collaboration with *AG Archäometrie* FU Berlin. Formerly a part-time employee at TOPOI, she is currently an associated member of the Institute for Prehistoric Archaeology FU Berlin and also runs ARCHEA, a laboratory in Warsaw for archaeometric analysis and research. Her main research interests are determining the technology and provenance of archaeological ceramics and devising techniques for the classification of bulk ceramic finds.

Dr. Małgorzata Daszkiewicz
Freie Universität Berlin
Institut für Prähistorische Archäologie
Fabeckstraße 23–25
14195 Berlin, Germany
and
ARCHEA
ul. Ogrodowa 8m95
00-896 Warszawa, Poland
E-mail: m.dasz@wp.pl

GERWULF SCHNEIDER

Gerwulf Schneider (Dr.rer.nat. 1968, habilitation 1979, both at Freie Universität Berlin) was a research associate at Excellence Cluster Topoi and now at the Insitute of Prehistoric Archaeology at FU Berlin. Since 1975 his main focus has been on chemical and mineralogical analysis of archaeological ceramics. His research focusses on Roman pottery in Germany, Hellenistic to Late Antique pottery in the Mediterranean region, and on pottery in Europe, Mesopotamia and Sudan. Schneider is a member of the German Archaeological Institute and of various archaeometric societies.

Dr. Gerwulf Schneider
Freie Universität Berlin
Institut für Prähistorische Archäologie
Fabeckstraße 23–25
14195 Berlin, Germany
E-mail: schnarch@zedat.fu-berlin.de

BERNHARD HEEB

Bernhard Heeb is archaeologist with a scientific focus on the Late Bronze Age in southeast Europe. He is a curator at the Museum for Pre- and Early History in Berlin for the Bronze Age, Troy and the anthropological collection. He obtained a PhD in 2009 (Frankfurt/Main). Since 2007, he has conducted a research project on the Late Bronze Age Mega-Site Corneşti-Iarcuri in collaboration with the Muzeul Naţional al Banatului in Timişoara and the Johann Wolfgang Goethe-Universität Frankfurt am Main.

Dr. Bernhard Heeb
Staatliche Museen zu Berlin – Stiftung Preußischer Kulturbesitz
Museum für Vor- und Frühgeschichte
Archäologisches Zentrum
Geschwister-Scholl-Str. 6
10117 Berlin, Germany
E-mail: b.heeb@smb.spk-berlin.de

ANDREI BĂLĂRIE

Andrei Bălărie is Head of Department of Archaeology at the Muzeul Național al Banatului, with a scientific focus on the Middle and Late Bronze Age in southeast Europe. He is the curator of the Bronze Age collection of the Muzeul Național al Banatului.

Andrei Bălărie
Muzeul Național al Banatului
Bastionul Maria Theresia, str. Martin Luther, nr.4
300054 Timisoara, Romania
E-mail: andrei.balarie@gmail.com

Małgorzata Daszkiewicz, Miriam Lahitte, Rudolf Naumann

Analysis of Ancient Beads from Gala Abu Ahmed, Sudan, Using pXRF and XRD

Summary

The potential and limitations of using pXRF in the analysis of ancient beads was tested on samples recovered from excavations held at the fortress site of Gala Abu Ahmed, situated along the lower reaches of Wadi Howar, North Sudan, some 110 km west of the Nile Valley. Miriam Lahitte selected 112 disc-shaped beads for analysis, each one measuring c. 5 mm in outer diameter and with a cross-section of c. 1.5 mm in diameter. Despite their small size, it proved possible to perform measurements on these beads. The tests showed that pXRF results could be used to group the beads; however, additional analyses, such as XRD and SEM-EDX are required to accurately determine what material the beads are made of.

Keywords: Gala Abu Ahmed; beads; pXRF; SEM-EDX

Die Möglichkeiten und Grenzen der Anwendung der pRFA bei der Analyse antiker Perlen wurden an Proben von Ausgrabungen in der Festungsanlage von Gala Abu Ahmed, gelegen im unteren Wadi Howar, Nord Sudan, etwa 110 km westlich vom Niltal geprüft. Miriam Lahitte hatte 112 scheibenförmige kleine Perlen für die Analyse ausgewählt, alle mit etwa 5 mm äußerem Durchmesser und etwa 1,5 mm Dicke. Trotz der kleinen Größe zeigte es sich möglich, Messungen mit pRFA an diesen Perlen durchzuführen. Es war möglich, die Perlen chemisch zu gruppieren, aber für die Bestimmung der Zusammensetzung waren zusätzliche Analysen wie Röntgenbeugung (XRD) und Analysen im Rasterelektronenmikroskop (SEM-EDX) notwendig.

Keywords: Gala Abu Ahmed; Perlen; pRFA; REM-EDX

We are very grateful to the National Corporation for Antiquities and Museums (NCAM) in Khartoum, and especially to the Director General, Abdel Rahman Ali Mohamed, and to the Director of the University of Cologne Mission, Friederike Jesse, for allowing us to analyse the beads from Gala Abu Ahmed.

Morten Hegewisch, Małgorzata Daszkiewicz und Gerwulf Schneider (eds.) | Using pXRF for the Analysis of Ancient Pottery – an Expert Workshop in Berlin 2014 | Berlin Studies of the Ancient World 75 (ISBN TODO; DOI: 10.17171/3-75) | www.edition-topoi.org

This article focuses on the potential and limitations of applying portable energy dispersive X-ray fluorescence (pXRF) to the analysis of ancient beads. In order to assess the scope of this analytical technique, measurement results obtained using pXRF were compared with conclusions drawn from the results of comprehensive analyses carried out on the same beads. The pXRF measurements were performed as part of a project conducted within the Excellence Cluster 264 TOPOI at the Freie Universität Berlin investigating whether pXRF can be used as a non-destructive method for analysing archaeological samples. The chemical composition of 112 beads was analysed by pXRF using a Niton XL3t 900S GOLDD RF-Analyser, MINING software, calibration using ceramic standards (calibration based on twelve own standards analysed by WD-XRF), an 8-mm window, a measurement time of 120 seconds (30 sec per filter), without helium, in a sample chamber. Most of the beads were no larger than 5 mm in outer diameter, therefore measurements were performed by placing the beads very carefully directly on the film above the detector (Fig. 1).

The following analytical methods were used: X-ray diffraction, thin-section studies using a polarising microscope, scanning electron microscopy and chemical composition analysis using a scanning electron microscope fitted with an EDX microprobe analyser. Qualitative analysis was carried out using a reflected light microscope.

The 112 beads examined in this study were selected for analysis by Miriam Lahitte based on macroscopic examination of a large unclassified assemblage of beads (most of them weathered), discovered during three seasons of excavation at the fortress site of Gala Abu Ahmed, situated along the lower reaches of Wadi Howar, North Sudan, some 110 km west of the Nile Valley. This fortress dates from *c.* 1100 to 400 BC, and was first recorded in 1984 during the course of a survey conducted by a team from the Cologne University DFG-Project B.O.S. ("Besiedlungsgeschichte der Ostsahara"). Combining forces with the Collaborative Research Centre ACACIA ("Arid Climate, Adaptation and Cultural Innovation in Africa"), the first two seasons of archaeological fieldwork took place in 2002 and 2006. Further excavations were undertaken in 2008 following the launch of the DFG-Project "At the borders of power – the fortress Gala Abu Ahmed in lower Wadi Howar, Sudan. A base of Kushite domination", directed by Friederike Jesse and based at the University of Cologne. Permission to take the beads on loan to Germany for the purposes of analysis was granted by the NCAM (National Corporation for Antiquities and Museums, General Director Abdel Rahman Ali), Khartoum, Sudan.

Information from the results of the pXRF measurements was used to group the beads according to their chemical composition. The groups arising from this classification cannot, strictly speaking, be called provenance groups; each one simply represents a collection of samples of similar composition, but with large variations in the content of individual elements. Groups were defined based on characteristic elements, i.e. elements which are distinctive for a given group of beads regardless of their exact con-

centrations. Within a single group, the coefficient of variation for distinctive elements is up to 50%. This means that a given group of beads is made from one particular type of material, but the material in question is not necessarily of the same provenance.

Fig. 2 shows black beads representing three different compositional groups distinguished by pXRF – see Tab. 1.

Comparing the results obtained by pXRF with those obtained by SEM-EDX (Figs. 3 and 4) clearly highlights differences in chemical composition, particularly in relation to Mg and Na levels, which were not determined by pXRF, thus placing significant limitations on the interpretation of results and hence on correctly identifying the material from which the beads were made.

Looking at all of the results of individual analyses reveals, as expected, that pXRF measurements do not provide any quantitative results for the beads from Gala Abu Ahmed. Nevertheless, the pXRF technique proved itself to be a valuable tool for identifying groups. This was a surprise finding given that most of the beads were very small (no more than 5 mm in outer diameter) and their surfaces contaminated. Additional destructive analyses will, however, be necessary to establish what material the beads are made of. It is particularly important that non-archaeometrists be made aware of the fact that the pXRF technique cannot be used for analysing Na, and that determining Mg and Al is often problematic. This means that performing quick pXRF measurements will not provide the information needed to accurately distinguish all types of glass/glaze. Soda glaze is identified based on the absence of lead, which can, however, result in mistakes, as seen in the case of red beads. Nonetheless, if pXRF is used as a classification tool together with careful macroscopic examination under a reflected light microscope, then destructive analysis can be restricted to individual representative samples chosen from each group.

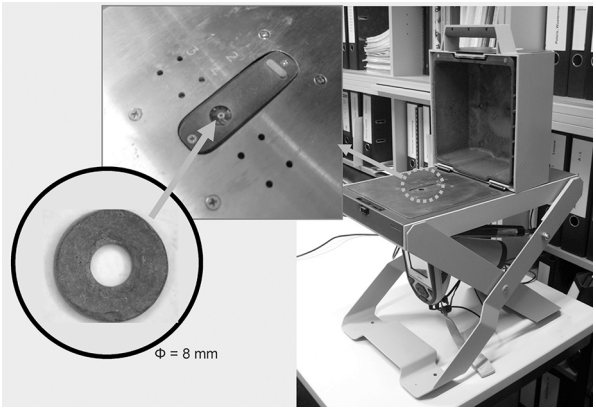

Fig. 1 Positioning of bead for measurement by pXRF.

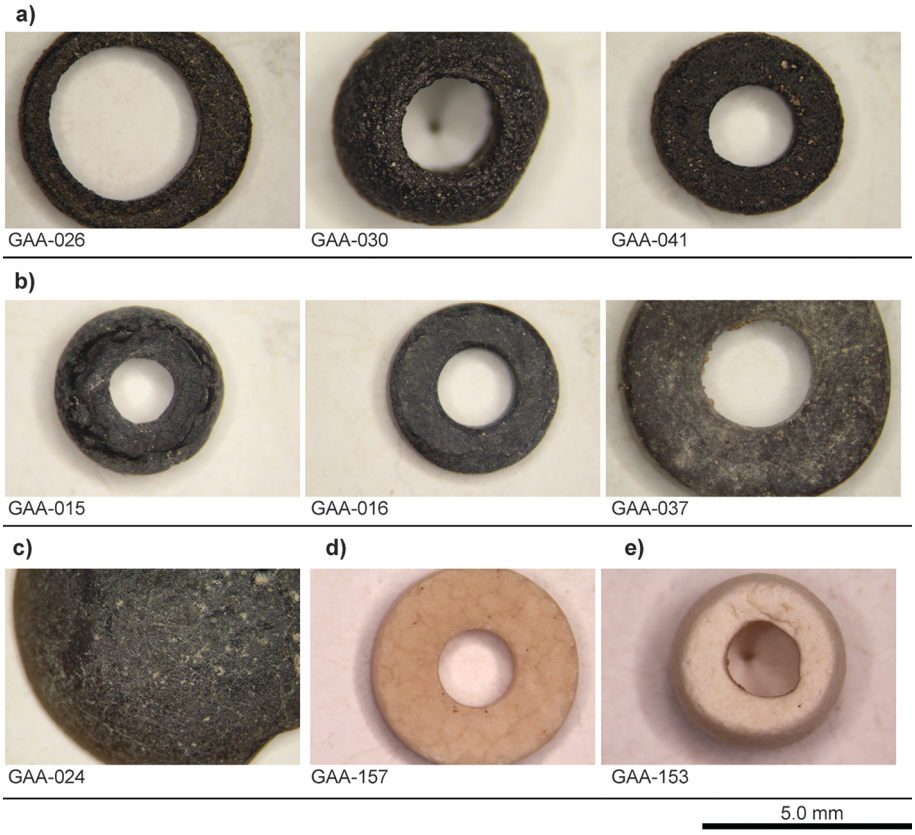

Fig. 2 Examples of black and white beads discovered during the excavation at the fortress site of Gala Abu Ahmed: beads made of quartz ceramics with black glaze (a); black beads made from ostrich egg shells (b); black bead made from obsidian (c); white beads made from ostrich egg shells (d); white bead made from ceramics (e).

SAMPLE	SiO_2	TiO_2	Al_2O_3	Fe_2O_3	MnO	MgO	CaO	K_2O	P_2O_5	S	Cl	V	Cr	Cu	Zn	Rb	Sr	Y	Zr	Ba	Pb	Co	As
	% by weight									ppm													
Black bead, obsidian, Tibesti-group 7 (Schneider data bank)																							
GAA-024	89.59	0.31	22.01	2.76	0.04		1.22	6.01			269	145	47		69	129	55	65	378	522	6		
Black beads, quartz ceramics with black glaze																							
GAA-Pe	456.84	1.34		4.35	14.45		4.09	0.59			209	1706		1856	154	22	163	21	109	5362	246	887	
GAA-026	74.28	1.43	15.86	5.27	15.53		2.43	0.89	0.34	14460	118	1783	125	3028	184	19	230	52	99	4534	5297	752	268
GAA-030	76.78	0.65		2.67	6.49		1.03	0.98			210	823		757	75	28	60	10	73	7446	139	258	
GAA-014	78.45	1.08		3.59	15.27		2.26	1.15			141	1657	97	5176	154	26	156	25	82	7027	487	967	38
GAA-041	88.71	0.98		4.54	5.67		4.23	1.06		1853	310	1223	36	561	78	20	86	15	92	3487	46		
Black beads, ostrich egg shells																							
GAA-037	12.61	0.05	8.69	0.23	0.01	13.81	61.65	0.10	0.67		65	32		54		9	335		19				
GAA-042	9.70	0.01	8.74	0.14	0.01	18.12	66.33	0.03	0.73		66	61		19	18	9	380						
GAA-015	10.01	0.02	3.08	0.13	0.01	9.24	61.39	0.09	0.44	967	176	33		93		9	302						
GAA-016	8.65		5.96	0.09	0.01	14.53	67.66	0.06	0.65		203	163		106		9	584						
White beads, ostrich egg shell																							
GAA 157	4.93	0.04	9.80	0.10		16.72	65.46	0.10	0.75		123	151				9	216						
GAM1-2	3.91	0.04	8.55	0.11	0.03	18.48	63.08	0.12	1.67		189	170			15	9	351						
GAM2-2	9.33	0.12	11.08	0.28		20.45	57.61	0.21	0.82		88	119			9	10	289						
GAM3-2	6.76	0.07	9.85	0.24		18.52	60.87	0.13	0.81	726	329	147				9	180						
GAM4-2	4.88	0.05	9.08	0.12		18.89	61.47	0.14	0.92		96	100			14	9	409						
Modern ostrich egg shell																							
MD5436a	1.87	0.02	6.55	0.02		20.15	57.62	0.22	1.34		78	109				9	137						
MD5436i	1.64	0.02	3.95	0.03		12.58	48.65	0.18	0.58	6306	179					9	105						
Modern ostrich egg shell, chemical analysis by WD-XRF																							
MD5436						0.55	99.31		0.23					16			245						
White bead, high fired ceramics																							
GAA-153	57.15	0.03	29.18	0.55			0.24	1.79				22	31	20		100	29				7		

Tab. 1 Results of chemical analysis by pXRF. One black bead made from obsidian is distinguished by its potassium content – sample GAA-024. All black beads made of quartz ceramics with black glaze are characterized by high levels of Fe and Mn. Black and white beads made from ostrich egg shells are characterized by very high levels of Mg and Ca. Chemical composition of contemporary ostrich egg shell: a = outer surface of shell, I = inner surface (chemical composition similar to beads found at Gala Abu Ahmed; the higher concentration of Si in ancient beads is attributable to the alteration process). Results of chemical analysis carried out by WD-XRF on the same shell only reveal the presence of Ca. White bead GAA-153 is a ceramic bead. X-ray diffraction analysis reveals the presence of mullite, indicating that this bead was fired at a high temperature.

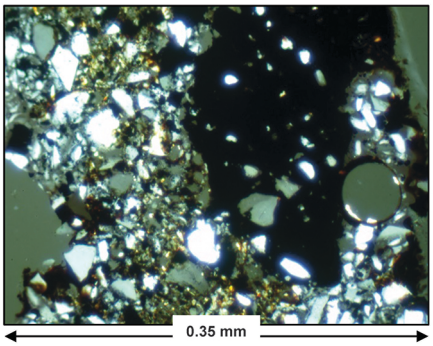

GAA-Pe4	SiO_2	TiO_2	Al_2O_3	Fe_2O_3	MnO	MgO	CaO	Na_2O	K_2O	Ba
	per cent by weight									
pXRF										
Pe4a	56.84	1.34		4.35	14.45		4.09		0.59	0.54
SEM-EDX										
Pe4-1	67.55		3.89	3.75	12.41		0.00	8.85	1.56	1.79
Pe4-2	70.57		3.42	4.65	12.37	0.37	1.38	3.19	0.63	1.95
Pe4-3	74.43		2.49	3.72	10.95		0.61	5.27	0.96	1.41

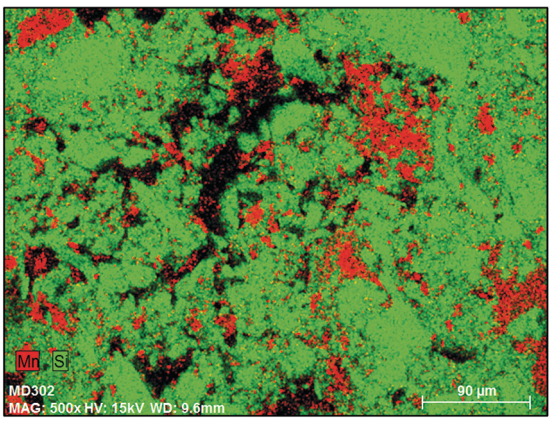

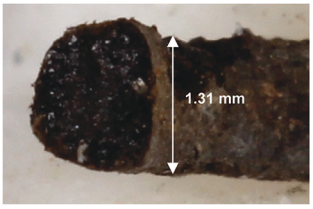

Fig. 3 Sample GAA-Pe4. This sample is from the group of beads which chemical composition analysis by pXRF showed to be distinctive in having high levels of iron and manganese. These beads vary in colour, appearing grey, brown-grey and dark brown when viewed using reflected light microscopy, and black or grey when viewed in daylight. One of the beads from this group is shown in this figure. It is a barrel disc bead with an asymmetrical profile. It is black and has a rough surface caused by the visible grain fragments protruding from it; it has a glassy sheen and exhibits grainy conchoidal fracture. Fine, unrounded, predominantly elongated quartz grains and black glass inclusions can be seen in thin-section (a). EDX analysis revealed that this is a soda glass with a high barium concentration of up to 1.9% Ba (adding BaO improves the mechanical properties of a glaze). Analysis results showed that this is a quartz ceramic bead with alkaline black glass: Na glaze with Fe and Mn as colorants (b = mapping showing Mn and Si). The black glass acts as a binding agent and as a surface glaze. Neither Na nor Al were detected by pXRF analysis, which also revealed a threefold lower Ba content.

a)

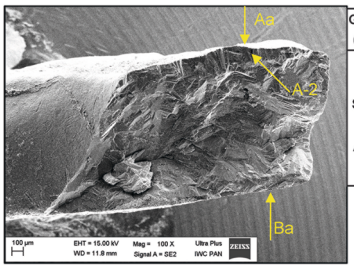

GAA 037	SiO_2	TiO_2	Al_2O_3	FeO	MgO	CaO	Na_2O	K_2O	P_2O_5	SO_3	Cl
	% by weight										ppm
pXRF											
Aa	12.61	0.05	8.69	0.17	13.8	61.6		0.10	0.67		65
SEM - EDX											
Aa	9.71		5.49	2.19	1.41	71.24	0.85	0.43	8.44	0.12	1200
A-2						100.0					
Ba	2.83		1.24		0.56	94.93			0.12	0.27	500

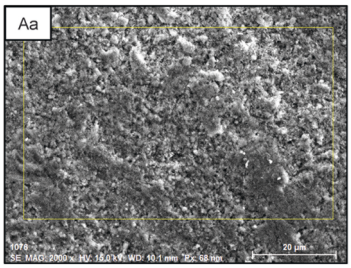

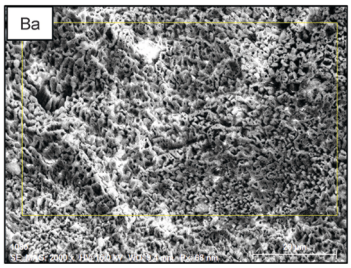

b)

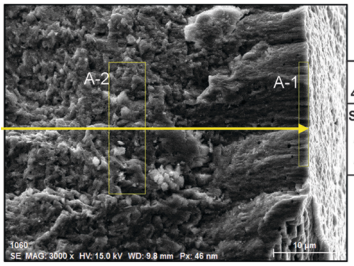

MD 4536	SiO_2	TiO_2	Al_2O_3	FeO	MgO	CaO	Na_2O	K_2O	P_2O_5	SO_3
	% by weight									
SEM - EDX										
A-1	0.25		0.32		8.86	87.55	0.95		2.01	0.06
A-2					1.71	96.89	0.91		0.49	

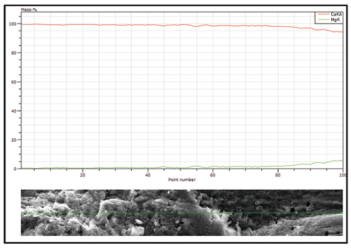

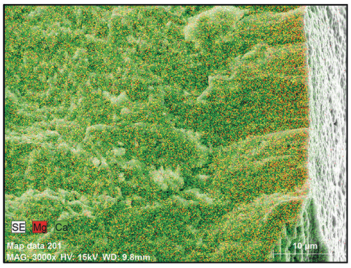

Fig. 4 Beads made from ostrich egg shells. a = bead GAA-037: a black bead made of an intentionally dyed ostrich egg shell. SEM-EDX analysis revealed differences in the concentration of Mg in the bead's cross-section; a higher Mg content is observed on one of the bead's surfaces than the other (1.41% and 0.56% MgO respectively), the chemical composition of its central portion is 100% CaO. There are significant differences between the results obtained by SEM-EDX and by pXRF analysis, particularly in the case of Mg and Ca levels. The results of pXRF analysis yield markedly exaggerated Mg levels. b = a similar Mg distribution is seen in contemporary ostrich egg shells (Mg varying from 8.86% near the egg shell's outer face to 1.71% at a depth of 40µm and down to 0% near the egg shell's inner face), the chemical composition of its central part is consistent with that detected by WD-XRF (100% CaO).

Illustration and table credits

ILLUSTRATIONS: 1 M. Daszkiewicz. 2 Photos by M. Baranowksi. 3–4 M. Daszkiewicz.

TABLES: 1 M. Dazkiewicz / M. Lahitte.

MAŁGORZATA DASZKIEWICZ

Małgorzata Daszkiewicz, MA Warsaw 1979 in Physical Geography, PhD Warsaw University 1993 in Humanities. Since 1994 she has worked in collaboration with *AG Archäometrie* FU Berlin. Formerly a part-time employee at TOPOI, she is currently an associated member of the Institute for Prehistoric Archaeology FU Berlin and also runs ARCHEA, a laboratory in Warsaw for archaeometric analysis and research. Her main research interests are determining the technology and provenance of archaeological ceramics and devising techniques for the classification of bulk ceramic finds.

Dr. Małgorzata Daszkiewicz
Freie Universität Berlin
Institut für Prähistorische Archäologie
Fabeckstraße 23–25
14195 Berlin, Germany
and
ARCHEA
ul. Ogrodowa 8m95
00-896 Warszawa, Poland
E-mail: m.dasz@wp.pl

MIRIAM LAHITTE

Miriam Lahitte is an archaeologist working since years in Sudan (Gala Abu Ahmed and Mograt island). Alumna and independent researcher at Humboldt University and Free University in Berlin.

Miriam Lahitte M.A.
Humboldt Universität zu Berlin
Archäologie und Kulturgeschichte Nordostafrikas
Unter der Linden 6
10117 Berlin, Germany
and Freie Universität Berlin, Lateinamerika Institut
E-Mail: miriamlahitte@web.de

RUDOLF NAUMANN

Rudolf Naumann, as a mineralogist (diploma in Leipzig), after work at the Bergakademie Freiberg, before he retired was the head of the laboratory for the analysis of rocks and minerals mainly using XRF and XRD, at the Geoforschungszentrum in Potsdam since 1979. He is co-author of numerous publications.

Dipl.-Min. Rudolf Naumann
Helmholtz Zentrum Potsdam
Deutsches GeoForschungsZentrum GFZ
Anorganische und Isotopengeochemie
Telegrafenberg, B 327
14483 Potsdam, Germany
E-Mail: ru-nau@t-online.de

Fleur Schweigart, Małgorzata Daszkiewicz

Cluster Analysis of Chemical Data vs. Matrix Classification by Refiring: Example of Imperial Period Wheel-Thrown Pottery from Olbia, Ukraine

Summary

In this article, the application of portable energy-dispersive X-ray fluorescence (pXRF), wavelength-dispersive X-ray fluorescence (WD-XRF), and matrix analysis by refiring (MGR-analysis) for the provenance study of ancient ceramics are discussed. This discussion focuses on the methodical approach and the specific considerations required for each technique, as well as the evaluation and interpretation of the data obtained. In particular, the potential and limits of cluster analysis of chemical data, the comparability of chemical data obtained by pXRF and WD-XRF, and insights from the results of the comparison with MGR-analysis are the main focus in this article.

Keywords: wheel-thrown pottery; Imperial Period; Olbia; pXRF; WD-XRF; cluster analysis; MGR-analysis

In diesem Artikel wird die Anwendung der pRFA, der WD-RFA und von MGR-Analysen für die Herkunftsbestimmung archäologischer Keramik diskutiert. Dabei stehen der methodologische Ansatz und die für jede Technik spezifischen Betrachtungen im Focus wie auch die Bewertung und Interpretation der erhaltenen Daten. Insbesondere sind die Möglichkeiten und Grenzen von Clusteranalysen chemischer Daten, die Vergleichbarkeit der mit pRFA und WD-RFA erhaltenen Daten und die Erkenntnisse aus dem Vergleich mit den Ergebnissen von MGR-Analysen das Thema dieses Artikels.

Keywords: scheibengedrehte Keramik; Kaiserzeit; Olbia; pRFA; WD-RFA; Clusteranalyse; MGR-Analyse

Morten Hegewisch, Małgorzata Daszkiewicz und Gerwulf Schneider (eds.) | Using pXRF for the Analysis of Ancient Pottery – an Expert Workshop in Berlin 2014 | Berlin Studies of the Ancient World 75 (ISBN TODO; DOI: 10.17171/3-75) | www.edition-topoi.org

1 Introduction

The following study is part of the Excellence Cluster Topoi research project "Wheel thrown pottery of the La Tène and Imperial periods".[1]

The project is targeting the examination of spatial distribution and economic distribution structures of wheel-thrown pottery of different predefined regions. For this particular study wheel-thrown pottery from Olbia (Ukraine) and its surrounding settlements was sampled.[2]

The sites in question are situated on the left and right bank of the lower Bug river, next to the Black Sea (Fig. 1). Wheel-thrown pottery of two different cultural origins was identified from these settlements: on the one hand pottery of the Graeco-Roman spectrum from the 1st to 3rd century AD (Fig. 2) and on the other hand pottery of the Chernyakhov spectrum of the late 3rd and 4th century AD (Fig. 3).[3] The Graeco-Roman spectrum contained only table ware, the Chernyakov wheel-thrown pottery was composed of tableware, kitchenware (e.g. pots) and storage vessels.[4] The tableware, which consisted, for example, of bowls, pots, jars and vases, differs typologically between the Chernyakhov and Graeco-Roman spectrum and is therefore clearly distinguishable.[5]

The aim of investigation was to reveal possible economic structures between these settlements in comparison with the respective cultural background.

For this purpose, various archaeometrical analyses were applied. First of all, chemical composition was analysed using the portable energy-dispersive X-ray fluorescence technique (hereafter referred to as pXRF).[6] Additional measurements were made using the wavelength-dispersive X-ray fluorescence technique (WD-XRF)[7] and examinations of the matrix were accomplished using MGR-analysis.[8]

All in all, 290 pottery samples collected by E. Schultze from ten different sites were analysed (Tab. 1) as were samples of three raw materials.

1 For further information regarding the project see: http://www.topoi.org/project/a-6-4/

2 All samples selected and classified by Dr. Erdmute Schultze (DAI Berlin)

3 Schultze, Magomedov, and Bujskich 2006, 318–319.

4 For a detailed insight into the pottery typology of the sampled sites see: Schultze, Magomedov, and Bujskich 2006, 295–322.

5 Schultze, Magomedov, and Bujskich 2006, 336.

6 Niton XL3t 900S GOLDD RF-Analyser; pXRF-analysis was made by Schweigart and Hegewisch.

7 Samples for the chemical analysis by WD-XRF were prepared by ARCHEA and measured by Schneider and Schleicher in GFZ Potsdam (GFZ = Helmholtz-Zentrum Potsdam, Deutsches GeoForschungsZentrum GFZ, Sektion 4.2, Anorganische und Isotopengeochemie).

8 MGR-analysis = Matrix Group by Refiring Daszkiewicz and Schneider 2001; Daszkiewicz 2014; Daszkiewicz and Maritan 2017 was made by M. Daszkiewicz, ARCHEA.

2 Analysis of chemical composition

The chemical composition of the sampled sherds was initially ascertained by pXRF (Niton XL3t 900S GOLDD RF-Analyser; mining mode; 8-mm spot; without helium, calibration on 12 ceramic standards by G. Schneider/M. Daszkiewicz).

Since the elements are scattered heterogeneously within the clay[9] and temper is capable of influencing the measured results,[10] it is recommended to run several pXRF measurements on different measurement spots. The result of this is the arithmetic means of these measurements.[11] Therefore each sample was measured at least thrice.

The pXRF-technique is often referred to as a non-destructive technique and, therefore, quite suitable for use on objects which cannot be destroyed. Nevertheless, the excavated pottery sherds required a specific type of preparation to minimise the effect of external influences on the chemical composition of analysed sherds (changes during use and/or alteration effect). For this purpose, two different preparation methods can be used:

– preparation of the surface for measurement by mechanical removal of the sherd's outer surface layer (the cleaned surface must be no smaller than the measurement spot aperture).

– preparation of the surface for measurement by creating a fresh break.

When using the first preparation method it must be remembered that the type of material from which the abrasive tool is made can affect the measurement result. An abrasive tool made of corundum is optimal because of its hardness and chemical composition. If other tools are used, the composition of the abrasive material should be determined before beginning the preparation process to check which elements could contaminate the sherd. Furthermore, once the surface has been removed, the sample should be rinsed in an ultrasonic cleaner in order to remove any contaminants from its open pores. This is time-consuming though not impossible to do when analysing fragments of pottery, but in the case of complete vessels it not really a feasible option.[12]

In order to assess what impact the use of a material other than corundum would have on the chemical composition results obtained from the analysed ceramic fragments M. Hegewisch made measurements on 61 sherds (mainly from Kozyrka, Tab. 1) having

9 Mecking, Mielke, and Behrendt 2013, 58–60.

10 Mecking, Mielke, and Behrendt 2013, 55.

11 The mean should not be calculated automatically; each measurement should be verified.

12 Daszkiewicz and Schneider, who have since 2009 been using pXRF to determine chemical composition in their analysis of ancient ceramics, believe that measurements should preferably be made on fresh breaks and that corundum should be the only abrasive material used.

first removed the outer layer of each one using an abrasive material widely available in DIY shops. A thin layer of about one millimetre was abraded to create a measurement spot.

F. Schweigart then made measurements on fresh breaks of the same samples. To do this a small break was created by using tile nippers with tungsten-carbide cutting blades. Table 2 shows a different material when analysed by pXRF (though theoretically the same) was used for the abrasive disc grinder and cylindrical tool. Analysis reveals that the composition of the coating of the tools differed significantly even though the abrasive material is theoretically the same (corundum). These were unexpected results for a composition of binding materials for corundum grains (e.g. 24% of CaO, 1500 ppm V or 8800 ppm Cr!).

Differences in chemical composition for each element when measured on fresh breaks or on polished surfaces were compared by using the coefficient of variation (cv). Figure 4 presents the average values of coefficient of variation (cv) in percent (grey dots), while the perpendicular lines show the range of cv values from minimum to maximum between the results for each element. Average cv values of less than 5% are observed for levels of Si, Ti, Fe, K, Rb, Zr and Nb, and over 10% for Mn, Ca, P, Zn, Ba and Pb. Although the increased Ca content could be attributable to contamination, the same does not apply to the differences in the levels of P and Ba because there is very little of these two elements in the abrasive material.

Comparison of the pXRF data with the results of samples measured with WD-XRF[13] (data recalculated to a dry basis) showed, in some cases, quite obvious differences between both preparation methods (Figs. 5 and 6). Especially in the case of P_2O_5 a measurement surface created by mechanical removing an outer layer could not prevent a high range variance (up to 93%) between the pXRF and WD-XRF results (with the arithmetic mean at 30.25%). The fresh-break method created much better results (according to the WD-XRF comparison), with an overall variance up to 35.51% and an average cv of 18.30% (which would still lead to an exclusion of these data for statistical analysis).

Another clear difference showed up in the case of CaO. The overall variance with a polished measurement spot (up to 30.24% with an average cv of 12.84%) was not quite as prominent as in the case of P_2O_5 but still differed noticeably from the fresh-break results (maximum variance: 10.34% and average cv of 2.80%).

13 Samples for chemical analysis by WD-XRF were prepared by pulverising fragments weighing *c.* 2g (sample size was determined by the number and size of the non-plastic components), having first removed their surfaces and cleaned the remaining fragments with distilled water in an ultrasonic device. The resulting powders were ignited at 900°C (heating rate 200°C/h, soaking time 1h), melted with a lithium-borate mixture (Merck Spectromelt A12) and cast into small discs for measurement. This data is, therefore, valid for ignited samples but, with the ignition losses given, may be recalculated to a dry basis. When comparing WD-XRF results with pXRF results the WD-XRF results should be recalculated to a dry basis due to the fact that the pXRF measurements concern original and not ignited samples.

The Ba results were in both cases (surface removal and fresh break) beyond reliable according to the comparison with the analogue WD-XRF results. As already stated earlier, the increased Ca content is potentially attributable to the abrasive material, unlike the levels of phosphorus and barium. The most likely explanation for this effect would be that preparation by polishing the measurement surface cannot sufficiently prevent the influence of alteration effects on the measurement results if too thin a layer is removed from the sherd surface. The experiment undertaken showed that, because of the potential of alteration effects as well as 'surface contamination' due to the polishing instrument used, more satisfactory results are obtained from measurements on fresh breaks.

Interestingly, in the case of Fe_2O_3, MnO, Zn and Y content the polishing preparation method delivered slightly better results (meaning that the results were closer to the results obtained using the WD-XRF technique). In the case of MnO and Y the average cv with the fresh-break preparation method was higher than 10%.

Regardless of the type of measurement spot preparation, further general reasons for the apparently low measurement reliability for some elements using the pXRF technique are, for example, the low penetration depth of the radiation[14], respectively a lower information depth of lighter elements[15] (elements with a low atomic number, such as Mg or Al). For this reason some elements are not measurable (Na) or can rarely be measured and only with great error (Mg) using the portable technique. Another role, especially in measurements on polished surfaces, is played by the depositional environment, which can result in storage and leaching of elements, which in turn leads to changes in chemical composition (this most often applies to P, Ba, Ca, Sr, Mn, Na and Fe).[16]

In every case, the comparison of WD-XRF results with pXRF results showed the reliability of the pXRF technique. The Ba results were in both cases (removed outer layer and fresh break) beyond reliable according to the comparison with the analogue WD-XRF results. This result is not surprising because Ba (together with P_2O_5) is highly susceptible to alteration effects.

This calculation for each element allowed the decision regarding which elements should be excluded in the following statistical evaluation. This comparison should be performed for every new study once again.

3 Statistical evaluation of chemical data

In order to combine the samples into groups with similar features based on their chemical composition a hierarchical cluster analysis was applied. The following elements

14 Schneider and Daszkiewicz 2010, 110–111.

15 Mecking, Mielke, and Behrendt 2013, 55.

16 Daszkiewicz 2014, 178.

were – according to the previous comparison (Figs. 5 and 6) – selected for usage in the statistical evaluation of pXRF data: Si, Ti, Al, Fe, Ca, K, V, Cr, Zn, Rb, Sr, Y, Zr, Nb.

It is recommended to consider the different existing cluster techniques regarding their suitability for the present data and question. Here, the obvious techniques would be Average-Linkage or Ward.

In the present case, the Ward's method was selected for agglomerative hierarchical clustering of a distance matrix (distance measure type – squared Euclidean distance, transformation of data in SPSS: reference range -1 to 1). In contrast to other clustering techniques (e.g. Average-Linkage, Complete Linkage, Single Linkage), the Ward's method creates groupings with the help of a defined heterogeneity measure. That is, by adding objects to a group, the sum of the variance within the group should increase as little as possible, which leads to particularly homogeneous groups.[17]

However, for the interpretation of the result it has to be regarded that the Ward's method tends to build equal-sized groups. This means that there is a possibility that minor groups can be "swallowed" within a larger cluster.[18] However, further studies from other projects have shown[19] that the Ward's method is principally able to create minor groups as well.

Also, the prior removal of "outliers" is important[20] but this is true for other techniques (e.g. Average Linkage) as well. This is necessary because outliers will affect the formation of the clusters and distort them, in most cases significantly. These outliers have to be considered separately.

Outliers can easily be detected with the so-called 'Single-Linkage-Technique' – a hierarchical cluster analysis with the tendency to build 'chains' instead of real groups. Outliers will appear at the end of the chain in the dendrogram. Especially when dealing with a great amount of data this preliminary test can be very helpful.

After the elimination of samples with pXRF outlier values, 255 samples were available for the statistical cluster analysis.[21]

The final decision to use the Ward´s method was made based on two initial steps which should always be performed in order to verify the quality of separation of clusters with a certain technique. The first step is to assign the approximate number of clusters with the help of the so-called 'elbow-criterion' (elbow shaped conjugation in the graph error sum of squares per merging step).

17 Backhaus et al. 2006, 522.

18 Backhaus et al. 2006, 528.

19 Fleur Schweigart. „Distributionssysteme kaiserzeitlicher Drehscheibenkeramik zwischen Elbe und Oder (Arbeitstitel)". Dissertationsprojekt in Bearbeitung.

20 Backhaus et al. 2006, 528.

21 A simple omission of a single outlier value is not possible in a cluster analysis by using the SPSS program, as here single missing values are leading to a general omission of the entire sample in the calculation.

This elbow is not always clearly recognisable and does not lead to an unambiguous result in every case, as indeed was the case in the present study. Here, using the Ward´s method the conjugation of the graph was detected somewhere between a three- and a five-cluster-solution for the pXRF data (Fig. 7).

With this approximate value the verification of the actual cluster number can be refined in the next step by a scatterplot matrix. Based on the performed scatterplot matrix, the four-cluster solution for pXRF data was selected since it showed the best possible cluster separation (Fig. 8). Particularly in the case of the Fe_2O_3/CaO matrix the separation of groups became quite visible.

In comparison, the Average-Linkage method provided a result which was not at all satisfactory. Here, the elbow criterion mostly indicates a 3-cluster solution with two major groups and one minor group containing only a single sample (Figs. 9 and 10).

This picture would have still remained by choosing a higher number of clusters (always two main clusters and further minor clusters consisting only of isolated samples). The two main clusters were thus very broad ranged in their composition (Fig. 10). Here, the Ward's method delivered the more precise clustering.

Therefore, for this study, Average-Linkage was not the favoured method. With another data set different conclusion may have been reached.

This described strategy would be the *statistically* correct approach for the clustering of data. However, a statistical evaluation will never completely substitute the independent interpretation of data. The question is, therefore, to what extent do the calculated clusters (for pXRF as well as for WD-XRF data) provide a reliable result in terms of grouping the analysed pottery according to the provenance of the raw materials used for making this pottery. To pursue this question, the results of an independent method (here the classification of the sherd matrix by MGR-analysis) were included in the evaluation.

4 MGR-analysis

MGR-analysis is done by firing fragments of pottery in controlled, standardised conditions[22] at a temperature exceeding that of the original firing, and subsequently assessing the appearance of the refired sample. The thermal behaviour of a pottery sherd refired at

22 In this instance four thin slices were cut from each sample in a plane at right angles to the vessel's main axis. One of these sections was left as an indicator of the sample's original appearance, whilst the remaining three were fired in an electric laboratory chamber furnace, each one at a different temperature. Firing was carried out at the following temperatures: 1100, 1150 and 1200°C in air, static, with a heating rate of 200°C/h and a soaking time of 1h at the peak temperature. The fragments were then glued on to paper.

a higher temperature than that of its original firing depends solely on the chemical and phase composition of the ceramic body. This makes it possible to classify samples by matrix type (the matrix being the plastic part of the ceramic body which hardens on firing) and hence also by the type of clay raw material used. Raw materials can be classified using abridged MGR-analysis, which consists of refiring at only three temperatures.[23]

The thermal behaviour of the sample refired at three temperatures (1100°C, 1150°C and 1200°C) is taken into account when defining different MGR-groups (the term 'group' is used even when groups are each represented by only a single sample[24]). Definitive classification is based on thermal behaviour at 1200°C. If samples display the same appearance, colour and shade after refiring at 1200°C this indicates that they were made using the same plastic raw material. All ceramic samples belonging to the same MGR-group were made of the same clay, or of the same ceramic body in those cases where they also belong to the same non-plastic material group. If samples of one MGR-group belong to the same non-plastic material group their chemical composition is the same. Figure 11 shows two samples before and after refiring. These samples were removed from a ceramic sherd discovered in Olbia (O-89) and from a sherd found in Novokondakove (Nk-3). Both samples belong to the same MGR-group and the same clastic-material group; as can be seen in the accompanying table, the chemical composition (determined by WD-XRF) of both sherds is the same (Table in Fig. 11). If samples of one MGR-group do not belong to the same non-plastic material group their chemical composition is not the same. Figure 12 shows two sherds made from the same clay. One of the sherds has no macroscopically visible non-plastic particles, whilst the other features non-plastic particles mostly comprising grains of quartz in coarse sand fraction (some in gravel fraction), which affects the chemical composition.

5 Results of MGR-analysis

In contrast to projects where a down-up sampling strategy[25] is employed and MGR-analysis is the first analytical procedure carried out, in the OLBIA project chemical analysis using pXRF was the first technique used. Next, after completion of cluster analysis,

23 So-called full MGR-analysis (refiring at nine temperatures) enables an estimate to be made of the original firing temperature range (indicated by a change in the colour of the refired sample in relation to the original colour of the sample); see Daszkiewicz and Maritan 2017; Daszkiewicz 2014.

24 It is unlikely that only a single vessel was made from one ceramic body, hence it is assumed that the sample submitted by archaeologists for analysis represents a group of vessels made from the same material. It is for this reason that the term 'group' is used even in relation to those groups which are represented solely by one sample.

25 See e.g. overview article Daszkiewicz 2014.

104 ceramic sherds were selected for MGR-analysis. This analysis revealed several instances where the same CaO levels were recorded in sherds made of calcareous clays as in sherds made of non-calcareous clays in which the CaO content is not linked to the presence of carbonates in the matrix (Fig. 13). These samples were attributed to the same chemical cluster. In order to investigate further, additional MGR-analysis was carried out on all ceramic sherds for which pXRF analysis revealed a CaO content of over 5%. Thus, MGR-analysis was carried out on a total of 216 ceramic sherds, including additional analysis of three fragments that had already been examined as part of the first analytical series (samples were removed from two different places). Heterogeneity of the ceramic body was not observed in the sherds fired as reference samples[26] (Fig. 14). In one instance, the macroscopically visible differences in fabric (grey and brown) are attributable to the firing process (Fig. 14, sample ES-StB-2).

Figure 15 shows examples of different matrix categories and matrix types. Based on the colour of samples after refiring, three fundamental categories of matrix can be identified: non-calcareous, coloured by iron compounds[27] (samples Ak-21, Ak-18, Nk-2, Pt-23, Pt-20, Stv-9, Koz-72, ZjM-7, Stv-11), calcareous[28] (samples Nk-8, ZjM-53), and mixed[29] (O-43). Different colours and shades can be distinguished within each category of matrix.

Sherds made of non-calcareous clays are coloured to varying degrees by iron compounds; the intensity of the colour is not directly proportional to the Fe_2O_3 content determined by chemical analysis. In the first two samples shown in figure 15 (Ak-21 and AK-18) the Fe_2O_3 content is less than 3% (so-called pale-firing samples). In sample Nk-2 and sample Pt-23 the Fe_2O_3 content is practically the same (4.43% and 4.32% respectively), though the first of these samples fired brick-red whilst the second fired dark reddish-brown, indicating that Fe occurs in different phases.

Two of the samples shown in Figure 15 are made of non-calcareous clays enriched with carbonates in sub-10 µm fraction. The CaO content of sample ZjM-7 is 8.78%, while that of sample StV-11 is 6.95%, and it is almost entirely attributable to the presence

26 In addition to the archaeological samples, reference samples are also included with each firing to monitor firing reproducibility, which is particularly important when ceramic series from the same site are fired several years apart (in theory the temperature in modern laboratory chamber furnaces ought to be stable; however, this type of check is still carried out).

27 Samples were deemed to have a non-calcareous matrix if no calcium silicate or calcium aluminium silicate phases formed during laboratory refiring in air at a temperature of 1200°C, which was indicated by the fact that the samples did not adopt a greenish tint.

28 Samples were said to have a calcareous matrix if calcium silicate or calcium aluminium silicate phases formed during laboratory refiring in air at a temperature of 1200°C, indicated by the fact that the samples became green in colour (or had a greenish tint).

29 Samples were considered to have a mixed matrix if various irregularly distributed patches of colour were noted in the fabric after refiring.

of carbonates in the matrix; only negligible aggregates of calcareous clays in sand fraction are observed.

Sherds made of calcareous clays (samples Nk-8 and ZjM-53) take on distinctly different colours when fired already at 1100°C in comparison to sherds made of non-calcareous clays. The CaO content of these two samples (10.86% and 21.11% respectively) is linked to the plastic part of the ceramic body. The mixed matrix category shown in Figure 15 is represented by sample O-43. A mixture of two clay types is clearly visible after refiring at 1150°C. In the case of pottery discovered in Olbia two types of clay mixtures are observed: either with a predominance of non-calcareous clay coloured by iron-compounds (Fig. 16 sample O-3) or a predominance of calcareous clay (Fig. 16 sample O-93).

Within the matrix categories described above, the following matrix types were identified based on the appearance of samples when refired at 1200°C: sintered matrix type (SN)[30]; over-fired (ovF)[31]; very slightly over-melted (vsovM)[32]; slightly over-melted (sovM)[33]; over-melted (ovM)[34]; semi-melted (sMLT)[35]; melted (MLT).[36] In addition, some samples also exhibit bloated behaviour (BL)[37]. A number of samples are slightly over-melted or over-melted already after refiring at 1150°C (Fig. 15, samples Pt-23, ZjM-7 and Stv-11).

The results of MGR-analysis demonstrate that various clay types were used to make the analysed pottery. Additionally, after refiring it is possible to make a more reliable estimate of the type and quantity of non-plastic ingredients present in the ceramic body. Figure 17 shows sherds in which non-plastic inclusions are much easier to assess macroscopically after refiring, and in which recognising two different clays within the matrix is virtually impossible before refiring (Fig. 17, sample O-12).

Of the 216 analysed samples, 64 are made from five types of calcareous clays (CC1–CC5). The majority of the calcareous clay samples are made of CC1 clay (52 samples), nine samples are made of CC2 clay, one each of CC3 and CC5 and two samples are made of CC4 clay. Various non-calcareous clays enriched with carbonates are represented by 63 sherds, 13 samples are made of mixed clays, 69 samples are made of non-calcareous clays coloured to varying degrees by iron compounds, ten samples exhibit features of both mixing and alteration and could not be definitively classified.

30 The sherd is well-compacted; it may or may not become smaller in size in comparison to the original sample, whilst its edges remain sharp.

31 The sample changes in shape, bloating, however, does not occur, nor does the surface of the sample become over-melted.

32 The surface of the sample becomes very slightly over-melted and its edges very slightly rounded.

33 The surface of the sample becomes slightly over-melted and its edges slightly rounded.

34 The surface of the sample becomes over-melted and its edges slightly rounded.

35 Over-melting of the surface occurs, changes in sample shape are noted (not just rounded edges) but no bloating.

36 The sample becomes spherical or almost spherical in shape.

37 The sample slightly expands in volume.

The MGR-analysis results presented above clearly indicate that the examined pottery was made using a variety of non-calcareous clays coloured by iron compounds (only a few MGR-groups are represented by more than one sample) and also that various recipes[38] were used. The opposite is true of pottery made from calcareous clay, where there is a predominance of vessels made using one particular type of clay – CC1 (81% of the total number of vessels made from calcareous clays).

Of the 216 samples examined through MGR-analysis, 41 were also subjected to chemical composition analysis using WD-XRF. Figure 18 shows these samples after refiring at 1150°C divided into matrix categories and matrix types. Various calcareous clays were identified (first column, CC), as well as a range of non-calcareous clays variously enriched with carbonates in the matrix (second column and top of third column, NC cc), non-calcareous clays slightly coloured by iron compounds (third column: NC Fe-) and various non-calcareous clays coloured by iron compounds (NC). Some of these samples belong to the same MGR-groups: MGR 14 (O-48, O54, Pt-16), MGR 51 (O-29, O-81, O-114), MGR 40 (samples Nk-6, Nk-3, O-89, O-103, O-105) and MGR 24 (samples Stv-8 and Stv-9). MGR grouping correlates very well with the results of chemical analysis by WD-XRF and differences in chemical composition between the individual MGR-groups are clear (Tab. 3).

5.1 Comparison of WD-XRF-cluster with MGR-groups

For the clustering of WD-XRF data (Fig. 19), the same approach as for the clustering of pXRF data (as described above) was performed. However, more elements (Mn, Mg, Na, Ni) were included. The cluster analysis contained the elements Si, Ti, Al, Fe, Mn, Mg, Ca, Na, K, V, Cr, Ni, Zn, Rb, Sr, Zr.

In contrary to the 4-cluster solution with pXRF data, the Ward´s clustering of the WD-XRF data resulted in a 5-cluster solution (Fig. 19 and Tabs. 3 and 4). Similar to the pXRF clusters the separation of the WD-XRF cluster was among other dependable on the Ca amount in % (Figs. 20 and 21), together with especially Al, Fe and Mg (as it will be discussed below).

On Figure 22 are shown samples after refiring at 1150°C in order of the calculated WD-XRF clusters (see dendrogram Fig. 19 and Tab. 4).

For the following description of clusters see also Tab. 4.

WD-XRF cluster 1 contained mostly samples made of non-calcareous clays with CaO contents up to 5% (with the exception of sample O-103 with a slightly higher CaO

38 Recipe = the ratio of plastic ingredients to intentionally added non-plastic ingredients in the ceramic body.

value of 6.96%). The samples in cluster 1 showed a quite similar Fe_2O_3 amount (more than 4 but less than 5%).

In contrary to cluster 1, WD-XRF cluster 2 contained samples with higher CaO amount (between 5.18–13.86% CaO). Misclassified appeared therefore on first sight sample "clay 2" within this group with its low CoO amount of 0.88%.

WD-XRF cluster 2 is a good example for the limitations of grouping of ancient pottery according to chemical composition. Cluster 2 contained – with the exception of sample "clay 2" – to nearly equal parts samples made of two different clay phases, namely calcareous (CaO 11.8%–13.86%) and non-calcareous clays with carbonate inclusions (CaO 5.5–9.98%). Therefore, these samples could not truly appear in the same group, since made of completely different clay types, nevertheless according to cluster analysis of chemical composition they do.

In this case, calcareous clay MGR-group CC 1.1 was exclusively connected to WD-XRF cluster 2. On the other hand, various non-calcareous MGR-groups (40, 51, Y3) were allocated in cluster 2 as well. The connection of these different samples within the same group was obviously in the first instance due to their similar Al, Fe and Mg values respectively their combination (for example cluster 4 features similar Mg values but is combined with lower Al and Fe values than samples connected to cluster 2). This Al, Fe, Mg – correlation is also the obvious reason for the allocation of sample clay 2 within this group despite its very low CaO amount.

This is true also for sample ZjM-7. The only recognizable indication for this in the chemical composition is the slightly higher K_2O value (4.02%; other samples of this group vary between 3.03–3.81% K_2O), which is also the second highest K_2O value measured with WD-XRF (highest value outliner sample ZjM-8 with K_2O = 4.90%).

Cluster 3 is insofar consistent as it only contains samples of the same clay type (NC clay according to MGR-analysis). It contained MGR-groups 7, 24 and 17. Chemically 'outstanding' is sample O-33 due to its lower Ti2O value (0,657%) and higher CaO amount (4.59%). The other samples of this cluster range between 0.725–0.994% TiO2 and 1.30–2.44% CaO.

Cluster 4 is again composed of samples with elevated CaO rates (7.02–21.11%). It differs chemically to cluster 2 due to slightly less Al, Fe and Mg values. Within cluster 4 are appearing the calcareous MGR-groups CC 1.2, CC3 and CC4 together with samples made of non-calcareous clay with carbonate inclusions.

Finally, cluster 5 is near-complete composed of samples of MGR-group CC2 (with the exception of sample Stv11). Again, the CaO amount is elevated in this cluster (6.95–10.86%), with less content of Fe (4.00–4.98%) and Al (10.64–12.84%).

To sum it up, the comparison of MGR-groups with the statistical WD-XRF cluster showed, that clustering can give an indication, but of course cannot show the real precise groupings of ceramic samples.

Same MGR-groups were at least associated to the same WD-XRF cluster, with one exception in case of MGR-group 40. Samples O-89 and Nk-3 were allocated in cluster 2, whereas O-105 and O-103 were connected to cluster 1. Here, the obvious explanation is the change of chemical composition due to temper.

As can also be seen in Fig. 12 and Fig. 13 the samples O-103 and O-105 were coarse tempered, samples O-89 and Nk-3 not. Although according to MGR-analysis all these mentioned samples were made of the same clay (MGR group 40), but the chemical composition of the coarse tempered samples was changed due to dilution effect (higher Si value due to quartz grains leads to lower percentages of the remaining elements in the analysis results). Therefore, the cluster analysis did not 'regard' them as identical to the non-tempered samples.

The exclusion of coarse tempered samples might solve this problem. However, the MGR-analysis revealed that in some cases temper grains, which were not visible in the first place, only appear in sight after refiring (Fig. 17). Therefore, 'hidden temper' can be considered a possible failure source by using the XRF technique.

5.2 Comparison of pXRF with WD-XRF cluster and analogue MGR results

On Figs. 23–27 are shown all samples analysed by MGR (samples after refiring at 1150°C) belonging to the particular pXRF clusters (Figs. 28 and 29).

A direct correlation of pXRF and WD-XRF cluster is not possible, since the clustering resulted in different cluster numbers (pXRF: 4-cluster solution; WD-XRF: 5-cluster solution). The correlation of samples associated to the respectively XRF clustering can be seen in Tab. 5.

WD-XRF cluster 1 contained for example mostly samples of pXRF cluster 3 and 4, WD-XRF cluster 2 was consisted of samples of pXRF cluster 1 and 2 and so on (Tab. 5 and colours in Boxplot Figs. 30 and 31). Only WD-XRF cluster 5 matched pXRF cluster 3 completely.

It appears also, that with the pXRF-data there was a slightly higher emphasis on the CaO amount for the grouping than with the WD-XRF cluster (Figs. 30 and 31).

pXRF cluster 2 contained therefore for example the majority of calcareous clay samples, additionally to a lesser extent samples of NC cc and mixed clays. pXRF cluster 2 is mostly represented in WD-XRF cluster 2 and 4. MGR groups CC1, CC3 and CC4 were aggregated in pXRF cluster 2, and separated in WD-XRF cluster 2 and 4 (see chapter above).

The separation of the calcareous MGR-groups CC1 and CC2 worked in both cases: pXRF: CC1 near-complete in cluster 2 and CC2 only in cluster 3 (Fig. 29 and Tab. 3), WD-XRF: CC1 completely in cluster 2 and CC2 only in cluster 5.

Apart from that, the connection of same MGR-groups to the same cluster worked

with the pXRF data as well (again with the exception of MGR-group 40; Tab. 3 and Tab. 4).

The pXRF clustering deals with the same issues as already discussed at the comparison of WD-XRF and MGR-groups. Again, there are no precise ceramic groups identifiable, rather than a more or less coarse overview.

5.3 Comparison of the results of analysis with archaeological parameters

The comparison of the archaeological parameter with the results of the applied analyses lead to the following results:

1. Samples made of calcareous clay (CC) were mostly associated with the Graeco-Roman spectrum, wherease Chernyakhov pottery was mostly made of non-calcareous clay (NC) and non-calcareous clay with calcit in matrix (NC cc). Here, a cultural induced difference regarding the usage of raw clays could be detected (Fig. 32).

2. Furthermore, the majority of the Graeco-roman pottery, which was modelled from calcareous clay was manufactured out of the same specific clay (MGR-group CC1.1).

Graeco-roman pottery belonging to MGR-group CC1 could be detected in Olbia, Kozyrka, Stara Bodanivka, Radsad and Zolotoyi Mys (Tab. 6). MGR-group CC1 could also almost entirely be detected on pottery, which was assigned to the earlier Graeco-Roman spectrum. There were a few exceptions in Petukhivka, Kozyrka and Olbia (Chernyakhov pottery made of MGR-group CC1 pottery).

On the contrary, the Graeco-roman pottery made of non-calcareous clay did not show any certain distribution between the sites (Tab. 5).

3. Chernyakhov pottery made of non-calcareous clay has shown a quite big variability within. Like before, none of the various Chernyakhov non-calcareous MGR-groups (with just two exceptions) were found in two different sites, but were rather connected to just one single site (Tab. 6).

The matching samples found in Novokondakove and Stara Bogdanivka (MGR group X3) provided a single matching sample each. This is to less a mass to assume a possible purposeful exchange respectively trade between the sites in question.

There were also all in all 8 matching samples found in Olbia and Novokonakove (MGR group 40) with six vessels in Olbia and two vessels in Novokondakove made from the same clay.

That means, (apart from probably MGR group 40) the Chernyakhov non-calcareous wheel-thrown pottery in the investigated area was obviously a local production, no distribution could be determined. Since there are various different clay types connected to each site, the interpretation might show evidence of various local workshops respectively a household production within the sites.

4. As already stated, the minority of Chernyakhov pottery was made of calcare-

ous clay and in these cases a certain distribution could actually be detected (e.g. CC2 Chernyakhov pottery was found in Olbia, Kozyrka, Adzhikolska Kosa, Petukhivka and Novokondakove, Tab. 4).[39]

6 Conclusions

In general, the evaluation of chemical composition (with clustering) is a suitable technique for an initial overview of data. However, a statistical technique never substitutes the independent interpretation of said data. More so, since the pure statistical evaluation is often providing a quite limited result, as was proved in this particular study. For further conclusions, the knowledge of more facts regarding the samples, in this case the archaeological parameters (cultural context, classification, archaeological site), is necessary.

In every case, a final conclusion and confirmation of the results required additional application of further analysis (here: WD-XRF, MGR). The comparison of the chemical data with the results of the MGR-analysis showed for example, that samples with similar chemical composition are not automatically made of the same clay or ceramic body, as different mineral phases could have similar chemical composition (e.g. Ca and Mg contents in magnesium rich calcite and dolomite).

Additionally problems occur when samples contain high amount of CaO. Such samples sometimes were made not of calcareous clay at all, as would be the first conclusion, but non-calcareous clays with carbonates in the matrix or in the non-plastic part of the body as carbonates aggregates (sometimes only visible after refirng). The single consideration of chemical data would have led to a false conclusion in these special cases. Generally, up to 5% CaO (measured per pXRF) the clay can be adressed as non-calcareous, and data beyond 12% CaO points to calcareous clay. Problematic are samples were in pXRF data CaO contents is between 5 and 12%.

The comparison of the described analysis with the added archaeological parameters was sketching a quite detailed picture. That is, with the help of the combined analyses, a cultural induced difference between Graeco-roman pottery and Chernyakhov pottery could be recognized regarding their production and distribution patterns.

All in all, the combination of archaeological data and archaeometric analysis has proven to be quite successful. If possible, during examination per pXRF it is highly recommended to apply additional archaeometric analyses to confirm the grouping.

39 For the results of the analysis see also Meyer et al. 2016, 204–209.

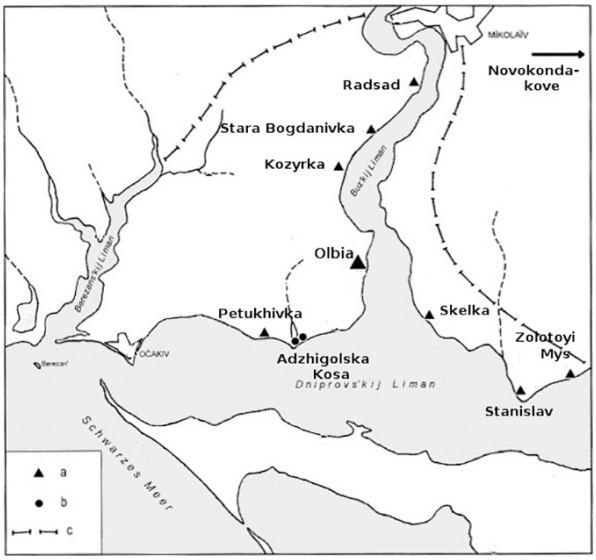

Fig. 1 Localisation of sites from which pottery samples have been analysed. (a) hillforts (b) rural settlements (e) border of the chora of Olbia (revised map after Schultze, Magomedov, and Bujskich 2006, Fig. 1).

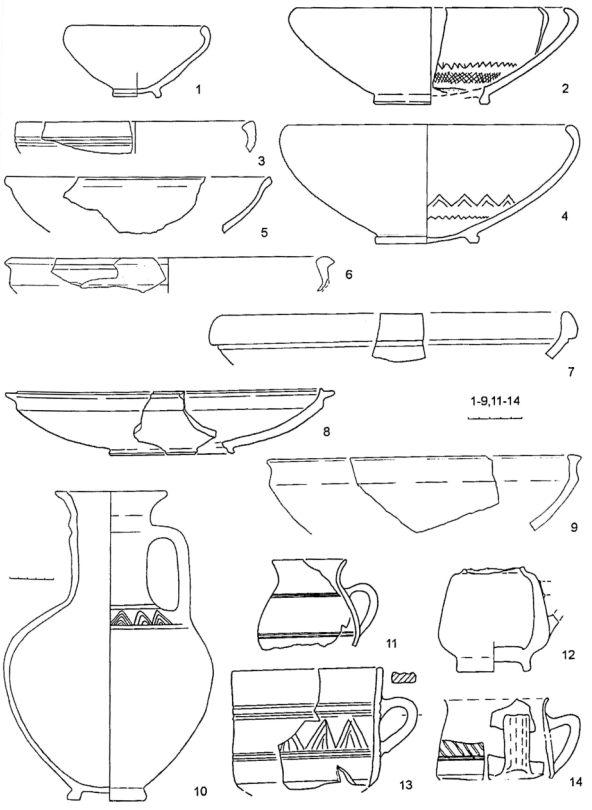

Fig. 2 Graeco-Roman pottery (1st–3rd century AD) from Olbia and its surroundings (after Schultze, Magomedov, and Bujskich 2006, Fig. 25).

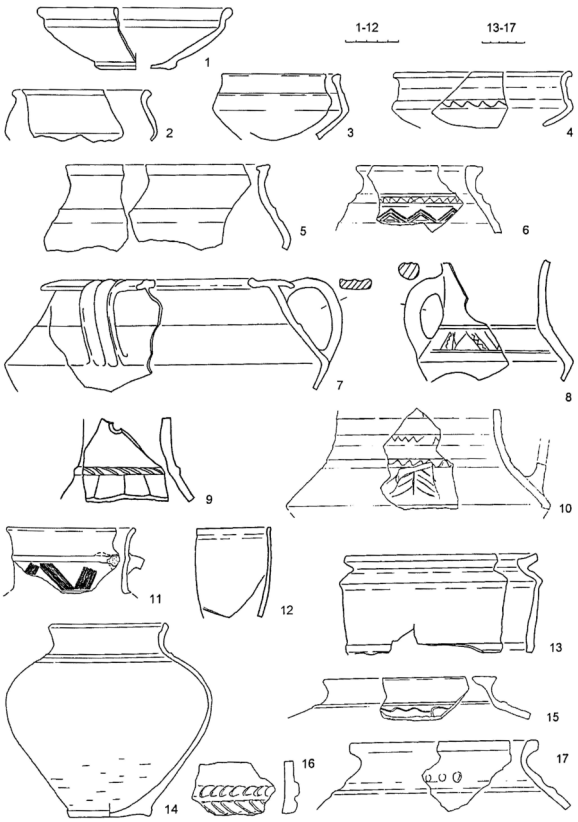

Fig. 3 Chernyakhov pottery (3rd–4th century AD) from Olbia and its surroundings (after Schultze, Magomedov, and Bujskich 2006, Fig. 26).

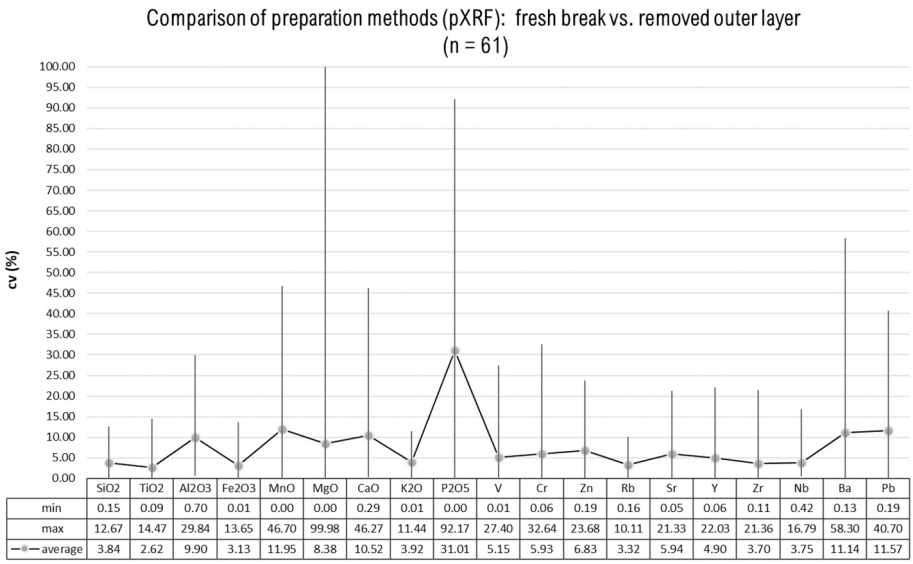

	SiO2	TiO2	Al2O3	Fe2O3	MnO	MgO	CaO	K2O	P2O5	V	Cr	Zn	Rb	Sr	Y	Zr	Nb	Ba	Pb
min	0.15	0.09	0.70	0.01	0.00	0.00	0.29	0.01	0.00	0.01	0.06	0.19	0.16	0.05	0.06	0.11	0.42	0.13	0.19
max	12.67	14.47	29.84	13.65	46.70	99.98	46.27	11.44	92.17	27.40	32.64	23.68	10.11	21.33	22.03	21.36	16.79	58.30	40.70
—■— average	3.84	2.62	9.90	3.13	11.95	8.38	10.52	3.92	31.01	5.15	5.93	6.83	3.32	5.94	4.90	3.70	3.75	11.14	11.57

Fig. 4 Comparison of preparation methods: pXRF results received twice for the same sample by measurements on fresh breaks and on vessel surfaces after removing a thin outer layer.

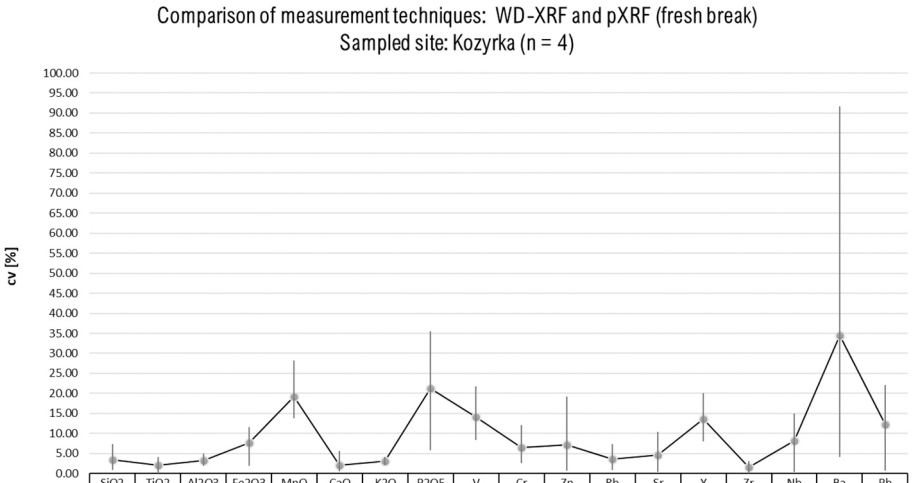

	SiO2	TiO2	Al2O3	Fe2O3	MnO	CaO	K2O	P2O5	V	Cr	Zn	Rb	Sr	Y	Zr	Nb	Ba	Pb
min	0.92	0.11	1.85	1.90	13.75	0.51	2.05	5.85	8.35	2.59	0.68	0.80	0.35	7.93	0.09	0.31	4.16	0.65
max	7.33	4.11	5.03	11.55	28.18	5.64	4.12	35.51	21.76	12.05	19.26	7.25	10.42	20.04	3.01	14.94	91.73	22.11
average	3.36	2.06	3.28	7.73	19.26	2.09	3.11	21.21	14.12	6.54	7.16	3.53	4.60	13.65	1.63	8.16	34.48	12.22

Fig. 5 Comparison of measurement techniques: results reiceived for the same sample once by pXRF (measurements on fresh break) and once by WD-XRF.

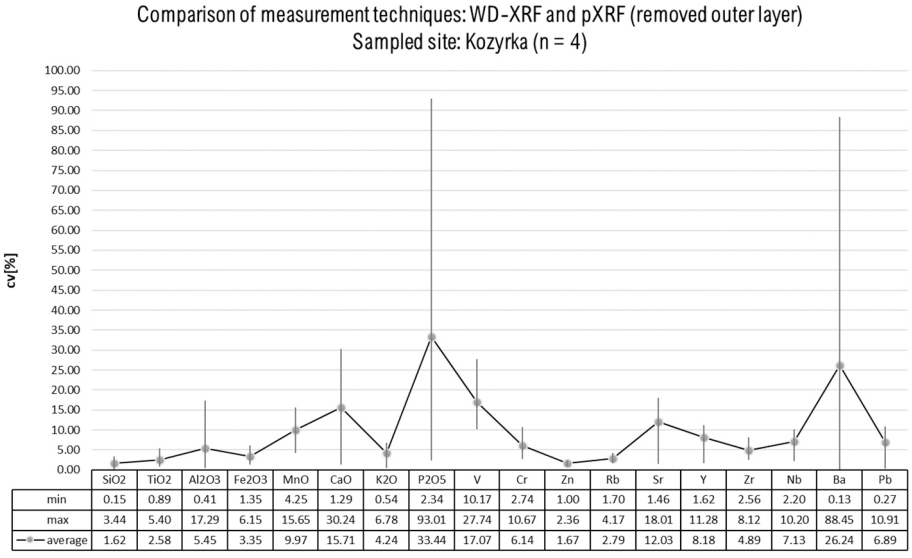

	SiO2	TiO2	Al2O3	Fe2O3	MnO	CaO	K2O	P2O5	V	Cr	Zn	Rb	Sr	Y	Zr	Nb	Ba	Pb
min	0.15	0.89	0.41	1.35	4.25	1.29	0.54	2.34	10.17	2.74	1.00	1.70	1.46	1.62	2.56	2.20	0.13	0.27
max	3.44	5.40	17.29	6.15	15.65	30.24	6.78	93.01	27.74	10.67	2.36	4.17	18.01	11.28	8.12	10.20	88.45	10.91
average	1.62	2.58	5.45	3.35	9.97	15.71	4.24	33.44	17.07	6.14	1.67	2.79	12.03	8.18	4.89	7.13	26.24	6.89

Fig. 6 Comparison of measurement techniques: results received for the same sample once by pXRF (measurements on surface after removing an outer layer) and once by WD-XRF.

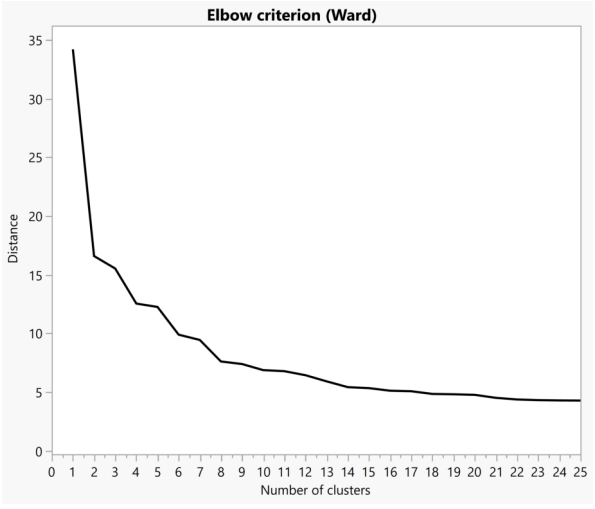

Fig. 7 Ward method: Elbow-criterion for statistical evaluation of pXRF data.

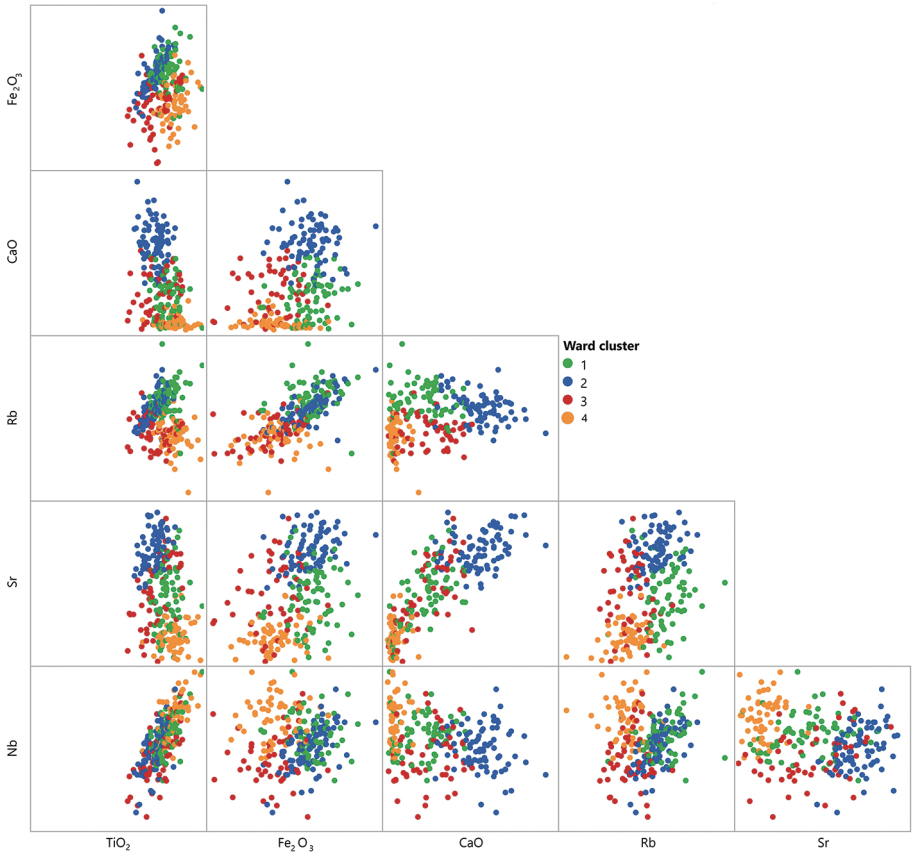

Fig. 8 Scatterplot matrix (4 cluster solution, Squared Euclidean distance, Ward method), comparison of Ti, Fe, Ca, Sr, Rb, Nb.

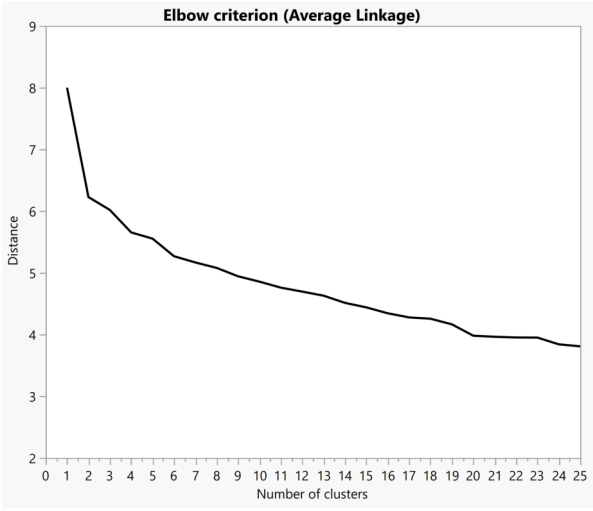

Fig. 9 Average-Linkage method: Elbow-criterion for statistical evaluation of pXRF data.

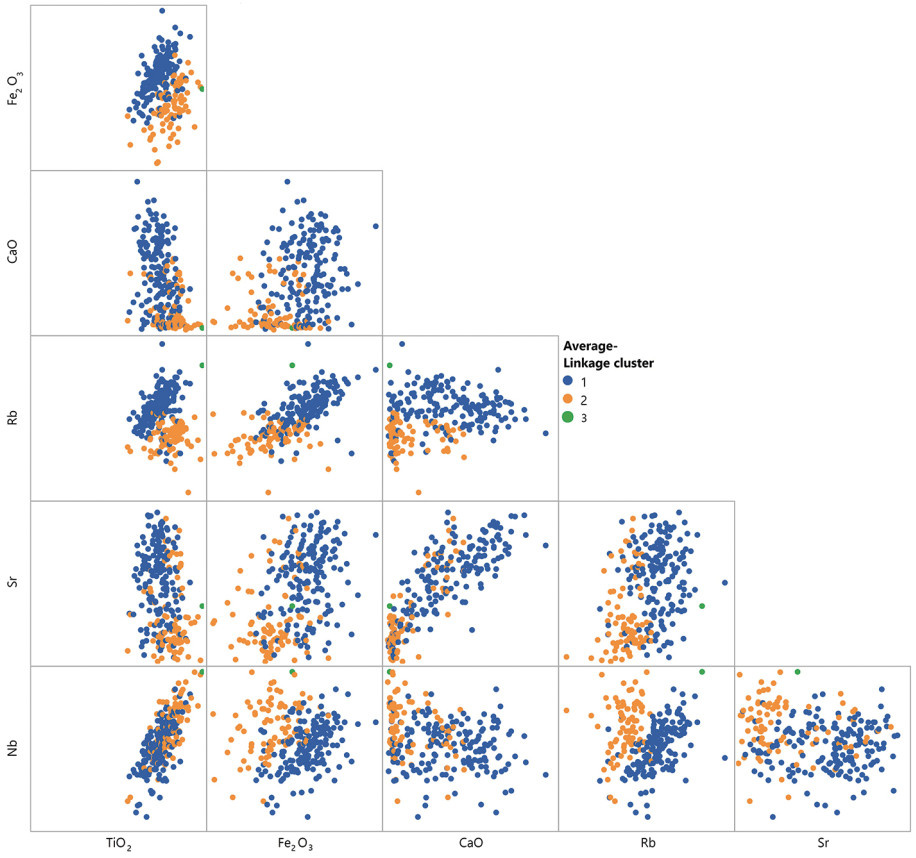

Fig. 10 Scatterplot-matrix (Average-Linkage method).

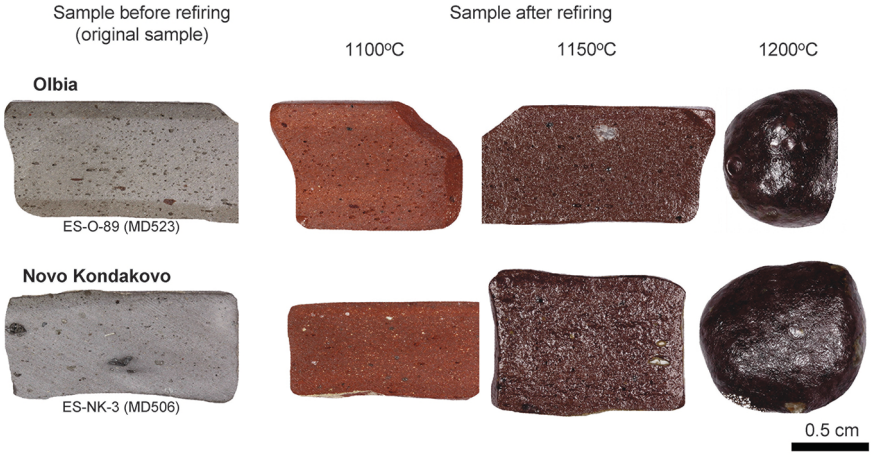

Lab. No.	SiO_2	TiO_2	Al_2O_3	Fe_2O_3	MnO	MgO	CaO	Na_2O	K_2O	P_2O_5	V	Cr	Ni	Zn	Rb	Sr	Y	Zr	Ba	l.o.i.	Sum
	per cent by weight										ppm									%	%
MD523	65.21	0.803	16.59	5.38	0.052	2.91	5.18	0.38	3.28	0.23	148	129	59	104	163	200	22	205	457	2.66	100.69
MD506	64.44	0.805	16.13	6.04	0.069	2.65	5.55	0.69	3.12	0.51	137	127	62	99	157	234	20	204	451	2.50	100.41

Fig. 11 Two ceramic samples (recovered from sites in Olbia and Novokondakove) belonging to the same MGR-group (MGR40, sMLT matrix type, NC cc clay). These samples have the same chemical composition. Samples (cut-sections) before and after refiring in air, with results of chemical analysis by WD-XRF (content of major elements normalized to a constant sum of 100%) shown below.

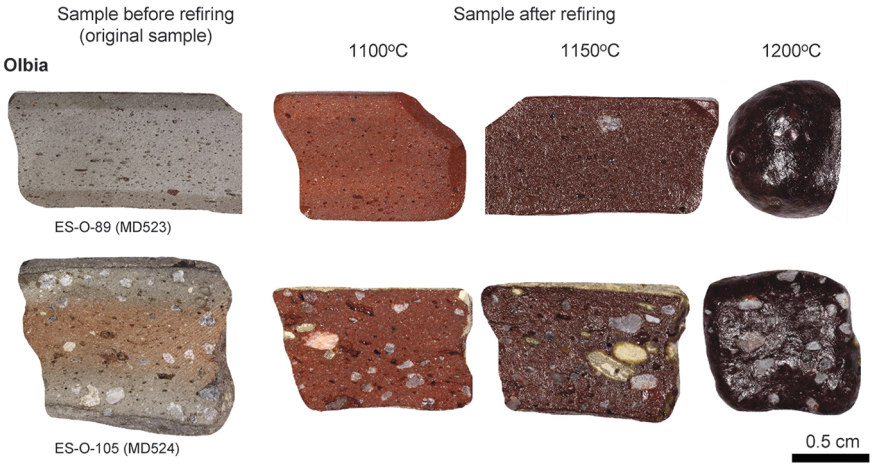

Lab. No.	SiO_2	TiO_2	Al_2O_3	Fe_2O_3	MnO	MgO	CaO	Na_2O	K_2O	P_2O_5	V	Cr	Ni	Zn	Rb	Sr	Y	Zr	Ba	l.o.i.	Sum
	per cent by weight										ppm									%	%
MD523	65.21	0.803	16.59	5.38	0.052	2.91	5.18	0.38	3.28	0.23	148	129	59	104	163	200	22	205	457	2.66	100.69
MD524	72.94	0.617	12.34	4.57	0.084	1.80	4.31	0.66	2.54	0.15	100	91	45	73	112	161	15	200	374	3.27	100.40

Fig. 12 Two ceramic samples found in Olbia belonging to the same MGR-group (MGR40, sMLT matrix type, NC cc clay). Sample O-89 has no macroscopically visible inclusions; sample O-105 features coarse non-plastic inclusions which affect the chemical composition. Samples (cut-sections) before and after refiring (cut-sections) in air, with results of chemical analysis by WD-XRF (content of major elements normalized to a constant sum of 100%) shown below.

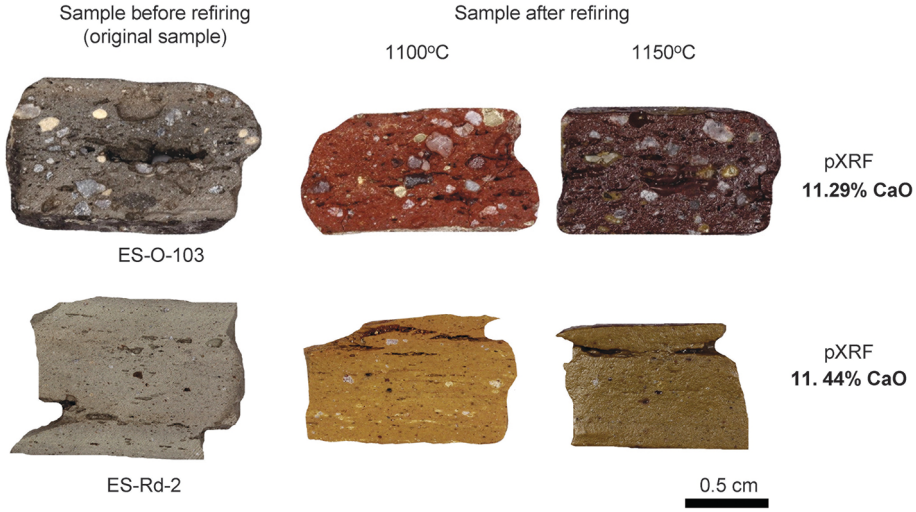

Fig. 13 Two ceramic samples with virtually identical CaO levels (chemical analysis by pXRF). Sample o-103 is made of non-calcareous clay while sample Rd-2 is made of calcareous clay. The CaO content is attributable to carbonates (non-plastic inclusions) in sample O-103, while in sample Rd-2 it is attributable jązebaetloneprzeszły to należy zzeszły to należy zaszarzone ' wytwórcy, a o daj znać.tego powtarzać, tym bardziej, że chyba poda to the plastic part of the ceramic body. Samples (cut-sections) before and after refiring in air.

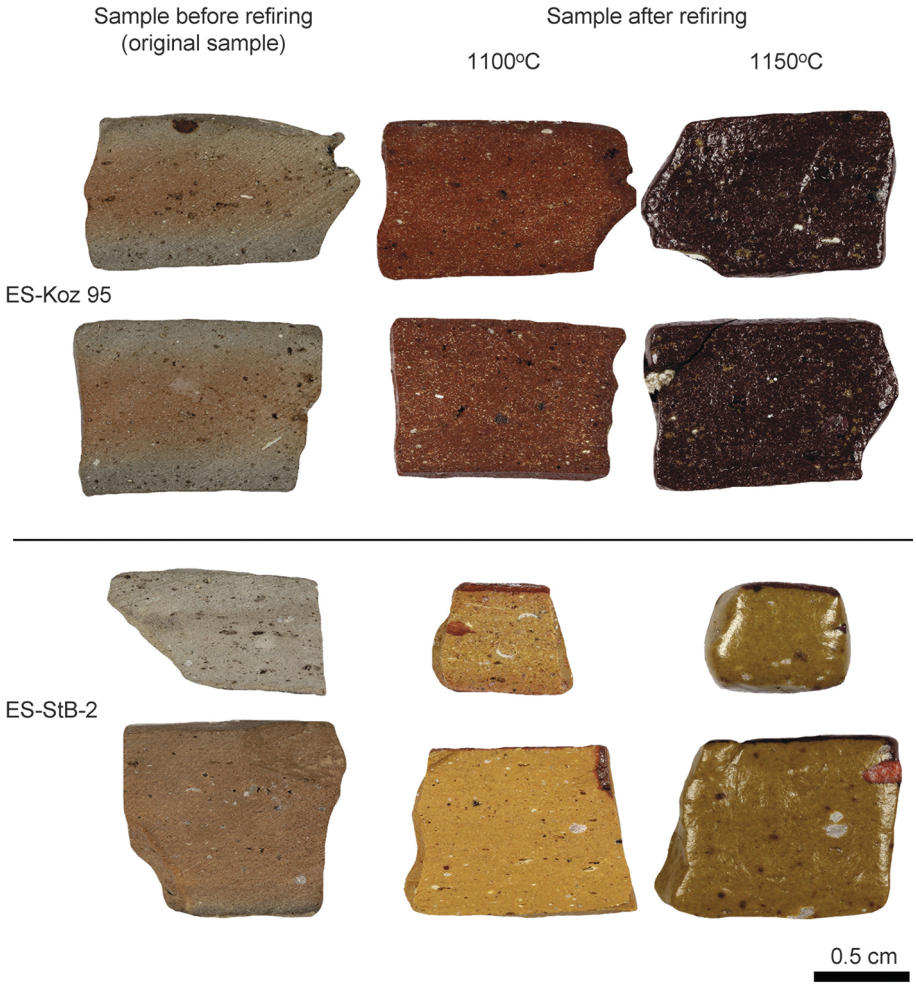

Fig. 14 Two ceramic samples (Koz-95 and StB-2) from which two pieces were removed from two different places and fired in two separate series. The ceramic body of both samples is homogeneous. Sample StB-2 was originally fired in non-standardised conditions, which is evident in the sample before refiring. Samples (cut-sections) before and after refiring in air.

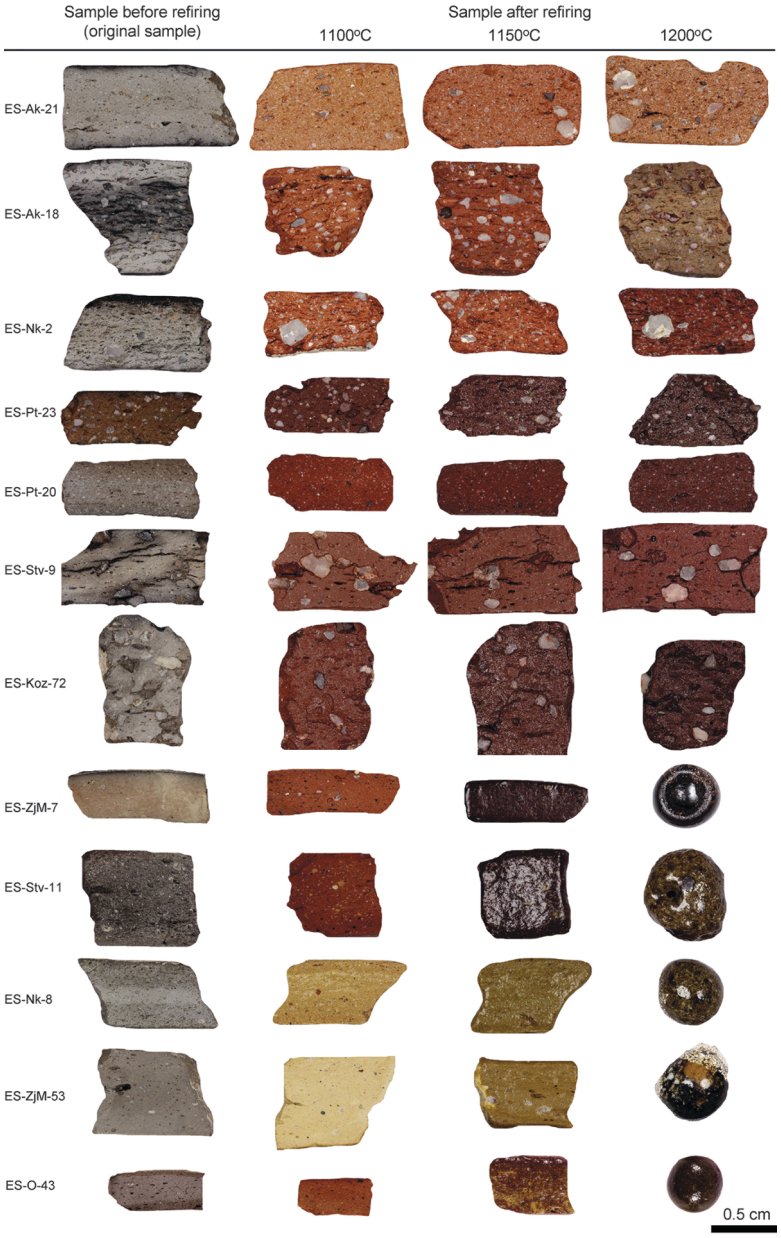

Fig. 15 Examples of various matrix categories and various matrix types. The seven first samples are made of various non-calcareous clays coloured to varying degrees by iron-compounds. Two of the samples (ZjM-7 and Stv-11) are made of non-calcareous clays enriched with carbonates in sub-10 μm fraction. The next two samples are made from calcareous clays. The last sample (O-43) is made of a mixed clay (with a predominance of non-calcareous clay). Samples (cut-sections) before and after refiring in air.

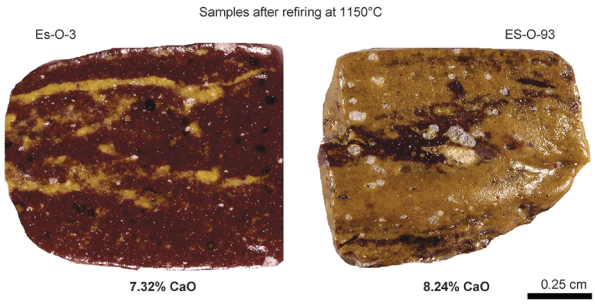

Fig. 16 Two pottery fragments discovered in Olbia representing two types of clay mixtures: one with a predominance of non-calcareous clay coloured by iron-compounds (sample O-3) and one with a predominance of calcareous clay (sample O-93). Samples (cut-sections) after refiring in air at 1150°C, CaO content determined by pXRF.

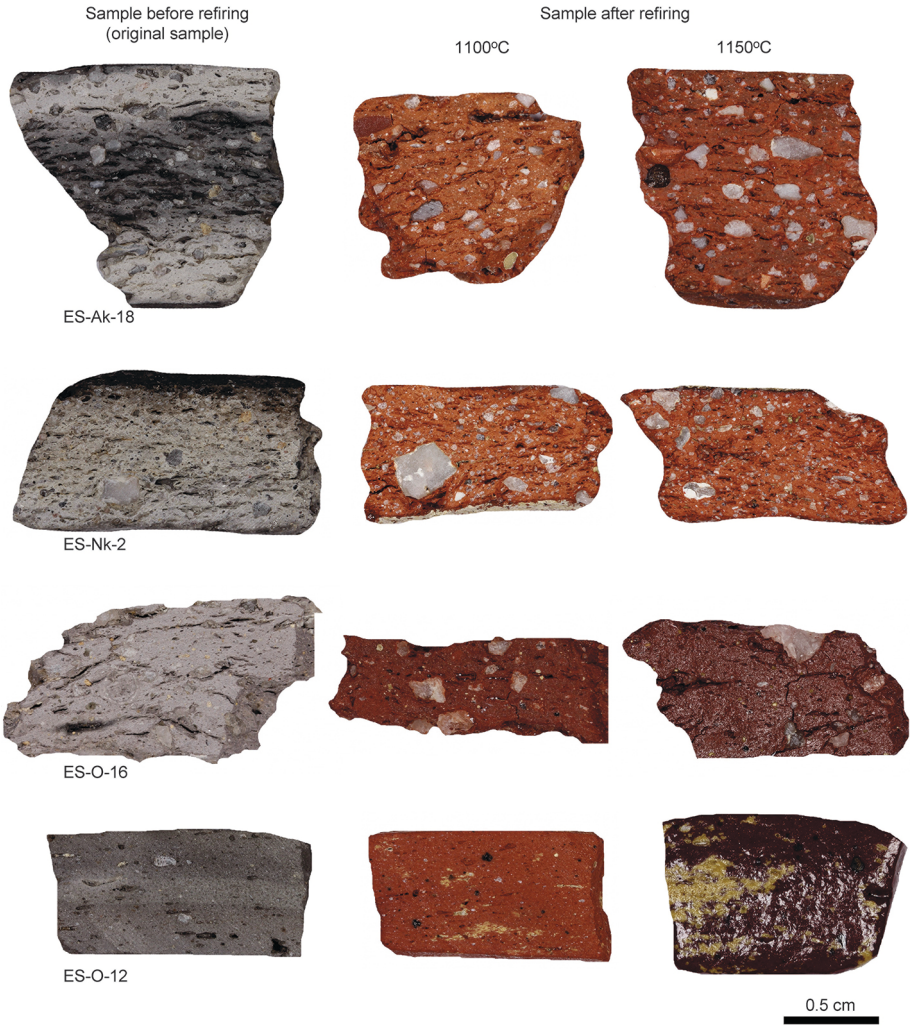

Fig. 17 Sherds in which non-plastic inclusions are much easier to assess macroscopically after refiring (three first samples) and one sherd (O-12) in which recognising two different clays within the matrix is virtually impossible before refiring. Samples (cut-sections) before and after refiring in air.

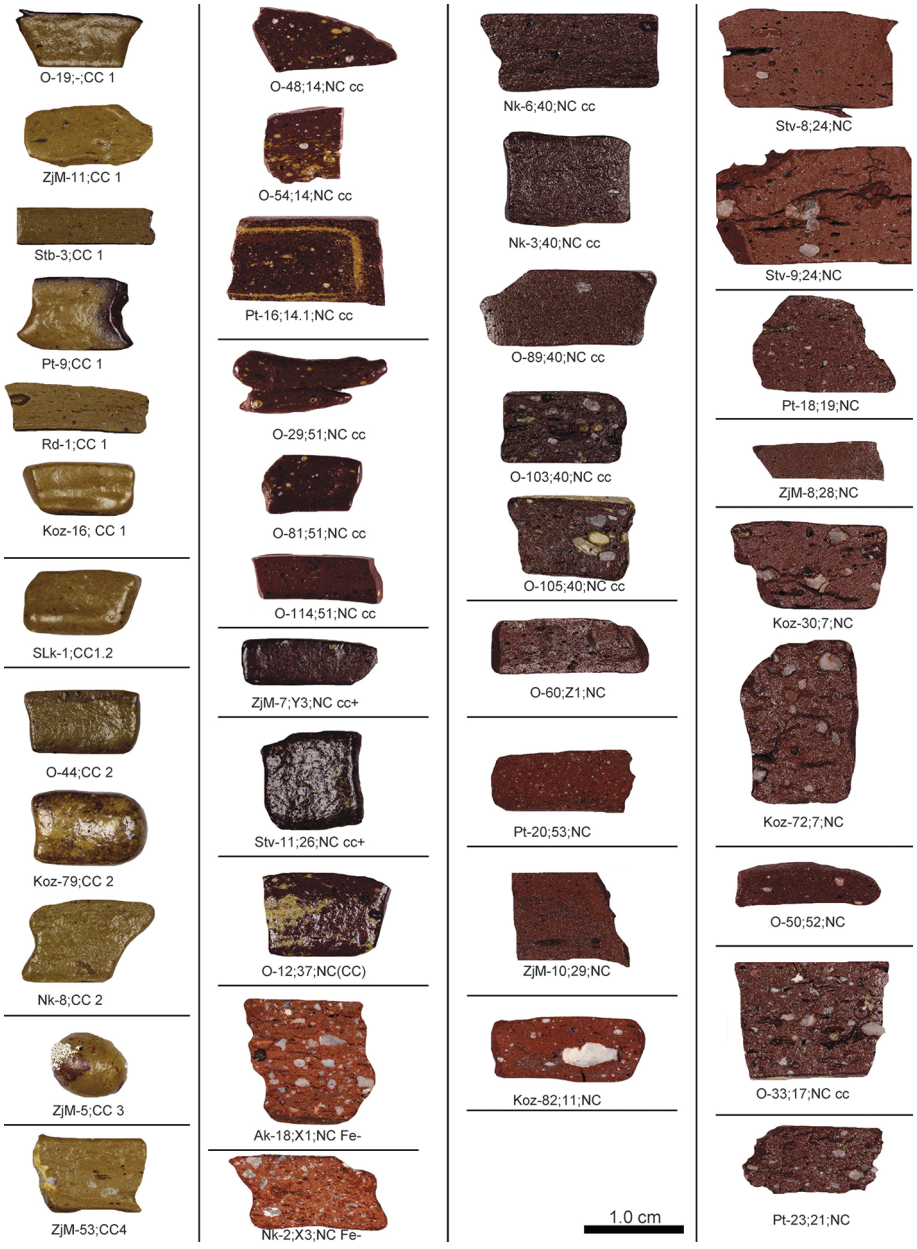

Fig. 18 Samples examined using both MGR-analysis and chemical analysis by WD-XRF. Samples are grouped according to MGR-analysis results, i.e. divided into sherds made from calcareous clays (first left column), samples made of non-calcareous clays enriched with carbonates in sub-10 µm fraction, mixed clays and various non-calcareous clays coloured to varying degrees by iron compounds. Samples (cut-sections) refired at 1150°C in air.

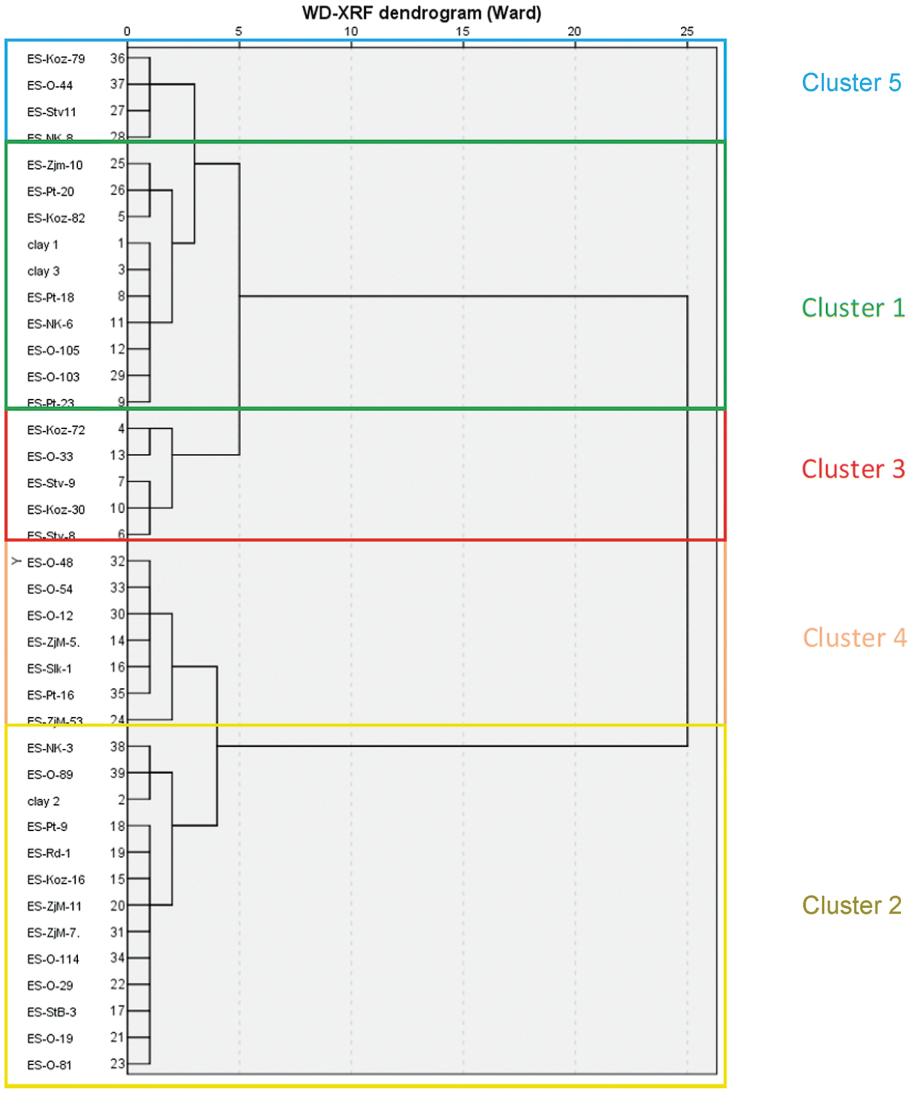

Fig. 19 Dendrogram of cluster analysis (Squared Euclidean distance, Ward method, elements used: Si, Ti, Al, Fe, Mn, Mg, Ca, Na, K, V, Cr, Ni, Zn, Rb, Sr, Zr).

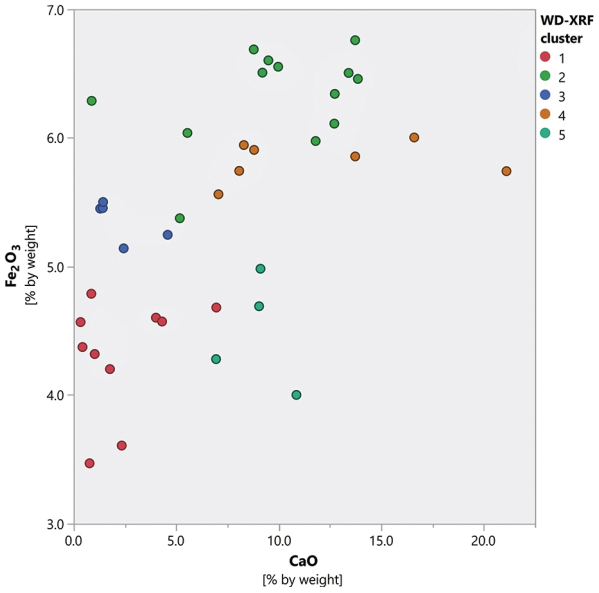

Fig. 20 WD-XRF data: Scatterplot of 5-cluster solution according to Fe_2O_3 and CaO in percent by weight.

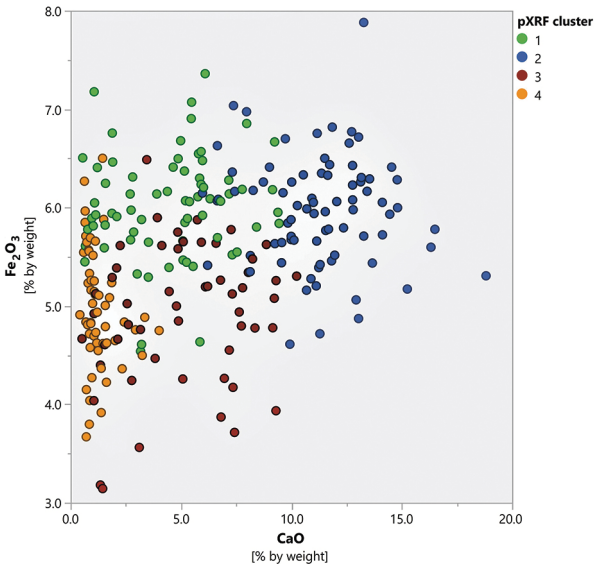

Fig. 21 pXRF data: Scatterplot of 4-cluster solution according to Fe_2O_3 and CaO in percent by weight.

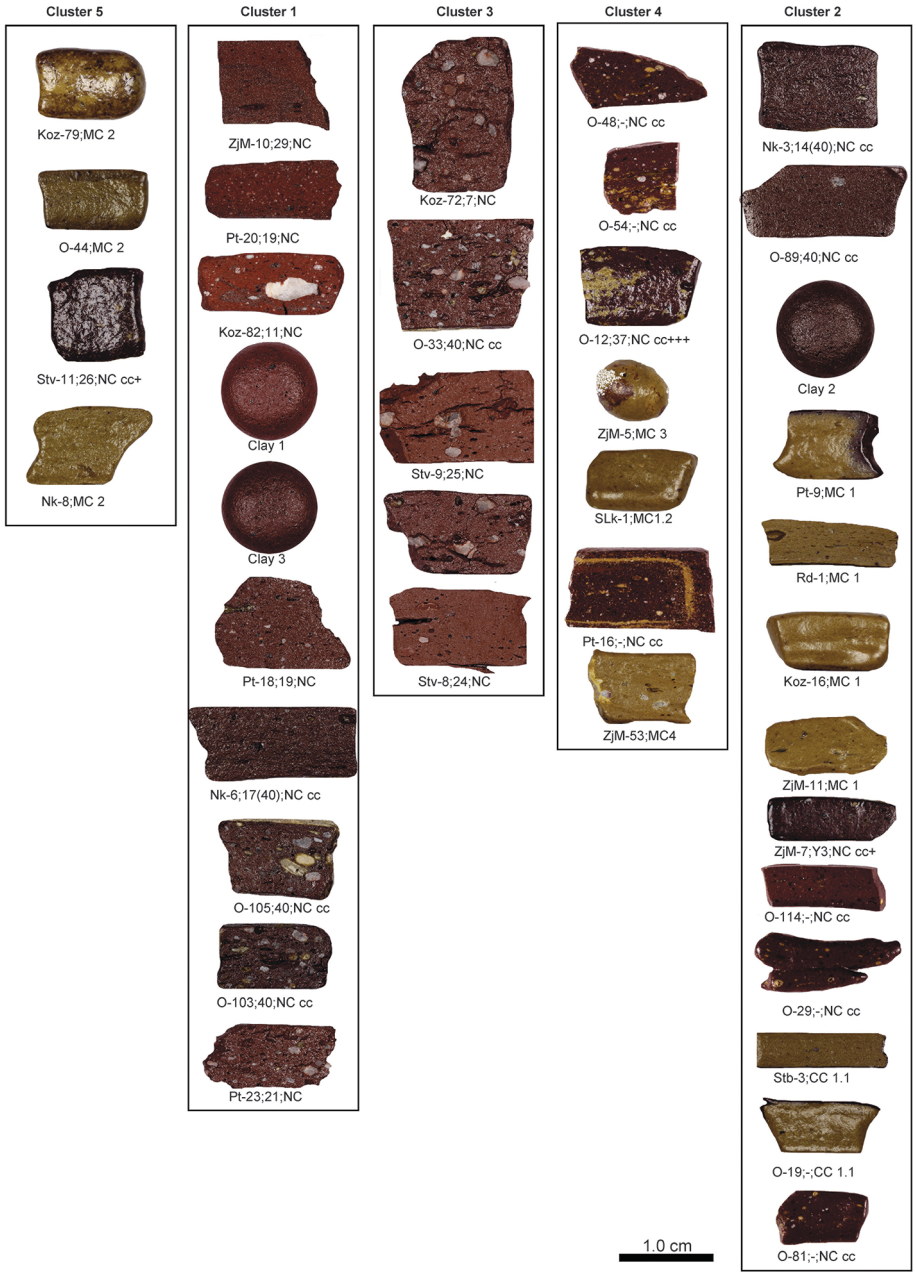

Fig. 22 Samples examined using both MGR-analysis and chemical analysis by WD-XRF. Samples arranged in order determined by cluster analysis, see dendrogram shown in figure 17. Samples (cut-sections) after refiring and three specimens of fired clay samples, refiring/firing at 1150°C in air.

Fig. 23 Samples of cluster 1 arranged in order determined by cluster analysis of pXRF data. Samples (cut-sections) after refiring at 1150°C in air.

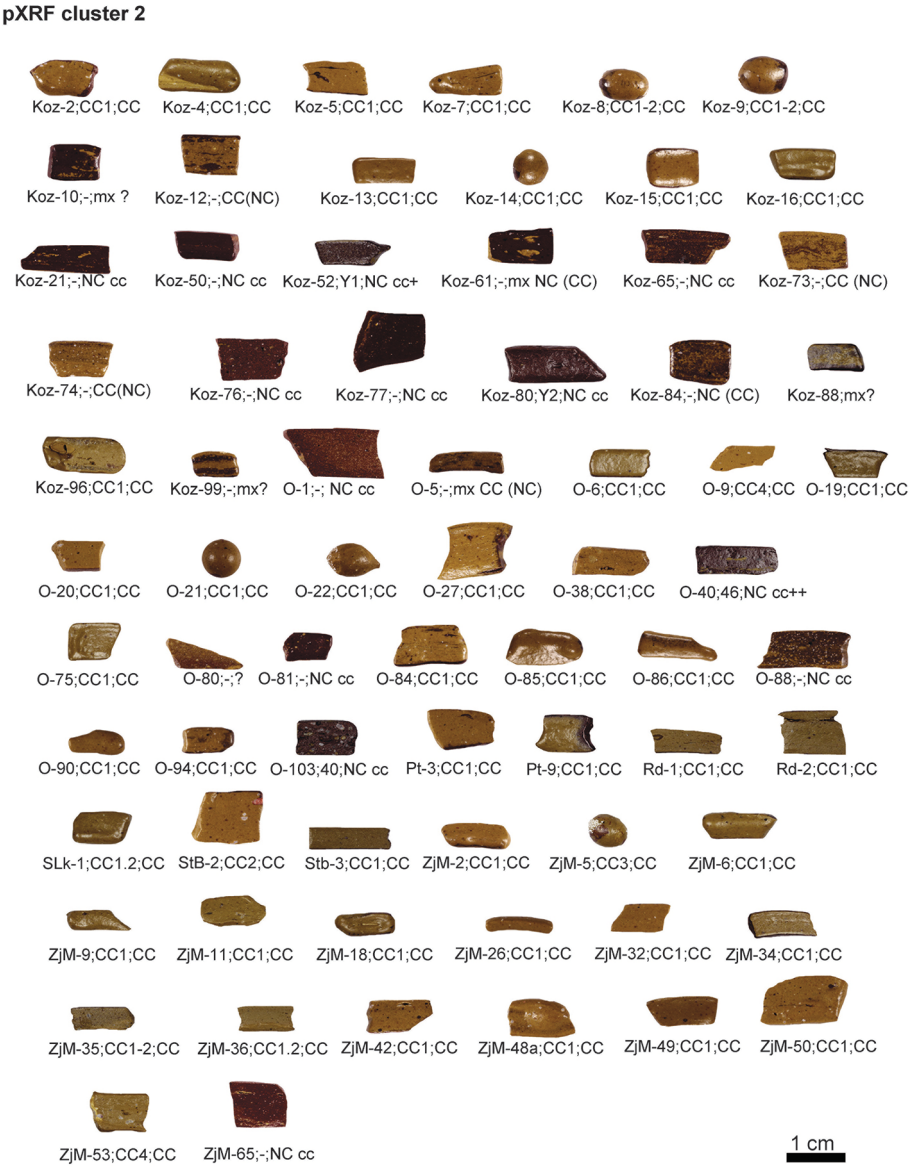

Fig. 24 Samples of cluster 2 arranged in order determined by cluster analysis of pXRF data. Samples (cut-sections) after refiring at 1150°C in air.

Fig. 25 Samples of cluster 3 arranged in order determined by cluster analysis of pXRF data. Samples (cut-sections) after refiring at 1150°C in air.

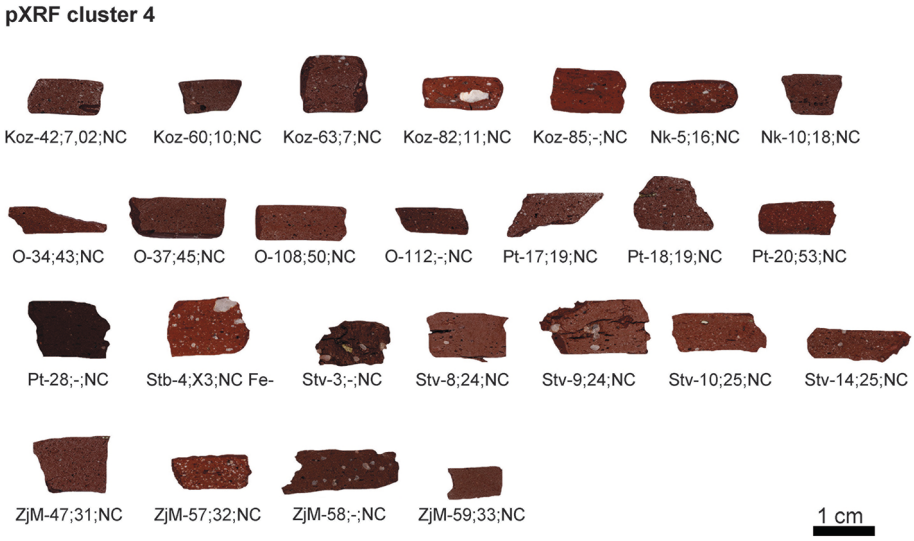

Fig. 26 Samples of cluster 4 arranged in order determined by cluster analysis of pXRF data. Samples (cut-sections) after refiring at 1150°C in air.

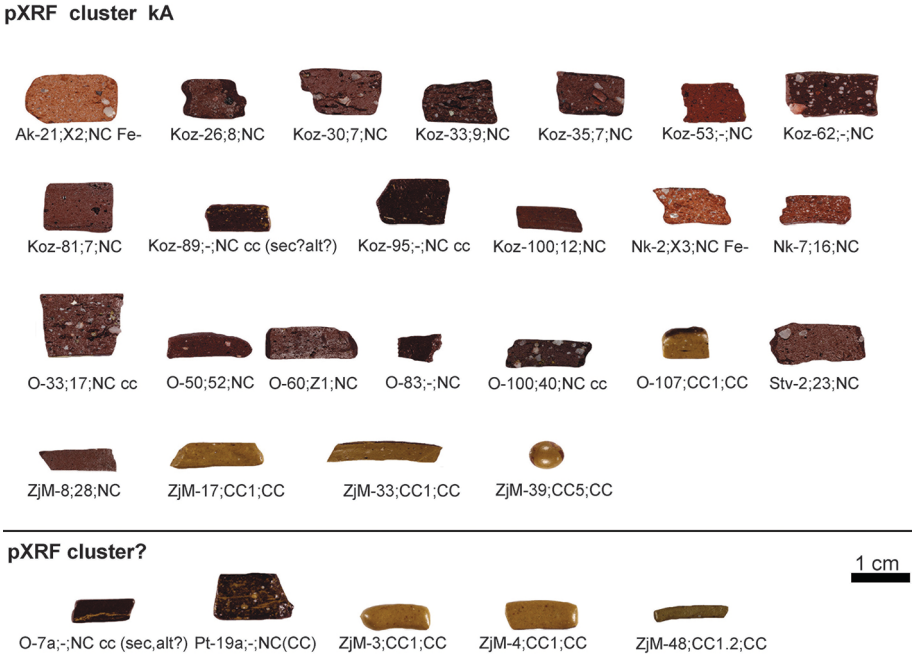

Fig. 27 Samples not attributed to any clusters (e.g. due to chemical outliers, very coarse tempered). Samples (cut-sections) after refiring at 1150°C in air.

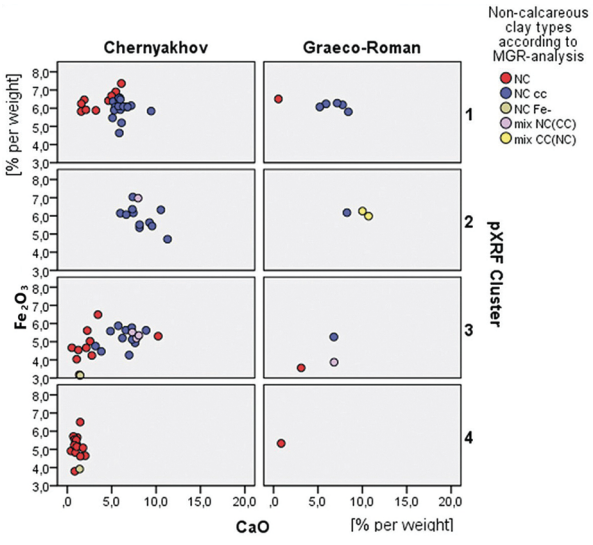

Fig. 28 Distribution of pXRF clusters with non-calcareous clay-types (according to MGR-analysis) and cultural spectra.

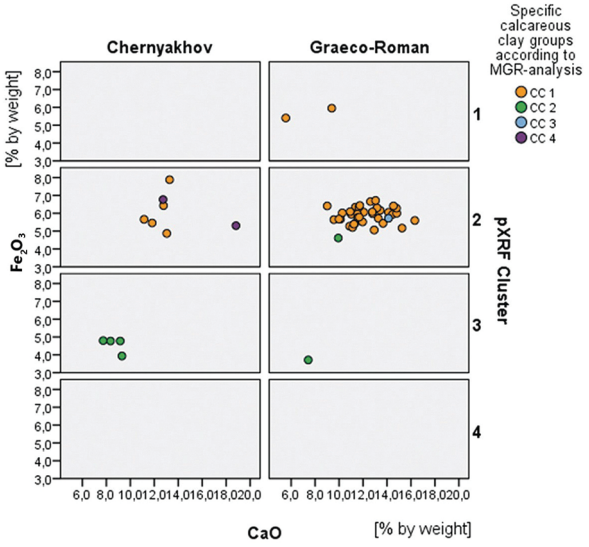

Fig. 29 Distribution of pXRF clusters with specific clay-groups (according to MGR-analysis) and cultural spectra.

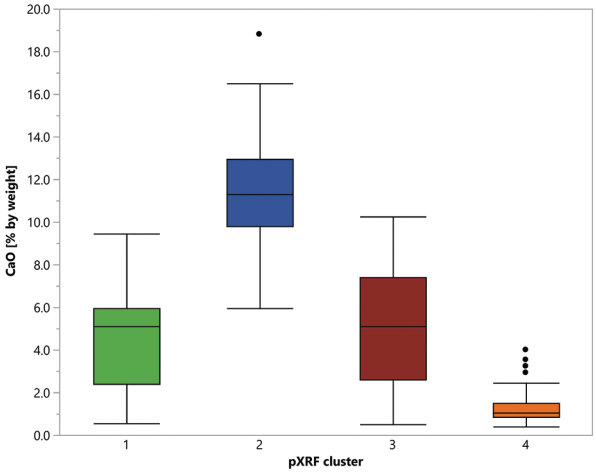

Fig. 30 Boxplot of proportion of CaO (% by weight) within pXRF clusters.

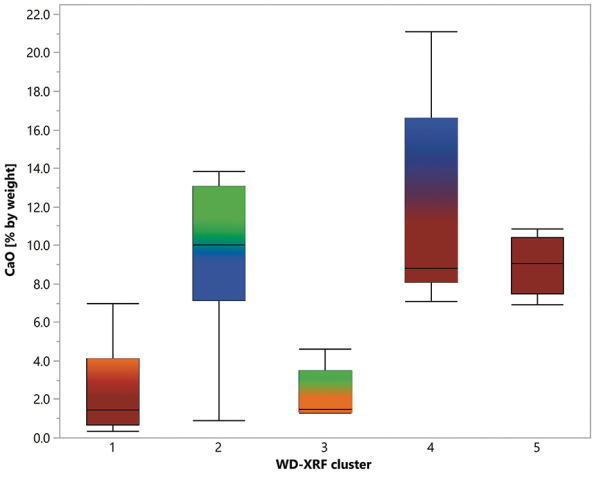

Fig. 31 Boxplot of proportion of CaO (% by weight) within WD-XRF clusters. The colours refer to the pXRF clusters (see Fig. 30) contained within the WD-XRF clusters per each analogue sample colour.

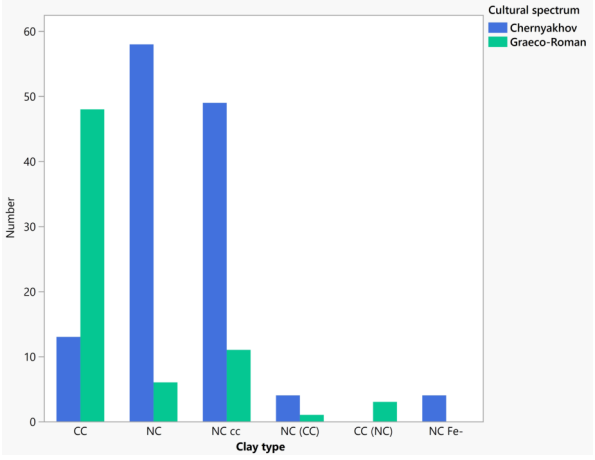

Fig. 32 Number of samples of particular clay-types in cultural spectra.

Site	Number of samples	Spectrum	Number of analysed samples		
			pXRF	WD-XRF	MGR
Olbia (O)	116	Graeco-Roman (29) Chernyakhov (80) Unknown (7)	116 (1)*	14	87
Kozyrka (Koz)	76	Graeco-Roman (19) Chernyakhov (50) Unknown (7)	76 (51)*	5	51 (2)*
Zolotoyi Mys (ZjM)	42	Graeco-Roman (27) Chernyakhov (13) Unknown (2)	37	6	34
Petukhivka (Pt)	20	Graeco-Roman (3) Chernyakhov (13) Unknown (4)	20	5	14
Novokondakove (Nk)	10	Chernyakhov	10 (1)*	5	8
Stanislav (Stv)	9	Chernyakhov	9	3	7
Adzhigolska Kosa (AK)	9	Chernyakhov	9	1	8
Stara Bogdanivka (StB)	4	Graeco-Roman (3) Chernyakhov (1)	4 (4)*	1	3 (1)*
Radsad (Rd)	3	Graceo-Roman	3 (3)*	1	3
Skelka (Slk)	1	Graeco-Roman	1 (1)*	1	1
Total	**290**		**285 (61)***	**42**	**217 (2)***

Tab. 1 Number of samples from individual sites analysed using various techniques. ( )* = Number of samples analysed two times for the purpose of validation and comparison of results using different preparation of measurement spots.

Sample	SiO_2	TiO_2	Al_2O_3	Fe_2O_3	MnO	MgO	CaO	K_2O	P_2O_5	S	Cl	V	Cr	Cu	Zn	Rb	Sr	Y	Zr	Nb	Sn	Ba	Pb
	per cent by weight									ppm													
grinding head pink	23.5	0.00	25.5	0.10	0.01		1.12	1.69	0.16		10	51	874		403	48	34		14	4		641	711
grinding disc	5.94	3.83	21.1	8.87	0.09		7.56	0.26	0.55	9859	65	197	8846	40	68	9	476	70	648	111	16		16
grinding disc	5.55	3.78	20.9	8.82	0.09		7.61	0.26	0.54	10152	69	204	8381	47	58	9	466	72	639	100			17
cylinder grinding wheel	2.55	12.9	1.76	0.01	4.16	24.40	0.23	0.41	314	97	1550			35	9	303	36	360	5		659	29	
cylinder grinding wheel	2.54	12.6	1.79	0.01	3.63	24.36	0.23	0.39		98	1541			34	9	311	36	366	6		673	30	

Tab. 2 Composition of grinding tools measured by pXRF.

cluster pXRF	cluster WD-XRF	MGR group	Sample No.	Lab. No.	SiO_2	TiO_2	Al_2O_3	Fe_2O_3	MnO	MgO	CaO	Na_2O	K_2O	P_2O_5	V	Cr	Ni	(Cu)	Zn	Rb	Sr	Y	Zr	(Nb)	Ba	(Ce	Pb	Th)	l.o.i.	Sum
					per cent by weight										ppm														%	%
					various calcareous clays (CC)																									
					clay CC 1																									
2	2	CC 1.1	O-19	MD520	59.44	0.74	14.61	5.98	0.109	2.31	11.80	0.91	3.81	0.29	152	106	57	52	110	135	251	22	199	11	479	60	24	20	9.57	99.96
2	2	CC 1.1	ZjM-11	MD519	58.52	0.75	15.24	6.11	0.113	2.29	12.71	0.63	3.12	0.50	146	113	57	49	77	136	295	23	183	10	453	82	12	14	1.34	100.21
2	2	CC 1.1	StB-3	MD510	57.72	0.78	15.40	6.34	0.106	2.34	12.74	0.75	3.59	0.23	136	112	59	49	118	136	294	22	184	12	433	53	21	21	11.08	100.19
2	2	CC 1.1	Pt-9	MD514	56.75	0.80	15.98	6.51	0.132	2.36	13.41	0.60	3.15	0.31	143	119	65	38	108	151	304	26	174	12	680	77	22	21	4.22	100.30
2	2	CC 1.1	Rd-1	MD518	55.90	0.83	16.42	6.76	0.171	2.30	13.73	0.54	3.07	0.28	119	119	64	37	87	150	319	24	184	14	727	67	22	21	2.57	100.23
2	2	CC 1.1	Koz-16	MD501	56.57	0.78	15.41	6.46	0.162	2.13	13.86	0.64	3.57	0.42	155	113	57	37	88	148	369	22	168	13	9277	83	16	17	1.94	98.69
2	4	CC 1.2	Slk-1	MD509	59.34	0.74	14.02	5.86	0.188	2.14	13.73	0.70	3.03	0.26	138	105	55	26	85	134	269	23	227	12	504	58	16	17	1.68	100.30
					clay CC 2																									
3	5	CC 2	O-44	MD522	67.82	0.81	12.36	4.69	0.079	1.99	9.04	0.68	2.35	0.18	102	92	45	25	64	100	273	26	404	14	487	71	18	17	1.62	100.63
3	5	CC 2	Koz-79	AD060	66.86	0.81	12.84	4.98	0.080	2.17	9.11	0.66	2.30	0.18	109	92	43	23	69	101	279	30	383	12	486	76	17	11	1.73	99.85
3	5	CC 2	NK-8	MD508	69.06	0.74	10.64	4.00	0.063	2.07	10.86	0.62	1.74	0.20	96	82	38	18	51	81	252	24	406	12	504	50	13	13	3.05	100.19
					clay CC 3																									
2	4	CC 3	ZjM-5.	AD061	55.38	0.73	14.69	6.00	0.152	2.13	16.61	0.78	3.09	0.44	142	103	50	22	86	124	266	19	191	11	426	54	15	16	6.41	94.10
					clay CC 4																									
2	4	CC 4	ZjM-53.	AD062	54.48	0.70	12.88	5.74	0.082	2.10	21.11	0.36	2.27	0.28	110	101	46	20	80	111	299	21	197	13	474	56	18	17	7.90	100.29
					various non-calcareous clays with carbonates in matrix (NC cc)																									
1	4	14	O-48	AD341	64.20	0.80	14.38	5.91	0.115	1.98	8.80	0.63	2.98	0.21	141	107	54	27	78	135	211	29	248	19	512	89	20	10	1.10	100.22
1	4	14	O-54	AD343	65.49	0.78	13.89	5.94	0.091	2.03	8.30	0.77	2.54	0.15	123	100	50	26	71	124	191	29	237	16	428	65	12	12	0.49	100.59
3	4	14.1	PT-16	AD346	65.91	0.77	13.29	5.56	0.159	2.51	7.06	1.03	3.37	0.34	128	107	51	10	86	123	251	31	276	17	488	78	20	12	6.17	100.62
1	2	51	O-114	AD345	59.89	0.85	16.42	6.60	0.135	2.43	9.50	0.76	3.24	0.18	131	122	63	24	93	152	235	29	180	16	482	78	24	9	1.05	100.56
1	2	51	O-29	AD340	58.90	0.78	16.66	6.55	0.123	2.68	9.98	0.67	3.38	0.27	165	130	60	56	108	148	198	25	140	15	403	65	21	14	9.94	99.95
2	2	51	O-81	AD344	60.59	0.80	15.21	6.51	0.118	2.52	9.21	0.90	3.55	0.58	128	106	66		95	121	201		154		717				2.57	92.95
1	2	Y 3	ZjM-7.	AD073	60.04	0.82	16.24	6.69	0.113	2.31	8.78	0.69	4.02	0.29	149	121	63	30	104	152	237	22	185	15	502	77	21	25	6.66	100.18
3	5	26	Stv11	MD513	72.77	0.79	10.77	4.28	0.063	1.87	6.95	0.68	1.66	0.17	82	83	39	18	61	81	189	19	392	12	415	68	7	18	0.93	92.50
					mixed clays NC with CC																									
3	4	37	O-12	AD058	65.02	0.85	14.42	5.74	0.087	2.41	8.07	0.63	2.61	0.15	121	106	45	22	69	116	226	28	316	13	537	84	20	16	0.98	99.91
					non-calcareous clay with some carbonates in matrix (NC cc)																									
1	2	40	NK-3	MD506	64.44	0.80	16.13	6.04	0.069	2.65	5.55	0.69	3.12	0.51	137	127	62	26	99	157	234	20	204	13	451	66	16	22	2.50	100.41
1	2	40	O-89	MD523	65.21	0.80	16.59	5.38	0.052	2.91	5.18	0.38	3.28	0.23	148	129	59	33	104	163	200	22	205	14	457	72	19	22	2.66	100.69

Tab. 3 Results of analysis by WD-XRF, sorted according clay-types.

cluster pXRF	cluster WD-XRF	MGR group	Sample No.	Lab. No.	SiO_2	TiO_2	Al_2O_3	Fe_2O_3	MnO	MgO	CaO	Na_2O	K_2O	P_2O_5	V	Cr	Ni	(Cu)	Zn	Rb	Sr	Y	Zr	(Nb)	Ba	(Ce	Pb	Th)	l.o.i.	Sum
					per cent by weight										ppm														%	%
clay 40 plus coarse non-plastic inclusions																														
3	1	40	O-105	MD524	72.94	0.62	12.34	4.57	0.084	1.80	4.31	0.66	2.54	0.15	100	91	45	30	73	112	161	15	200	9	374	46	16	16	3.27	100.40
3	1	40	NK-6	MD507	72.41	0.78	12.89	4.60	0.050	1.97	4.01	0.69	2.28	0.31	105	95	46	21	76	90	167	23	285	13	432	62	17	22	3.48	100.62
2	1	40	O-103	AD059	70.67	0.62	12.01	4.68	0.103	1.80	6.96	0.64	2.30	0.21	104	92	42	21	70	113	193	20	207	11	470	62	16	17	3.60	100.14
various non-calcareous clays slightly coloured by iron compounds (NC Fe-)																														
3	-	X 1	AK-18	MD500	75.57	0.74	16.53	2.84	0.033	0.92	1.22	0.29	1.76	0.09	113	100	35	29	57	112	123	19	205	12	518	76	21	20	1.01	100.04
2	-	X 3	NK-2	MD505	76.14	0.88	15.77	4.43	0.018	0.41	1.86	0.01	0.32	0.18	86	59	24	13	32	17	93	29	407	20	375	76	26	25	1.79	100.74
various non-calcareous clays (NC)																														
1	3	7	Koz-30	MD502	71.64	0.83	14.66	5.14	0.065	1.93	2.44	0.62	2.12	0.55	107	106	46	25	78	119	184	23	258	12	411	83	19	21	0.81	100.21
1	3	7	Koz-72	MD503	73.48	0.72	14.25	5.45	0.093	1.65	1.42	0.36	2.36	0.20	120	102	48	19	80	127	144	21	228	13	687	69	23	20	0.87	100.15
4	1	11	Koz-82	MD504	74.91	0.78	14.26	4.20	0.058	1.07	1.77	0.37	2.48	0.11	98	84	38	14	58	103	119	27	392	12	647	99	19	29	1.41	99.70
-	3	17	O-33	MD521	70.35	0.66	13.82	5.25	0.099	1.97	4.59	0.27	2.83	0.18	127	106	55	33	87	136	140	18	163	12	418	46	16	15	2.10	100.29
4	1	19	Pt-18	MD515	75.48	0.76	13.34	4.79	0.091	1.36	0.86	0.62	2.58	0.13	102	98	48	25	76	112	94	22	280	12	489	63	19	22	2.36	98.80
3	1	21	Pt-23	MD517	77.92	0.60	11.71	4.32	0.046	1.61	1.03	0.42	2.22	0.13	100	82	42	23	67	100	91	16	170	10	338	61	14	19	3.43	100.48
4	3	24	Stv-8	MD511	69.65	0.99	17.81	5.50	0.081	1.85	1.44	0.39	2.19	0.10	119	121	52	25	86	103	159	28	269	16	532	88	22	24	3.85	100.57
4	3	24	Stv-9	MD512	72.72	0.88	15.73	5.45	0.053	1.51	1.30	0.33	1.86	0.16	114	110	45	23	77	104	199	25	247	14	554	67	19	28	2.72	100.59
-	-	28	Zjm-8	AD347	63.76	0.76	21.11	4.79	0.089	1.17	2.53	0.63	4.90	0.26	115	95	40	24	86	181	145	27	225	16	672	82	34	22	2.36	99.53
3	1	29	Zjm-10	AD348	78.22	0.77	11.13	3.61	0.092	1.27	2.35	0.64	1.74	0.18	96	85	32	9	53	79	152	22	334	18	534	76	19	11	2.72	100.62
-	-	52	O-50	AD342	68.90	0.89	16.08	6.91	0.107	1.96	1.29	1.67	2.06	0.14	142	184	84	36	92	82	142	31	182	15	403	62	17	10	0.80	99.46
4	1	53	Pt-20	MD516	80.83	0.77	10.89	3.47	0.056	0.93	0.78	0.48	1.71	0.09	75	79	30	16	51	95	71	22	364	13	343	58	16	17	0.47	100.53
-	-	Z 1	O-60	AD071	61.44	0.85	19.65	8.17	0.103	2.67	3.45	0.23	3.29	0.17	183	149	86	37	118	189	167	24	167	16	475	69	25	19	0.83	100.43

Tab. 3 (Continued) Results of analysis by WD-XRF, sorted according clay-types.

cluster		MGR	Clay	Sample	Lab.	SiO_2	TiO_2	Al_2O_3	Fe_2O_3	MnO	MgO	CaO	Na_2O	K_2O	P_2O_5	V	Cr	Ni	(Cu)	Zn	Rb	Sr	Y	Zr	(Nb)	Ba	(Ce	Pb	Th)	l.o.i.	Sum
pXRF	WD-XRF	group	type	No.	No.	per cent by weight										ppm														%	%
1	4	19	NC	ES-Pt-18	MD515	75.48	0.760	13.34	4.79	0.091	1.36	0.86	0.62	2.58	0.127	102	98	48	25	76	112	94	22	280	12	489	63	19	22	2.36	98.80
1	3	40	NC cc	ES-NK-6	MD507	72.41	0.782	12.89	4.60	0.050	1.97	4.01	0.69	2.28	0.310	105	95	46	21	76	90	167	23	285	13	432	62	17	22	3.48	100.62
1	4	11	NC	ES-Koz-82	MD504	74.91	0.778	14.26	4.20	0.058	1.07	1.77	0.37	2.48	0.108	98	84	38	14	58	103	119	27	392	12	647	99	19	29	1.41	99.70
1	3	40	NC cc	ES-O-105	MD524	72.94	0.617	12.34	4.57	0.084	1.80	4.31	0.66	2.54	0.146	100	91	45	30	73	112	161	15	200	9	374	46	16	16	3.27	100.40
1	2	40	NC cc	ES-O-103	AD059	70.67	0.621	12.01	4.68	0.103	1.80	6.96	0.64	2.30	0.213	104	92	42	21	70	113	193	20	207	11	470	62	16	17	3.60	100.14
1	3	21	NC	ES-Pt-23	MD517	77.92	0.596	11.71	4.32	0.046	1.61	1.03	0.42	2.22	0.132	100	82	42	23	67	100	91	16	170	10	338	61	14	19	3.43	100.48
1	4	53	NC	ES-Pt-20	MD516	80.83	0.773	10.89	3.47	0.056	0.93	0.78	0.48	1.71	0.089	75	79	30	16	51	95	71	22	364	13	343	58	16	17	0.47	100.53
1	3	29	NC	ES-Zjm-10	AD348	78.22	0.770	11.13	3.61	0.092	1.27	2.35	0.64	1.74	0.179	96	85	32	9	53	79	152	22	334	18	534	76	19	11	2.72	100.62
1	kA		NC	clay 1	MD525	78.13	0.757	12.10	4.37	0.048	1.36	0.43	0.70	1.97	0.128	78	87	38	18	65	104	102	29	293	12	333	50	12	18	3.69	99.69
1	KA		NC	clay 3	MD527	77.23	0.786	12.58	4.57	0.082	1.48	0.34	0.77	2.08	0.075	87	94	44	20	68	106	100	19	293	11	335	71	16	22	3.80	97.64
2	2	CC 1.1	MC	ES-Koz-16	MD501	56.57	0.781	15.41	6.46	0.162	2.13	13.86	0.64	3.57	0.415	155	113	57	37	88	148	369	22	168	13	9277	83	16	17	1.94	98.69
2	2	CC 1.1	MC	ES-StB-3	MD510	57.72	0.780	15.40	6.34	0.106	2.34	12.74	0.75	3.59	0.231	136	112	59	49	118	136	294	22	184	12	433	53	21	21	11.08	100.19
2	2	CC 1.1	MC	ES-Pt-9	MD514	56.75	0.800	15.98	6.51	0.132	2.36	13.41	0.60	3.15	0.315	143	119	65	38	108	151	304	26	174	12	680	77	22	21	4.22	100.30
2	2	CC 1.1	MC	ES-Rd-1	MD518	55.90	0.829	16.42	6.76	0.171	2.30	13.73	0.54	3.07	0.283	119	119	64	37	87	150	319	24	184	14	727	67	22	21	2.57	100.23
2	2	CC 1.1	MC	ES-ZjM-11	MD519	58.52	0.753	15.24	6.11	0.113	2.29	12.71	0.63	3.12	0.503	146	113	57	49	77	136	295	23	183	10	453	82	12	14	1.34	100.21
2	2	CC 1.1	MC	ES-O-19	MD520	59.44	0.743	14.61	5.98	0.109	2.31	11.80	0.91	3.81	0.293	152	106	57	52	110	135	251	22	199	11	479	60	24	20	9.57	99.96
2	1	51	*NC cc*	O-29	AD340	58.90	0.783	16.66	6.55	0.123	2.68	9.98	0.67	3.38	0.274	165	130	60	56	108	148	198	25	140	15	403	65	21	14	9.94	99.95
2	1	Y 3	NC cc+	ES-ZjM-7.	AD073	60.04	0.823	16.24	6.69	0.113	2.31	8.78	0.69	4.02	0.289	149	121	63	30	104	152	237	22	185	15	502	77	21	25	6.66	100.18
2	1	51	NC cc	O-114	AD345	59.89	0.845	16.42	6.60	0.135	2.43	9.50	0.76	3.24	0.184	131	122	63	24	93	152	235	29	180	16	482	78	24	9	1.05	100.56
2	1	40	NC cc	ES-O-89	MD523	65.21	0.803	16.59	5.38	0.052	2.91	5.18	0.38	3.28	0.228	148	129	59	33	104	163	200	22	205	14	457	72	19	22	2.66	100.69
2	kA		NC	clay 2	MD526	70.49	0.800	15.45	6.29	0.064	2.10	0.88	0.81	3.03	0.092	126	119	64	37	102	142	136	18	258	13	330	83	22	23	4.70	100.42
2	2	51	NC cc	O-81	AD344	60.59	0.803	15.21	6.51	0.118	2.52	9.21	0.90	3.55	0.584	128	106	66		95	121	201		154		717				2.57	92.95
2	1	40		Nk-3																											
3	1	7	NC	ES-Koz-72	MD503	73.48	0.725	14.25	5.45	0.093	1.65	1.42	0.36	2.36	0.204	120	102	48	19	80	127	144	21	228	13	687	69	23	20	0.87	100.15
3	1	7	NC	ES-Koz-30	MD502	71.64	0.832	14.66	5.14	0.065	1.93	2.44	0.62	2.12	0.552	107	106	46	25	78	119	184	23	258	12	411	83	19	21	0.81	100.21
3	4	24	NC	ES-Stv-8	MD511	69.65	0.994	17.81	5.50	0.081	1.85	1.44	0.39	2.19	0.098	119	121	52	25	86	103	159	28	269	16	532	88	22	24	3.85	100.57
3	4	24	NC	ES-Stv-9	MD512	72.72	0.881	15.73	5.45	0.053	1.51	1.30	0.33	1.86	0.162	114	110	45	23	77	104	199	25	247	14	554	67	19	28	2.72	100.59
3	kA	17	NC	ES-O-33	MD521	70.35	0.657	13.82	5.25	0.099	1.97	4.59	0.27	2.83	0.177	127	106	55	33	87	136	140	18	163	12	418	46	16	15	2.10	100.29

Tab. 4 Results of analysis by WD-XRF, sorted according clusters.

cluster		MGR	Clay	Sample	Lab.	SiO_2	TiO_2	Al_2O_3	Fe_2O_3	MnO	MgO	CaO	Na_2O	K_2O	P_2O_5	V	Cr	Ni	(Cu)	Zn	Rb	Sr	Y	Zr	(Nb)	Ba	(Ce	Pb	Th)	l.o.i.	Sum
pXRF	WD-XRF	group	type	No.	No.	per cent by weight										ppm														%	%
4	2	CC4	MC	ES-ZjM-53.	AD062	54.48	0.704	12.88	5.74	0.082	2.10	21.11	0.36	2.27	0.284	110	101	46	20	80	111	299	21	197	13	474	56	18	17	7.90	100.29
4	2	CC3	MC	ES-ZjM-5.	AD061	55.38	0.727	14.69	6.00	0.152	2.13	16.61	0.78	3.09	0.443	142	103	50	22	86	124	266	19	191	11	426	54	15	16	6.41	94.10
4	2	CC 1.2	MC	ES-Slk-1	MD509	59.34	0.736	14.02	5.86	0.188	2.14	13.73	0.70	3.03	0.261	138	105	55	26	85	134	269	23	227	12	504	58	16	17	1.68	100.30
4	3	37	NC cc++	ES-O-12	AD058	65.02	0.853	14.42	5.74	0.087	2.41	8.07	0.63	2.61	0.146	121	106	45	22	69	116	226	28	316	13	537	84	20	16	0.98	99.91
4	1	14	NC cc	O-48	AD341	64.20	0.802	14.38	5.91	0.115	1.98	8.80	0.63	2.98	0.213	141	107	54	27	78	135	211	29	248	19	512	89	20	10	1.10	100.22
4	1	14	NC cc	O-54	AD343	65.49	0.782	13.89	5.94	0.091	2.03	8.30	0.77	2.54	0.154	123	100	50	26	71	124	191	29	237	16	428	65	12	12	0.49	100.59
4	3	14.1	NC cc	ES-Pt-16	AD346	65.91	0.769	13.29	5.56	0.159	2.51	7.06	1.03	3.37	0.337	128	107	51	10	86	123	251	31	276	17	488	78	20	12	6.17	100.62
5	3	CC2	MC	ES-NK-8	MD508	69.06	0.740	10.64	4.00	0.063	2.07	10.86	0.62	1.74	0.200	96	82	38	18	51	81	252	24	406	12	504	50	13	13	3.05	100.19
5	3	26	NC cc+	ES-Stv11	MD513	72.77	0.786	10.77	4.28	0.063	1.87	6.95	0.68	1.66	0.171	82	83	39	18	61	81	189	19	392	12	415	68	7	18	0.93	92.50
5	3	CC2	MC	ES-Koz-79	AD060	66.86	0.815	12.84	4.98	0.080	2.17	9.11	0.66	2.30	0.176	109	92	43	23	69	101	279	30	383	12	486	76	17	11	1.73	99.85
5	3	CC2	MC	ES-O-44	MD522	67.82	0.812	12.36	4.69	0.079	1.99	9.04	0.68	2.35	0.177	102	92	45	25	64	100	273	26	404	14	487	71	18	17	1.62	100.63
			Outliers																												
	3	X 1	NC Fe-	ES-AK-18	MD500	75.57	0.740	16.53	2.84	0.033	0.92	1.22	0.29	1.76	0.092	113	100	35	29	57	112	123	19	205	12	518	76	21	20	1.01	100.04
	kA	52	NC	O-50	AD342	68.90	0.892	16.08	6.91	0.107	1.96	1.29	1.67	2.06	0.141	142	184	84	36	92	82	142	31	182	15	403	62	17	10	0.80	99.46
	kA	28	NC	ES-Zjm-8	AD347	63.76	0.763	**21.11**	4.79	0.089	1.17	2.53	0.63	4.90	0.259	115	95	40	24	86	181	145	27	225	16	672	82	34	22	2.36	99.53
	kA	Z 1	NC	ES-O-60	AD071	61.44	0.848	19.65	8.17	0.103	2.67	3.45	0.23	3.29	0.171	183	149	86	37	118	189	167	24	167	16	475	69	25	19	0.83	100.43
	4	-	-	ES-NK-9	AD072	76.07	0.870	14.87	4.56	0.036	0.83	1.55	0.03	0.79	0.462	117	82	30	10	61	**33**	79	22	244	14	152	62	19	12	1.51	100.96
	2	X 3	NC Fe-	ES-NK-2	MD505	76.14	0.882	15.77	4.43	0.018	0.41	1.86	0.01	0.32	0.183	86	59	24	13	32	**17**	93	29	407	20	375	76	26	25	1.79	100.74

Tab. 4 (Continued) Results of analysis by WD-XRF, sorted according clusters.

		pXRF Cluster				
WD-XRF cluster		**1**	**2**	**3**	**4**	Total
1	Number		1	4	3	8
	% within WD-XRF cluster		12.5%	50.0%	37.5%	100.0%
2	Number	5	7			12
	% within WD-XRF cluster	41.7%	58.3%			100.0%
3	Number	1			2	3
	% within WD-XRF cluster	33.3%			66.7%	100.0%
4	Number	2	3	2		7
	% within WD-XRF cluster	28.6%	42.9%	28.6%		100.0%
5	Number			4		4
	% within WD-XRF cluster			100.0%		100.0%
Total	Number	8	11	10	5	34
	% within WD-XRF cluster	23.5%	32.4%	29.4%	14.7%	100.0%

Tab. 5 Comparison of accordances between WD-XRF and pXRF clusters. The table shows the number of matching samples within the same Ward cluster with pXRF and WD-XRF data.

Site	MGR-group		Graeco-Roman	Chernyakhov	Unknown
	calcareous	*non-calcareous*		*No. of samples*	
Olbia	**CC1.1**		**11**	**3**	**1 (Cerny.?)**
	CC2		2	2	1
	CC4		-	1	
	mx				
		14	2		
		17		1	
		34		1	
		35		1	
		36		1	
		37		1	
		38		1	
		39		1	
		40		6	
		41		1	
		42		1	
		43		1	
		44		1	
		45		1	
		46	1		
		48		1	
		49		1	
		50		1	
		51	3		
		52	1		
		Y4		1	
		Z1		1	
		47/CC2		1	

Tab. 6 Number of samples in particular MGR-groups and clay-types occurring at particular cultural spectra and sites.

Site	MGR-group		Graeco-Roman	Chernyakhov	Unknown
	calcareous	*non-calcareous*		*No. of samples*	
Kozyrka	**CC1.1**		**9**	**1**	
	CC1.2		2		
	CC2				1 (Cerny.?)
	mx		1 (mx?)	1	1(Cerny.?)
		7		6	
		7,02		1	
		8		1	
		9		2	
		10		1	
		11		1	
		12	1		
		Z2		1	
		Y1		1	
		Y2		1	
Zolotoyi Mys	CC1.1		15		1 (G-R?)
	CC1.2		2	1	
	CC3		1		
	CC4			1	
	CC5		2		
		28	1		
		29	1		
		30		1	
		31		1	
		32		1	
		33	1		
		Y3	1		

Tab. 6 (Continued) Number of samples in particular MGR-groups and clay-types occurring at particular cultural spectra and sites.

Site	MGR-group		Graeco-Roman	Chernyakhov	Unknown
	calcareous	*non-calcareous*		*No. of samples*	
Petukhivka	**CC1.1**			**1**	**1**
	CC2			1	
	mx				1
		19		2	
		21		1	
		53		1	
		20		1	
		22	1		
		14,1		1	
Adzhikolska Kosa		1		1	
		2		1	
		3		1	
		4		1	
		5		1	
		6		1	
		X1		1	
		X2		1	
Stanislav		23		1	
		24		2	
		25		2	
		26		1	
Stara Bodanovka	CC1.1		1		
	CC2		1		
		X3		1	

Tab. 6 (Continued) Number of samples in particular MGR-groups and clay-types occurring at particular cultural spectra and sites.

Site	MGR-group		Graeco-Roman	Chernyakhov	Unknown
	calcareous	*non-calcareous*		*No. of samples*	
Novokondakove	**CC2**			**1**	
		15		1	
		16		2	
		18		1	
		40		2	
		X3		1	
Radsad	**CC1.1**		2		
		27	1		
Skelka	**CC1.2**		1		

Tab. 6 (Continued) Number of samples in particular MGR-groups and clay-types occurring at particular cultural spectra and sites.

Bibliography

Backhaus et al. 2006
Klaus Backhaus, Bernd Erichson, Wulff Plinke, and Rolf Weiber. *Multivariate Analysemethoden. Eine anwendungsorientierte Einführung*. Berlin and Heidelberg: Springer, 2006.

Daszkiewicz 2014
Małgorzata Daszkiewicz. "Ancient Pottery in the Laboratory – Principles of Archaeoceramological Investigations of Provenance and Technology." *Novensia* 25 (2014), 177–197.

Daszkiewicz and Maritan 2017
Małgorzata Daszkiewicz and Lara Maritan. "Experimental Firing and Re-firing." In *The Oxford Handbook of Archaeological Ceramic Analysis*. Ed. by A. Hunt. Oxford: Oxford University Press, 2017, 487–508.

Daszkiewicz and Schneider 2001
Małgorzata Daszkiewicz and Gerwulf Schneider. "Klassifizierung von Keramik durch Nachbrennen von Scherben." *Zeitschrift für Schweizerische Archäologie und Kunstgeschichte* 58 (2001), 25–32.

Mecking, Mielke, and Behrendt 2013
Oliver Mecking, Dirk Paul Mielke, and Sonja Behrendt. "Methodenvergleich, Anwendungsbeispiele und Grundlagen der portablen Röntgenfluoreszenzanalyse (P-RFA) in der Keramikforschung." In *Naturwissenschaftliche Analysen vorund frühgeschichtlicher Keramik 3*. Ed. by B. Ramminger, O. Stilborg, and M. Helfert. Universitätsforschungen zur prähistorischen Archäologie 238. Bonn: Habelt, 2013, 49–67.

Meyer et al. 2016
Michael Meyer, Małgorzata Daszkiewicz, Gerwulf Schneider, Reinhard Bernbeck, Bernhard S. Heeb, Morten Hegewisch, Kay Kohlmeyer, Claudia Näser, Silvia Polla, Erdmute Schultze, Fleur Schweigart, and David Alan Warburton. "Economic Space. On the Analysis and Interpretation of Pottery Production and Distribution." In *Topoi Research Papers*. Ed. by G. Gerd and M. Meyer. eTopoi Journal for Ancient Studies 6. Edition Topoi, 2016, 200–204. URL: http://edition-topoi.org/articles/details/economic-space.-on-the-analysis-and-interpretation-of-pottery-production-an (visited on 08/02/2018).

Schneider and Daszkiewicz 2010
Gerwulf Schneider and Małgorzata Daszkiewicz. "Testmessungen mit einem tragbaren Gerät für energiedispersive Röntgenfluoreszenz (P-XRF) zur Bestimmung der chemischen Zusammensetzung archäologischer Keramik." In *Archäometrie und Denkmalpflege*. Ed. by O. Hahn, A. Hauptmann, D. Modarressi-Tehrani, and M. Prange. Metalla Sonderheft 3. Bochum: Deutsches Bergbau-Museum, 2010, 110–112.

Schultze, Magomedov, and Bujskich 2006
Erdmute Schultze, Boris V. Magomedov, and Sergej B. Bujskich. *Grautonige Keramik des Unteren Buggebietes in römischer Zeit. Nach Materialien der Siedlungen in der Umgebung von Olbia*. Eurasia Antiqua 12. von Zabern, 2006.

Illustration and table credits

ILLUSTRATIONS: **1** After Schultze, Magomedov, and Bujskich 2006, Fig. 1. **2** After Schultze, Magomedov, and Bujskich 2006, Fig. 25. **3** After Schultze, Magomedov, and Bujskich 2006, Fig. 26. **4–10** F. Schweigart. **11–18** M. Daszkiewicz (with Macrophotos by M. Baranowski). **19–21** F. Schweigart. **22–27** M. Daszkiewicz (with Macrophotos by M. Baranowski). **28–32** F. Schweigart. **TABLES:** **1** F. Schweigart. **2–3** M. Daszkiewicz. **4–6** F. Schweigart.

FLEUR SCHWEIGART

Fleur Schweigart, MA in Berlin 2014, finished her PhD thesis at the Berlin Graduate School of Ancient Studies (BerGSAS) with a stipend from the Excellence Cluster Topoi. She was a part of the Topoi research group (A-6) Economic Space, working on the topic 'Wheel-Thrown Pottery between Elbe and Oder. Production, Distribution and Consumption.'

Dr. des. Fleur Schweigart
Institut für Prähistorische Archäologie
Freie Universität Berlin
Fabeckstraße 23–25
14195 Berlin, Germany
E-mail: fleur.schweigart@gmail.com

MAŁGORZATA DASZKIEWICZ

Małgorzata Daszkiewicz, MA Warsaw 1979 in Physical Geography, PhD Warsaw University 1993 in Humanities. Since 1994 she has worked in collaboration with *AG Archäometrie* FU Berlin. Formerly a part-time employee at TOPOI, she is currently an associated member of the Institute for Prehistoric Archaeology FU Berlin and also runs ARCHEA, a laboratory in Warsaw for archaeometric analysis and research. Her main research interests are determining the technology and provenance of archaeological ceramics and devising techniques for the classification of bulk ceramic finds.

Dr. Małgorzata Daszkiewicz
Freie Universität Berlin
Institut für Prähistorische Archäologie
Fabeckstraße 23–25
14195 Berlin, Germany
and
ARCHEA
ul. Ogrodowa 8m95
00-896 Warszawa, Poland
E-mail: m.dasz@wp.pl

Małgorzata Daszkiewicz, Ewa Bobryk

Analysis of Ceramic Vessel Surfaces Using pXRF: Preliminary Results of Experiments with Gypsum Moulds and Salt Production by Boiling Brine

Summary

Like all analytical techniques, pXRF has its advantages and disadvantages. Chemical analysis by pXRF is of limited use in provenance studies, but using this technique opens up new possibilities for rapidly classifying large numbers of archaeological pottery sherds and analysing the surfaces of ceramic vessels. The results of pXRF analyses not only provide information about layers intentionally applied to vessel surfaces, but also about the alteration process. Model tests also show that pXRF results can be useful in reconstructing vessel forming techniques and in assessing functional properties.

Keywords: surface analysis; pXRF; gypsum mould; salt boiling

Wie alle analytischen Techniken hat pRFA ihre Vor- und Nachteile. Chemische Analysen mit pRFA sind für Herkunftsbestimmungen von begrenztem Nutzen, jedoch bietet diese Technik neue Möglichkeiten für eine schnelle Klassifikation großer Mengen archäologischer Keramik und bei der Analyse von Gefäßoberflächen. Die pRFA-Ergebnisse geben nicht nur Information über intentionell aufgebrachte Schichten auf Gefäßen, sondern auch über Alterationsprozesse. Modellversuche zeigten auch, dass pRFA-Ergebnisse nützlich sein können bei der Rekonstruktion von Formgebungsverfahren und bei der Beurteilung von Funktionseigenschaften.

Keywords: Oberflächenanalyse; pRFA; Gipsmodel; Salzsieden

Morten Hegewisch, Małgorzata Daszkiewicz und Gerwulf Schneider (eds.) | Using pXRF for the Analysis of Ancient Pottery – an Expert Workshop in Berlin 2014 | Berlin Studies of the Ancient World 75 (ISBN TODO; DOI: 10.17171/3-75) | www.edition-topoi.org

1 Introduction

The surface composition of pottery cannot be determined by the type of conventional chemical analysis used to establish pottery provenance. For the purposes of provenance studies, the information about a sherd's chemical composition gleaned from chemical analysis must be as precise as possible, i.e. analysis must provide details of the sherd's original chemical composition. To achieve this goal, prior to analysis each sample is thoroughly cleaned, and a thin layer of the sherd's surface is removed, as this layer may have been affected by bidirectional migration of elements resulting from the pottery having been buried in the ground (elements can both leach out from the sherd as well as penetrate into the sherd). Any intentional surface coatings, such as slip, gloss, glaze and painted decoration, are also removed.

In contrast to conventional chemical analysis, multiple measurements can be performed quickly using the portable X-ray fluorescence technique. However, the application of pXRF in provenance studies is partly limited because it does not always provide sufficiently precise and accurate results in determining the concentrations of individual elements.[1] Nevertheless, this technique provides new opportunities for multifaceted analysis of ceramic materials e.g. through integration into a down-up strategy,[2] especially for the analysis of surfaces and intentional as well as non-intentional surface coatings.[3] The impetus for carrying out model tests using pXRF to analyse the surface of ceramic vessels for a purpose other than examining intentional surface coatings arose from analysis of pottery found in Petra.

Thirty-two samples of Nabataean pottery from Petra[4] were measured by pXRF on the unpainted parts of their surfaces (inside or outside) after all sherds had been cleaned with acetic acid for one hour in an ultrasonic device to remove any potential thin calcite deposits on their surfaces. In the case of twelve samples, fresh fractures or cut cross-sections were also measured, even if the cross-sections only covered a small part of the 8-mm-window of the pXRF analyser. The results of the measurements were consistently different. Not all differences could be explained by the samples' different geometries, which account, for example, for the differing values of the light elements Al and Si

1 See in this volume contribution 8 by Daszkiewicz et al.; contribution 5 by Baranowski et al.; contribution 10 by Schweigart and Daszkiewicz.

2 See in this volume contribution 8 by Daszkiewicz et al.

3 E.g. analysis of slip on Roman pottery from Moesia, see contribution 5 by Baranowski et al. in this volume, and analysis of black layers coating Hellenistic pottery found in Risan, Montenegro: Baranowski et al. 2018.

4 Nabataean pottery is a unique eggshell-thin ceramic ware which is barely 1–4 mm thick. It represents a range of dates between the 2nd century BC and the 4th century AD and has been found at Petra in Jordan and at other Nabataean sites. The most common form of this ware is a shallow open bowl, probably used as a drinking vessel. These bowls usually feature characteristic painted decoration on the inside, which varies in style depending on the date of the vessel, see e.g. Schmid 2000.

(Mg was only detected in a few cases). Concentrations of Ba and Cl (as well as Mn) were generally lower at the surfaces and were not detected in many cases. Ca levels were higher on the outer surfaces by an average factor of 1.8 compared to the inner surfaces, and higher than the values of measurements taken on fresh fractures or cut cross-sections, as well as being higher than the WD-XRF control measurements. Two samples were shown to represent calcareous pottery by analysis on fresh fractures and by WD-XRF. Lower Ca on both surfaces of one of these samples was caused by elements leaching from this sherd during its deposition. The high P concentration suggests that this sherd is strongly weathered. It is well known that P levels become elevated due to absorption from the surrounding soil during burial and are usually highest near the sherd surface. The high value on the outer surface must, therefore, be ascribed to the two surfaces having different qualities. In the case of the second sample, the elevated Ca content, particularly on the outer surfaces, can only be attributed to gypsum because any potential calcite layers were removed with acid.

In this article the authors outline the results of a model analysis aimed at answering the following questions regarding the use of the pXRF technique:

– Could it be that we can detect the presence of calcium and sulphur associated with the influence of forming techniques (forming in gypsum moulds, Fig. 1)?

– Could it be that we can detect chlorine by pXRF at the surface of vessels used for crystallising salt by boiling brine (sodium cannot be detected by pXRF)?

In order to examine the feasibility of using pXRF, measurements were performed on samples prepared in a laboratory under strictly specified conditions. Model analyses were carried out on samples made of non-calcareous iron-rich clays (clay from Olbia for experiments with a gypsum mould and clay from Rheinzabern for experiments with boiling salt solutions). These model analyses were undertaken at ARCHEA and at the Faculty of Chemistry of the Warsaw University of Technology;[5] pXRF measurements were performed at the Free University Berlin Excellence Cluster 264 TOPOI as part of a series of tests designed to assess the potential and limitations of using this technique in the analysis of ancient pottery. Measurements were performed using a Niton XL3t 900S GOLDD RF-Analyser and MINING software, calibration based on twelve ceramic standards analysed by WD-XRF,[6] 8-mm measuring spot, measurements on fresh fractures, three measurements per sample (three different spots), measurement time of 120 seconds (30 seconds per filter), in a sample chamber; helium was not used.

5 This work was financially supported by Warsaw University of Technology.

6 Preparation and measurements by M. Daszkiewicz and G. Schneider.

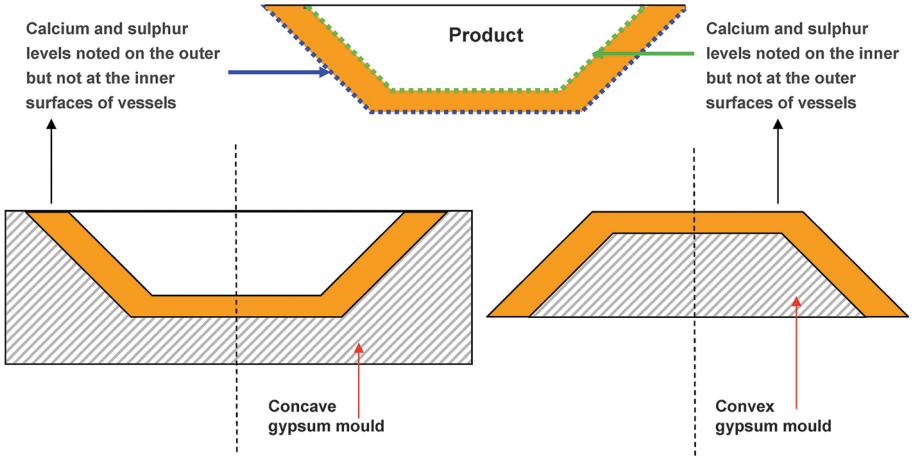

Fig. 1 Schematic representation of vessels being formed in concave and convex gypsum moulds. Depending on the type of mould used, it is expected that there will be a greater concentration of calcium and sulphur either on the inner or the outer surface of the vessels.

2 Results

2.1 Forming in a gypsum mould

A non-calcareous clay (OLBIA-MD525) was used to create specimens of ceramic body and pottery (pottery = ceramic body fired at 900°C). Three types of plastic mass made up with distilled water were prepared from this clay: the first mass was not enhanced with any additives, the second featured added gypsum, while both NaCl and gypsum were added to the third (pure p.a. NaCl was added so that the salinity of the make-up water equated to the average salinity of seawater – 35‰; the quantity of added pure p.a. gypsum amounted to 2g CaO in 100g of clay).[7] Various techniques were used to produce specimens from these three masses: a) specimens made without any exposure to gypsum: the plastic mass was prepared by hand and rolled out, after which specimens were either formed in a porcelain mould or cut out using a cutter made of glass; b) specimens made with exposure to gypsum: produced by forming in plaster moulds (wet and dry). The various forming techniques yielded specimens with different surface

7 Saline make-up water was used in view of the fact that to this day, as has been the case for centuries, potters add either saline or freshwater to the same calcareous clay depending on the surface colour they wish to achieve, resulting in an effect known as self-slip. In many regions the use of saline water or water that introduces gypsum to the ceramic body was not an intentional measure but was linked to environmental factors – the Near East region being one such example. Salt is also added to ceramic bodies made of non-calcareous clays in order to improve their rheological properties (no self-slip effect).

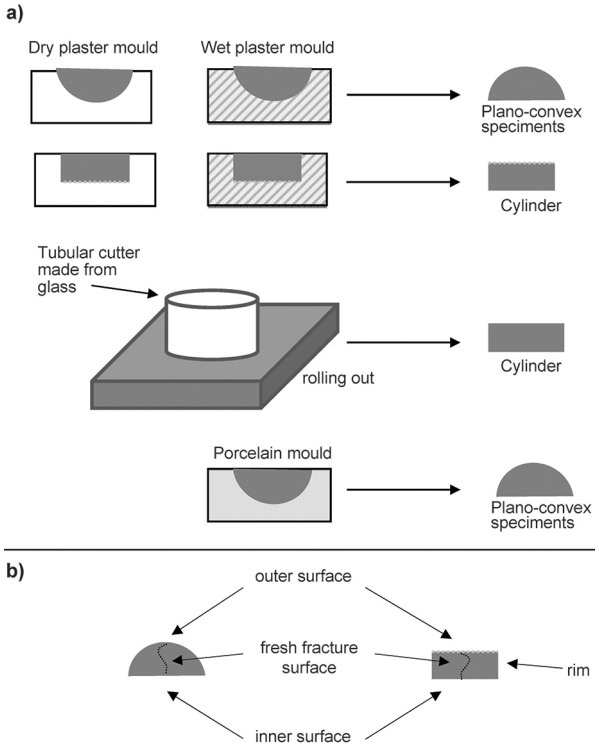

Fig. 2 a) The various forming techniques used to produce specimens for the experiment; b) measurement spots for pXRF analysis.

geometries, see Fig. 2a. All specimens were dried on blotting paper. Measurements by pXRF were taken on the outer and inner surface of each specimen and on fresh fracture surfaces, as well as on rim surfaces (see Fig. 2b). Three measurements were taken on each surface, altering the position of the sample each time. Measurements were also performed on flat, pressed pellets prepared from a dry mass.

Fig. 3 shows calcium (Ca) and sulphur (S) distribution detected in unfired specimens and in fired specimens made from the same ceramic body made up with distilled water and distilled water featured added gypsum and NaCl. Ca, S and Cl levels determined by pXRF for variously formed specimens (averages of three measurements) as predicted are showing the same changes. Due to loss on ignition the concentrations of these elements detected in unfired specimens were different to those detected in fired specimens made from the same ceramic body.[8] The model analyses revealed that inferences can be drawn about whether or not a ceramic product was made in a plaster

8 This fact must be taken into account when writing up the results of chemical analysis carried out using pXRF on pottery and clay raw materials (previously unfired) in provenance studies, as well as when analysing ceramic sherds fired at significantly different temperatures.

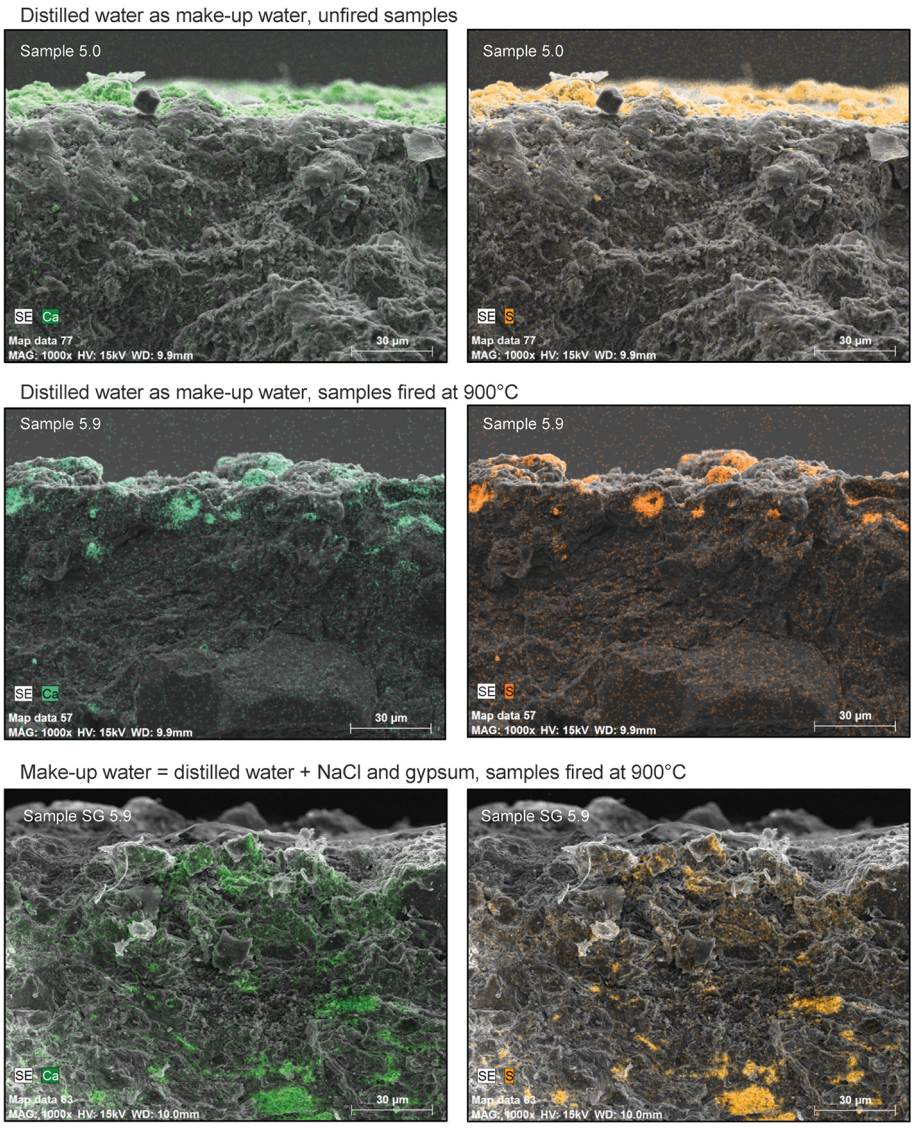

Fig. 3 Mapping of calcium and sulphur distribution detected in unfired specimens (5.0) and in fired specimens (5.9) made from the same ceramic body made up with distilled water; SG 5.9 = fired specimens made from the same ceramic body made up with distilled water featuring added gypsum and NaCl.

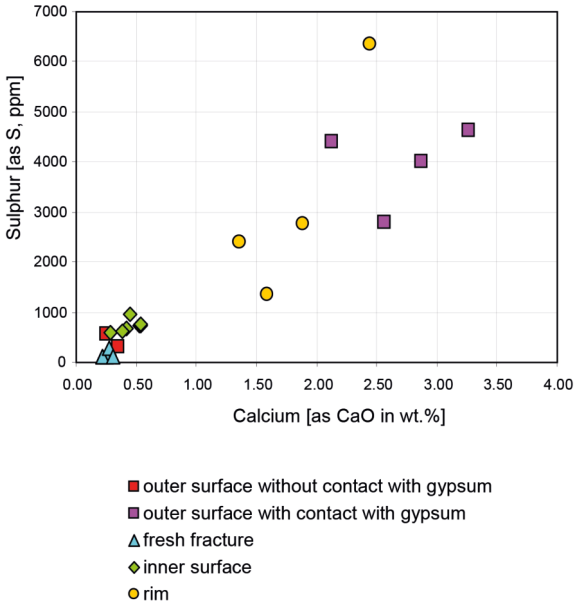

Fig. 4 Sulphur contents (as S in ppm) versus calcium contents (as CaO in wt.%). Specimens made of the same ceramic body formed either without exposure to gypsum or in concave gypsum moulds. Analysis by pXRF was performed on the outer and inner vessel surfaces and on rim and fresh fracture surfaces (each point represents the average of three measurements).

mould by correlating Ca content (and to a lesser degree S content) in sherd surfaces with the results of fresh fracture analysis (Fig. 4). These tests also showed that a similar migration process takes place in sherds made from non-calcareous clays to that which takes place in calcareous sherds; however, a visibly pale surface (so-called self-slip) does not develop. Fig. 5 shows Ca contents in three Nabataean pottery fragments and in laboratory created specimens formed in wet plaster mould.

Is the presence of gypsum on the outer surface of a Nabataean vessel evidence of its having been formed in a gypsum mould or is it due to the other effect?

2.2 Salt boiling

A project conducted by Eberhard Bönisch included analysis of five samples of Briquetage-Kelche, one of them found in Saalhausen.[9] All of the samples were made from non-calcareous clays with various amounts of iron-compounds. A very characteristic feature of these samples is that they are heavily tempered, as can be seen macroscopically in the original samples. Thin-section analysis revealed that the non-plastic ingredients are primarily quartz grains, with quartzite and particles of magmatic and metamorphic rocks also present. From a technological point of view such a large amount of temper stems

9 Bönisch, Daszkiewicz, and Schneider 2012.

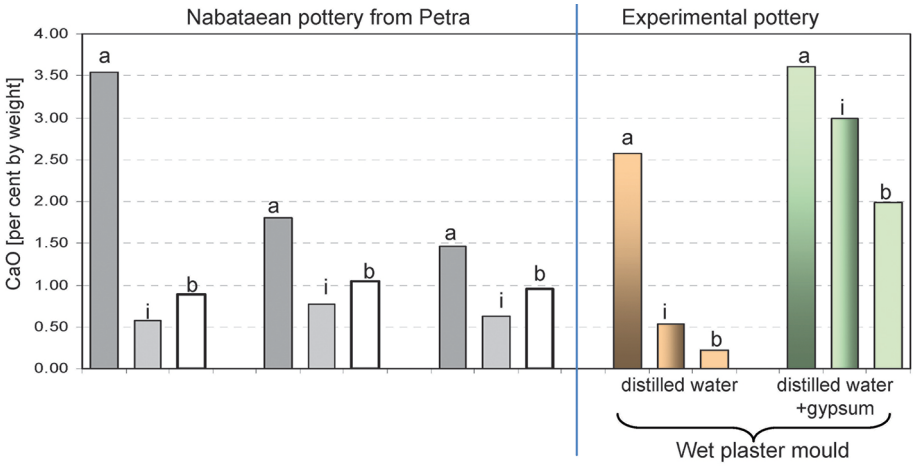

Fig. 5 Calcium (as CaO in wt.%) content in three Nabataean pottery fragments and in laboratory-made specimens formed in wet plaster moulds made up either with distilled water or with distilled water and added gypsum.

from the necessity of producing vessels highly resistant to thermal shock and with higher resistance to crack growth, to which the ceramic material would have been vulnerable during repeated cycles of heating and cooling associated with the salt boiling process.

In order to establish whether we can detect chlorine by pXRF at the surface of vessels used for producing salt, a salt-boiling experiment was conducted in laboratory conditions. This experiment involved the following steps: 1) selecting raw materials for making plastic masses, 2) formulating the composition of the plastic masses, 3) determining firing temperatures, 4) vessel forming and firing, 5) salt boiling as a periodic and a continuous process, 6) vessel conditioning after the salt production process, 7) vessel analysis. A schematic diagram of the experiment is presented in Fig. 6.

Selecting raw materials for plastic masses: Rheinzabern clay was chosen as the matrix material, with rounded quartz sand grains of 1–1.5 mm being used as a non-plastic ingredient. The clay was dried, crushed and passed through a sieve with a 0.5 mm mesh. The quartz sand was repeatedly rinsed in distilled water, dried and fractionated.

Formulating the composition of plastic masses: Based on preliminary studies, two formulas were chosen for the composition of the plastic masses: A – mass containing 50% by weight clay and 50% by weight temper, B – mass containing 35% by weight clay and 65% by weight temper. Adding such a significant quantity of non-plastic material was dictated by the need to produce vessels highly resistant to thermal shock and with good resistance to crack growth caused by thermal stress during repeated cycles of heating and cooling in the course of the vessel's use. The amount of make-up water was calculated as 18% for formula A and 15.5% for formula B. A batch of 2000 g of each

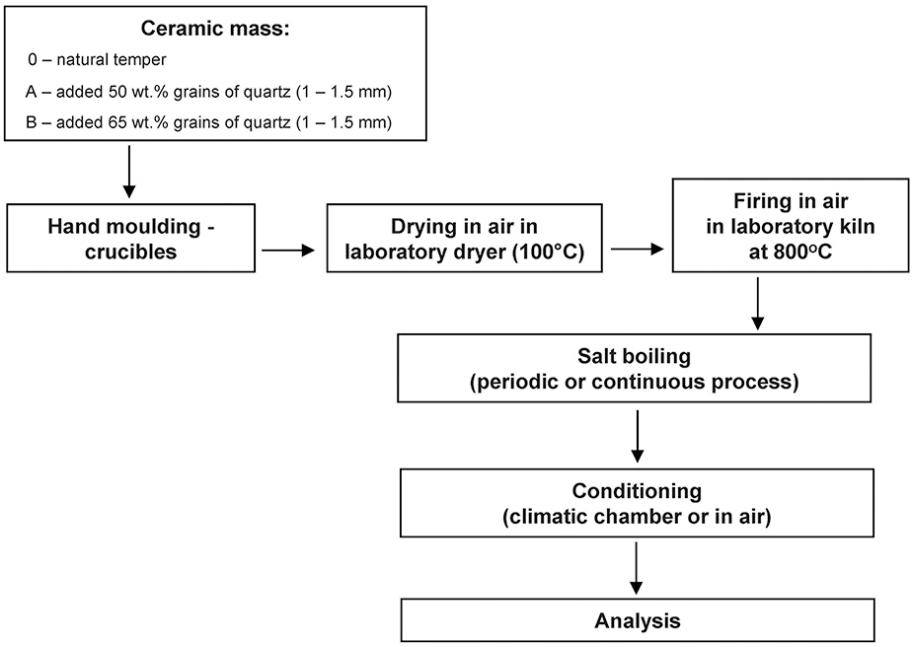

Fig. 6 A schematic diagram of the salt-boiling laboratory experiment.

mass was prepared.

Determining firing temperatures: Firing temperatures for fabrics A and B were determined based on the ceramic properties of specimens fired at the following temperatures: 600, 700, 800, 900, 1000, 1100, 1150 and 1200°C. Hydrostatic weighing was used to gauge apparent density, open porosity and permeability. Based on these results it was decided to fire vessels at 800°C – the lowest temperature at which a sufficiently resistant vessel with a high porosity of 30% could be produced.

Vessel forming and firing: A simplified vessel form – as shown in Fig. 7. – in the shape of an elongated crucible with a capacity of 50–60 ml was selected for the purposes of this experiment. The vessels were formed by hand, with several being made from each fabric.

Once formed, the crucibles were dried for 48h at room temperature and then for a further 24h in a laboratory drier at 100°C. The dried crucibles were fired in a Carbolite resistance furnace at 800°C at a heating rate of 5°C/min with peak temperature maintained for 1 hour.

Salt boiling as a periodic and a continuous process, the technological details of this experiment were as follows:

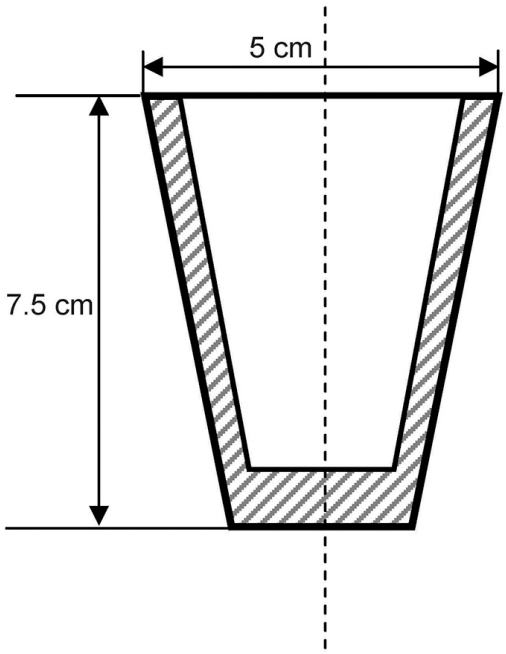

Fig. 7 Cross-section of vessel in the shape of an elongated crucible with a capacity of 50–60ml used in laboratory salt-boiling experiment.

– the salt extraction process was undertaken using water from Ciechocinek's natural saline springs with a salt concentration of 5% and 30% by weight.

– the apparatus used consisted of a laboratory burner and a tripod with a porcelain triangle on which the crucible was placed, as shown in Fig. 8.

– the process was carried out in two ways: continuously and periodically.

The periodic process involved a crucible filled with brine being heated until all of the water had evaporated. After the salt-filled crucible had dried out, the salt was removed and the whole process was repeated a further five times for both the 5% and the 30% solutions.

In the continuous process, the crucible was topped up with brine during the course of its being heated. The volume of water evaporated in this process amounted to 500 ml for the 5% saline solution and 200 ml for the 30% solution.

The salt-boiling process was a turbulent one. When the brine-filled crucible was heated, the solution began to boil and become more concentrated. Salt was deposited at the bottom of the vessel, but the intense evaporation of the water also encouraged salt to crystallise at the top of the vessel, on its outer surface which had a lower temperature,

Fig. 8 Salt boiling in the laboratory.

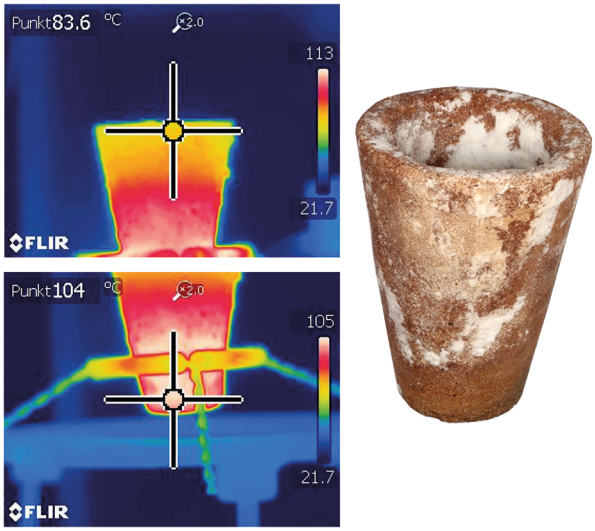

Fig. 9 Infrared images taken during salt boiling: the image on the right shows the crucible after completion of the salt-boiling process.

as confirmed by infrared measurements taken using a thermal imaging camera. The use of a thermal imaging camera (FLIR T335) enabled the temperature of the brine to be gauged in various parts of the crucible during the process. The infrared images shown in Fig. 9 confirm that there was a temperature gradient within the vessel – from 105°C near the bottom to 80°C below the surface of the liquid. This explains why the heating process was so dynamic.

The continuous process of boiling the 30% saline solution was a very efficient one. Keeping the crucible, which had a capacity of 50–60 ml, constantly full required three to five 'top-ups' (around 150 ml in total) over a period of 20–30 minutes. As the volume of the salt deposits increases so the amount of available space for the solution decreases

and the process becomes less efficient. Therefore, it is preferable to successively remove the crystallised salt from the crucible. In contrast, the same process carried out using a 5% solution becomes considerably drawn out, and at least 16–18 'top-ups' are needed to obtain the same amount of salt. It can be assumed that this type of elongated crucible, which did not provide a large surface for evaporation, was more effective for the final phase of salt crystallisation rather than for the preliminary concentration of the saline solution. None of the vessels made for this process was damaged during use, confirming the initial assumption that this simple technology would be effective for the purposes of this experiment.

Once the experiment had been completed, the crucibles were rinsed in distilled water and divided into pieces. Some of them were placed in a Memmert climate chamber (to simulate the alteration process) programmed to run for 50 hours at a constant temperature of 30°C and 90% humidity, while the remainder were dried in air. After removal from the climate chamber, these samples were also dried in air. Samples prepared in this manner were measured using pXRF.

Measurements were performed on three parts of each crucible: the rim, bottom and middle, in each instance on the outside, inside and on a fresh fracture. All together 27 measurements were taken per crucible. The results of these measurements show that the amount of temper used did not make a difference to the Cl content. In the case of original archaeological samples, if possible, it is best to analyse the bottom of the vessel, as the salt from other parts of it disappears after it has been in the climate chamber. The faster disappearance of salt from the outer surface of the upper and middle portion of a vessel is probably linked to the various processes responsible for salt deposition (evaporation, sedimentation). At the time of writing this text, pXRF analysis results were available for one briquetage-Kelch found in Saalhausen (sample submitted for analysis by Eberhard Bönisch); for preliminary results see Daszkiewicz[10] and for ten rim sherds of briquetage-type pottery recovered from the excavation of a site in Lossow Burgwall (samples submitted for analysis by Agnes Beilke-Voigt). Cl content was also determined on an old fracture in order to examine the impact of the alteration effect. There is a very clear tendency towards higher Cl levels on the vessel's outer wall. Cl content was also measured on a fresh fracture and was found to be higher than in other types of ceramic vessels. Cl levels were determined by pXRF on the fresh fracture of various ceramic sherds. The Cl content did not exceed 89 ppm in 1229 sherds of pottery from: the Banat region (Romania), Brandenburg (Germany), the Lublin area (Poland), in and around Voitenki (Ukraine) and Gorsleben (Germany). Bimodal distribution is observed, but the differences in Cl levels are not related either to the site from which the samples were recovered or the date when the measurements were performed (Fig. 10). Of the total

10 Daszkiewicz, Bobryk, and Bönisch 2016.

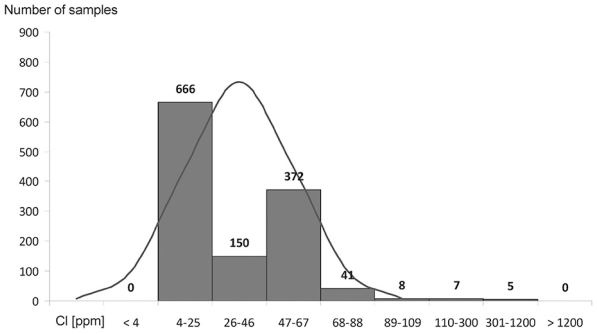

Fig. 10 Histogram of Cl content measured by pXRF on fresh fracture surfaces; measurements were performed on 1249 samples. Cl content of one sample = average from measurements on three different spots, precision of measurement (2 Sigma): ± 5 rel.% (statistically), ± 10 rel.% (long term precision, 3 years).

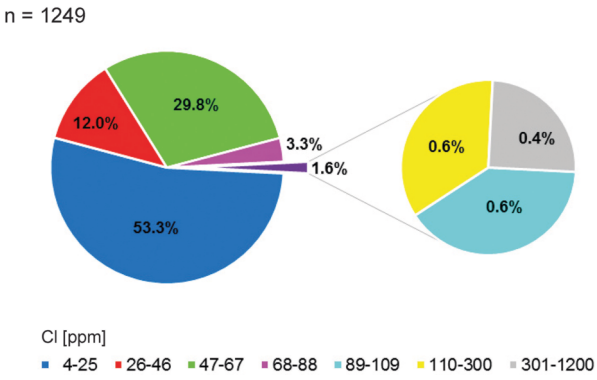

Fig. 11 Percentage of samples representing particular ranges. Cl content (ppm) measured on fresh fracture surfaces of 1249 samples.

number of 1249 analysed sherds, only 20 samples (Fig. 11) had a Cl content of more than 90 ppm (92–1190 ppm). These were sherds of briquetage-type pottery recovered from the excavation of a site in Lossow Burgwall, briquetage-type pottery found in Saalhausen and sherds found at a site in the Banat region. Fig. 12 shows Tukey boxplot, in green are marked outliers (Cl content of more than 109 ppm) and in red samples having extreme values – these are sherds of briquetage-type pottery found in Lossow Burgwall and in Saalhausen and samples from the Banat region.

An assessment was also made of the Cl levels on the inner and outer walls as well as on an old fracture of the briquetage-type sherds found in Lossow Burgwall (Fig. 13 shows one vessels without contact with salt). In some vessels, in keeping with the experiment results, the Cl content was greater on the outer/inner wall and the Cl content on the old fracture was almost the same as on the fresh fracture. It is with a high degree of probability that this can be taken as evidence of the analysed ceramic sherds having been used for salt extraction, as had earlier been determined based on typological analysis. For the briquetage-type sherd the high Cl content measured only on the fresh fracture surface can be sufficient proof that it was used in contact with salt (Fig. 14).

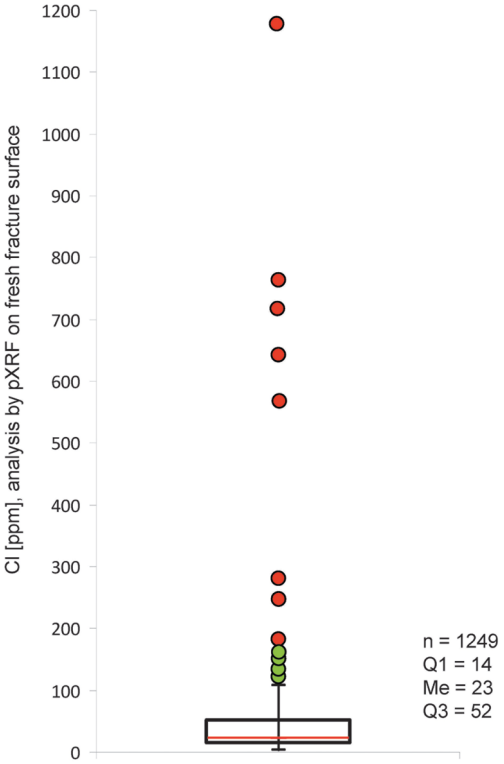

Fig. 12 Tukey boxplot: green = outliers (Cl content of more than 109 ppm), red = extreme outliers. Atypical samples are represented by sherds of briquetage-type pottery found in Lossow Burgwall and in Saalhausen and in samples from the Banat region.

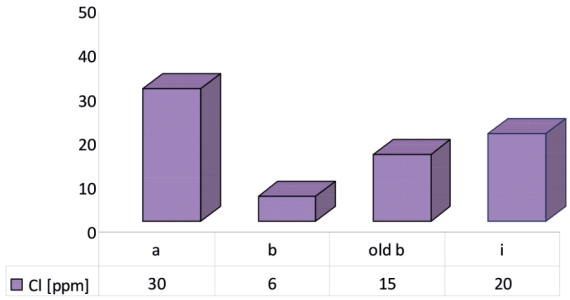

Fig. 13 Briquetage-type sherds found in Lossow Burgwall without contact with salt. a = outer surface, b = fresh fracture, old b = old fracture surface, I = inner surface.

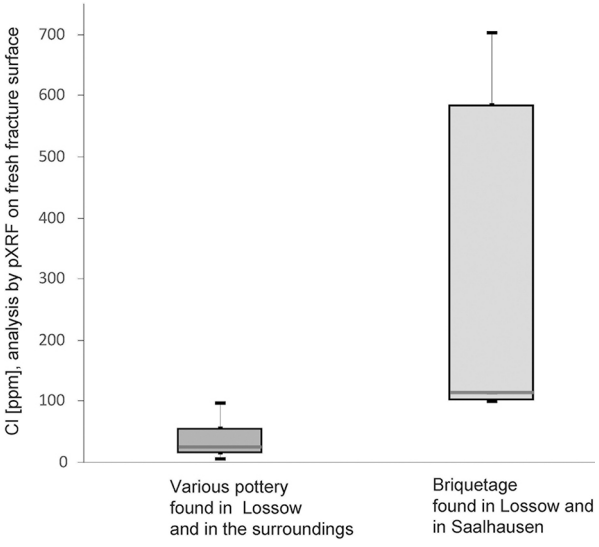

Fig. 14 Two different distribution patterns. On the left: samples analysed as part of Agnes Beilke-Voigt's LOSSOW project, found at Lossow and at other sites in Brandenburg; on the right: samples found at Lossow-Burgwall and Saalhausen (Eberhard Bönisch's project), most of which are samples typologically identified as Briquetage-type sherds.

3 Conclusions

The model analysis revealed that using pXRF introduces new possibilities in the analysis of vessel surfaces in the context of studying ancient technologies, specifically in the analysis of forming techniques using moulds and in functional analysis, in particular of briquetage. Nonetheless, when analysing historic pottery it must be borne in mind that the results of measurements made on a vessel surface are also affected by the alteration process.

Bibliography

Baranowski et al. 2018
Marcin Baranowski, Klaus Bente, Christoph Berthold, Ewa Bobryk, Małgorzata Daszkiewicz, Monika Ganeczko, and Bartłomiej Witkowski. "MGR-Analyis, textgreekμ-Raman Spectroscopy and Gas Chromatography-Mass Spectrometry Analysis of an Exceptional Fragment of Black-Voated Gnathia-Type Pottery Found in Risan (Montenegro)." In *Archäometrie und Denkmalpflege 2018. Jahrestagung am Deutsches Elektronen-Synchrotron, Hamburg, 20.–24. März 2018*. Ed. by L. Glaser. Hamburg: Verlag Deutsches Elektronen-Synchrotron, 2018, 34–37.

Bönisch, Daszkiewicz, and Schneider 2012
Eberhard Bönisch, Małgorzata Daszkiewicz, and Gerwulf Schneider. "Gefäßausstattung eines jüngstbronzezeitlichen Kammergrabes der Lausitzer Kultur mit Briquetage – Interpretation unter Einbeziehung von Keramikanalysen." In *Finden und Verstehen. Festschrift für Thomas Weber zum sechzigsten Geburtstag*. Vol. 66. Beiträge zur Ur- und Frühgeschichte Mitteleuropas. Langenweissbach: Beier & Beran, 2012, 195–222.

Daszkiewicz, Bobryk, and Bönisch 2016
Małgorzata Daszkiewicz, Ewa Bobryk, and Eberhard Bönisch. "Salz aus Halle – Natriumchlorid an Niederlausitzer Briquetage nachgewiesen." In *Ausgrabungen im Niederlausitzer Braunkohlenrevier 2013/2014*. Ed. by E. Bönisch and F. Schopper. Wünsdorf: Brandenburgisches Landesamt für Denkmalpflege und Archäologisches Landesmuseum, 2016, 77–88.

Schmid 2000
Stefan G. Schmid. *Petra ez-Zantur II. Ergebnisse der Schweizerisch–Liechtensteinischen Ausgrabungen, Teil I: Die Feinkeramik der Nabatäer: Typologie, Chronologie und kulturhistorische Hintergründe*. Mainz: Philipp von Zabern, 2000.

Illustration credits

1–2 E. Bobryk. **3–5** M. Daszkiewicz. **6** E. Bobryk / M. Daszkiewicz. **7–9** E. Bobryk. **10** M. Daszkiewicz / H. Baranowska. **11–13** M. Daszkiewicz. **14** M. Daszkiewicz / H. Baranowska.

MAŁGORZATA DASZKIEWICZ

Małgorzata Daszkiewicz, MA Warsaw 1979 in Physical Geography, PhD Warsaw University 1993 in Humanities. Since 1994 she has worked in collaboration with *AG Archäometrie* FU Berlin. Formerly a part-time employee at TOPOI, she is currently an associated member of the Institute for Prehistoric Archaeology FU Berlin and also runs ARCHEA, a laboratory in Warsaw for archaeometric analysis and research. Her main research interests are determining the technology and provenance of archaeological ceramics and devising techniques for the classification of bulk ceramic finds.

Dr. Małgorzata Daszkiewicz
Institut für Prähistorische Archäologie
Freie Universität Berlin
Fabeckstraße 23–25
14195 Berlin, Germany
and
ARCHEA
ul. Ogrodowa 8m95
00-896 Warszawa, Poland
E-mail: m.dasz@wp.pl

EWA BOBRYK

Ewa Bobryk, Master of Science. She graduated from the Faculty of Chemistry of the Warsaw University of Technology in 1978. A leading specialist in designing advanced ceramic materials, she has authored and co-authored numerous publications and patents in the field of ceramic technology, and is also involved in a long-standing collaboration with Małgorzata Daszkiewicz and Gerwulf Schneider on archaeometric research projects.

Ewa Bobryk, MSc
Division of Inorganic Technology and Ceramics
Faculty of Chemistry
Warsaw University of Technology
ul. Noakowskiego 3
00-664 Warszawa, Poland
E-mail: bobryk@ch.pw.edu.pl

Małgorzata Daszkiewicz, Hans-Jörg Karlsen

Possibilities and Limitations of Using pXRF in Analysis of Ancient Glasses – an Example of 3rd and 4th Century AD Glasses Found in Komariv, Ukraine

Summary

This article looks into the possibilities and limitations of using portable energy dispersive X-ray fluorescence (pXRF) to analyse ancient glasses. The scope of this technique was examined by comparing measurement results obtained using pXRF with conclusions drawn from the results of analyses carried out on the same samples using wavelength dispersive X-ray fluorescence (WD-XRF). PXRF measurements were performed as part of a project on the application of pXRF in the non-destructive analysis of archaeological samples conducted at the Excellence Cluster 264 TOPOI of the Freie Universität Berlin.

Keywords: Glass; pXRF; WD-XRF; Komariv

In diesem Beitrag werden die Projektziele und erste Untersuchungsergebnisse zur Siedlung von Komariv vorgestellt. Es handelt sich um den derzeit bedeutendsten Fundplatz im europäischen Barbaricum, der mit einer technologisch hoch entwickelten Glasherstellung in Verbindung gebracht werden kann. Neben neuen Feldforschungen auf dem Siedlungsplatz stand die Analyse einer ersten Probenserie von Glasfragmenten mittels WD-RFA im Vordergrund des Projekts. Zugleich wurde an derselben Serie die Einsatzmöglichkeit des portablen RFA-Geräts getestet.

Keywords: Glas; pRFA; WD-RFA; Komariv

Morten Hegewisch, Małgorzata Daszkiewicz und Gerwulf Schneider (eds.) | Using pXRF for the Analysis of Ancient Pottery – an Expert Workshop in Berlin 2014 | Berlin Studies of the Ancient World 75 (ISBN TODO; DOI: 10.17171/3-75) | www.edition-topoi.org

1 Introduction

The samples of glass used in this study come from Komariv (Ukraine), one of the best-known sites within the European *barbaricum* in connection with glass finds. The settlement at Komariv is noted for its production of glassware, which reflected a high level of technological know-how based on Roman recipes. Analysis of 23 glasses using WD-XRF revealed them to be soda-lime glasses typical of the Roman period, made following a recipe based on three components (natural soda + pure lime + glass sand).[1] This study allowed to distinguish seven groups of Komariv glasses (KOM-1 to KOM-7). Vessels made in the glass workshops of Komariv had a wide-ranging distribution, having been noted not only at regional sites but also, for example, as grave goods in Scandinavia.[2]

2 Results of test measurements by pXRF

Analysis using pXRF encompassed a total of 36 fragments. In choosing samples for analysis, the condition of the glass fragments was assessed and, where possible, well-preserved specimens exhibiting as little weathering as possible were selected. PXRF readings (using a Niton XRF analyser)[3] were taken from three different spots (with several exceptions where only two readings were possible) on the outer and inner surfaces of each of the 36 samples. The results of the measurements are subject to limitations because of the fact that we are dealing with portable energy-dispersive X-ray fluorescence and because of the sampling error associated with the geometry of the samples (quite apart from the problems caused by the weathering of the glass surface). It is not possible to determine sodium content using pXRF, and only a general, semi-quantitative determination of magnesium can be made. Therefore, the rhombic diagram of concentrations of Na, K, Mg, and Ca, which is widely used in the classification of glasses,[4] cannot be applied to the results of pXRF analysis.

Measurements by pXRF were also performed on fresh fractures of seven samples of glass. The only significant differences between measurements taken on the surface and on a fresh fracture are observed in the case of Al and K (and P) concentrations.

1 See Hans-Jörg Karlsen and Małgorzata Daszkiewicz. „Glass Production of the 3rd and 4th Century AD in Komariv, Ukraine". In *Approaching Economic Spaces – Archaeometric Ceramic Analysis: Methods and Interpretation*. Ed by M. Meyer, in preparation.

2 It would be advisable to carry out analyses of these glasses to check whether they have been made in Komariv.

3 Measurements were performed using a Niton XL3t 900S GOLDD RF-Analyser and MINING software, calibration based on twelve ceramic standards analysed by WD-XRF (also checked with three standard glasses), 8-mm measuring spot, measurements on fresh fractures, three measurements per sample (three different spots), measurement time of 120 seconds (30 seconds per filter), in a sample chamber; helium was not used.

4 e.g. Kronz, Simon, and Dodt 2018; Wedepohl 2003.

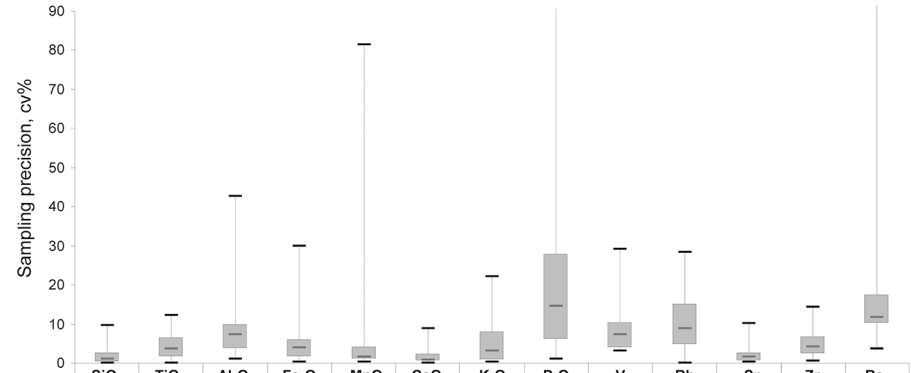

	SiO_2	TiO_2	Al_2O_3	Fe_2O_3	MnO	CaO	K_2O	P_2O_5	V	Rb	Sr	Zr	Ba
Q1	0.38	1.49	3.7	1.62	0.94	0.46	0.8	5.92	3.89	4.71	0.62	2.34	10.3
– min	0.03	0.07	1.13	0.3	0.36	0.11	0.3	1.08	3.12	0	0.17	0.56	3.68
– median	0.97	3.63	7.35	3.94	1.51	0.84	3.24	14.5	7.23	8.87	1.63	4.13	11.7
– max	9.68	12.2	42.8	29.9	81.3	8.74	22.1	90.5	29.2	28.3	10.2	14.4	173.2
Q3	2.56	6.54	9.8	5.94	4.14	2.22	8.1	27.8	10.3	15.0	2.51	6.69	17.5

Fig. 1 Sampling precision, measurements by pXRF.

PXRF analysis of the glasses from Komariv yielded surprisingly good results in terms of sampling precision for SiO_2, CaO and Sr (Fig. 1). Very big sampling errors were noted when determining the content of Al, Mn and P – which was entirely foreseeable. However, a large sampling error was also noted in determining concentrations of Fe, K and Rb; this may be connected to gross error or to the condition of the glass fragments (whether the surfaces are weathered or not) and/or their geometry (fresh fracture surfaces are mostly not as flat as in the case of pottery). Sampling precision for Zr is worse than accepted.

The concentration of Si, Ca and Sr was determined by pXRF analysis with an average precision (precision of average value) of less than 1%; this means that analysis precision was good (Fig. 2a). Concentrations of Fe_2O_3, MnO (very wide variation in sampling precision), CaO and Sr were determined with acceptable analysis accuracy[5] (Fig. 2b). Unfortunately, the Zr content, which is important in establishing the provenance of quartz sand[6], was determined with poor accuracy.

5 See, for example, Hodgkinson 2015 who used the same equipment for glass analysis. As with pottery analysis, differences are noted in the accuracy with which specific elements are determined depending on the particular glass analysed. For example, aluminium and potassium were determined with poor accuracy in the glasses from Komariv.

6 Adlington and Freestone 2017, 1798, also noted that: "Zirconium is indicative of the sand source, and can be used to differentiate glass from different production sources or regions."

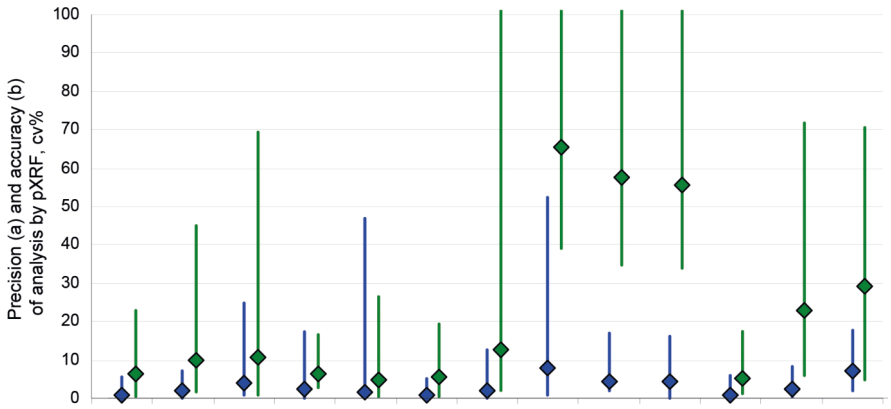

		SiO_2	TiO_2	Al_2O_3	Fe_2O_3	MnO	CaO	K_2O	P_2O_5	V	Rb	Sr	Zr	Ba
a)	min	0.02	0.04	0.65	0.17	0.21	0.07	0.17	0.62	1.80	0.00	0.10	0.32	2.13
	max	5.60	7.03	24.7	17.3	47.0	5.05	12.8	52.3	16.9	16.3	5.90	8.34	17.5
	◆ g.aver.	0.59	1.78	4.06	2.23	1.42	0.61	1.77	7.86	4.19	4.48	0.84	2.23	7.06
b)	min	0.23	1.64	0.96	2.59	0.53	0.36	1.83	39.1	34.8	34.2	1.39	5.78	4.74
	max	23.0	45.4	69.9	16.6	26.6	19.6	112.7	102.4	110.4	124.4	17.4	72.4	71.0
	◆ g.aver.	6.44	10.1	10.6	6.16	4.84	5.75	12.6	66.1	57.9	56.0	5.12	23.0	29.2

Fig. 2 Precision (a) and accuracy (b) of analysis by pXRF.

Tab. 1 presents the results of WD-XRF[7] and pXRF analysis of two samples for which measurements were performed on the outer surface and on a fresh fracture surface (glass fragments shown on Fig. 3). There is no doubt that the accuracy of measurements performed on a fresh fracture is better. Unfortunately, this type of analysis can only be carried out on artefacts that survive in fragmentary form rather than on complete vessels.

The test measurements carried out in our study indicate that the pXRF technique is particularly useful for analysing colourants in glasses with multicolour decoration or single-colour decoration, as well as for decolourising agents in colourless glass or opacifying agents in opaque glasses. Tab. 2 shows the results of pXRF analysis carried out on both transparent colourless base glass and on inlaid blue glass (Fig. 3, sample 637). The base glass was decolourised by manganese ions (physical decolourisation), while the blue colour is attributable to cobalt (Co).

7 Glass standards Corning A, B and D, Schott 1, DGG 2, CRM126B, VS-N were available for comparison.

pXRF / WD-XRF	SiO_2	TiO_2	Al_2O_3	Fe_2O_3	MnO	MgO	CaO	NaO	K_2O	P_2O_5	S	Cl	V	Cr	Ni	Cu	Zn	Rb	Sr	Y	Zr	Sn	Ba	Pb	Co	Nb	La	Ce	Sb	As	Mo	Nd
	per cent by weight										ppm																					
sample 422 (MD5177)																																
a	75.21	0.10	3.49	0.46	0.93		4.46	*na*	0.66	0.21	553	512	40				8	11	407		38		366									
c	71.42	0.10	1.26	0.47	0.94		4.63	*na*	0.31	0.11	722	825	37					12	407		39		382					49				
WD-XRF	71.99	0.09	1.82	0.49	1.05	0.67	5.52	17.98	0.34	0.03	*na*	*na*	11	5	14	9	8	6	416	<5	79	23	295	5	<5		<5	9	20		21	25
sample 650 (MD5171)																																
a	71.15	0.27	2.46	1.28	1.42		4.33	*na*	1.22	0.13	660	750	56				20	18	496		125		419	5		3				5		
c	65.84	0.28	1.64	1.19	1.35		4.31	*na*	0.53	0.12	815	767	62	22			21	13	479		119		339			4						
WD-XRF	68.64	0.27	2.88	1.21	1.47	1.03	5.03	18.84	0.57	0.06	*na*	*na*	29	30	17	17	26	6	483	5	148	19	318	6	6	<5	<5	24	<5	*5*	21	29

Tab. 1 Comparison of the results of analysis by pXRF (average) done on surface and fresh fracture surface with the results of chemical analysis by WD-XRF (analysis of melted samples after mechanical cleaning of surfaces, preparation by ARCHEA, measurements by G. Schneider, A. Schleicher and A. Gottsche in GFZ Potsdam). na = not analyzed; empty space = not detected. Values not detected by both techniques: Se, Ag, Au, Bi, U, Cd, Hg.

Sample No.	SiO_2	TiO_2	Al_2O_3	Fe_2O_3	MnO	MgO	CaO	NaO	K_2O	P_2O_5	Cl	V	Cr	Cu	Zn	Rb	Sr	Y	Zr	Sn	Ba	Pb	Co	Sb	As	Se	Ag	Au	Bi	U
	per cent by weight										ppm																			
transparent colourless glass																														
KOM 637a	77.1	0.13	2.8	0.58	1.27	nd	5.4	na	0.77	0.16	926	50	21	nd	7	9	465	16	47	nd	nd	106	nd	nd	nd	nd	nd	nd	nd	120
blue decoration																														
KOM 637i	78.8	0.21	5.5	1.76	0.27	nd	6.0	na	0.62	0.76	624	53	32	1209	76	9	458	19	62	nd	nd	1539	848	nd	nd	nd	nd	nd	nd	110

Tab. 2 Results of analysis by pXRF of colorless glass and blue glass decoration.

Collating the results of individual analyses using WD-XRF and pXRF shows that, in the case of glass samples, non-destructive measurement by pXRF (measurement on surface of objects) does not provide (as expected) results with sufficient accuracy for network former and network modifier elements; however, pXRF is nonetheless useful in helping to identify major groups (Fig. 4) – which was a surprise. However, the groups exhibit a tendency towards lower Zr contents and the distinctions are much less clear than when using WD-XRF analysis results for samples with a Zr content lower than 90 ppm when measured by WD-XRF and lower than 70 ppm by pXRF (groups KOM-1, KOM-2 and KOM-4). One sample of KOM-7 differs significantly in having a very high Al content (maybe a gross error).

Regression curves fitted to the set of paired data obtained by WD-XRF and pXRF for Si, Fe. Mn and Ca concentrations are shown in Fig. 5. Bearing in mind the limitations in accuracy, the non-destructive pXRF technique, however, can be used as a pre-classification tool that will help reduce the number of samples selected for more reliable destructive analyses. Besides, using pXRF in combination with chemical analysis by WD-XRF to analyse the glasses found in Komariv made it possible to determine a greater number of elements (particularly in the case of WD-XRF analysis carried out on samples of 100mg, in which some elements are not determined).

3 Conclusion

The fact that the pXRF technique cannot be used for analysing Na, and that determining Mg, as well as Al, is often problematic means that a quick pXRF measurement cannot be used to accurately distinguish all types of glass. Soda glass is identified based on the absence of lead, which can, however, result in mistakes. Determining what material any given glass fragment was made of (interpretation of glass types) will require additional destructive analyses. However, in situations when samples cannot be taken for laboratory analysis by pXRF the concentration of trace elements can be used to identify differences between major sources of sand glass (Zr) or glass making technology (e.g. it is possible to differentiate between physical and chemical decolourisation).

Note

The authors started to use pXRF before 2014, when this text was written (with some later corrections). Since then the potential of using this technique in the analysis of glass has also been recognized by other researchers, such as Laura W. Adlington and Ian C. Freestone in their 2017 article: *Using handheld pXRF to study medieval stained glass: a methodology using trace elements* (Material Research Society, 2017, 1785–1800).

Fig. 3 Examples of analyzed glass fragments.

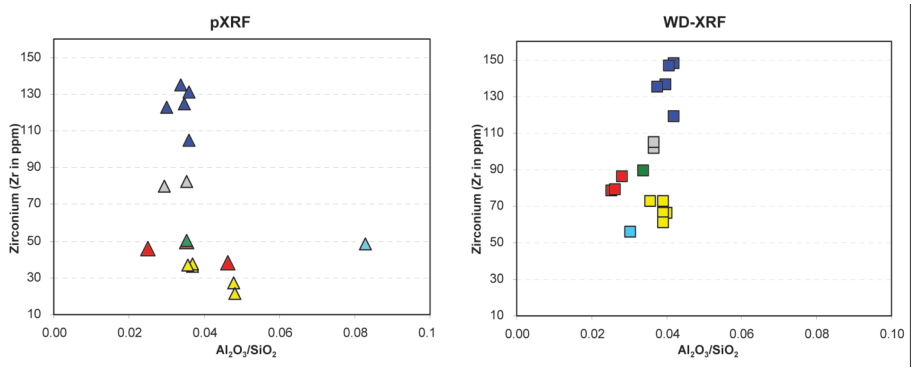

Fig. 4 Grouping by WD-XRF and pXRF.

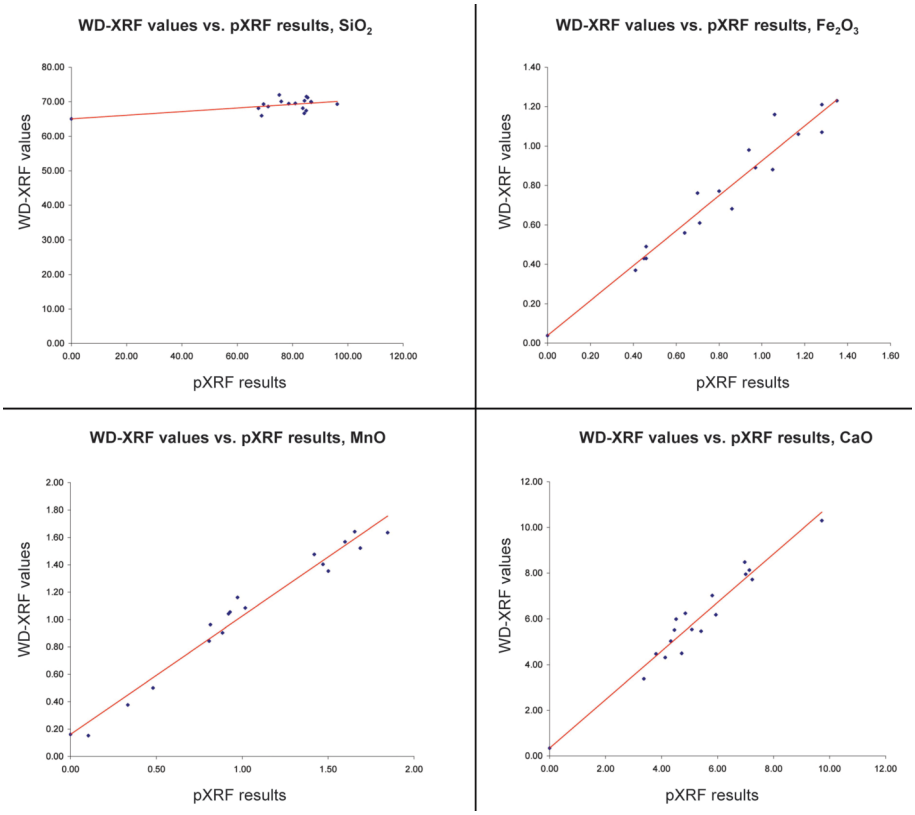

Fig. 5 Regression curves fitted to the set of paired data obtained by WD-XRF and pXRF.

Bibliography

Adlington and Freestone 2017
Laura W. Adlington and Ian C. Freestone. "Using Handheld pXRF to Study Medieval Stained Glass: A Methodology Using Trace Elements." *MRS Advances* 2.33/34 (Material Issues in Art and Archaeology XI) (2017), 1785–1800.

Hodgkinson 2015
Anna K. Hodgkinson. "Amarna Glass: from Egypt trough the Ancient World." *Egyptian Archaeology* (2015), 23–27.

Kronz, Simon, and Dodt 2018
Andreas Kronz, Klaus Simon, and Michael Dodt. "Frühmittelalterliche Glaswerkstätten am Kölner Hafen." In *Archäometrie und Denkmalpflege 2018. Jahrestagung am Deutsches Elektronen-Synchrotron, Hamburg, 20.–24. März 2018*. Ed. by L. Glaser. Hamburg: Verlag Deutschen Elektronen-Synchrotron, 2018, 124–127.

Wedepohl 2003
Karl Hans Wedepohl. *Glas in Antike und Mittelalter – Geschichte eines Werkstoffs*. Stuttgart: Schweizerbart'sche Verlagsbuchhandlung, 2003.

Illustration and table credits

ILLUSTRATIONS: 1–3 M. Daszkiewicz. 4 H.-J. Karlsen. 5 M. Daszkiewicz. **TABLES:** 1–2 M. Daszkiewicz.

MAŁGORZATA DASZKIEWICZ

Małgorzata Daszkiewicz, MA Warsaw 1979 in Physical Geography, PhD Warsaw University 1993 in Humanities. Since 1994 she has worked in collaboration with *AG Archäometrie* FU Berlin. Formerly a part-time employee at TOPOI, she is currently an associated member of the Institute for Prehistoric Archaeology FU Berlin and also runs ARCHEA, a laboratory in Warsaw for archaeometric analysis and research. Her main research interests are determining the technology and provenance of archaeological ceramics and devising techniques for the classification of bulk ceramic finds.

Dr. Małgorzata Daszkiewicz
Institut für Prähistorische Archäologie
Freie Universität Berlin
Fabeckstraße 23–25
14195 Berlin, Germany
and
ARCHEA
ul. Ogrodowa 8m95
00-896 Warszawa, Poland
E-mail: m.dasz@wp.pl

HANS-JÖRG KARLSEN

Hans-Jörg Karlsen (né Nüsse) Dr. phil. (Göttingen 2003), Habilitation (FU Berlin 2011), before he became a professor of Protohistoric Archaeology at the University of Rostock in 2016, he has been a member of the central administration of Excellence Cluster Topoi. He is specialized in settlement archaeology and social development of the Iron Age.

Prof. Dr. Hans-Jörg Karlsen
Universität Rostock
Heinrich Schliemann-Institut für Altertumswissenschaften, Lehrstuhl für Ur- und Frühgeschichte
Neuer Markt 3
18055 Rostock, Germany
E-mail: hans-joerg.karlsen@uni-rostock.de

MORTEN HEGEWISCH, archaeologist (2003 Dr.phil., FU Berlin) specializing in the Roman Imperial age in Germanic regions. He worked at various universities and archaeological institutions in Germany including the Cluster of Excellence Topoi, and is now at the Institute for Prehistoric Archaeology FU Berlin, as editor of the Praehistorische Zeitschrift.

MAŁGORZATA DASZKIEWICZ, physical geographer/archaeologist (1993 PhD in Humanities, Warsaw University). Since 1994 she has worked in collaboration with AG Archäometrie FU Berlin. Formerly a part-time employee at Topoi, she is currently an associated member of the Institute for Prehistoric Archaeology FU Berlin and also runs ARCHEA, a laboratory in Warsaw for archaeometric analysis and research.

GERWULF SCHNEIDER, mineralogist/geochemist (1968 Dr.rer.nat., 1979 Habilitation, FU Berlin). Since 1975 he has been involved in chemical and mineralogical analysis of archaeological ceramics. He was an associated member of Topoi. His many research projects encompass Roman and other pottery in Germany, the Mediterranean region and the Near East.

Within the BERLIN STUDIES OF THE ANCIENT WORLD series, monographs and volumes of all fields of ancient studies are published. These publications form the results of research conducted within the Excellence Cluster *Topoi. The Formation and Transformation of Space and Knowledge in Ancient Civilizations*, a research association between the Freie Universität Berlin and the Humboldt-Universität zu Berlin as well as the partner institutions Berlin-Brandenburgische Akademie der Wissenschaften, Deutsches Archäologisches Institut, Max-Planck-Institut für Wissenschaftsgeschichte and Stiftung Preußischer Kulturbesitz.
The series is part of the research platform *Edition Topoi* and fully accessible at www.edition-topoi.org.

ISBN 978-3-9819685-9-0

75 BERLIN STUDIES OF THE ANCIENT WORLD

www.edition-topoi.org